Metal flow analysis for automation of incremental open die forging

Aksakal, Bunyamin

Award date:
1993

Awarding institution:
University of Bath

METAL FLOW ANALYSIS FOR AUTOMATION OF INCREMENTAL OPEN DIE FORGING

submitted by

Bünyamin Aksakal

for the degree of Ph.D

of the

University of Bath

1993

ProQuest LLC
789 East Eisenhower Parkway
P.O. Box 1346
Ann Arbor, MI 48106-1346

ABSTRACT

Open die forging is a long established process which can be used to produce a wide range of shapes. Deforming the workpiece is essentially incremental and only a part of workpiece is compressed. Shape transformation is achieved by laborious manipulation of the workpiece while repeated blows are effected in order to reduce, locally, the cross section of the workpiece, which plays an important part in producing the required profiled product. This however has resulted in a diminished utilisation of the process. Its characteristic features in relationship to closed die forging processes are that it requires low forming loads, and with a small range of simple tools a wide variety of shapes can be produced. Whilst the process is generally associated with the production of large forgings, an automated version could be attractive for small batch manufacturing of low weight forgings. Such a system could compete effectively against machining process.

In this work for the sake of developing an automation in open die forging the nature of deformation of small size parts was investigated. The elementary analysis of open die forging of long bars were searched via the upper bound method by constructing a number of kinematically admissible velocity fields. From these velocity fields the deformation and friction power and hence the total power was minimised with respect to a pseudo independent parameter thus enabling load requirement and metal flow to be predicted. To enable correlation of the analysis, idealised quadrapiped billets with various aspect ratios of sections were locally deformed between two flat dies. The theoretical analysis enabled the determination of the amount of spread in the lateral direction and also the volume displaced from under the tools in the axial direction after each compression step for differ-

ent friction conditions. The compression steps were applied to the relevant billets in single step and in an incremental plus rotational manner with different depth of penetrations where the load required and the resultant pattern of deformation were predicted.

In order to develop an automated open-die forging process it is essential to be able to predict the shape changes occurring at each step. Therefore a general computerised methodology is proposed for small batch manufacture via a theoretical model producing rapid predictions of metal flow for continuing incremental deformation. The validity of the theoretical analysis have been assessed by comparison with experiments and found to be in a good agreement.

Acknowledgment

The author wishes to thank all those who helped to make this work possible. In particular I wish to express my deepest gratitude to my supervisors, Prof. A.N. Bramley and Dr. F.H. Osman, who being most generous with their time, provided many useful ideas, valuable guidance and encouragement through the work.

I would like to thank to Mr. I. Walker and the other postgraduate colleagues in the department of Mechanical Engineering and the staff of the laboratories and workshop for their technical assistance.

The author is also indebted to the Turkish Government and the Ataturk University for the financial support of the work.

LIST OF SYMBOLS

h_0 : Initial height of the billet (mm)

h : Final height of the billet (mm)

l_0 : Initial length of the billet before compression(mm)

l : Length of the deformed region after compression(mm)

m : Friction factor,

w_0 : Initial width of the billet (mm)

w : Final width of the billet (mm)

b : Tool width (mm)

p_{ave} : Mean forging pressure,

$\dot{u}_x$, $\dot{u}_y$,$\dot{u}_z$: Velocities in the x,y,z directions respectively,

$\dot{u}_{y_{max}}$: Maximum velocity in the y direction,

$\dot{v}_p$: The upper tool velocity

$\dot{W}_d$: Deformation power or internal power,

$\dot{W}_f$: Friction power,

$\dot{W}_s$: Shear power,

$\dot{W}_t$: External traction power,

$\dot{\epsilon}_x$: Strain rate in x direction,

$\dot{\epsilon}_y$: Strain rate in y direction,

$\dot{\epsilon}_z$: Strain rate in z direction,

σ_0 : Yield strength of the deformed material,

w_0/h_0 : Initial aspect ratio of the workpiece(IAR)

w/h : Final aspect ratio of the workpiece(FAR)

CRAR : Compressed and rotated aspect ratio of the workpiece.

Contents

List of Figures

Chapter 1

INTRODUCTION

Forging is probably one of the most ancient of the metal-working operations, as practised on a small scale by the village blacksmith. Basically the process is one of simple compression and can be dated back to 5000 B.C. Very simple forgings can be made with a heavy hammer and an anvil with techniques that have been used by blacksmiths for centuries. It has been used for making parts of widely varying sizes and shapes from a variety of metals. Typical parts made by forging today are crankshafts and connecting rods for engines, turbine discs, gears, wheels, bolt heads, hand tools, and a great variety of structural components for machinery and transportation equipment. The data available from previous forging of the same or similar parts were the main basis of development of the process. Then some empirical formulae were developed by experience with laboratory forging work but primarily before computers became available the evolution of metalforming processes relied extensively on the experience of the forgemaster.

Forging can be classified into closed and open-die forging on the basis of whether the workpiece is constrained to flow into impressions contained in tools or allowed

to flow freely by being locally compressed between simple tools. Closed die forged products whilst reflecting benefits in terms of material utilisation and homogeneity are invariably associated with large batch size production where die sinking costs can be amortised to a small proportion of the individual component cost. At the present time where forging plants are being obliged to work with increasingly smaller batches, that portion of the final component cost attributable to the tooling can be as much as 30 %. Although metal-forming operations are diverse, the primary objective is to produce a desired shape change. The major concerns of the engineer are the load requirements and the metal flow prediction. The ability to produce forgings economically in small batches would yield dramatic benefits by recovering old markets lost to castings, reducing lead times, opening up new markets for forgings by competing against traditional full machining systems and advantageously enabling the forging processes to be integrated into flexible manufacturing systems. Open die forging could provide this opportinuity.

Open-die forging is a deformation method in which a workpiece is manually manipulated and shaped under a hammering action and has not lost its importance in recent times. Forging is carried out under hot or cold working conditions. Hot forging of a metal occurs when metals are plastically deformed above their recrystallization temperature and usually involves severe geometrical changes from an initially simple geometry. Cold forging can also be used directly for the production of small and precise products such as parts in automotive, aviation and some large parts in shipping industries. In open die forging the process is carried out incrementally and only a part of workpiece is being deformed at each stage.

The system comprises a set or sets of flat or curved dies which can be produced economically. The tools are small compared with overall sizes of the forging. The resultant reduced forging loads mean that lower load capacity and therefore lower capital press equipment cost machine can be used to produce a given part. The principle of such an incremental forging processes is simply compressing or upsetting of the material step by step until it reaches the final target shape. Using simple flat or radiused tools of varying width, products of various shapes can be manufactured, mainly by simple upsetting. In the further developement of this type of forming operation requirments are for accuracy of load prediction and metal flow. There have been several attempts to analyse the block forming processes using new techniques such as the Finite element and the upper bound method in order to achieve these requirements.

Incremental forming however, has been gaining ground in the area of sheet metal working and various new forms of swaging techniques have been emerged which to automate and systematise the process. For example, in an industrial context, the Siemel Kempf Company in Germany produces a robot and press combination which can be used for automatic open die forging but whilst the facility is programmable it has to learn the appropriate sequence of steps based on experience, trial and error...etc, in order to produce a particular shape. Clearly a modelling/simulation facility coupled to their system would be valuable.

In a wider context production methods throughout industry worldwide have undergone radical changes over recent years. The most notable of these changes has been the move towards the Japanese production method called "just-in-time",

JIT. Adopting JIT philosophies enables companies to reduce stock levels to a bare minimum, saving money on work-in-progress, and reducing lead times, whilst ensuring quality control of the highest level.

As a part of Flexible Forging System(FFS) a system is proposed in this work to automate the open die forging process using a robot to manipulate the workpiece and a numerically controlled forging press linked together via a controlling computer. The system would be programmed and controlled to enable a given shape to be produced by a series of pressing operations and workpiece manipulations. This would provide an appropriate flexibility for the forging industry. A basic forging step in this set-up is a simple 3D upsetting operation. The geometrical changes in the workpiece have to be continously observed and monitored by the operator who will accordingly apply appropriate rotational and longitudinal manipulations. Sufficient knowledge of the flow behaviour of the workpiece during compression is therefore required.

One of the main purposes of this investigation is to enable the rapid prediction of material flow and allow for flexibility in process utilization so as to save material and reduce the total cost of production. An important part of this system is its capability to provide a complete schedule to produce various formed features and profiles. This requires a reasonably accurate and rapid analysis of the deformation pattern for each individual bite. In incremental open-die forging the predicted metal flow has a substantial importance which enables the control of the process rather than relying on trial and error method to make an expert system for process design. The schedule can also be optimised with respect to the bite size so that

minimum effort and workpiece manipulation are required. Detailed information on the deformation pattern such as metal flow and load predictions is necessary in order to incorporate a process planning system for automation of open die forging.

The main subject of the work in this thesis is to analyse the three dimensional deformation pattern and to enable the rapid prediction of material flow and allow for flexibility in process utilization then to establish a method that can be used to produce a profile in incremental open die forging. The thesis includes seven chapters. Chapter II deals with a historical review of open die forging. Chapter III explains the upper bound method and its previous applications. Chapter IV relates to the three dimensional analysis of open die forging of long bars having various aspect ratios. Three different solutions are introduced employing different velocity fields for forging load prediction and the associated flow pattern produced in a single bite, incremental and 90° rotation operations. The upper bound solution results are compared with three of other previous work in open die forging and also in rolling process. Chapter V describes a progamme of experimental work directed towards ascertaining the effects of aspect ratio, height reduction, tool width in single compression and also in an incremental continous compression-rotation process to validate the theoretical solutions. The results of these theoretical and experimental investigations into the mechanics of forging of long bars by predicting load, spread and elongation rapidly may, in their own right, be useful for industrial purposes. These may also be useful for further investigations into differently shaped bars and tools. Furthermore Chapter VI exploits the theoretical solutions to build a method which accommodates a

profiling sequence of forging steps to produce profiles from initial long square and rectangular bars by using flat tools. Chapter VII draws the conclusions of this work and indicates the need for future work. Finally a number of displaced volume calculation methods are described in Appendix-A.

Chapter 2

HISTORICAL and LITERATURE REVIEW

2.1 Introduction

There is an increasing demand for improving the precision of the forging process by providing accurate predictions of forging load and metal flow. However, owing to the complexity of the deformation pattern in forging processes metal flow simulation and loading predictions are still major areas of research. The theory of plasticity deals with the methods of calculating the main characteristics such as flow stress, strains, load and material flow. Applications are aimed at predicting forming loads, overall geometry changes of deforming workpieces, quantifying metal flow and optimising process conditions. Analysing the deformation pattern in open die forging is very important but the detailed analysis of deformation patterns is very limited and does not seem to provide detailed information suitable for process planning. Also they are not applicable or practical enough for incre-

mental and continuous forging processes. Several methods are in existence with which both the forming load and metal flow can be worked out. In recent years numerical solutions in open die forging such as Finite Element and Upper Bound methods which are based on one of the extremum principles have attracted many investigators into analysing deformation process in open die forging. In most of these analytical methods the elastic strains were neglected and the material is considered rigid plastic. However, the yield stress of the forged material may vary at different stages in the deformation.

The purpose of this chapter is to give a brief review of the historical development and of the techniques which are currently available and have been and can be used for predicting the load and metal flow in open die forging. Since many of these techniques are described in plasticity and metalforming text books eg [7, 8, 10, 31, 37, 40] some detail is omited. Table 1 shows a summary of the methods which are used in metalforming processes.

2.2 Historical review

The blacksmithes is one of the oldest arts in history. Just when and where the art of forging came into use, history is not able to define very clearly. However it can be deduced from legends, records, and relics that the forging was in long use before there existed written records. Most records of past civilisations indicate that the forgeman has always held a leading position, since the products of the forge were the weapons that defended the people against their enemies. The quality of their products depended largely upon the grade of ore which they were

able to find and upon the skill of the smith in working the metal. The early smith had practically no knowledge of chemistry or metallurgy to guide him.

The thirtheenth century witnessed the introduction of gun powder and this brought about a complete change in the manufacture of iron and the art of forging. The old style weapons of war became obsolete and were replaced by firearms (see Fig 2.1). The change in the mechanical operation of forges brought larger forges into existence which in turn increased the demand for iron and steel products. The iron was first hammered lightly under hand sledges to force out some of the slag, then it was reheated and forged under the heavy waterwheel hammer into short, thick squares, reheated and drawn out under smaller waterwheel hammers or finished by hand sledging.

It has to be said that up to the nineteenth century very little change had been made in the design of power hammers and no other forging method was in use. In the meantime during the eighteenth century into the nineteenth, the use of steam for power grew and forced its way into industrial use through development of the steam engine. It was in 1838 that James Naysmith, a Scottish engineer, conceived the idea and developed plans for the first direct acting unit which made available the means of making forgings of considerable size. In Fig 2.2 the Naysmith hammer is seen [67].

Up to about 1850 all power hammers generally used had either flat faces on the hammer and anvil or were simply profiled to the rough shape of the piece to be forged. These forgings eliminated a great deal of hand work such as filling and grinding to finish them. The first general use of these duplicate forgings was

in the manufacture of firearms and it was one of the means that made possible the rapid production of firearms during the American civil war. After that a few forging plants with power hammer began to make their appearance. Further developments occurred with the introduction of mechanical and hydraulic forging presses.

The forger has learned through his experience the basic laws that govern the action of metal under pressure. He had, however, a mental picture of the path of metal flow from the shape of the raw forging stock to the finished forging and his experience indicated the path, in the various forging steps which needed to be taken by the flowing metal in order to reach the desired shape. He considered such factors as height and surface area of the raw forging stock and of the finished piece.

As a general rule, such forgings require machining all over where they are parts for machinery, such as gear, rings, shafts etc. There were, however, many forgings made by the steam hammer process that require little or no machining, and many of these were forged to fairly close dimensional tolerances. The steam hammer was much used in the larger production forging plants on maintenance repairs. One of the products of the steam hammer was the forged weldless rolled ring. These rings were produced from the solid billet by a piercing and rolling operation, also called a saddling operation. The procedure was to flatten a cut piece of steel into a disk of suitable diameter and thickness[67].

By the end of nineteenth century several attempts had been made by experience to develop suitable data and tables from which production on any given forging

could be determined approximately.

2.3 Previous work on Open Die Forging

The first pioneering work in bar forging analysis was introduced by Tomlinson and Stringer [83]. They developed an empirical formula for the prediction of elongation and sideways spreading in open die forging. The experimental work was based on square bars. The effects of temperature, reduction in height, longitudinal movement of the bar between strokes and shape of cross sections were investigated. The range of reductions in height was examined to see whether the proportion of spreading to elongation varied with different reductions. The change of bar height and length was expressed in terms of the ratio between the original and final bar size. Using their experimental data and the condition of volume constancy the following empirical expression was determined:

$$s = 0.29 - 0.16\,(\frac{h_1}{h_0}) + 0.343\,(\frac{b}{w_0}) - 0.048\,(\frac{b}{w_0})^2 \qquad (2.1)$$

h_1 is height after forging, h_0 is initial height, b is width after compression, w_0 is initial width before compression and s is referred to as the spread coefficient. The physical meaning of this coefficient can be defined as a measure of the proportion of the deformed material moving sideways and can be obtained as follows:

$$s = \frac{ln\frac{w_1}{w_0}}{-ln\frac{h_1}{h_0}} \qquad (2.2)$$

The effect of friction was not considered and it was pointed out that the coefficient of spread (s) depended mainly on the shape of the tool contact area, as defined by the bite ratio $(\frac{b}{w_0})$.

In the same year similar work on this topic was reported by Wistreich and Shutt [84] in which they presented a theory for cogging of square blooms and billets. They worked out a series of empirical formulae to predict the shape of the final forging. A simple workpiece was chosen for the analysis as shown in Fig 2.3. In this work a spread factor β and spread ratio s were introduced.

$$s = \theta/(1 + \theta) \tag{2.3}$$

$$\beta = (1/\gamma)^s \tag{2.4}$$

where θ is the bite ratio ($\theta = b/w$) and $\gamma = h_1/h_0$

Braun, Angott and Berger [16] presented work which dealt with an upper bound solution for spread and pressure. A long rectangular bar was compressed by an opposed pair of flat tools. Spread and elongation were calculated in terms of the spread coefficient s, given in Eqn. 2.3 which was defined as a function of velocities, thickness and the width of the bite as,

$$s = 1 - \frac{h\,\dot{U}}{b\,\dot{V}} \tag{2.6}$$

where h is thickness, b the width of the bite, $\dot{U}$ velocity in longitudinal direction and $\dot{V}$ is the magnitude of the tool velocity. In order to calculate s, the velocity of the rigid body motion associated with plastic flow was determined by applying the Upper Bound principles. Values for spread s and pressure calculated were

compared with measured values.

In 1960 Kudo [42] presented a procedure to facilitate the analysis of complicated problems for plane strain forming operations by introducing the concept of a "unit rectangular deforming region". It was assumed that a unit region can be surrounded by rigid bodies which may be considered to be either a rigid tool or a rigid part of the material. The velocity field for plane-strain compression between two parallel flat dies. Fig 2.4 shows Kudo's velocity field. The rate of energy dissipation for various unit regions of different height-width ratios were tabulated. Optimization was carried out with respect the aspect ratio of the deforming elements.

In Kudo's work there were some restrictions where it was assumed that the overall forging must be capable of being split into elements of rectangular cross section only. Also flow was restricted to two boundaries of the element. One boundary for inward flow and the other for outward flow which satisfies the volume constancy. Subsequently, he extended the solution to include axisymmetric shapes by introducing cylindrical regions [43].

In more recent years metal flow investigations in open die forging have been empirically based. Raughunathan and Sheppard [75] investigated the factors that affected spread during slab rolling in two commercial Al-Mg alloys(AA 5056 and AA 5083) with a new spread formulae which was derived from their experiments. The material characteristics under the appropriate deformation conditions were introduced into the spread function. The spread coefficient in this work originated from the theoretical analysis of roll gap deformation by Hill [22] utilizing the

Levy-Mises flow rule.

Baraya and Johnson [14] analysed bar forging using the upper bound technique. Three solutions were suggested through triangular velocity fields in which each one denoting to work out p_{ave}/σ_0 and load using three different metals. It was assumed that straight boundaries remain straight after compression. All three solution themselves had some restrictions as to their suitability depending upon the working range of the aspect ratio, w_0/h_0 values. It was also noted that the velocity field did not take friction conditions into account and none of the solutions gave a satisfactory fit to all the experimental results for the various aspect ratios. Therefore the applicability of this approach to practice does not seem to be promising.

Sagar and Juneja [46] introduced work on the problem of determining load requirments by taking the bulging into account. Their aim was to determine the die pressure for rectangular bar with flat tools using the upper bound method. To find out the nature of flow of the material, experiments were conducted with rectangular bars of aluminium and flat tools of various widths. It was noted that when the height of the specimen was smaller than the width, bulging was predominant. It was also shown that for the same values of w_0/b and w_0/h_0 the tendency to bulging increases as the friction on the tool workpiece interface increases. Attempts were also made by Sagar and Juneja [47, 48] for analysing the flow and relative die pressure of four sided irregular and rhombus shaped discs in open die forging. They used the upper bound method in which the irregular shape was divided into three zones, each zone having a separate velocity field.

In this work the bulging was taken into account and the velocity field and power dissipation in different regions of the disc was determined by minimising a shape factor which signified the extent of nonuniformity of material flow in the plane sections thus indicating the extent of bulging. The compressions took place under different lubrication conditions thus varying the friction factor values.

An investigation was carried out by Kemp [54] in which he examined whether the upper bound technique is suitable for hot rolling, and generally for the modelling of three dimensional forming processes. A rectangular shape was considered for simple compression and a kinematic admissible velocity field constructed. Energy dissipation was computed and spread values, which were predicted, for a given aspect ratio were compared with the experimental work. It was reported that theoretical predictions were in a good agreement with experiments.

Kennedy [44] analysed spread, elongation and bulge in flat rolling using the upper bound approach. The shape of bulging was predicted and compared with experimental measurements. It was shown that the predicted true spread values which are directly related to the actual elongation, significantly underestimated the measured values, especially at heavy reductions.

Kiefer and Shah [50] simulated open die forging by a three dimensional analysis based on the Finite element model. They used the model to show the distribution of internal stresses and strains in rectangular ingots which were compressed to analyse the effect of different type of flat die widths under different height reductions. They showed the width strain increases with increasing aspect ratio of b/h, where b is the die width, while the length strain initially increases.

Kanacri et al [51] investigated the compression of rectangular blocks between two parallel platens by modifying Hill's formulated theory [22] for the calculation of stress and displacement in a thin sheet that is being plastically compressed. It was shown from the flow lines that the amount of spread becomes higher with increased friction values.

During last two decades a few more attempts were made for analysing compression of blocks in open die forging using different numerical techniques. For example Shiau and Kobayashi [78] used the finite element method to analyse one bite operations and sequences for square to round and round to square operations in open die forging. They developed a theoretical model in which the workpiece is compressed and rotated in a single and then multi-bite operations to reduce the cross section by assuming $m = 0.2$. However it was noted that only one compression step took 75-100 seconds of CPU time.

Park and Kobayashi [74] employed the three dimensional finite element method which took eight-node hexahedral elements in order to analyse simple block compression. Although theoretical results were in good agreement with experiment, computation took considerable time.

Experimental investigations into the strain distribution and surface cracks using photoelastic technique were carried out by Mulc [66] in an attempt to evaluate the practical workability limits in open die forging. Accurate modelling of the process using finite element plasticity has also been reported by Lange [58], especially in relation to a radial forging process.

Incremental forming however has been gaining ground in the area of sheet metal working, rotary forming and various new forms of swaging techniques and attempts have been made to automate and systematise the process. For example, in an industrial context, the Siemel Kempf Company [70, 71] in Germany produces a robot and press combination which can be used for automatic open die forging but whilst the facility is programmable it has to learn the appropriate sequence of steps based on experience and trial and error in order to produce a particular shape. The GFM machine and the MRPM [81] forging machine using a multi-die arrangement also exploit the concept but are generally associated with large components and do not offer a great deal of flexibility in setting up for different shapes. Lange [58] also developed a four die radial machine, RUMX 2000, suitable for flexible production of medium size components. This was coupled with some analytical modelling work but the concept does not appear to have been taken up commercially. This may be a reflection of the general over-capacity in the forging industry and a consequent natural is the reluctance to invest in new equipment. From the mid-70's, decreasing batch sizes due to growing product variety and shorter product life cycles resulted in growing pressure for flexibility [59]. Flexible automation, irrespective of the process, is not an end in itself, but a means of lowering the production costs, especially in the case of small batch sizes. Better, quicker and hence less costly adaptation, while retaining the same degree of automation, reduces the minimum economically viable batch size and therefore opens up further applications.

The forging industry, like many others, is having to make some significant adjustment to accommodate shorter production runs and a greater variety of parts.

The small batch manufacturing mode is becoming more common to meet changing customer requirements. Accordingly, flexibility and cost effectiveness are increasingly important in the utilisation of forging equipment [82]. The economic benefits of small batch production in manufacturing, and of the forging process itself as a shape maker, suggest that a promising line of development could be to couple an automated open die forging process with a flexible on-line process design and modelling system. This has the potential for making use of existing equipment possibly with the need to retro-fit some form of computer control. The ultimate objective is to have a system which for a given required component shape could automatically prescribe a sequence of incremental deformation steps and workpiece manipulations. At the core of this is the need to have a systematic model for the prediction of spread and elongation in open die forging. Some empirical approaches to modelling the open die forging process have been made earlier [83]. But they are restricted to a limited range of configurations and are not rapid enough for the process.

Forging is one of the most hazardous environments in industry because of its noise, heat and pollution. The repetitive, tedious and also monotonous nature of the process makes working conditions extremely difficult. In order to increase productivity and reduce the labouring costs for forging industries automation would seem to be necessary. The use of manipulators in open die forging can be dated back about 60 years when development started in both Europe and USA. In the application of manipulating the workpiece by robots a feasibility study was undertaken by Appleton et al [4] Tomlinson's formulae was used for the prediction of spread and this led to a computer technique [5, 6] for generating an

optimum forging schedule which can be used as a basis for robot programming. Lead was used as a model material through the experiments to simulate hot steel. The program determined the optimum number of squeezes per pass, the forging ratios and elongation. They used a Versetran D301 point-to-point manipulator robot with a gripper and a mechanism to allow the elongation without disturbing the robot arm position. These studies took place by using the computer software developed in the interactive graphics unit by Heginbotham et al [29, 30].

Introducing JIT manufacturing in open-die forging will increase the productivity. The practice of JIT in which materials are purchased or parts produced in an exact quantity just as they are needed has been one of the distinct features of a system that has contributed substantially to Japan's high product quality and productivity. The primary objective in this kind of technique is reduction of cost through the elimination of waste. Waste is defined as anything other than the minimum amounts of equipment, materials, workers, and time that are absolutely essential to production[34]. The central idea of reducing waste means that the pull mechanism, which supports the focus on producing only what is required, ensures that no money is wasted on producing unneccessary inventory and 'Work In Progress'[76]. Manufacturing process control relates to design control through two phases of diagnosis and problem solving. The object is to maintain process and product specifications according to the design standards and to ensure production of uniform products. These objectives can be obtained by diagnosing and solving the problems within the production process. Diagnosis and problem solving constitute a method of logically analysing process data to arrive at a decision on process control.

In an effort to automate the open die forging process, the determination of process data is essential and knowledge of the material flow at each single squeeze with a cyclic sequential operation is needed in order to interact with the manipulator with the press via controlling computer. This computer will be providing automatic control and supervision of the whole production process by data and program distribution to attached subprograms in a direct numerical control system.

Recently Shimizu et al [77] presented a work which deals with a process design also using FEM. In their analysis a multi ram press with a fixed tool width was used to enable the reduction of the cross section of aluminium billets in three different ways, hexagonal reducing by rotating 45° and, square reducing by rotating billet 90°. They showed deformation and strain distribution obtained while the cross section of the billet is reducing. In the analysis no friction was considered and it was noted that the analysis process is limited by computing time which it was given 40 minutes CPU time for only four steps of compression process. As far as the whole process is concerned in order to complete one component a few hours or may be days are needed.

Table 2 shows a summary of the methods and solutions, described above, in comparison with each other. It is clear that the current practice and existing empirical formulae which have been used before are restricted to a limited range of configurations and are not suitable or rapid enough on-line process in the field of open die forging. Hence this work was executed in order to provide a number of upper bound solution which can predict accurate load and metal flow rapidly

and to produce shapes in a systematic way. This will also allow for flexibility in process utilisation so as to save material and reduce the total cost of production.

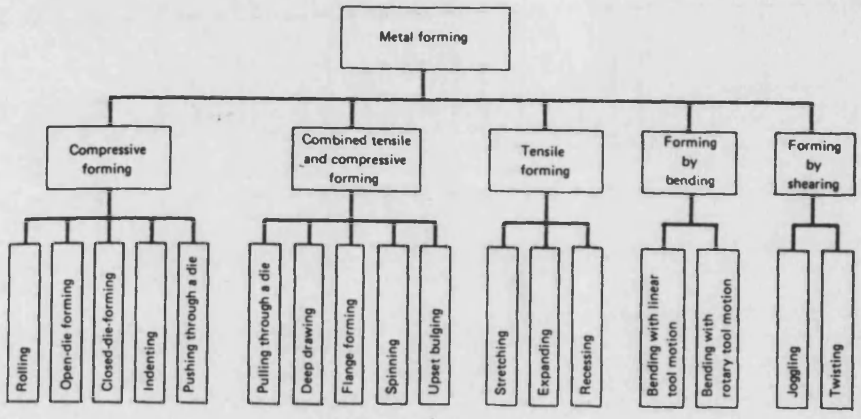

Table 1. Methods in metalforming area[59].

Table 2. A summary of work in open die forging.

Ref.no:	Analytical solution	Experiment	Workpiece description	Correlation Theory-Experiment	Tool configuration	Process limitations	Forging process type
[82]	—	✓	Long square sections	—	Flat tools	-No friction $-0.5 < \frac{w_0}{h_0} < 2$	Single squeeze Open-die
[83]	—	✓	Long square sections	—	Flat tools	—	Single squeeze Open-die
[14]	Upper bound method	✓	Long rectangular sections	Not very good	Flat tools	-No friction - Limited working range for theory	Single squeeze Open-die
[16]	Upper bound method	—	Long rectangular sections	—	Flat tools	$2/3 < \frac{w_0}{h_0} < 1$	Single squeeze Open-die
[45,46,47]	Upper bound method	—	Small rectangular bars Irregular shaped discs Rhombic shaped discs	Good	Flat tools	-Limited w_0/h_0 range No bulging[45] Limited results	Single squeeze open-die Dies cover whole specimen
[50]	Finite element method	—	Large and long rectangular sections	—	Flat tools	Only strain distribution was investigated	Single squeeze Open-die
[51]	Modified Hill's formulae	✓	Rectangular blocks	Good	Flat tools	Analysis valid only for small frictions	Single squeeze Open-die
[77]	Finite element method	—	Round and square billets	—	Flat tools	- Long CPU time m = 0.2	Single squeeze and multi-cycled open-die process
[74]	Finite element method	✓	Rectangular blocks	Good	Flat tools	- No friction - Long CPU time	Single squeeze Open-die
[76]	Finite element method	—	Round billets	—	Multi-die arrangment	- Long CPU time	Multi-cycled compression-rotation process
[80]	Finite element	—	Large components	—	Multi-die arrangment	No flexibility in setting-up for different shapes	Single squeeze and multi-cycled open-die process
Current work	Upper bound method	✓	Small size parts Rectangular and square cross-sectioned long billets	Very good	Flat tools with various widths	No limits for theory Experimental: $0.3 < \frac{w_0}{h_0} < 2$	Open-die: -Single squeeze -Multi-cycled incremental

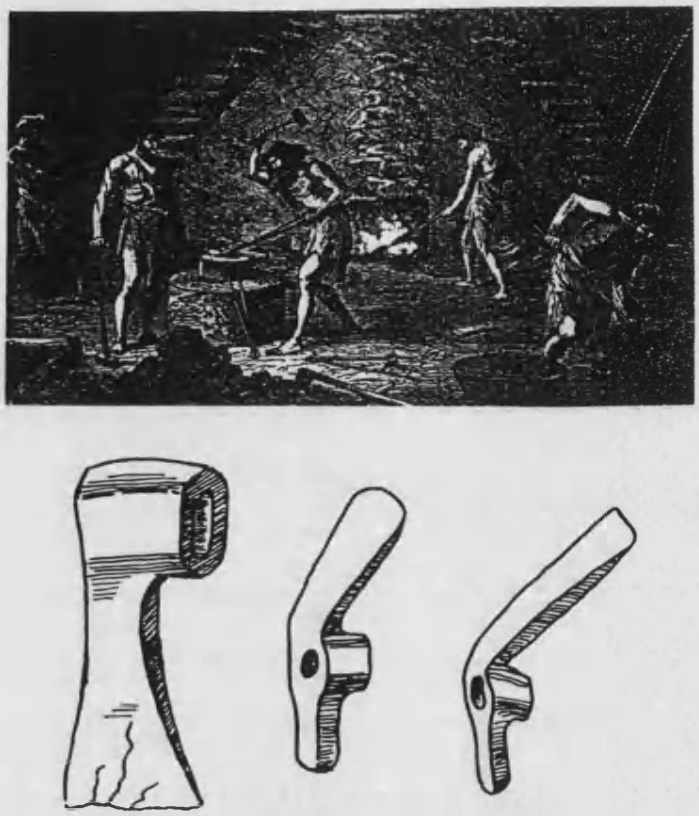

Figure 2-1: Early Roman Forging

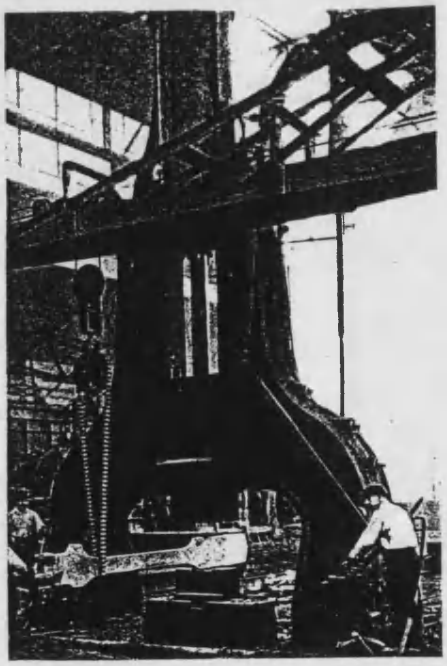

Figure 2-2: Nasmyth Hammer in operation.

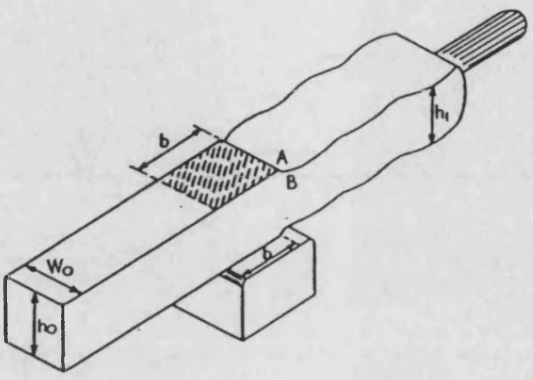

Figure 2-3: The billet for elementary cogging steps[84].

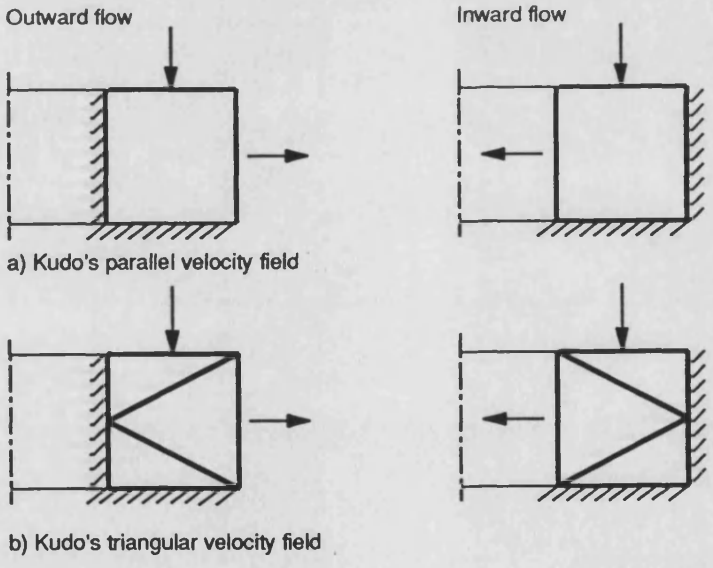

Figure 2-4: Kudo's velocity field[42].

Chapter 3

THE UPPER BOUND METHOD

3.1 Introduction

In metal forming it is of interest to predict a force that will certainly cause a body to deform plastically to produce the desired shape change. An upper bound analysis which predicts a load that is at least equal to or greater than the exact load needed to cause plastic flow satisfies that requirement. The upper bound theorem formulation was introduced by Prager and Hodge [72]. The method provides a means by which prediction of an over estimation of forging loads can be established using plasticity theory. Many investigators have used this approach with different geometrical representations of the deforming volume. If it was necessary to explain the upper bound method physically perhaps the best way to describe it is to assume that a body is deformed by equating internal rate of dissipation of energy to the rate at which external forces do work to cause a

postulated mechanism of deformation inside the body. The main requirement of this method is to build up a kinematically admissible velocity field which satisfies the incompressibility, continuity and velocity boundary conditions. Among the kinematically admissible velocity fields the best solution minimises the rate of energy dissipation. The estimation of the required external forces will be either high or correct thus being oriented to applications in practice. Since velocity fields are better suited to describe the flow than stress fields, the method has become attractive in metal forming where the stress fields are generally complex. Many researchers have adopted and expanded the use of the upper bound method to metal forming.

3.2 The Formulation of Upper Bound Method

The basis of the theory is relatively simple and easy to understand and also to compute. In applying the upper bound method the following assumptions are made:

- a) The material is isotropic and incompressible,
- b) The elastic deformation and inertia forces are negligible,
- c) The plastically deforming material obeys Levy-Mises flow rule and von Mises yield criterion and is perfectly plastic(no strain hardening)
- d) The flow stress of the material assumed is constant.

The total power is considered as the sum of the power dissipated to cause the deformation, internal shearing and to overcome the frictional resistance between the workpiece and the tools.

3.2.1 Deformation Power

The deformation power is the power required to deform the material plastically. The friction in the tool/material interface is ignored and the material is assumed to be free from internal discontinuities. The rate of the work per unit volume for von Mises material is given by;

$$\dot{w} = \sigma_{ij}\, \dot{\epsilon}_{ij} \tag{3.7}$$

expansion of 3.7 leads to,

$$\dot{w} = \sigma_{11}\, \dot{\epsilon}_{11} + \sigma_{22}\, \dot{\epsilon}_{22} + \sigma_{33}\, \dot{\epsilon}_{33} + 2\,(\sigma_{12}\, \dot{\epsilon}_{12} + \sigma_{23}\, \dot{\epsilon}_{23} + \sigma_{31}\, \dot{\epsilon}_{31}) \tag{3.8}$$

The stress tensor can be separated into stress deviator and hydrostatic stress as follows;

$$\dot{w} = (S_{11} + S)\, \dot{\epsilon}_{11} + (S_{22} + S)\, \dot{\epsilon}_{22} + (S_{33} + S)\, \dot{\epsilon}_{33} + 2\,(S_{12}\, \dot{\epsilon}_{12} + S_{23}\, \dot{\epsilon}_{23} + S_{31}\, \dot{\epsilon}_{31}) \tag{3.9}$$

and because of incompressibility; $\dot{\epsilon}_{ii} = 0$ and it follows that

$$\dot{w} = S_{11}\, \dot{\epsilon}_{11} + S_{22}\, \dot{\epsilon}_{22} + S_{33}\, \dot{\epsilon}_{33} + 2\,(S_{12}\, \dot{\epsilon}_{12} + S_{23}\, \dot{\epsilon}_{23} + S_{31}\, \dot{\epsilon}_{31}) \tag{3.10}$$

by simplifying eq. 3.10,

$$\dot{w} = S_{ij}\, \dot{\epsilon}_{ij} \tag{3.11}$$

and substituting $\dot{\epsilon}_{ij}$, from von Mises' stress- strain law,

$$\dot{\epsilon}_{ij} = \frac{\sqrt{\frac{1}{2}\dot{\epsilon}_{ij}\ \dot{\epsilon}_{ij}}}{k}\ S_{ij} \tag{3.12}$$

it follows that,

$$\dot{w} = \frac{\sqrt{\frac{1}{2}\ \dot{\epsilon}_{ij}\ \dot{\epsilon}_{ij}}}{k}\ S_{ij}\ S_{ij} \tag{3.13}$$

von Mises yield condition in terms of hydrostatic stress is,

$$k^2 = \frac{1}{2} S_{ij}\ S_{ij} \tag{3.14}$$

$$ie \qquad {S_{ij}}^2 = 2\ k^2 \tag{3.15}$$

substituting this into 3.13 the following is obtained:

$$\dot{w} = 2\ k \sqrt{\frac{1}{2}\dot{\epsilon}_{ij}\ \dot{\epsilon}_{ij}}$$

and substituting k where,

$$k = \frac{\sigma_0}{\sqrt{3}} \tag{3.16}$$

$$\dot{w} = \frac{2}{\sqrt{3}}\ \sigma_0 \sqrt{\frac{1}{2}\ \dot{\epsilon}_{ij}\ \dot{\epsilon}_{ij}} \tag{3.17}$$

The expression for total power of deformation is then obtained by integration of Eqn.3.17, over the deforming volume ,

$$\dot{W}_d = \int_V \dot{w}\, dV \tag{3.17}$$

$$\dot{W}_d = \int_V \dot{w}\, dV = 2\, k \int_V \sqrt{\frac{1}{2}\, \dot{\epsilon}_{ij}\, \dot{\epsilon}_{ij}} dV \tag{3.18}$$

and the final formula for deformation power, which is linearly proportional to the flow stress of the material, becomes as follows:

$$\dot{W}_d = \frac{2}{\sqrt{3}}\, \sigma_0 \int_V \sqrt{\frac{1}{2}\, \dot{\epsilon}_{ij}\, \dot{\epsilon}_{ij}\, dV} \tag{3.19}$$

The work per unit volume is obtained by integrating the power with respect to time as follows:

$$\dot{W}_d = \int_t \dot{w}\, dt \tag{3.20}$$

substituting $\dot{w}$ into 3.20;

$$\dot{W}_d = \frac{2}{\sqrt{3}}\, \sigma_0 \int_t \sqrt{\frac{1}{2}\, \dot{\epsilon}_{ij}^2}\, dt \tag{3.21}$$

3.2.2 The Shear Power

Considering Fig 3.1 along the surface I, the divided discontinuity leads to a shear within the deformed material. Material flows from zone I to zone II. Along these surfaces the discontinuity leads to a shear within the deformed material. Accordingly a shear losses does exist along the surface.

The volume crossing the surface remains constant before and after the crossing. Therefore the velocity component normal to the surface in both sides v_{1N} and

v_{2N} respectively are equal. There will be a velocity discontinuity on the direction parallel to the surface, v_1 in zone I and v_2 in zone II. The power dissipated along the velocity discontinuity can be expressed as follows

$$\Delta v = v_1 - v_2 \tag{3.22}$$

From von Mises's yield criteria the maximum resistance of the material to shear is found to be,

$$\tau = \frac{\sigma_0}{\sqrt{3}} \tag{3.23}$$

The shear power is then found by an integration of the shear losses over the surface, thus

$$\dot{W}_s = \frac{\sigma_0}{\sqrt{3}} \int_s |\Delta v| \, dS \tag{3.24}$$

3.2.3 The Friction Power

In plastic deformation processes friction occurs between tool and material. The friction resistance has a considerable effect on the forging load and the metal flow. Lubricants are often used to reduce frictional forces and improve material flow. The friction losses can be expressed as a function of the material shear stress in a similar manner as for the internal shear.

$$\tau = m \frac{\sigma_0}{\sqrt{3}} \tag{3.25}$$

m is the friction factor which acts on the tool/workpiece interface and varies from

zero to unity when sticking friction occurs. The friction power dissipated in the tool/workpiece interface contact is given by;

$$\dot{W}_f = \frac{m}{\sqrt{3}} \int_A \sigma_0 \Delta v \, dA \tag{3.26}$$

where Δv is the velocity discontinuity in a direction parallel to the tool/workpiece interface.

3.2.4 External tractions

This term represents the power associated with external tractions where $\dot{v}_i$ is the tool velocity on the surface S_i on which the external stress, T_i is the normal component of traction. The body traction associated with T_i is in the same direction with v_i and this external force aids the process thus to decrease the actual power needed to deform the material.

$$\dot{W}_t = \int_{S_i} T_i \, v_i \, dS \tag{3.27}$$

3.2.5 The total energy dissipation

From equation 3.19, 3.24, 3.26 and 3.27 the total power;

$$J^* = \dot{W}_d + \dot{W}_s + \dot{W}_f - \dot{W}_t \tag{3.28}$$

$$J^* = \frac{2}{\sqrt{3}} \sigma_0 \int_V \sqrt{\frac{1}{2}(\dot{\epsilon}_{ij} \, \dot{\epsilon}_{ij})} dV + \int_S \tau \, \Delta v \, dS$$

$$+ \frac{m}{\sqrt{3}} \int_A \sigma_0 \, \Delta v \, dA - \int_{S_i} T_i \, v_i \, dS \tag{3.29}$$

The first term of the equation 3.29 represents the rate of plastic deformation power dissipation of the material in metalforming problems, where;

$$\dot{\epsilon}_x = \frac{\partial \dot{u}_x}{\partial x} \tag{3.30}$$

$$\dot{\epsilon}_y = \frac{\partial \dot{u}_y}{\partial y} \tag{3.31}$$

$$\dot{\epsilon}_z = \frac{\partial \dot{u}_z}{\partial z} \tag{3.32}$$

The total energy exerted by the external tools can be represented as,

$$J^* = p_{ave} \, . A \, . \dot{v}_p \tag{3.32}$$

p_{ave} is the mean pressure acting on the tool, A is the contact area between the tool and workpiece at a given stage of compression, $\dot{v}_p$ is the velocity of the moving die. The total power is then calculated and the minimum rate of energy dissipation is obtained by using a minimisation procedure.

Avitzur [7] used the method to take into account the bulging effect in analysing the cylindirical forging problem. The velocity field was an exponential function to present the bulging effect but could not fully satisfy the physical boundary conditions. Another attempt by the same author [8] was made for plain strain condition of rectangular strips.

In most forging operations, shape complexity and bulging at the free surfaces make an exact analysis of metal forming operations impossible . Therefore some approximations are necessary in order to facilitate the formulation and obtain an approximate estimation of the forging load and the amount of bulge. One of the most important advantages of this method is that analytical solutions can be evaluated quickly with lower computing requirements if it is compared with Finite Element Method(FEM) . The Upper Bound approach therefore has become a valuable method in the analysis of more complicated problems.

Using Upper bound method, McDermott and Bramley [65] showed that Kudo's method can be applied to more general and complex forging problems. They also introduced curved boundary elements as shown in Fig 3.2a and an axi-symmetric forging shape is shown in Fig 3.2b which is divided into eight regions. For each of these eight regions shown a general admissible velocity field was considered and equations were established to determine the contribution of each element to the forging load. Also a series of experiments were carried out to verify the theoretical prediction and reasonable agreement with the theoretical results was noted. This technique is so called the Upper Bound Elemental Technique (UBET). The method at that time still did not accommodate flow on all boundaries of the elements.

There appears to be no limit to the complexity of forging shapes that can be analysed by this method, not only for load prediction but also for optimum flash geometry determination. The UBET was further developed for plane strain and axial symmetry where three general elements with flow on all boundaries; one

rectangular and two triangles were introduced as shown in Fig 3.3.

Cramphorn and Bramley [17] then produced a computer package which could divide the shape automatically into rectangular and triangular elements. The energy dissipation was optimised with respect to the unknown velocity component across the velocity discontinuity between elements, improved agreement with experimental results was achieved.

A generalised computer simulation technique for the prediction of load and metal flow in forging and extrusion was developed by Osman and Bramley [69]. This was a further development of the Upper Bound Elemental Technique which provided metal flow simulation for the process from start to finish in an incremental manner. In order to obtain the best velocity field which gives the lowest upper bound load and describes the metal flow, some considerations of the physical nature of the process were considered. The metal flow prediction was in agreement with the criterion that the material tends to flow in the direction which requires minimum power. Furthermore it was shown that the theoretical prediction of both load and gross metal flow that was based on the optimised velocity field was in very good agreement with the experimental results.

Lugora and Bramley [60] introduced a theoretical model based on the same technique for prediction of forging load and metal flow in three dimensional closed-die forging processes. In their work, three spatial figures, rectangular parallelepiped and pentahedron with rectangular base, were considered. Experiments were carried out to evaluate the validity of the load prediction using UBET. From this work a reasonable correlation was found between theoretical load prediction and

experiments. It was also pointed out that this theoretical model itself requires some improvements in regard to computational efficiency.

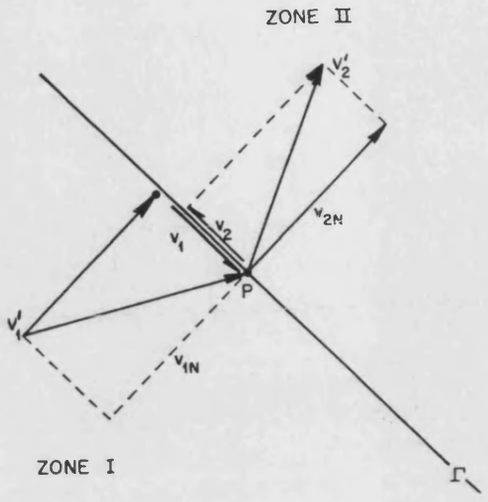

Figure 3-1: Surfaces of velocity discontinuity.

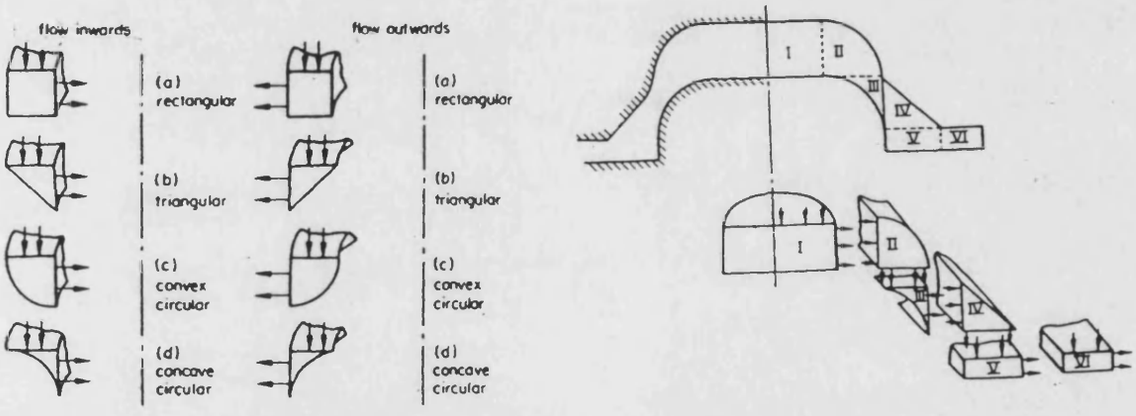

a) b)

Figure 3-2: a) General eight basic elements b) Hypothetical forging[65].

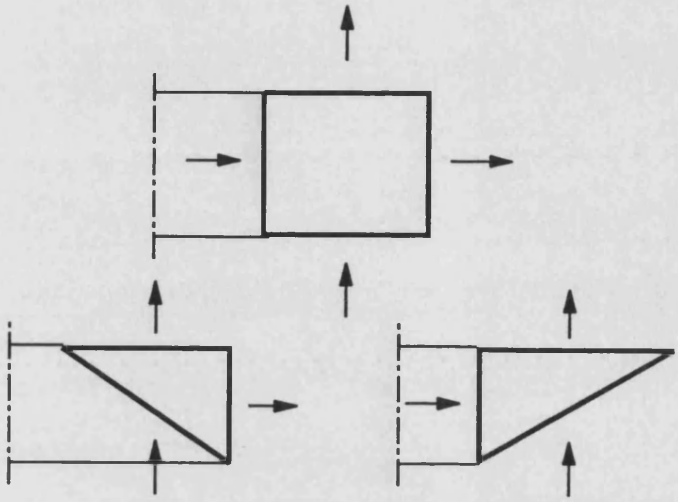

Figure 3-3: Generalised elements[65].

Chapter 4

METAL FLOW ANALYSIS FOR OPEN DIE FORGING

4.1 Introduction

The benefits of material utilizitation and energy saving in metal forming processes depend upon detailed, accurate and rapid theoretical analysis. The deformation pattern in open-die forging operations need to be investigated theoretically for each individual single step in order to construct a methodology for automation. The prediction of metal flow in the forging process has substantial importance in terms of developing a production sequence to achieve a final required shape. As it was described in chapter two, there are a number of methods to analyse the mechanism of deformation pattern in open die forging. These methods have some advantages and disadvantages when compared with each other. However among the various methods of solutions, the upper bound method appears to be used in metal forming more widely because of its simplicity as well as accuracy and

modest use of computational time. The programming of open die forging process can be accomplished with a press and manipulator but this requires accurate and rapid theoretical analysis.

This chapter presents a number of approaches which have been developed and they are based on the upper bound method for predicting forging load and the flow pattern produced in a single bite - incrementation - rotation operations. Friction and the lateral sideways bulging are taken into account in these analysis. In the theoretical analysis the deformation steps were simulated in three dimensions through three different upper bound solutions in which different velocity fields were constructed to describe the metal flow and hence to optimise the solution.

The configuration considered is that of a rectangular cross section billet being squeezed partially between two flat dies. When the element is compressed flow occurs in both longitudinal and lateral directions. Three different flow patterns have been proposed and evaluated; a simple homogeneous deformation pattern, SODIREC a nonhomogeneous triangular flow pattern, SODITRI and one incorporating a parabolic function in the lateral direction, SODIPAR. The analysis for all these solutions in both one step compression with fixed penetration and tool widths are investigated and then extended into incremental compression with various penetration levels, tool widths and friction levels. A combination of those solutions is shown schematically in Fig 4.1

For the first solution material flow was described by a kinematically admissible velocity field with a homogeneous and parallel deformation pattern ie spread does not vary in the longitudinal direction. Secondly the material flow was assumed to

take a nonhomogeneous triangular shape in the lateral direction with respect to the distance from the centre of the element. The third solution was developed by assuming the spread in the sideways lateral direction is going to be described by a parabolic function. Initially, the analysis for all these solutions was restricted to one step of the compression process with fixed penetration and tool width. Subsequently the analysis was developed for incremental compression with various penetration levels, tool widths and friction levels. Finally the workpiece was continuously compressed and rotated through 90^o to reduce the cross section gradually. The developed theoretical algorithms enable the prediction of the load and displacement of material at each step from under the dies in the axial direction.

4.2 Homogeneous Pattern of Deformation

One of the analyses presented for the investigation of deformation patterns in open die forging has been performed assuming a homogeneous parallel flow of the material. The main factors affecting deformation characteristics are friction, flow stress of the material, penetration and the tool geometry. These factors interact in a complicated manner and are themselves affected by the working conditions. The actual spread shape in this type of forming operation is normally a parabola which is affected and varied by forming conditions, friction and tool width. The main interest in this approach is to predict the flow ratio in the axial and longitudinal directions. When a quadrapiped billet is compressed partially between two flat dies, the amount of material volume squeezed to reduce the height will be flowing into the axial and lateral directions. The idea here is

simply to represent the material flow by a parallel velocity field in which the spread cross section remains rectangular. For predicting forging load and metal flow in both lateral and axial directions, a kinematically admissible velocity field distribution which describe the shape of bulging theoretically was constructed. Fig 4.2 shows the idealised and actual spread shapes which can be found in a locally forged long bar.

4.2.1 Velocity field

Fig 4.3 shows the rectangular pattern of deformation of a long bar of width w_0, thickness h_0 and length of deforming zone l_0 which is in contact with the die width. Considering one quarter of the billet, the velocity in the z direction is linear and increases from 0 at the centre of the element to the platen velocity $\dot{v}_p$ while the bottom die is stationary. Hence the velocity in the z direction is assumed linear, ie;

$$\dot{u}_z = -\frac{2\,\dot{v}_p}{h_0}\,z \tag{4.1}$$

where $\dot{v}_p$ is the die velocity and assuming that $\dot{\epsilon}_x$ is linearly proportional to $\dot{\epsilon}_z$

$$\alpha = \frac{\dot{\epsilon}_x}{\dot{\epsilon}_z} \tag{4.2}$$

or;

$$\dot{\epsilon}_x = -\alpha\,\dot{\epsilon}_z \tag{4.3}$$

α is the ratio between longitudinal and vertical strain rates,

$$\dot{\epsilon}_z = -\frac{2\dot{v}_p}{h_0} \tag{4.4}$$

substituting 4.4 into 4.3

$$\dot{\epsilon}_x = \frac{2\dot{v}_p}{h_0}\alpha$$

and also, $\dot{\epsilon}_y$ can be defined using the volume constancy equation

$$\dot{\epsilon}_y = -(\dot{\epsilon}_z + \dot{\epsilon}_x) = -\dot{\epsilon}_z\,(1 - \alpha) \tag{4.5}$$

and then,

$$\dot{\epsilon}_y = \frac{2\dot{v}_p}{h_0}\,(1 - \alpha) \tag{4.6}$$

For a linear velocity field the strain rate distribution is homogeneous and remains constant through out the deforming volume. Also, the flow in all directions must satisfy the preservation of volume which is given as:

$$\dot{\epsilon}_x + \dot{\epsilon}_y + \dot{\epsilon}_z = 0 \tag{4.7}$$

The velocity field is then determined as:

$$\dot{u}_x = \frac{2\dot{v}_p}{h_0}\,x$$

$$\dot{u}_y = \frac{2\dot{v}_p}{h_0}\,(1 - \alpha)\,y$$

$$\dot{u}_z = -\frac{2\dot{v}_p}{h_0} z$$

4.2.2 Deformation Power

The internal power of deformation $\dot{W}_d$ is calculated from the derived strain rate field.

$$\dot{W}_d = \frac{2}{\sqrt{3}} \sigma_0 \int_V \sqrt{\frac{1}{2} (\dot{\epsilon}_x^2 + \dot{\epsilon}_y^2 + \dot{\epsilon}_z^2)} \, dV \tag{4.8}$$

Substituting the strain rate components in Eqn(4.8),

$$\dot{W}_d = \frac{2}{\sqrt{3}} \sigma_0 \int_x \int_y \int_z \left[\frac{1}{2}\left[\frac{4\dot{v_p}^2}{h_0^2} \alpha^2 + \frac{4\dot{v}_p^2}{h_0^2} (1-\alpha)^2 + \frac{4\dot{v_p}^2}{h_0^2}\right]\right]^{\frac{1}{2}} dx \, dy \, dz \tag{4.9}$$

$$\dot{W}_d = \frac{w_0 \, l_0}{2\sqrt{3}} \dot{v}_p \sigma_0\} \int_x \int_y \left[\frac{1}{2}\left(\alpha^2 + (1-\alpha)^2 + 1\right)\right]^{1/2} dx \, dy \tag{4.10}$$

by solving Eqn 4.10

$$\dot{W}_d = \frac{w_0 \, l_0}{2\sqrt{3}} \dot{v}_p \, \sigma_0 \left[(\alpha^2 - \alpha + 1)\right]^{\frac{1}{2}} \tag{4.11}$$

4.2.3 Friction Power

As it was shown before the friction power is:

$$\dot{W}_f = \frac{\sigma_0}{\sqrt{3}} m \int_A |\Delta \dot{V}| dA \tag{4.12}$$

$$\Delta \dot{V} = \sqrt{\dot{u}_x^2 + \dot{u}_y^2} \tag{4.13}$$

$$\dot{u}_x^2 = \frac{4\dot{v}_p^{\,2}}{h^2} \alpha^2 x^2 \tag{4.14}$$

$$\dot{u_y}^2 = \frac{4\dot{v}_p^{\,2}}{h^2} (1 - 2\alpha + \alpha^2) y^2 \tag{4.15}$$

therefore:

$$\Delta \dot{V} = \frac{2\dot{v}_p}{h_0} \left[\alpha^2 x^2 + (\alpha^2 - 2\alpha + 1) y^2\right]^{1/2} \tag{4.16}$$

Substituting 4.16 into 4.12 the friction power formula becomes;

$$\dot{W}_f = \frac{2}{\sqrt{3}} \frac{\dot{v}_p}{h_0} \sigma_0 m \int_x \int_y [\alpha^2 x^2 + (\alpha^2 - 2\alpha + 1) y^2]^{1/2} dx\, dy \tag{4.17}$$

4.2.4 Optimisation of Total Power

The total internal power is given by the sum of the deformation and friction power. The average pressure is therefore determined by equating the external power to internal power. The total deformation power $\dot{W}$ is;

$$\dot{W} = \dot{W}_d + \dot{W}_f \tag{4.18}$$

and substituting 4.11 and 4.17 into 4.18 and since the external power being supplied by the platens is the force times the platen velocity, the applied power

is:

$$\dot{W} = p_{ave} \frac{w_0 \, l_0}{4} \dot{v}_p \tag{4.19}$$

By equating the power supplied to the power required to deform the bar, the final expression can be derived for the relative average pressure of p_{ave}/σ_0 and from eqn. 4.18 and 4.19 the final total energy dissipation formula becomes;

$$\frac{p_{ave}}{\sigma_0} = \frac{2}{\sqrt{3}} \left[\alpha^2 - \alpha + 1\right]^{\frac{1}{2}} + \frac{8}{\sqrt{3}} \frac{m}{h_0 \, w_0 \, l_0} \int_x \int_y [\alpha^2 \, x^2$$

$$+ (\alpha^2 - 2\alpha + 1) \, y^2]^{1/2} dx \, dy \tag{4.20}$$

This final energy formula can be optimised with respect to the independent parameter α using NAG minimisation routine E04CCF and D01DAF for solving the double integral numerically. For homogeneous deformation the optimum value of minimisation parameter $\alpha = 0.5$ for all values of w_0 ,b and h_0 for frictionless condition $(m = 0.0)$

4.3 Triangular Pattern of Deformation

The second approach provides an improved definition of the lateral spread in that it allows for uneven but linear variation in the magnitude of spread along the region being deformed.

Fig 4.4 illustrates the actual and approximated bulge shapes schematically and Fig 4.5 the velocity field which represents the proposed pattern of deformation on a rectangular bar element of width of $w_0/2$, thickness h_0 and length of deformation

zone l_0 which contacts with the die width. As it can be seen from the figures the material flow sideway or in the y direction is a function of the deforming length of the bar.

4.3.1 Velocity field

The metal flow in the direction of lateral spread is assumed to conform to a triangular velocity field distribution at each compression step. Fig 4.4 shows the velocity distribution on a quarter of billet. The total power is minimised with respect to a pseudo independent parameter that is the maximum flow rate $\dot{u}_{y_{max}}$ in the direction of lateral spread.

Assuming that the dies approach the billet at a unit speed $\dot{v}_p$ and that the velocity in the z direction will vary linearly through the deforming zone, the following equations can be written:

$$\dot{u}_z = -\frac{2\dot{v}_p}{h_0} z \tag{4.21}$$

$$\dot{\epsilon}_z = \frac{\partial \dot{u}_z}{\partial z} = -\frac{2\dot{v}_p}{h_0} \tag{4.22}$$

Considering a triangular velocity field distribution the spread velocity $\dot{u}_{y_{max}}$ in the direction of lateral spread can be written as:

$$\dot{u}_y = \frac{4\dot{v}_p}{w_0\, l_0}\, \dot{u}_{y_{max}} \left(\frac{l_0}{2} - x\right) y \tag{4.23}$$

This velocity distribution satisfies the boundary conditions, that is,

$$\left.\begin{array}{rl} & x = 0 \\ at & \\ & y = 0 \end{array}\right\} \qquad \dot{u}_y = 0$$

$$\left.\begin{array}{rl} & x = 0 \\ at & \\ & y = \frac{w_0}{2} \end{array}\right\} \qquad \dot{u}_y = \dot{u}_{y_{max}} \tag{4.24}$$

$$\left.\begin{array}{rl} & x = \frac{w_0}{2} \\ at & \\ & y = \frac{l_0}{2} \end{array}\right\} \qquad \dot{u}_y = 0$$

the strain rate $\dot{\epsilon}_y$ becomes,

$$\dot{\epsilon}_y = \frac{4\dot{v}_p}{w_0\, l_0}\, \dot{u}_{y_{max}} \left(\frac{l_0}{2} - x\right) \tag{4.25}$$

if the volume constancy equation is introduced;

$$\dot{\epsilon}_x + \dot{\epsilon}_y + \dot{\epsilon}_z = 0 \tag{4.26}$$

then,

$$\dot{\epsilon}_x = 2\dot{v}_p\left[\frac{1}{h_0} - \frac{2}{w_0\, l_0}\, \dot{u}_{y_{max}} \left(\frac{l_0}{2} - x\right)\right] \tag{4.27}$$

and the longitudinal velocity distribution $\dot{u}_x$ becomes,

$$\dot{u}_x = \dot{v}_p \left[\frac{2}{h_0} - \frac{4\dot{u}_{y_{max}}}{w_0\, l_0} \left(\frac{l_0}{2} - \frac{x}{2}\right)\right] \tag{4.28}$$

$$\dot{\epsilon}_{xy} = \frac{1}{2}\left[\frac{\partial \dot{u}_x}{\partial y} + \frac{\partial \dot{u}_y}{\partial_x}\right] \tag{4.29}$$

$$\dot{\epsilon}_{xy} = -2\dot{v}_p \left(\frac{\dot{u}_{y_{max}}}{w_0\, l_0}\right) y \tag{4.30}$$

The other strain rate components, $\dot{\epsilon}_{yx}$ and $\dot{\epsilon}_{yz}$,are zero.

4.3.2 Deformation power

For this strain rate field the deformation power is written as follows:

$$\dot{W}_d = \frac{2}{\sqrt{3}}\sigma_0 \int_V \left[\frac{1}{2}(\dot{\epsilon}_x^2 + \dot{\epsilon}_y^2 + \dot{\epsilon}_z^2) + \dot{\epsilon}_{xy}^2\right]^{1/2} \tag{4.31}$$

where $\dot{W}_d$ is the deformation power. Substituting strain rates from 3.22 , 3.25, 3.26 gives:

$$\dot{W}_d = \frac{2\dot{v}_p}{\sqrt{3}}\sigma_0 \int_x \int_y \int_z [\frac{1}{2}[\frac{2}{h_0} - f(x)^2 + f(x) + \frac{2}{h_0}^2] + f(y)^2]^{1/2} dx \tag{4.32}$$

where;

$$f(x) = \frac{4\dot{v}_p\, \dot{u}_{y_{max}}}{w_0 l_0}\left(\frac{l_0}{2} - x\right) \tag{4.33}$$

$$f(y) = \frac{2\dot{v}_p\, \dot{u}_{y_{max}}}{w_0 l_0}\, y \tag{4.34}$$

$$\dot{W}_d = \frac{h_0}{\sqrt{3}}\, \dot{v}_p \int_{x=0}^{l_0/2} \int_{y=0}^{w_0/2} \left[\frac{1}{2}\left[\left(\frac{2}{h_0} - f(x)\right)^2 + f(x)^2 + \frac{4}{h_0^2}\right] f(y)^2\right]^{1/2} dx\, dy \tag{4.35}$$

4.3.3 Friction Power

The friction occurs between tool and contact area A which is given by,

$$\dot{W}_f = \sigma_0 \frac{1}{\sqrt{3}} m \int_A |\Delta \dot{V}| \, dA \tag{4.36}$$

The velocities along the velocity discontinuity is ;

$$\Delta \dot{V} = \sqrt{\dot{u}_x^2 + \dot{u}_y^2} \tag{4.37}$$

Substituting the velocity components in the x and y directions into Eqn 4.37 $\Delta \dot{V}$ becomes,

$$\Delta \dot{V} = \dot{v}_p \left[\left[\frac{2}{h_0} - (\frac{l_0}{2} - \frac{x}{2}) \frac{4 \, \dot{u}_{y_{max}}}{w_0 \, l_0} \right]^2 x^2 + [f(x) \, y \,]^2 \right]^{1/2} \tag{4.38}$$

and substituting 4.38 into 4.36 the friction power is found by;

$$\dot{W}_f = \frac{\sigma_0}{\sqrt{3}} \dot{v}_p m \int_{x=0}^{l_0/2} \int_{y=0}^{w_0/2} \left[[\frac{2}{h_0} x - f(x)']^2 + [f(x) \, y]^2 \right]^{1/2} dx \, dy \tag{4.39}$$

where;

$$f(x)' = [\frac{l_0}{2} - \frac{x}{2}] \frac{4 \dot{u}_{y_{max}}}{w_0 \, l_0}$$

4.3.4 Optimization of Total Power

The total power is expressed as follows;

$$\dot{W} = \dot{W}_d + \dot{W}_f \tag{4.40}$$

and substituting 4.34 and 4.39 into Eqn 4.40 and then equating to Eqn. 4.19, the nondimensional pressure is found:

$$\frac{p_{ave}}{\sigma_0} = \frac{4}{\sqrt{3}}\frac{h_0}{w_0\, l_0}\int_{x=0}^{l_0/2}\int_{y=0}^{w_0/2}[\frac{1}{2}\,[[\frac{2}{h_0} - f(x)]^2 + f(x)^2\, y^2 + \frac{4}{{h_0}^2}] +$$

$$f(y)^2]^{1/2}dx\, dy + \frac{4\, m}{\sqrt{3}}\int_{x=0}^{l_0/2}\int_{y=0}^{w_0/2}[[\frac{2}{h_0}\, x - f(x)'\}]^2\, f(x)^2\, y^2]^{1/2}dx\, dy \tag{4.41}$$

The optimum value of $\dot{u}_{y_{max}}$ is obtained when;

$$\frac{\delta\dot{W}}{\delta\dot{u}_{y_{max}}} = 0 \tag{4.42}$$

is optimized numerically using the same minimisation and numerical integral routines mentioned before.

4.4 Parabolic Pattern of Deformation

The third upper bound solution to the material flow analysis in open die forging approaches the most probable bulging shape by describing a parabolic curve. In the analysis the free boundaries are assummed to be of parabolic form. The spread and elongation were predicted after each compression step using a kinematically admissible velocity field optimised to yield the minimum power require-

ments.

4.4.1 Velocity field

Fig 4.6 shows a partially compressed long bar showing the primary and secondary bulges in the deforming zone and Fig 4.7 shows a quarter of parabolic velocity field used to describe the sideway bulging. Secondary bulging is ignored and the metal flow in the lateral direction, y, is assumed parabolic reaching a maximum value of $\dot{u}_{y_{max}}$ at the centre and zero at the edge of tool ($x = \frac{l_0}{2}$). $\dot{u}_{y_{max}}$ will subsequently be used as a pseudo independent parameter determined by minimisation of the total power.

During the compression in the z-direction material will flow in the longitudinal(x) and lateral(y) directions. From the boundary conditions metal flow in the y direction can be expressed by:

$$ie. \qquad \dot{u}_y = (\frac{l_0}{2} - \frac{2\,x^2}{l_0})\,\dot{v}_p\,\frac{4\,\dot{u}_{y_{max}}}{w_0\,l_0} \tag{4.43}$$

The velocity in the z direction is assumed to be a linear function of z with a maximum value equal to the die velocity, $\dot{v}_p$ at $z = \frac{h_0}{2}$

$$ie. \qquad \dot{u}_z = -\frac{2\dot{v}_p}{h_0}\,z \tag{4.44}$$

where $\dot{u}_{y_{max}}$ is the maximum velocity representing the maximum metal flow in the sideway direction and $\dot{v}_p$ is the tool velocity which is assummed as unity.

$$at \quad \left.\begin{array}{l} x = 0 \\ y = 0 \end{array}\right\} \qquad \dot{u}_y = 0$$

$$\left.\begin{array}{rl} x &= 0 \\ y &= \frac{w_0}{2} \end{array}\right\} \quad \dot{u}_y = \dot{u}_{y_{max}} \qquad (4.45)$$

$$\left.\begin{array}{rl} x &= 0 \\ y &= \frac{l_0}{2} \end{array}\right\} \quad \dot{u}_y = 0$$

As it is seen the boundary conditions satisfy the velocity field. After compression the volume of the workpiece will have to remain the same. The volume constancy condition enables the strain rate in the x direction to be determined.

$$\dot{\epsilon}_x + \dot{\epsilon}_y + \dot{\epsilon}_z = 0 \qquad (4.46)$$

$$ie. \qquad \dot{\epsilon}_x = -(\dot{\epsilon}_y + \dot{\epsilon}_z) \qquad (4.47)$$

$$ie. \qquad \dot{\epsilon}_x = \dot{v}_p[\frac{2}{h_0} - (\frac{l_0}{2} - \frac{2\,x^2}{l_0})\frac{4\,\dot{u}_{y_{max}}}{w_0\,l_0}] \qquad (4.48)$$

By integrating Eqn. 4.48 the velocity in the x-direction is obtained as,

$$\dot{u}_x = \dot{v}_p[\frac{2}{h_0}\,x - (\frac{l_0}{2}\,x - \frac{2\,x^3}{3\,l_0})\,\frac{4\,\dot{u}_{y_{max}}}{w_0\,l_0}] \qquad (4.49)$$

The strain rates now become as follows;

$$\dot{\epsilon}_x = \frac{\partial \dot{u}_x}{\partial x} = \dot{v}_p[\frac{2}{h_0} - (\frac{l_0}{2} - \frac{2\,x^2}{l_0})\,\frac{4\,\dot{u}_{y_{max}}}{w_0\,l_0}] \qquad (4.50)$$

$$\dot{\epsilon}_y = \frac{\partial \dot{u}_y}{\partial y} = \dot{v}_p[(\frac{l_0}{2} - \frac{2\,x^2}{l_0})\,\frac{4\,\dot{u}_{y_{max}}}{w_0\,l_0}] \qquad (4.51)$$

$$\dot{\epsilon}_z = \frac{\partial \dot{u}_z}{\partial z} = -\frac{2\dot{v}_p}{h_0} \tag{4.52}$$

and,

By derivation of $4.29 \dot{\epsilon}_{xy}$ is worked out;

$$\dot{\epsilon}_{xy} = -\left[\frac{8\dot{v}_p}{w_0\, l_0^2}\, x\, y\, \dot{u}_{y_{max}}\right]^2 \tag{4.53}$$

Now deformation and shear power can be calculated through strain rates and velocity field.

4.4.2 Deformation power

In general form deformation power is given as follows:

$$\dot{W}_d = \frac{2}{\sqrt{3}}\, \sigma_0 \int_x \int_y \int_z \left[\frac{1}{2}(\dot{\epsilon}_x^2 + \dot{\epsilon}_y^2 + \dot{\epsilon}_z^2) + \dot{\epsilon}_{xy}^2\right]^{1/2} dx\, dy\, dz \tag{4.54}$$

where $\dot{W}_d$ is the deformation power. Substituting strain rate equations 4.50, 4.51, 4.52 and 4.53 into 4.54 the deformation power formula becomes as follows:

$$\dot{W}_d = \frac{\dot{v}_p\, h_0}{\sqrt{3}}\, \sigma_0 \int_{x=0}^{l_0/2} \int_{y=0}^{w_0/2} \left[\frac{1}{2}\,(f(x)^2 - f(x) + 2\, f(x,y)^2 + \frac{4}{{h_0}^2}\right]^{1/2} dx\, dy \tag{4.55}$$

where;

$$f(x) = \left[(\frac{l_0}{2} - \frac{2\, x^2}{l_0})\, \frac{4\dot{u}_{y_{max}}}{w_0\, l_0}\right] \tag{4.56}$$

$$f(x,y) = -\left[\frac{8}{w_0\, l_0^2}\, x\, y\, \dot{u}_{y_{max}}\right] \tag{4.59}$$

4.4.3 Friction Power

The friction occurs between tool and contact area A which is given by,

$$\dot{W}_f = \frac{\sigma_0}{\sqrt{3}}\, m \int_A \Delta\dot{V}\, dA \tag{4.60}$$

The velocities along the velocity discontinuity is ;

$$\Delta\dot{V} = \sqrt{\dot{u}_x^2 + \dot{u}_y^2} = [(\frac{2\dot{v}_p}{h_0}\, x - g(x))^2 + f(x)^2\, y^2]^{1/2} \tag{4.61}$$

Substituting 4.61 into 4.60 the friction power formula becomes;

$$\dot{W}_f = \frac{\dot{v}_p}{\sqrt{3}}\, \sigma_0\, m \int_{x=0}^{l_0/2} \int_{y=0}^{w_0/2} \left[(\frac{2\dot{v}_p}{h_0}\, x - g(x))^2 + f(x)^2\, y^2\right]^{1/2} dx\, dy \tag{4.62}$$

where $g(x)$,

$$g(x) = (\frac{l_0}{2}\, x - \frac{2\, x^3}{3\, l_0})\, \frac{4\dot{u}_{y_{max}}}{w_0\, l_0} \tag{4.63}$$

4.4.4 Optimization of Total Power

The total internal power is given by the sum of the deformation and friction power. The average pressure is therefore determined by equating the external to internal power. Since the external deformation power:

$$\dot{W}_d \;=\; p_{ave}\;\dot{v}_p\;(\frac{w_0\;l_0}{4}) \tag{4.64}$$

Thus the total power formula becomes;

$$\frac{p_{ave}}{\sigma_0} \;=\; \frac{4}{\sqrt{3}}\;\frac{h_0}{w_0\;l_0}\{\int_{x=0}^{l_0/2}\;\int_{y=0}^{w_0/2}\;[\frac{1}{2}\;[f(x)^2\;+\;f(x)\;+\;2\;f(x,y)^2\;+\;\frac{4}{h^2}]^{1/2}\;+$$

$$\frac{4}{\sqrt{3}}\;\frac{m}{w_0\;l_0}\{\int_{x=0}^{l_0/2}\;\int_{y=0}^{w_0/2}\;[(\frac{2\dot{v}_p}{h_0}\;x\;-g(x))^2\;+\;f(x)^2\;y^2]^{1/2}dx\;dy \tag{4.65}$$

The final total power Eqn. 4.65 is then optimised numerically to the $\dot{u}_{y_{max}}$ for which;

$$\frac{\delta\dot{W}}{\delta\dot{u}_{y_{max}}} \;=\; 0 \tag{4.66}$$

4.5 Computer Programs

Consider a long quadripiped billet of which only a part is subjected to compression. The purpose of the first part of the programming, a flow chart for which are given in Fig 4.8 and appropriate schematic illustration in Fig 4.10, is to calculate the load and dimensional changes which occurs incrementally after each compression step. This program optimises the total energy dissipation, comprising the deformation and friction power, and gives the optimum relative pressure p_{ave}/σ_0. If the flow stress σ_0 of the material is known the forging load requirement can

be found by substituting p_{ave} value and the contact area between workpiece and tool, load is found by following equation,;

$$Load = p_{ave} \ A \tag{4.72}$$

For a given penetration the program predicts the final maximum width of a partially compressed billet in an incremental manner. The dimensions of the workpiece after compression become the initial dimensions for the next compression stage of the process. As the relevant flow chart is shown in Fig 4.9 and the appropriate schedule in Fig 4.11 the second part of programming deals with again the prediction of load, dimensions and in addition enables the effect of various tool widths on metal flow in a long idealised bar to be determined. The program also predicts metal flow for various aspect ratios of the bar and friction factors m. To change the aspect ratio the height h_0 was fixed and the width w_0 of the billet is varied for each compression cycle.

The third part of the programming is not only to predict load and the metal flow for a given penetration in height at varying aspect ratios but also to analyse the workpiece when it is subjected to a multi-cycle of compression - rotation through 90^0 . Again here the program works for various friction factors for each cycle of compression-rotation process. The relevant sequential figure and flow chart can be seen in Fig 4.12 and 4.13. All these process variations were programmed individually using of the three Upper Bound solutions introduced earlier in this chapter.

4.6 Results and Discussion

In open die forging the accuracy of load and metal flow predictions will vary and depend upon the method and approximations used in the analysis. In this work, as described above, three different solutions were developed by looking at various aspects of the problem. In all solutions the method of analysis is based on the Upper Bound method and the analysis took place to investigate mainly the effect of aspect ratio, tool width, penetration and friction factor on metal flow. In that respect the minimum power with respect to the velocity field was calculated at each compression step or increment. Knowledge of the energy is important where energy restricted forming machines, such as hammers, screws, mechanical cranks and presses are used. The area under such a curve is the total energy consumed in the process.

The computer programs devised to predict metal flow can also be thought of as a load prediction program which incorporated a NAG optimisation routine. This also means that the load can be calculated at every step and the $load/deformation$ characteristics for the process determined. The results will be presented in three groups each accommodating a different solution in which the three dimensional solutions were presented.

The results were especially focussed on a comparison of the second and third solutions. It has also to be said here that the programs for all those solutions were taken to beyond the normal working range and extreme cases in order to show the reliability, continuity and consistency of the theoretical solutions.

Minimisation of total power took place for the SODIREC and SODITRI solutions using both a written subroutine and a *NAG* routine but for the SODIPAR only the *NAG* routine was used due to the relevant function requirement. It is shown that the methods provide minimum power and load for each compression step. In Fig 4.14 the nondimensional average power was plotted against the minimisation parameter α for different friction factors for the SODIREC. At $m = 0$ ie frictionless conditions the minimum total power occurs at unity and increases with increasing friction. The optimum value of α decreases with increasing friction factor. In Fig 4.15 the optimum values of average pressure are shown in variation with initial aspect ratios. In Fig 4.16 and 4.17 the same type of graphs are shown for the SODITRI, and in Fig 4.18 for the SODIPAR. In these figures solutions also show the minimum power and load requirements for different friction conditions. For both second and third solution the optimum values of p_{ave}/σ_0 increase simultaneously with increasing aspect ratio of the workpiece and after an aspect ratio of 4 remains constant but in the first solution the optimum p_{ave}/σ_0 is linear and continuous. This linearity is a result of the homogeneous velocity field which is assumed in the solution.

In Fig 4.19, 4.20 and 4.21 load predictions are plotted with varying aspect ratios and friction factors for these three solutions. From this figure the required load for forming the billet increases with increasing aspect ratio and friction factor. In the upper bound method the velocities are the main governing characteristics of metal flow. The magnitude of velocities determines the amount of metal flow in the x, y and z directions and Fig 4.22 shows the variation of the velocities in axial direction against different initial billet aspect ratios for both frictionless condition

and friction factor $m = 0.5$. Fig 4.23 shows the same relationship between the lateral velocity and the various aspect ratios of the billets. These figures show that the SODITRI gives higher values for the axial and lateral velocities than SODIPAR. While the friction increases velocity in axial direction also increases but the velocity in the lateral direction decreases. For both solution the material flow in axial direction increases with increasing initial aspect ratio. The flow in lateral direction increases with increasing aspect ratio of the workpiece up to a certain level thereafter remaining constant. If these results are compared it is seen that while the axial velocity begins to remain constant at its maximum value the lateral velocity increment passes through a maximum at a certain value of aspect ratio.

The trend of velocity in the lateral direction is a reflection of the characteristic of spread. In Fig 4.24 and 4.25 for the SODITRI, the average maximum spread values were plotted with the variation of initial aspect ratio, IAR, for frictionless and for $m = 0.5$. In Fig 4.26 the physical shapes/profiles of spread in the lateral direction was plotted against the distance from the centre line and given for all three solutions for two different IAR values of 0.5 and 1.0. The figures were produced for the tool width of $b = 40mm$ and friction factors of $m = 0.0$ and $m = 0.5$ respectively. Owing to the symmetry the figures show only a quarter of the spread in one lateral side. For each IAR value a half of the spread in one free side of the billet was calculated for various penetration levels for both frictionless conditions and $m = 0.5$. If these figures are compared with each other in terms of shape characteristics, which was determined by an approximated function, the amount of spread increases with increasing aspect ratio and penetration. Higher

friction increases spread for all IAR values. Fig 4.27 and 4.28 show the average maximum spread values plotted for the SODIPAR. The average of maximum spread values in the second solution is higher than the third solution because in the second solution the flow was assumed as a triangular shape and in the third solution as a parabola. These cases are clearly seen from the Fig 4.26.

Most interesting is that spread tends to drop considerably beyond a certain aspect ratio with a maximum occurring at an aspect ratio of 3. However, the magnitude of spread is not only dependent upon the IAR, penetration and friction but also on tool width. Fig 4.29 and 4.30 for the SODITRI and Fig 4.31 and Fig 4.32 for the SODIPAR show the varation of spread with IAR and friction for different tool widths at a fixed 25% penetration. It is shown that spread increases with increasing tool width and reaches its maximum value then decreases. This maximum point varies with increasing tool width and IAR and friction value. The friction effect becomes especially obvious at higher IAR and tool widths. From these results it can be seen that although the number of cycles will be higher when using small tool widths, at small IAR values the effect of friction on metal flow in the lateral direction reduces. It is also noticed from the figures that increasing tool width and friction make the maximum spread point increase to higher IAR values.

Although Kennedy's [44] work was dealing with spread in the rolling process a comparison can be made in order to show the spread zones and the effect of height reduction and friction. A comparison of lateral spread values has been made and given in Fig 4.33 for the range of $m = 0.5$ to 1.0 and $w_0/h_0 = 1.0$. This shows the

spread increases with increasing height reduction and friction factor. The friction has a different effect in the rolling process compared with flat bar forging.

In Fig 4.34 a comparison of spread against bite ratio is made with the work reported in the references of [83, 16, 14]. Because of difficulties in converting their results, given in percentage spread form, the spread values for the SODIPAR were converted into the form of spread factors. The figure shows that the trend is similar but the spread-factor- values in the current work with SODIPAR were found to be higher. This is probably because they used empirical formulae and the Upper Bound method used in this work provides an overestimate. However the spread values given in [14] are very small when compared to the current and some other work [16, 83]. This is may be a result of measurement problems and of ignoring bulging in the sideways direction.

Prediction of final dimensions is important particularly in incremental forging and the three solutions presented in this work enable this to be done in a way which can be used to describe the metal flow in an incremental sequence. For that purpose Fig 4.35 and 4.36 for the SODITRI and Figs 4.37 and 4.38 for the SODIPAR shows the initial aspect ratio(IAR) of the billet before compression plotted against predicted final aspect ratio after compression. The results are given at different penetration levels for frictionless and $m = 0.5$ respectively. From these figures it was shown that final aspect ratio increases linearly with increasing initial aspect ratio of the deformed billet and with the penetration. The second solution presents a slightly higher values of final aspect ratio than third solution because in this solution the approximated spread values from the

triangular field solution are higher than these obtained using the parabolic field. However, friction has no major effect under these conditions. In addition the effect of tool width on final aspect ratio were plotted in Fig 4.39 and 4.40 for the SODITRI and in Fig 4.41 and 4.42 for the SODIPAR at frictionless conditions and at a friction factor of $m = 0.5$ respectively. It was shown that the final aspect ratio increases with increasing tool width and slightly decreases with increasing friction values.

When a long billet is compressed between two flat tools some material elongates or moves away in the two opposite direction longitidunually. The variation of material elongation in the axial direction with IAR is shown in Fig 4.43 and a comparison with previous work [14] given in Fig 4.44. This flow is perhaps best described as displaced volume of material and is shown in Fig 4.45 and 4.46 for the SODITRI and in Fig 4.47 and 4.48 for the SODIPAR against variation of initial aspect ratio at $m = 0$ and $m = 0.5$ respectively. The volume displacement was altered with different height reductions subjected from the initial billet heights individually. As it can be seen from these figures the value of displaced volume increases with increasing height reductions and initial aspect ratios. While there is no friction, the volume displaced in the axial direction is especially higher at small initial aspect ratio values. For example in Fig 4.48 at small initial aspect ratio values, from 0.1 to 2.5, the variation in the amount of displaced volume was more noticeable than at higher values of aspect ratios and after an aspect ratio of 10 remains constant . However if the figures are compared with each other it is seen that when friction increases, the amount of material displaced from between the tools in the axial direction decreases.

The tool width also has an effect on the amount of volume displaced. Fig 4.49 and 4.50 show the variation of volume displacement with different tool widths and aspect ratios at a fixed penetration 25% for the SODITRI and Fig 4.51 and 4.52 for the SODIPAR. It can be concluded from these results that while tool width increases the displaced volume in the longitudinal direction decreases at higher friction values. This means that the magnitude of volume displacement depends on the initial aspect ratio of the billet, tool width, friction and also penetration level. Although large initial aspect ratios are not of practical relevance, the programs were extended to such extreme cases to examine the validity and viability of the solutions. The results for volume displacement were plotted in Fig 4.53 against initial global aspect ratio of workpiece for a friction factor of $m = 0.5$. In comparison, the theoretical approaches show that SODIREC due to the simplicity of its assumptions, eg homogeneity of flow in both lateral and axial directions, gives considerably lower results for loading, spread than that obtained via the results of SODITRI and SODIPAR solutions which are fairly close to each other.

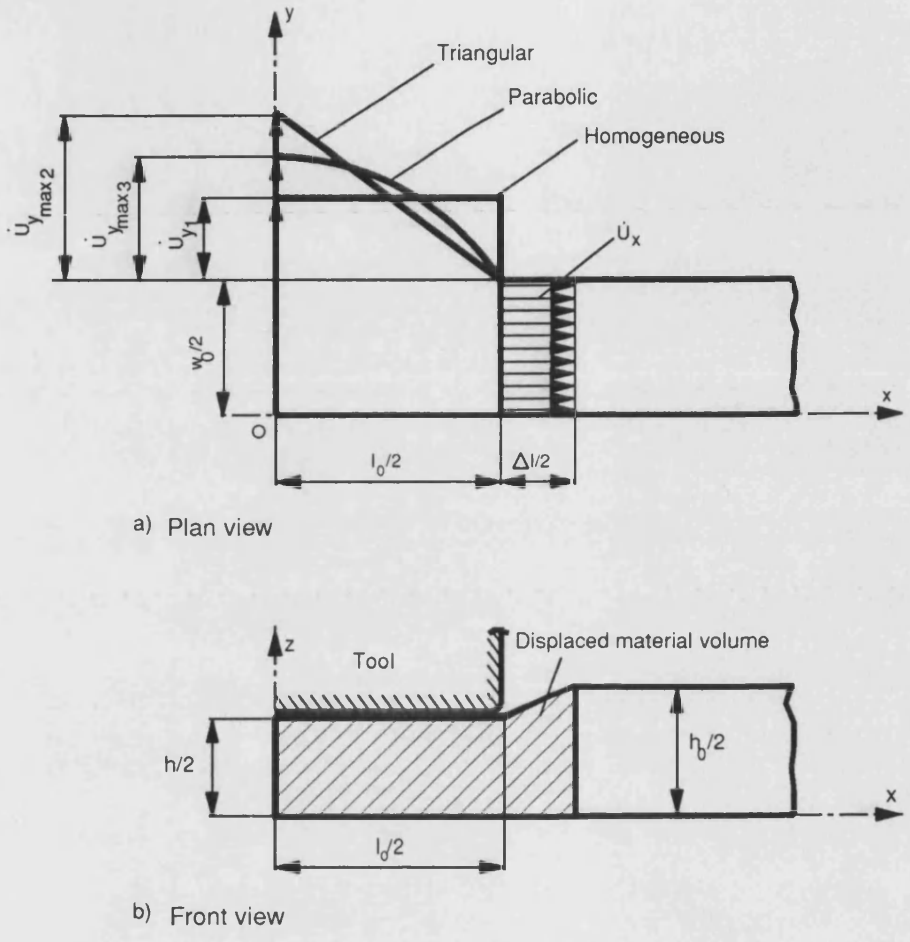

Figure 4-1: Schematic illustration of the velocity fields in the a)x-y plane and b) x-z plane.

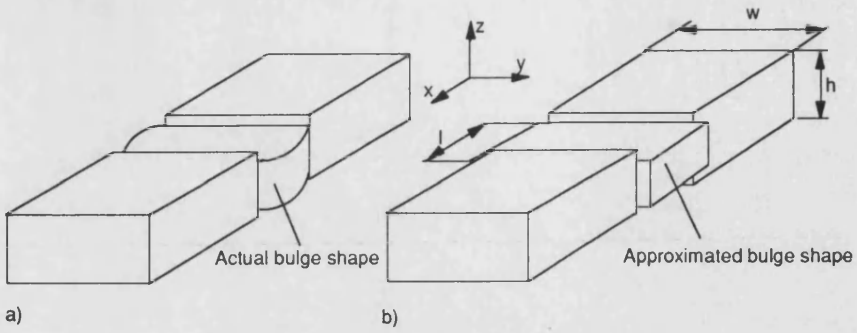

Figure 4-2: A partially compressed long bar.

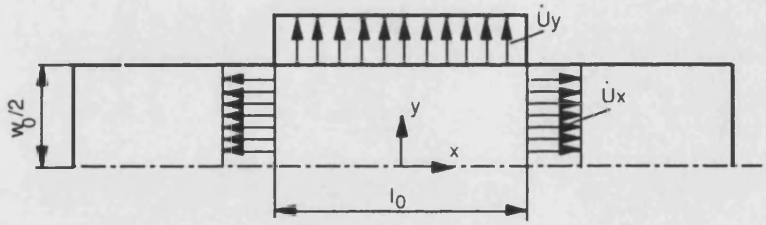

Figure 4-3: A partially compressed long bar with approximated velocity field.

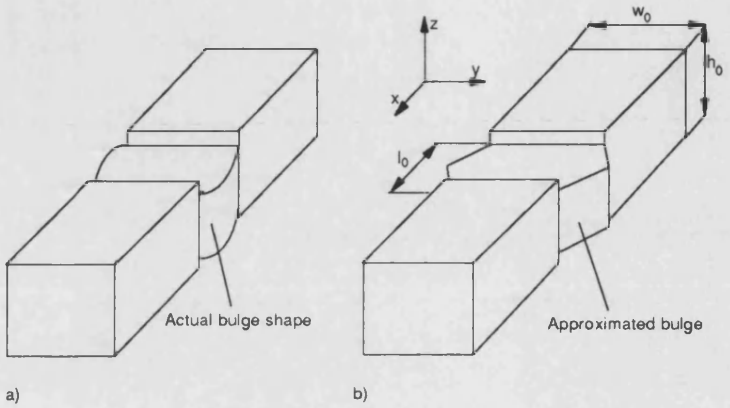

Figure 4-4: Partially compressed block element a) with actual bulge b) with approximated bulge.

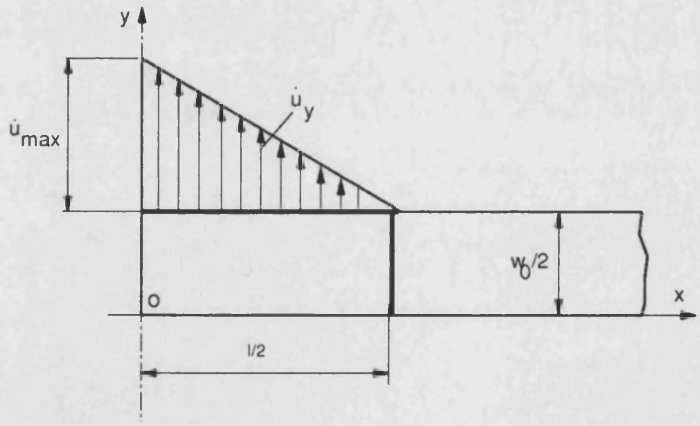

Figure 4-5: The estimated triangular velocity field.

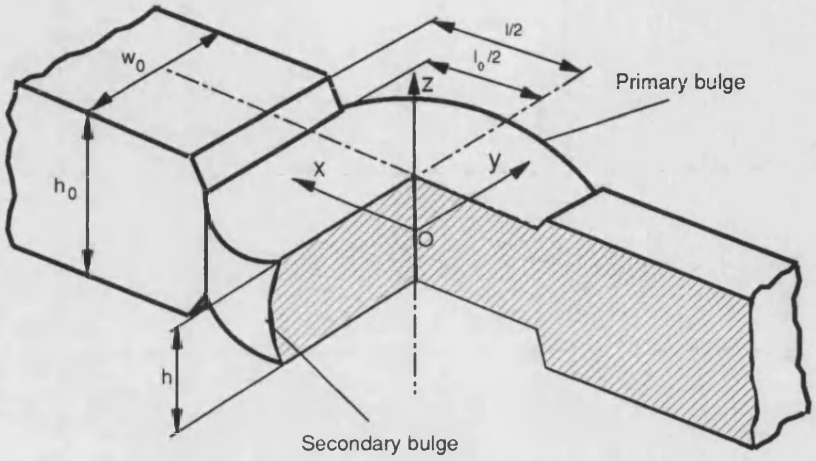

Figure 4-6: A partially compressed long bar.

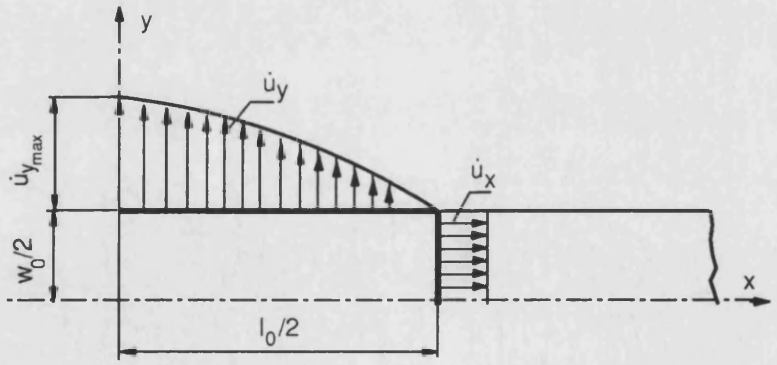

Figure 4-7: The proposed parabolic velocity field for the lateral spread.

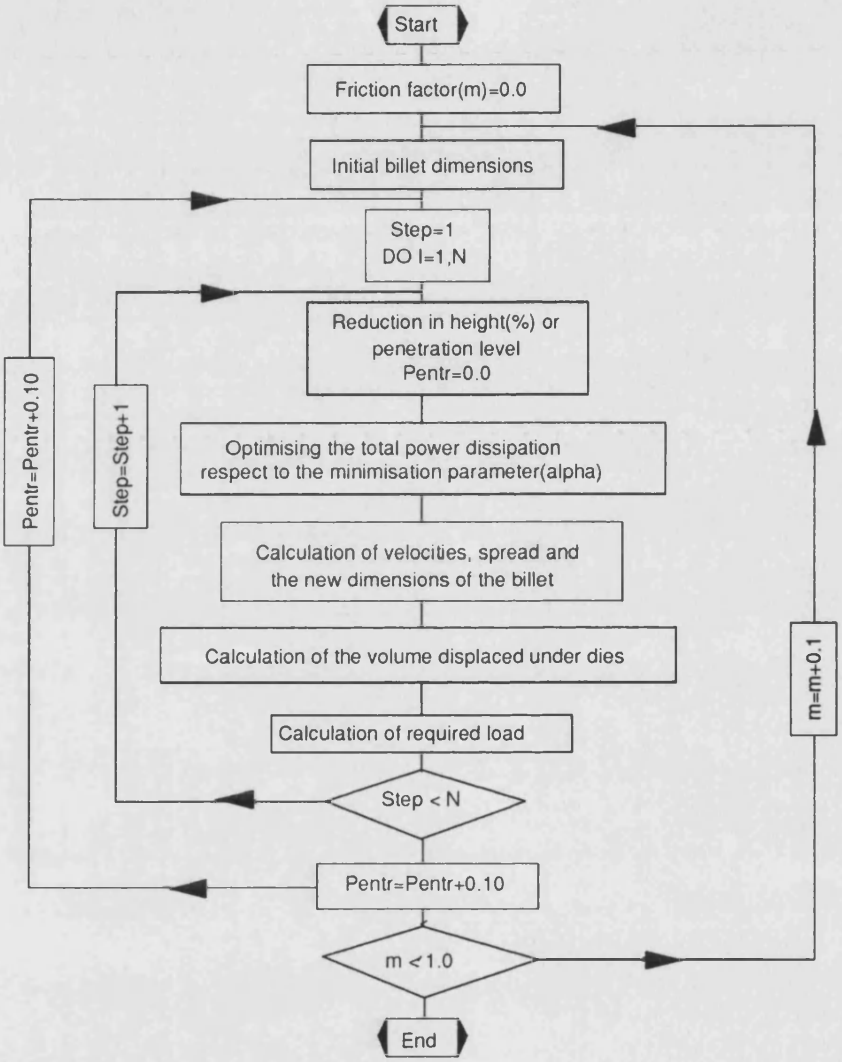

Figure 4-8: Flow chart for simple incremental compression of a long bar.

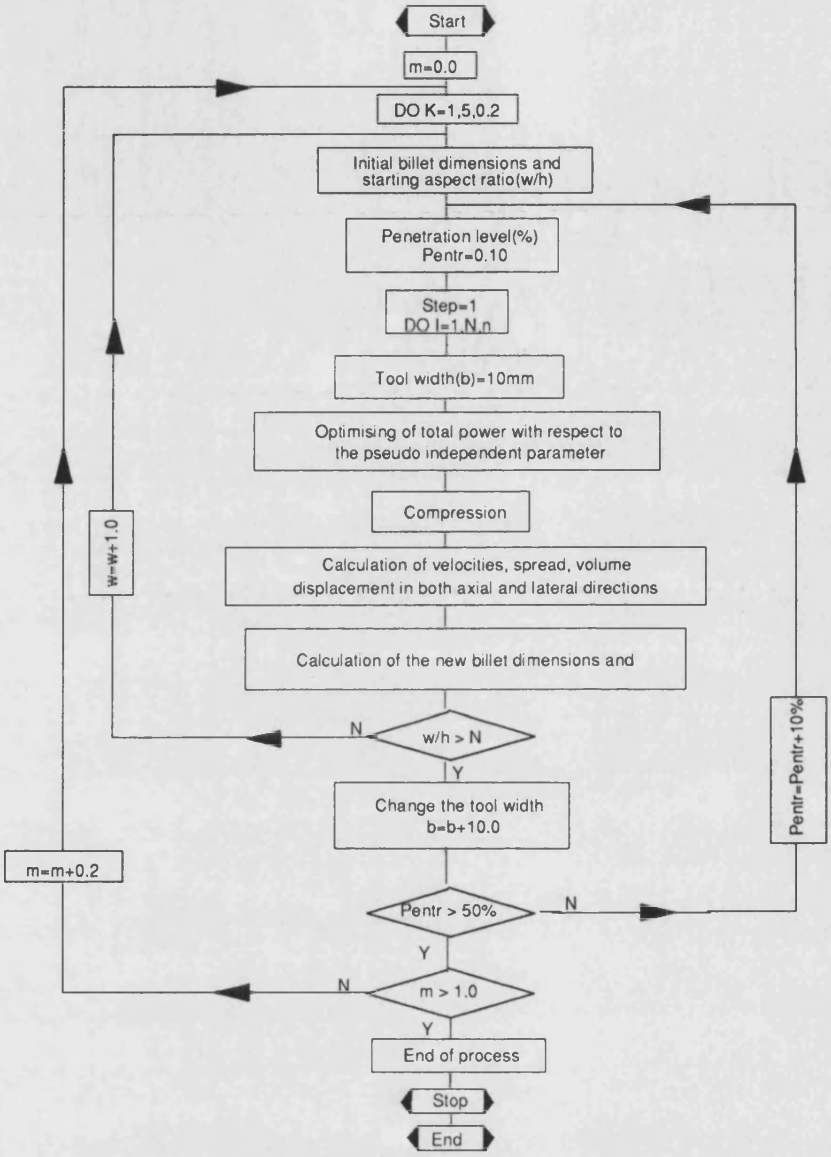

Figure 4-9: Flow chart for incremental compression for various aspect ratio and tool widths of a long bar.

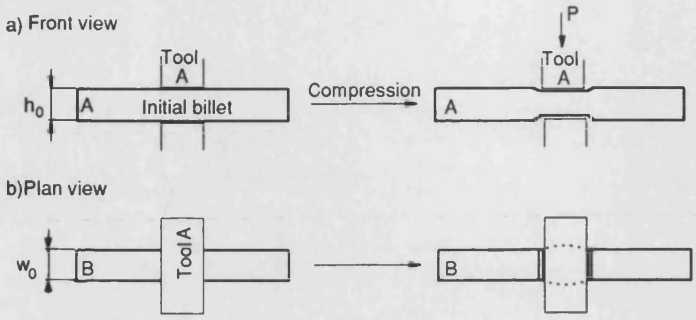

Figure 4-10: One step schematic example to incremental compression with a fixed tool width.

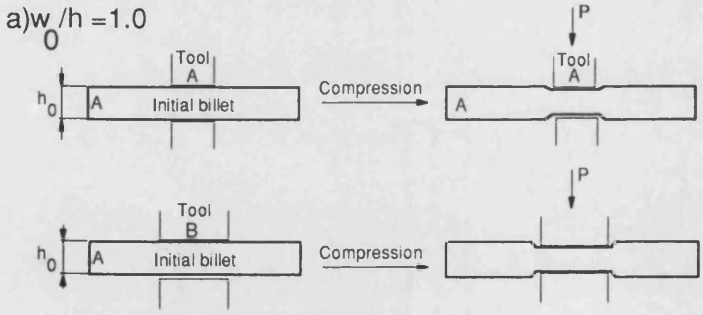

Figure 4-11: A one step schematic example for the compression with various tool widths.

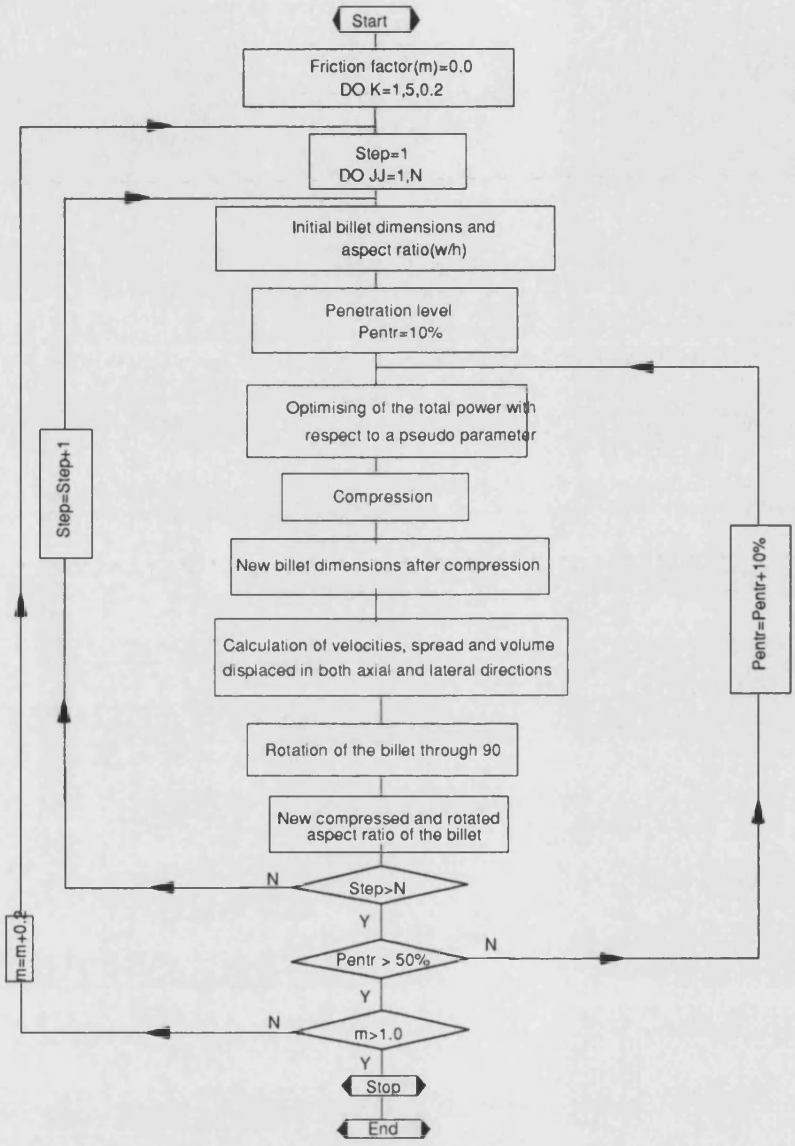

Figure 4-12: Flow chart for incremental compression-rotation of a long bar.

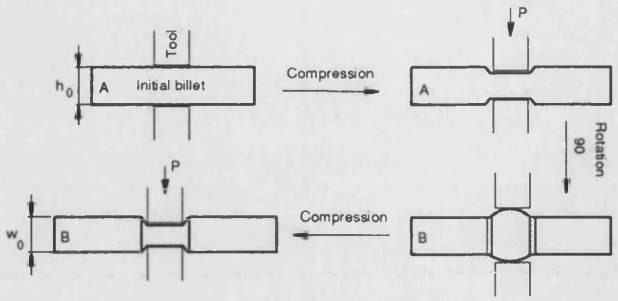

Figure 4-13: A schematic example to one cycle incremental compression-rotation of a long bar

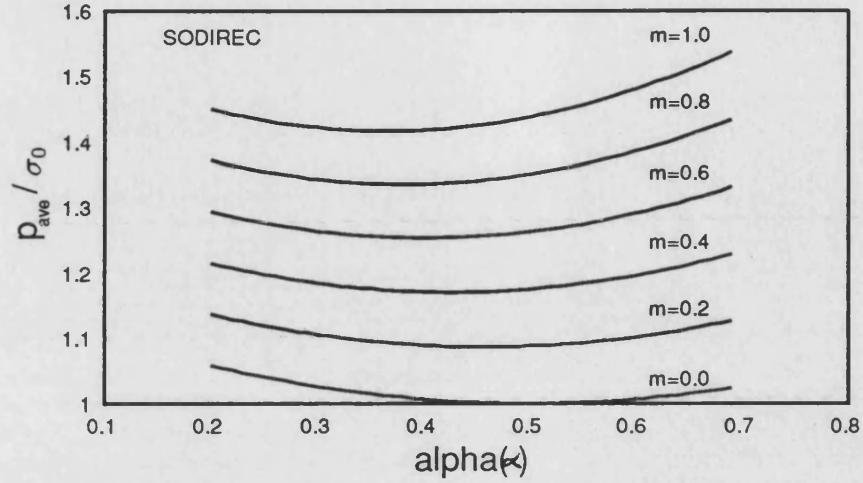

Figure 4-14: Relationship between relative pressure and spread parameter

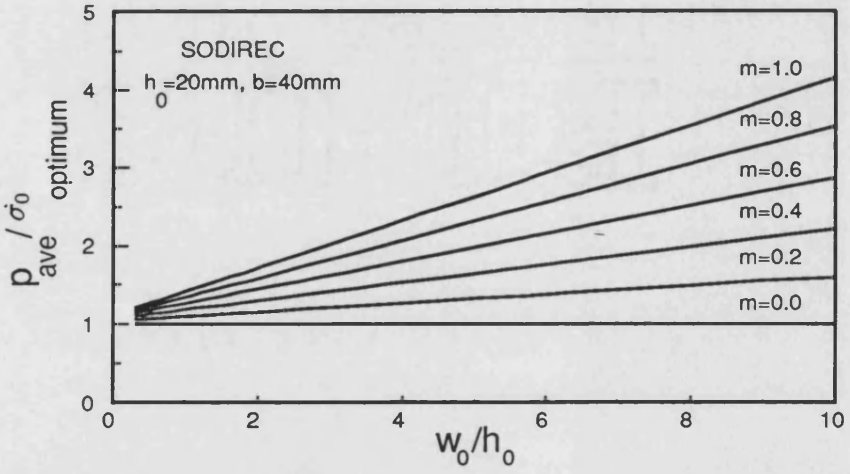

Figure 4-15: Relationship between optimum relative pressure and aspect ratio of the billet

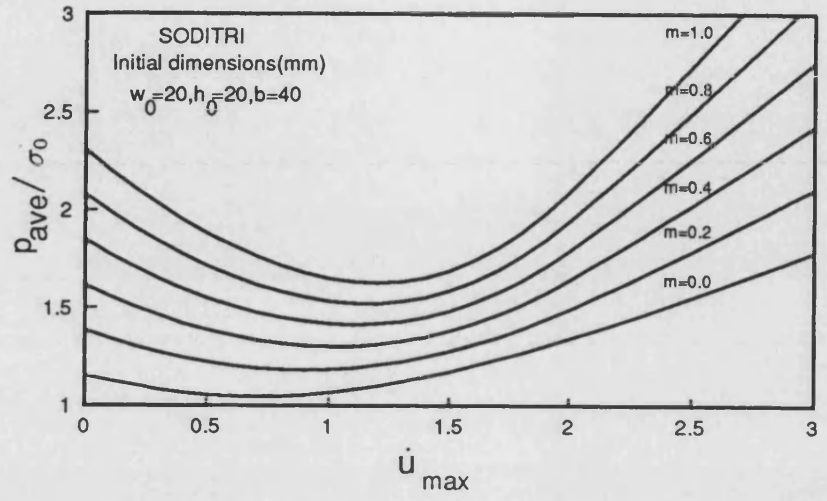

Figure 4-16: Variation of relative pressure with aspect ratio Triangular velocity field,SODITRI

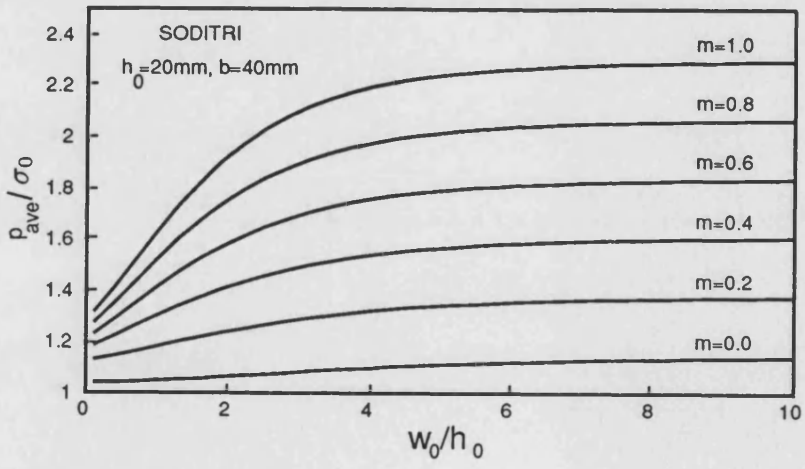

Figure 4-17: Variation of optimum relative pressure with aspect ratio Triangular velocity field,SODITRI

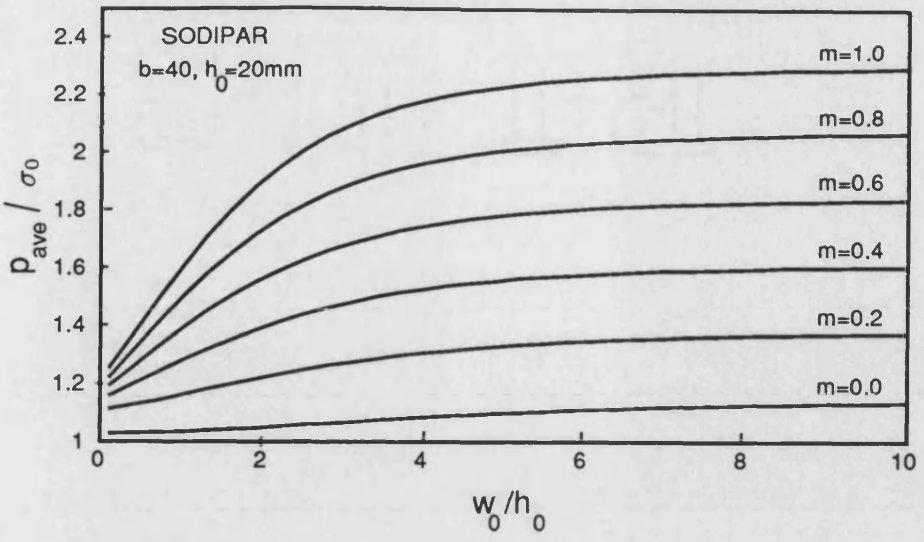

Figure 4-18: Variation of optimum relative pressure with aspect ratio Parabolic velocity field,SODIPAR

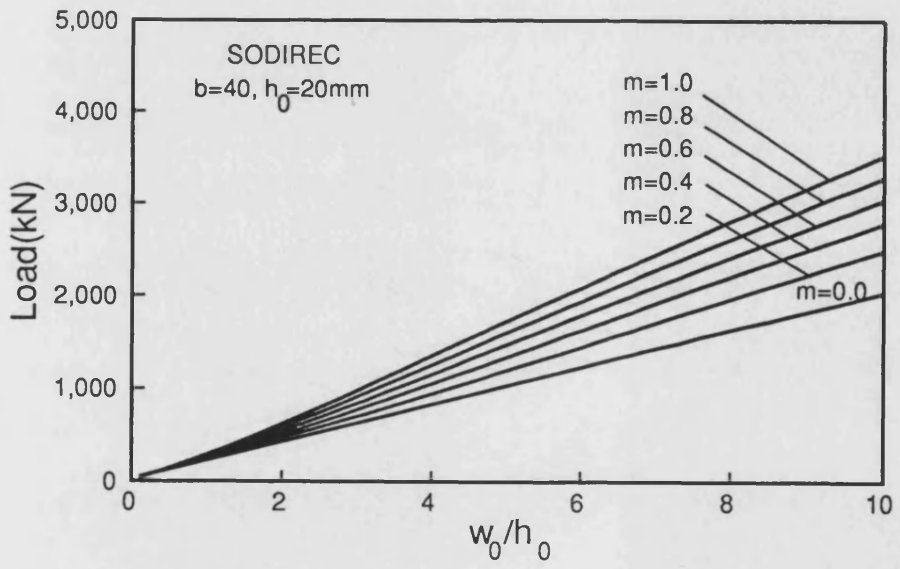

Figure 4-19: Prediction of load for different aspect ratios -Rectangular velocity field,SODIREC

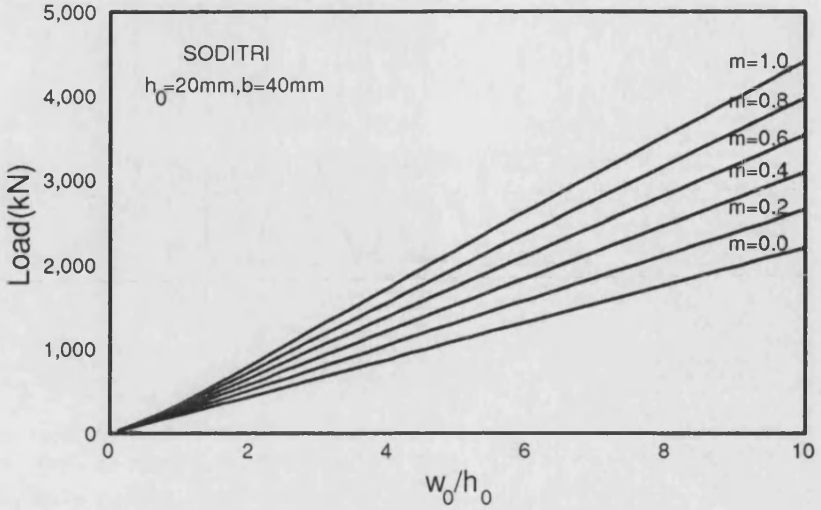

Figure 4-20: Prediction of load for different aspect ratios - Triangular velocity field,SODITRI

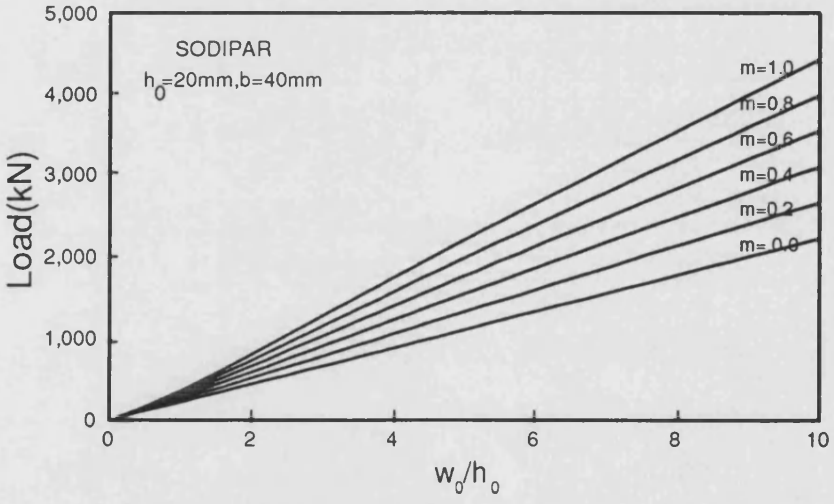

Figure 4-21: Prediction of load for different aspect ratios - Parabolic velocity field,SODIPAR

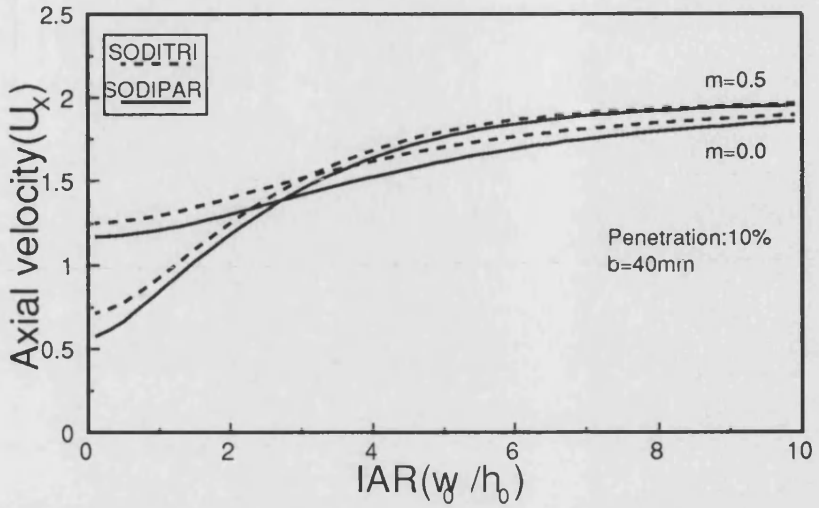

Figure 4-22: Variation of axial velocity with initial aspect ratio .

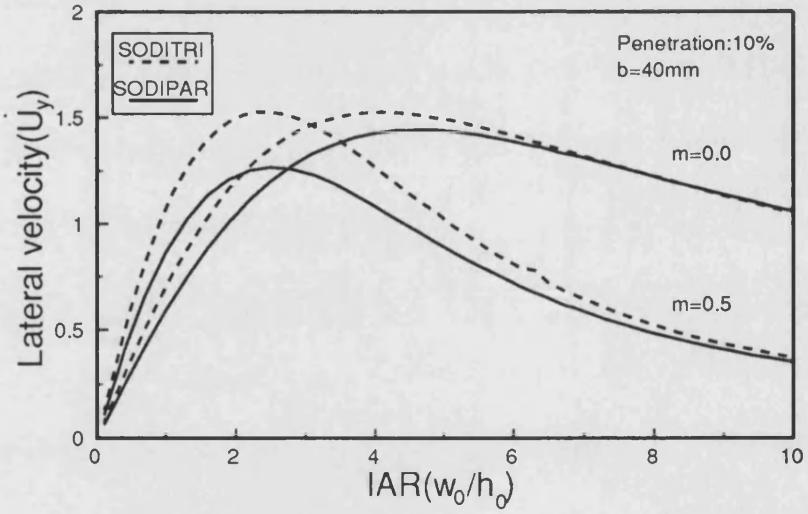

Figure 4-23: Variation of lateral velocity with initial aspect ratio .

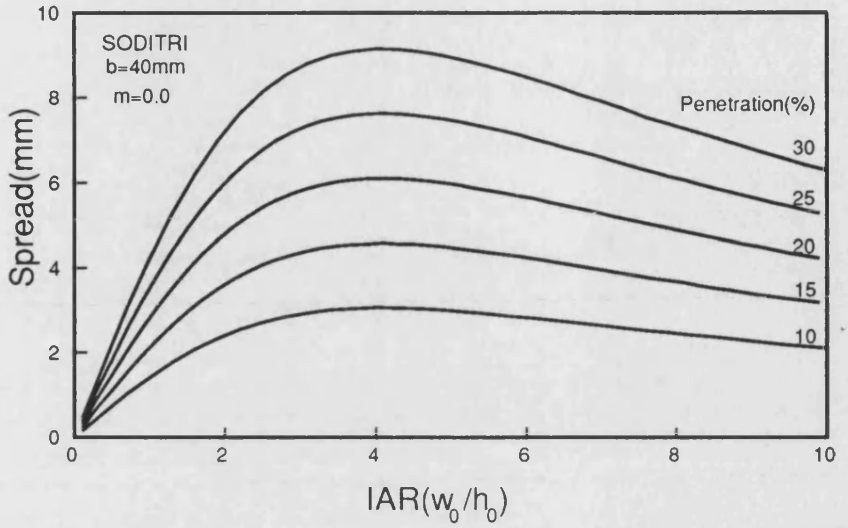

Figure 4-24: Prediction of spread for various aspect ratios of a long bar - Triangular velocity field -SODITRI

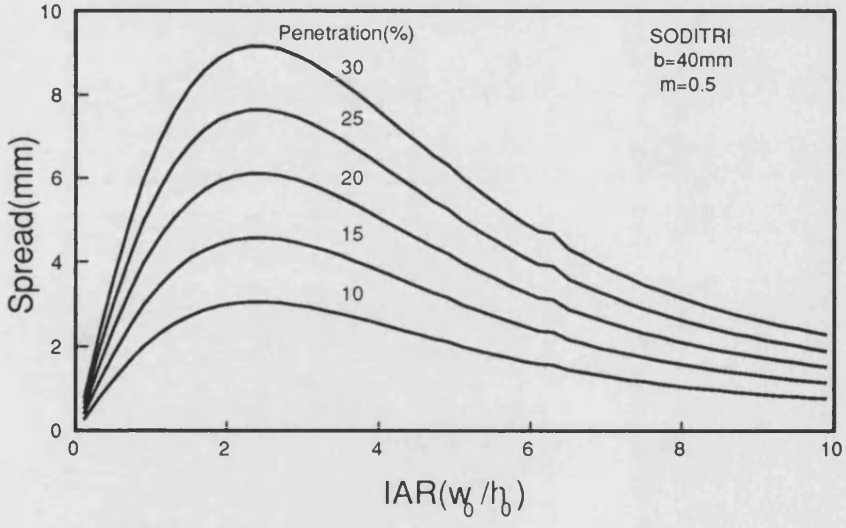

Figure 4-25: Prediction of spread for various aspect ratios of a long bar - Triangular velocity field -SODITRI

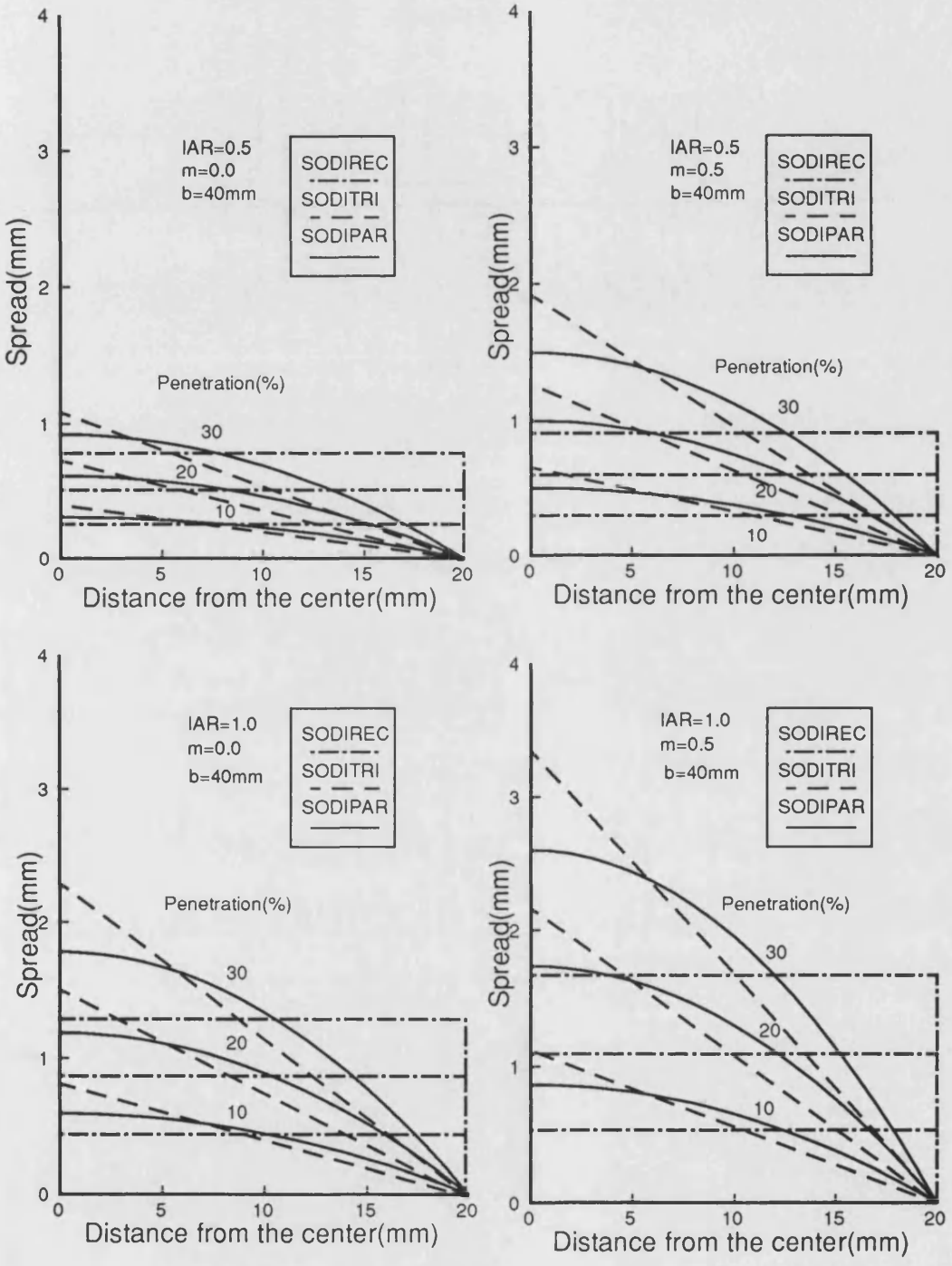

Figure 4-26: Prediction of spread profile.

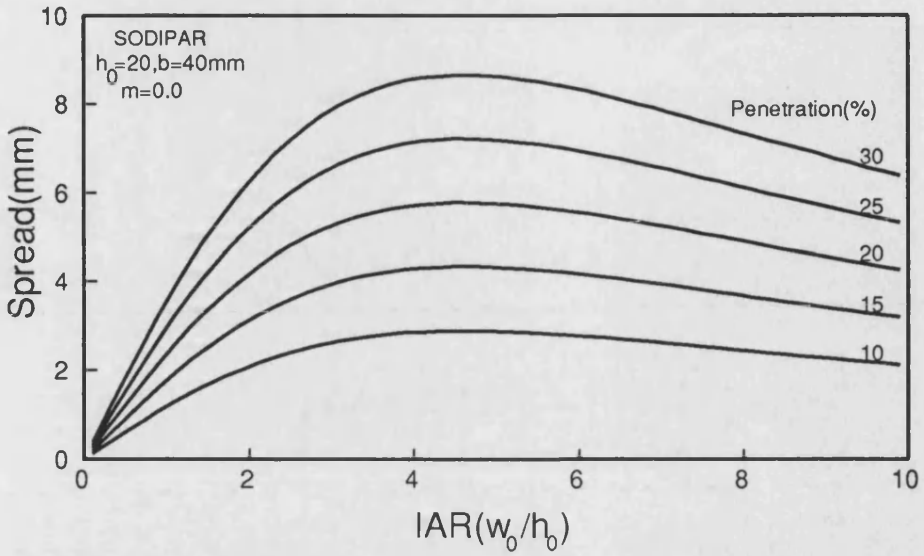

Figure 4-27: Prediction of spread for various aspect ratios of a long bar -Parabolic velocity field -SODIPAR.

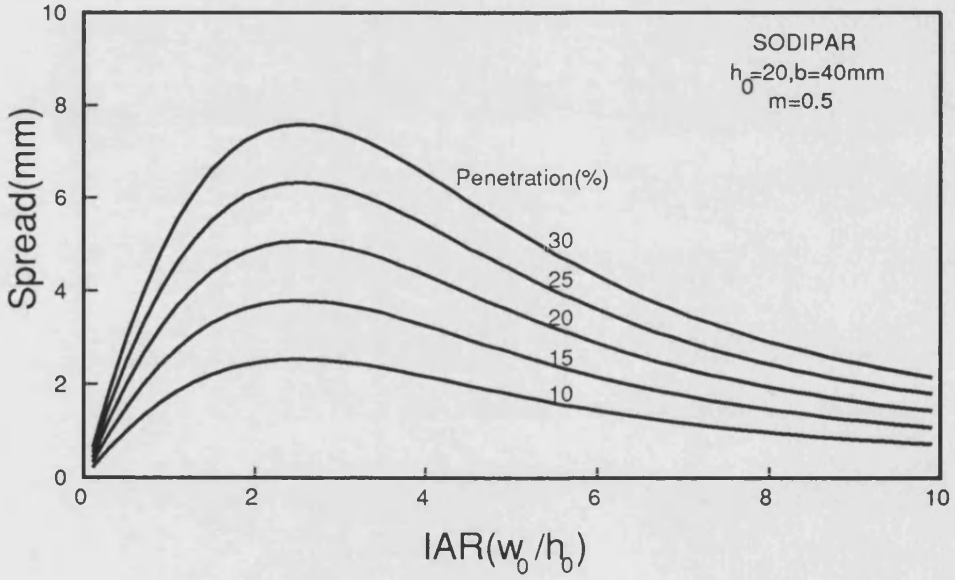

Figure 4-28: Prediction of spread for various aspect ratios of a long bar -Parabolic velocity field -SODIPAR

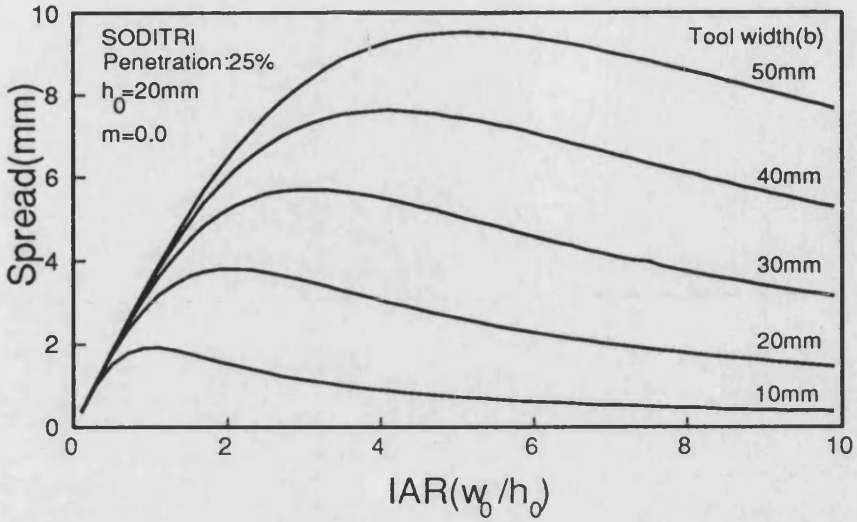

Figure 4-29: Prediction of spread for various tool widths -Triangular velocity field -SODITRIlabelfig:fig4.30

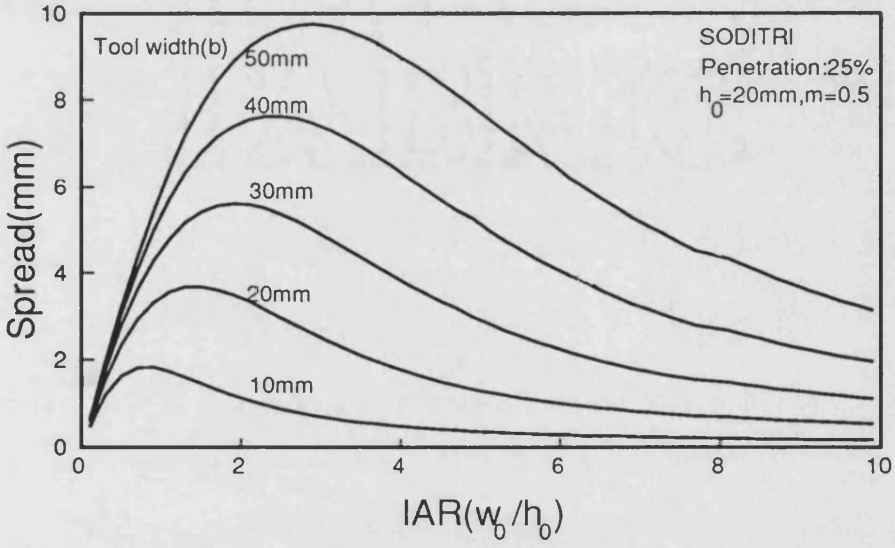

Figure 4-30: Prediction of spread for different tool widths -Triangular velocity field -SODITRI

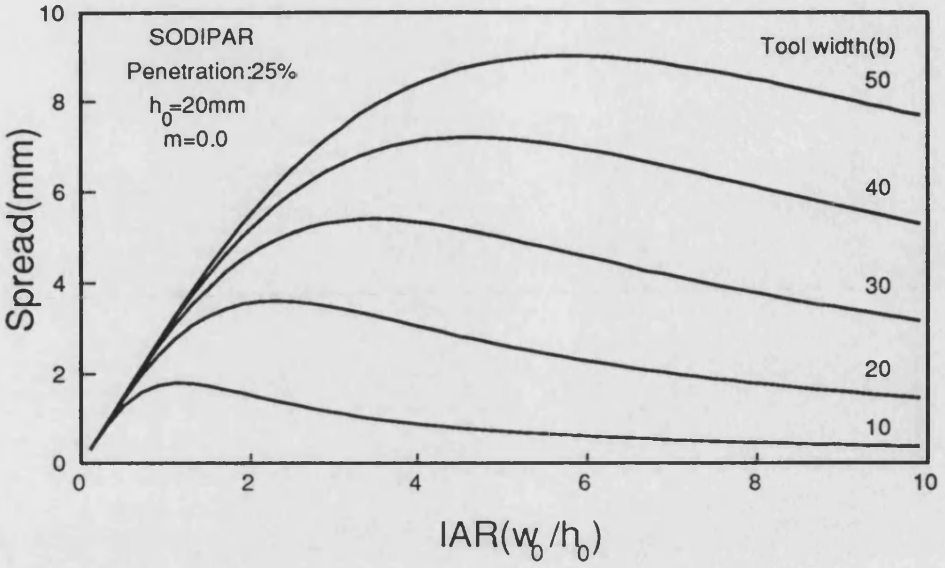

Figure 4-31: Prediction of spread for various tool widths -Parabolic velocity field -SODIPAR.

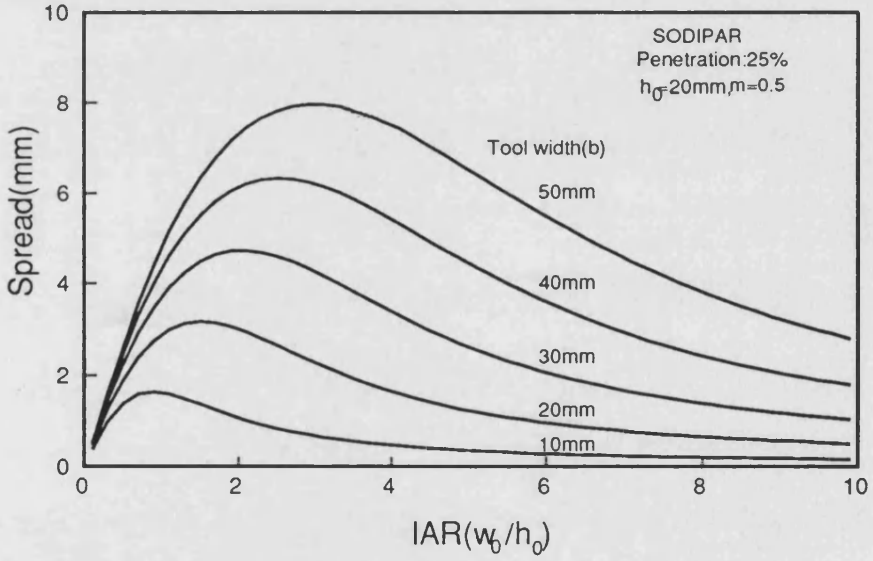

Figure 4-32: Prediction of spread for various tool widths -Parabolic velocity field -SODIPAR

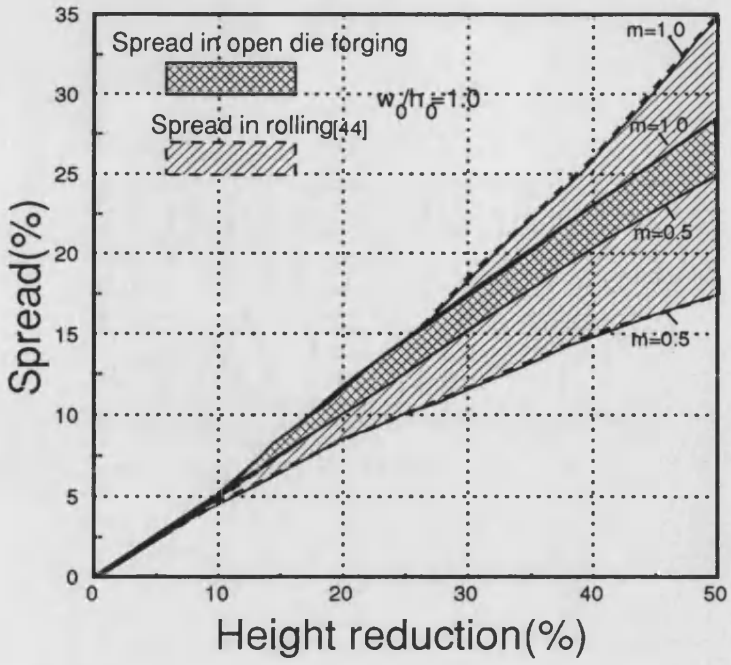

Figure 4-33: Comparison of percentage spread zones with rolling and flat bar forging processes.

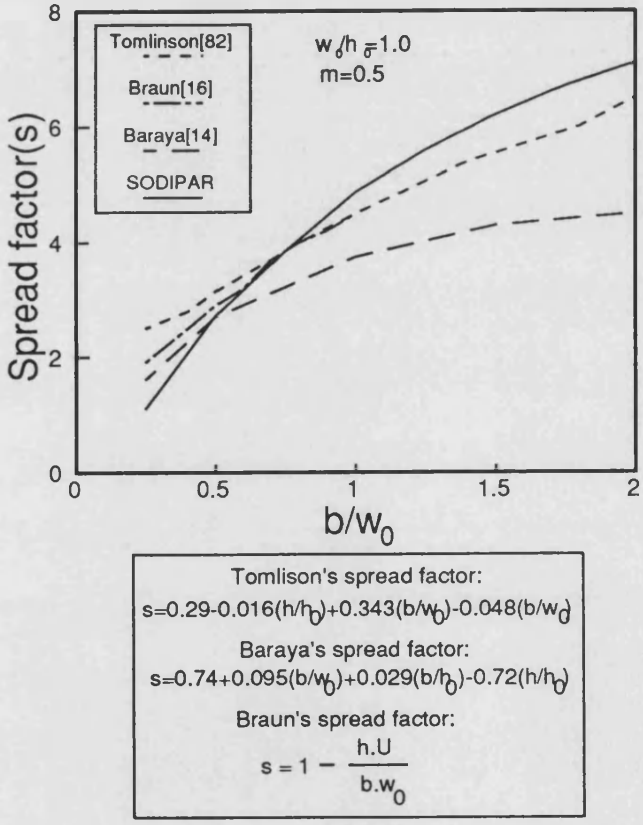

Figure 4-34: Comparison of spread-s against bite ratio.

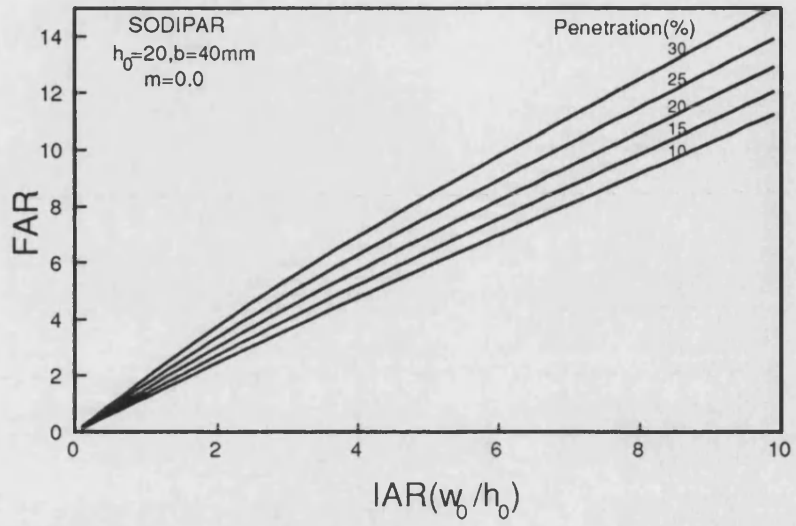

Figure 4-37: Prediction of final aspect ratio(FAR) for various initial aspect ratios(IAR) -Parabolic velocity field -SODIPAR

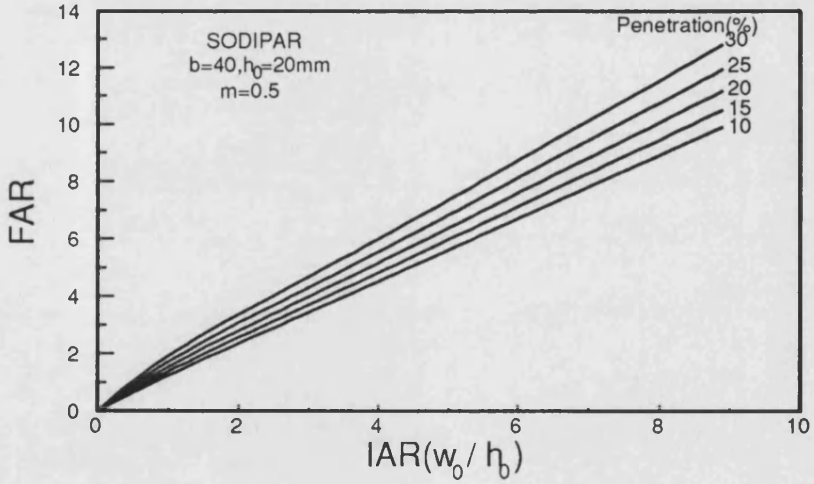

Figure 4-38: Prediction of final aspect ratio(FAR) for various initial aspect ratios(IAR) -Parabolic velocity field -SODIPAR

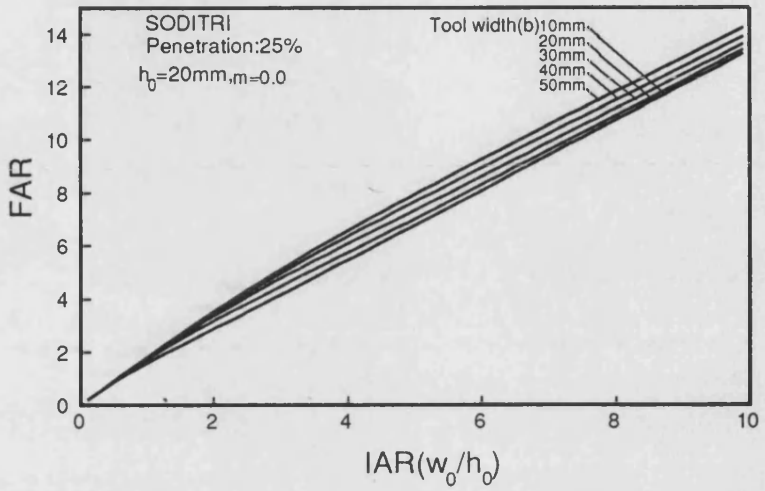

Figure 4-39: Prediction of final aspect ratio(FAR) for various tool widths - Triangular velocity field -SODITRI

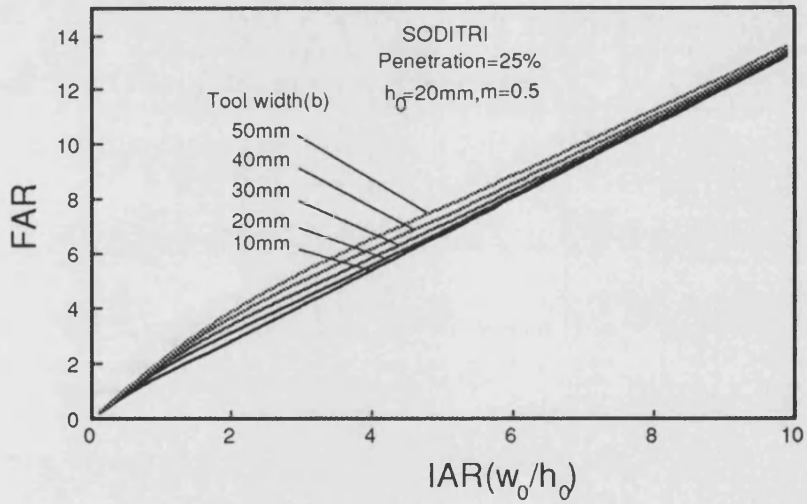

Figure 4-40: Prediction of final aspect ratio(FAR) for various tool widths - Triangular velocity field -SODITRI

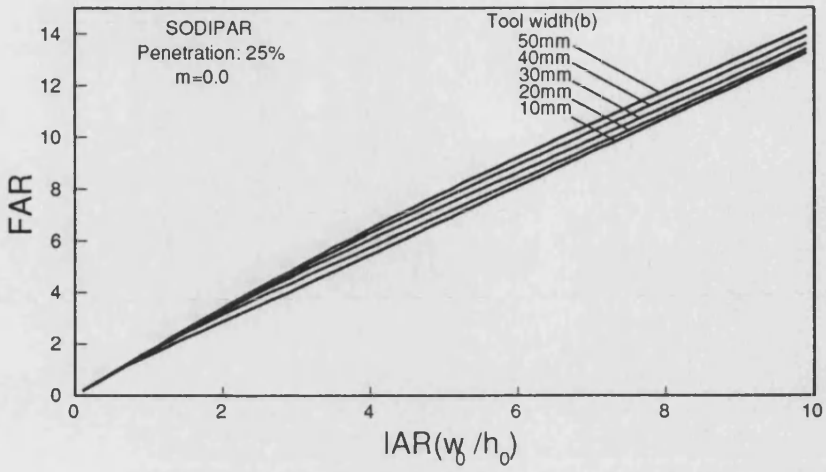

Figure 4-41: Prediction of final aspect ratio(FAR) for various tool widths - Parabolic velocity field -SODIPAR

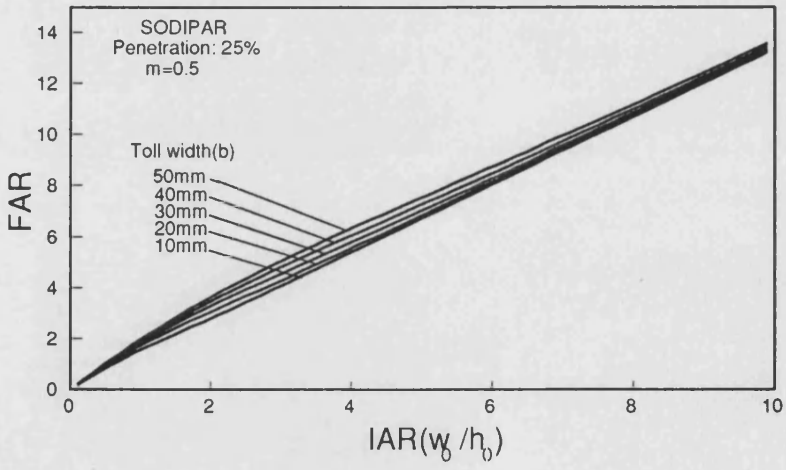

Figure 4-42: Prediction of final aspect ratio(FAR) for various initial aspect ratios(IAR) -Parabolic velocity field -SODIPAR

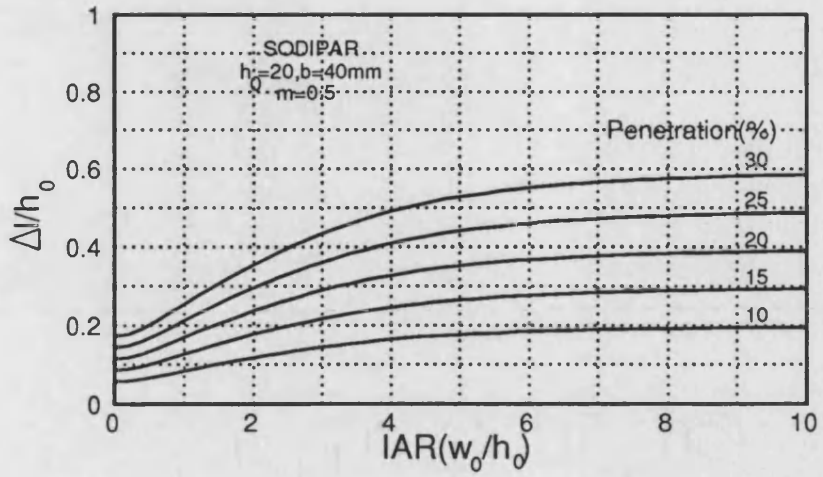

Figure 4-43: The variation of elongated material in axial direction with initial aspect ratio,IAR

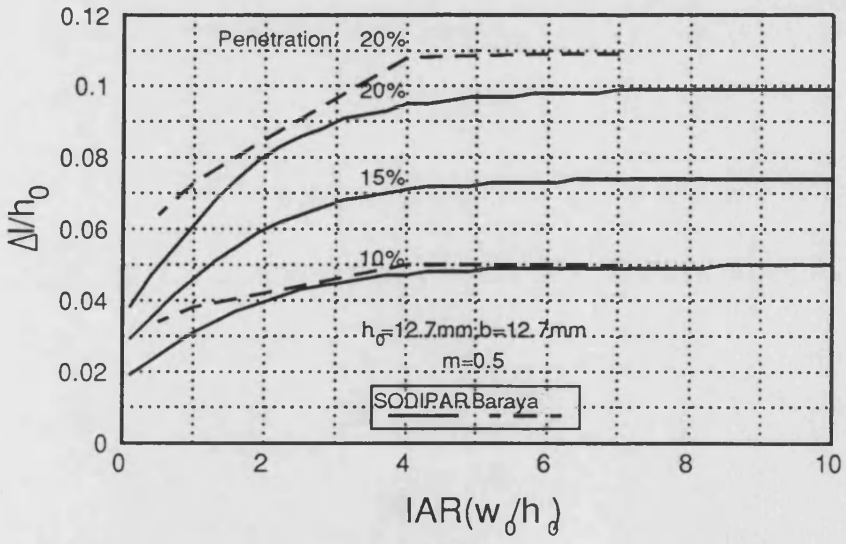

Figure 4-44: Comparison of elongation with a previous work[14]

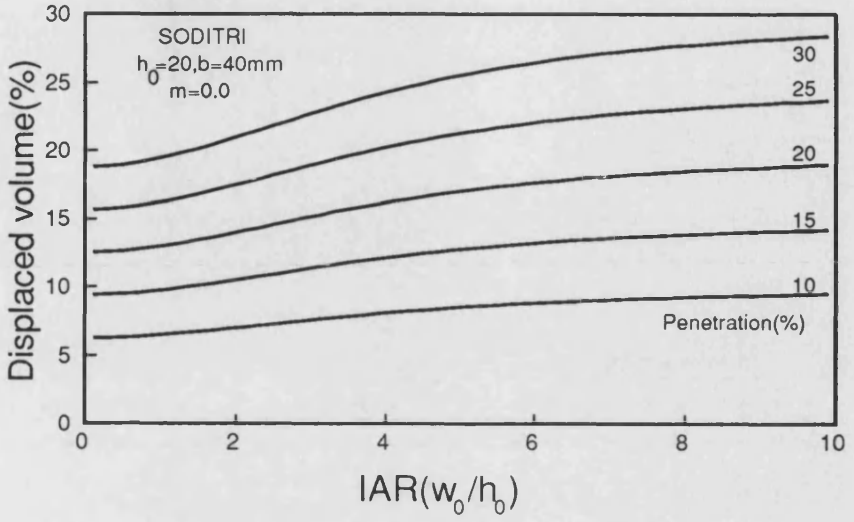

Figure 4-45: Variation of displaced material volume with aspect ratio -Triangular velocity field -SODITRI

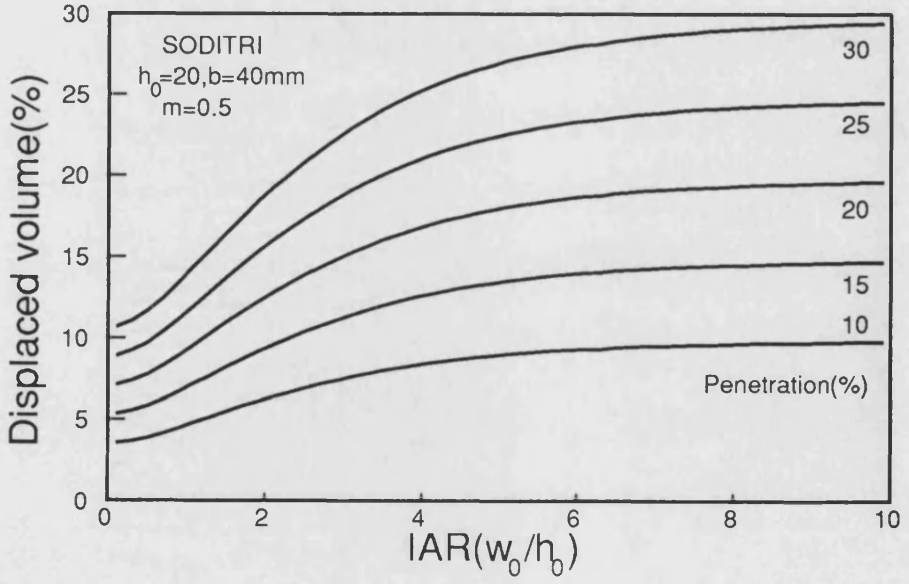

Figure 4-46: Variation of displaced material volume with aspect ratio -Triangular velocity field -SODITRI

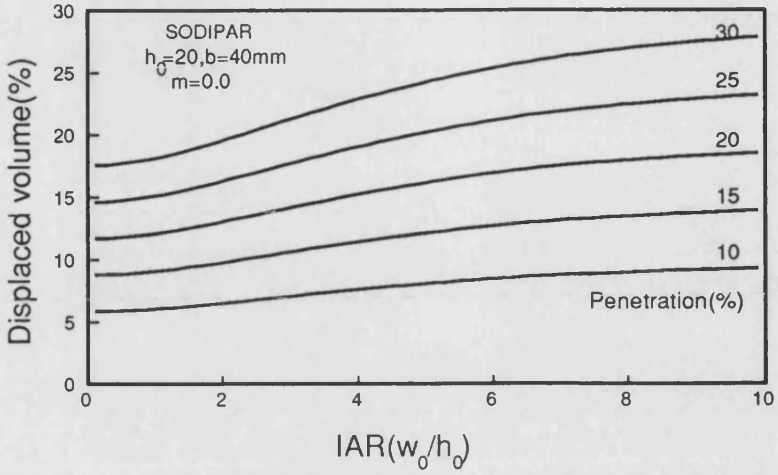

Figure 4-47: Variation of displaced material volume with aspect ratio -Parabolic velocity field -SODIPAR

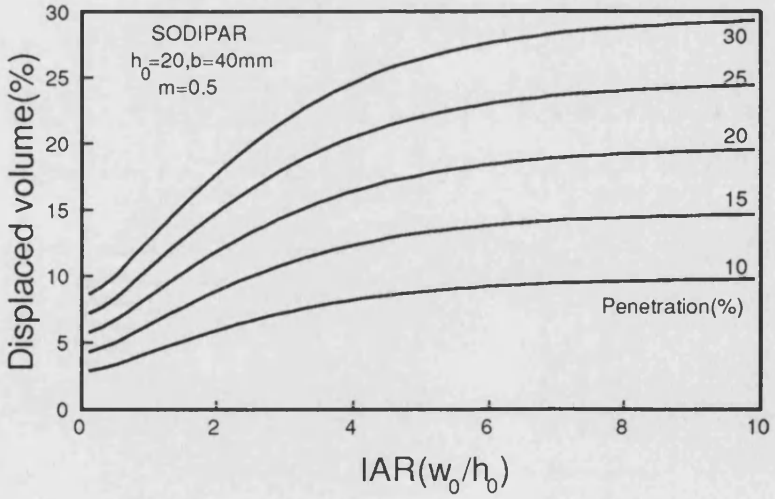

Figure 4-48: Variation of displaced material volume -Parabolic velocity field - SODIPAR

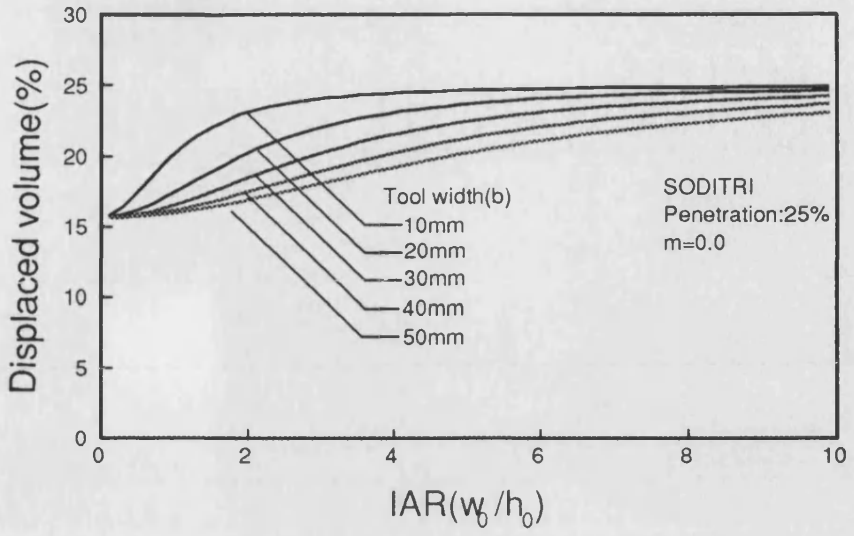

Figure 4-49: Variation of displaced material volume with aspect ratio for various tool widths -Triangular velocity field -SODITRI

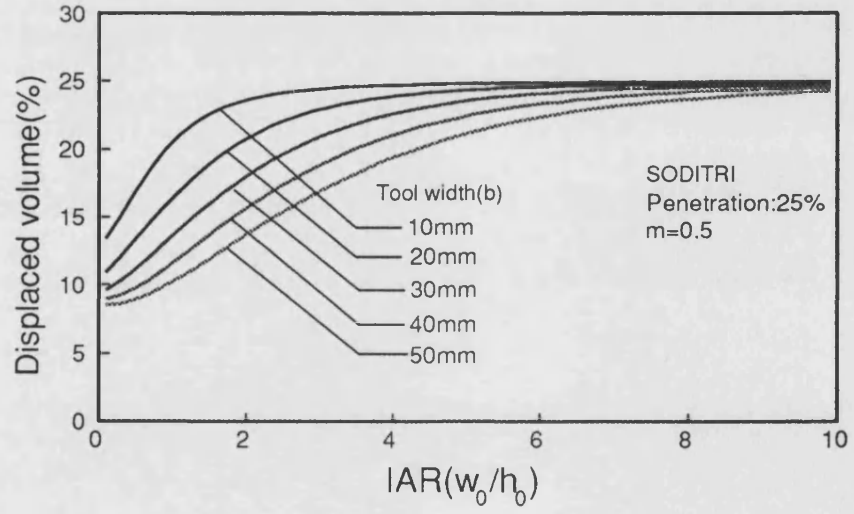

Figure 4-50: Variation of displaced material volume with aspect ratio for various tool widths -Triangular velocity field -SODITRI

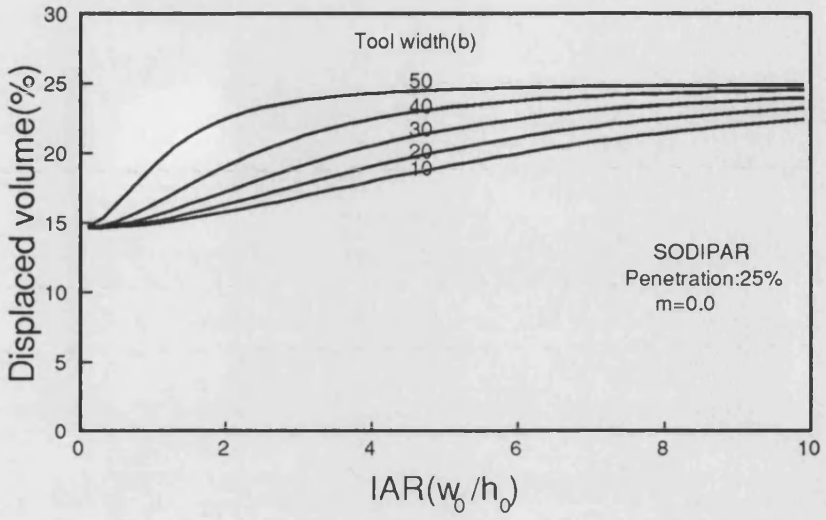

Figure 4-51: Variation of displaced material volume with aspect ratio for various tool widths -Parabolic velocity field -SODIPAR

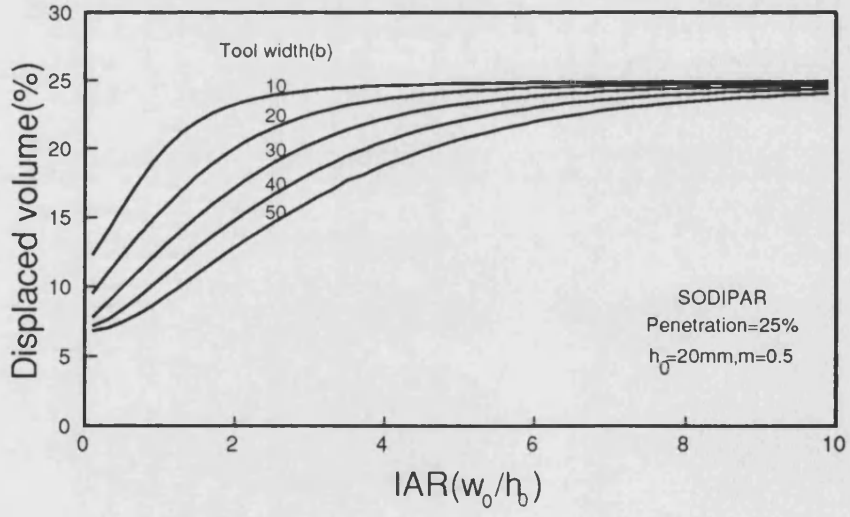

Figure 4-52: Variation of displaced material volume with aspect ratio for various tool widths -Parabolic velocity field -SODIPAR

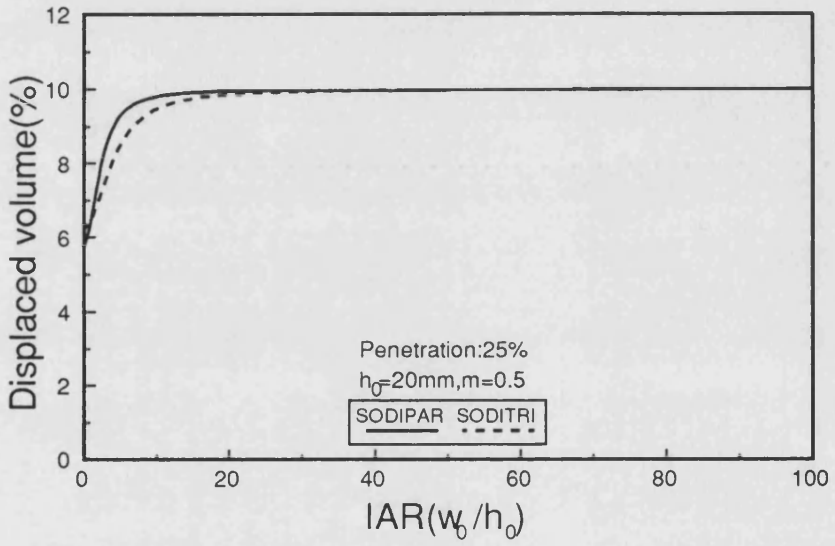

Figure 4-53: Prediction of displaced material volume with aspect ratio in extreme cases.

Chapter 5

EXPERIMENTAL WORK

5.1 Introduction

This chapter describes a programme of experimental work which was carried out to compare and validate the theoretical predictions. Although much work has been undertaken to analyse the deformation in the area of open die forging there appears to be little evidence correlating the theory with experiments in a way which provides full details of flow characteristics.

The experimental work has been undertaken in order to investigate the mode of deformation and can be divided into five main parts.

I) Single step and incremental compression of a billet with a rectangular cross section.

II) Experiments on a series of billets with various aspect ratios.

III) Experiments with various tool widths.

IV) Incremental compression followed by rotation of the billet.

V) Bar profiling experiments ie cyclic incremental compression and rotation.

The above tests were conducted on half hard (6082) aluminium using simple flat tools under dry conditions. The microstructure of some forged billets were examined to show the grain distribution and flow before and after compression. The friction factor was determined via ring tests.

5.2 Experimental set up

Initial forging experiments were performed using a 1000kN NC Rhodes hydraulic press as shown in Fig 5.1a. Later experiments were performed using a manually operated 1500kN hydraulic press(Fig 5.1a,b). The forging tools were mounted on a two pillar Desoutter die set as shown in Fig 5.2a and Fig 5.2b. A range of different tool widths was used and all the experiments were carried out at toom temperature.

A load cell fitted with a full bridge strain gauge circuit and capable of recording up to the maximum capacity 1000kN was used and is shown in Fig 5.3. This was fitted on the press and used to calibrate the Rhodes and the manually operated presses. The forging load was measured by the help of a data acquisition system which was connected to the load cell placed between the bottom die and the press base. The press ram displacement was registered simultaneously by a potentiometer placed vertically between the base and top ram of the press and by a linear displacement dial gauge used manually.

Handling of the workpiece is difficult in open-die forging experiments since it

must be repositioned and manipulated many times during compression-rotation forging tests cycle. A workpiece holder for this type of work must not only hold the workpiece but also should be able to accommodate the deformation of the workpiece during deformation. When the workpiece is forged elongation occurs and the movement of the centre line of the workpiece moves vertically. This can cause severe distortions with resultant undesirable features. In order to hold and compress the workpiece between two flat dies a simple holding device was designed and manufactured at an early stage of the work. This is shown in Fig 5.4. While pressing the workpiece between the flat tools, the horizontal centre line of the workpiece, which is parallel to the press surface, changes its vertical position. Providing a pair of springs around the two cylinder legs of the holder enables the tilting of the workpiece to be absorbed while the vertical displacement occurs continuously without any major effect on metal flow. When a compressed billet is rotated through 90^0, due to the sideway bulging in both free sides, the horizontal centerline moves to a new position for the next compression step. Poor centralisation of workpiece sometimes causes undesirable features and distortions. In a later stage of the work the improved workpiece holder shown in Fig 5.5, 5.6 and 5.7 was designed and manufactured. This workpiece holder device is able to accommodate metal flow in longitudinal and lateral directions with the vertical motion again accommodated by springs. The workpiece is held from both ends by a pair of inner sliding cylinders. These cylinders are movable and slide in the outer cylinders. The most important advantage of this is that workpiece can be rotated with much better accuracy during the multi cycling experiments without disturbing the workpiece position between dies.

5.3 Simple Compression and Ring Test

The determination of friction is important in open die forging in terms of the total load and power required for deformation. In this work, the ring test was used for determining the friction. In order to work out the flow stress σ_0 of the 6082 Al material simple compression tests was carried out using a number of cylindrical specimens having 30 mm in height and 25 mm in diameter. The specimens were annealed at 425^0 for two hours. The output from the load cell and the change of specimen height from a displacement transducer were recorded simultaneously. Since the volume remains constant during deformation the continous reduction in height can be converted into the contact area. Thus the stress can be determined simultaneously and hence the progressive stress-strain curve of the material can be determined as shown in Fig 5.8. Fig 5.9a shows a series of compressed specimens.

In open-die forming process the flow of the metal workpiece between the tools is opposed by frictional forces at the metal/tool interface. To determine the friction factor m for dry conditions ring test experiments were carried out using specimens of $20mm$ internal diameter, $40mm$ outer diameter and $13.33mm$ height. The ring specimens were made of 6082Al alloy each of which was taken from the same bars as the billets used during experimental forging tests. The specimens were also annealed at (425^0C) for two hours.

Fig 5.9b shows a series of rings which have been subjected to different deformation levels corresponding to $7, 19, 29, 35, 41\%$ height reductions and Fig 5.10 schematic illustration of deformed specimen dimensions. The friction factor values were

determined for each specimen using the calibration charts as proposed by Male and Cockcroft [61, 62]. The results is given in Table 4. It can be seen that the friction factors m, obtained for 6082Al varied between 0.20 and 0.70 with increasing deformation under dry conditions. Ideally the ring test requires only the initial and final dimensions of the specimens to determine a coefficient of friction to use for comparison with the theoretical solutions. As a result of these tests the friction factor was determined as $m = 0.5$.

5.4 Deformation Patterns in Open Die Forging

5.4.1 Single incremental and progressive compression

In this part two sets of experiments were carried out, first a number of billets of rectangular cross section of $25mm$ in width and $16.66mm$ in height were machined to $100mm$ in length. Fig 5.11 illustrates the cross-sections of the long aluminium specimens. No annealing took place for these specimens of 6082 Al. The billets were upset using the N.C Rhodes hydraulic press and their height reduced incrementally between flat dies. The load was recorded and maximum spread measured after each compression step and presented in Tables 5,6 and 7. In Fig 5.12a locally and incrementally compressed billets are illustrated.

In the second set of experiments a number of billets, having the same aspect ratio of w_0/h_0 and dimensions as given above were subjected to one deformation step varying from 5% to 50% height reduction. Fig 5.12b shows the examples of some billets subjected to progressive penetration. After reaching the required height the dimensional changes were measured and cross sectional area of the locally

compressed billets was calculated after each compression step. The figures show that the sideway bulge and elongation increase with the amount of reduction in height imparted to the billets. The results of measurements are given in Table 8.

5.4.2 Single compression of billets with various aspect ratios

The purpose of this part of work was to investigate the effect of aspect ratio and the penetration on spread and elongation. In this experiments the height of the billet and the tool width were kept constant, while the specimen width was variable. The experiments were carried out using the 1500 kN press at room temperature. 12 groups of specimen with different aspect ratios were used. Each group consists of 5 specimens each one was subjected to 5 different height reductions as shown in Table 9. In order to soften the metal sufficiently all these specimens were annealed at 425^0 for two hours and then cooled in air as in the other cases. In Fig 5.13 a series of partially compressed billets with different initial aspect ratios are shown in horizontal and vertical views.

5.4.3 Cyclic compression and rotation of the billet

In this part of the work initially square section billets were used to facilitate specimen alignment and location between increments. The billets had an initial cross-section 17mmx17mm, a length of 110mm and were annealed at 425^0C for two hours. Two types of test were conducted

a) Single cycle compression-rotation process

In this part, the workpieces were subjected to only one compression-rotation cycle to reduce the cross-section of the billet incrementally with a given penetration. The workpiece was compressed locally and rotated through 90^0 and then compressed again. Fig 5.14 shows some forged specimens, the corresponding data being given in Table 10.

b) Multi cycle compression-rotation process

In this second part the compression-rotation cycles were repeated. Some of the specimens compressed in the same way are shown in Fig 5.15 with the corresponding data in Table 11.

5.4.4 Single squeeze compression using various tool widths

The effect of tool width on the metal flow was investigated by using four different tool widths of 10, 20, 30 and $40mm$ to compress four groups of specimens, each group comprising four different aspect ratios as shown in Table 3. The spread was measured and volume displacement in the axial direction was calculated for each compressed billet individually. In Fig 5.16 one step compressed billets by using 10, 30, and 40mm tool widths are shown.

5.5 Displaced Volume Calculation Methods for Experimental Work

In forging the nature of metal flow is usually complicated and difficult to predict because of the shape complexity after each forging step. In open-die forging the calculation of the volume of material displaced from under the tool in the axial

direction and lateral bulged profile is crucial.

The actual shape of workpiece after compression is not easily defined due to bulging and this makes it difficult to measure the exact forged dimensions. Because of bending and distortions it is also not easy to work out the amount of bulging and elongation and this impedes the determination of spread, the volume of material remained under the die and of longitudinal material displaced in the longitudinal direction after each single squeeze. The remaining volume under dies can be worked out in a variety of ways based on the following methods:

1) Cutting off the partially forged material and weighing its mass.

2) Using Archimedes principle.

3) Measuring maximum width of the billet and using a corresponding function to quantity an assumed profile form.

4) Use of Imaging machine

5) Digitising the bulge profile

6) Measuring the length after compression

During the experiments only methods 3 and 6 were used successfully. Therefore these methods will be described below, details of the others being given in Appendix-A.

5.5.1 Calculation of displaced volume based on measuring maximum width of the billet

In this method the remaining volume under the tool is calculated by measuring the maximum spread, at the centre of the billet. By using minimum and maximum points numerically a theoretical function can be found to describe the assumed spread profile and for rapid calculations this area can be converted to an equivalent rectangular area during rotation of the billet. The mean width of the sideway bulging can then be found by substracting the remaining volume from the original contact area, between tool and material. The amount of displaced volume in the longitudinal direction can be determined by multiplying this area with current height of the billet.

In order to work out an equivalant volume of the lateral bulging "Lagrange's Interpolation Polynomial" method is used based on at least three known points. The relevant figure is shown in Fig 5.17 and the generalised formula for this is given as follows;

$$f(x) = f(x_0) + (x - x_0)\frac{f(x_0)}{(x_0 - x_1)} + \frac{(x - x_0)(x - x_1)}{(x_0 - x_1)(x_0 - x_2)} f(x_0)$$

$$+ \frac{(x - x_0)(x - x_1)}{(x_1 - x_0)(x_1 - x_2)} f(x_1) + \frac{(x - x_0)(x - x_1)}{(x_2 - x_0)(x_2 - x_1)} f(x_2) \qquad (5.7)$$

Here, first, second and third terms become zero due to the geometry of the billet, Substituting the numerical values of x_0, x_1, x_2 from the geometry of bulge, shown

above, into Eqn 5.7 a parabolic function for the sideway bulge is found as follows;

$$f(x) = (1 - \frac{4\,x^2}{l^2})\,\Delta w \tag{5.8}$$

Integration of (5.8), gives the hatched area under the parabolic curve

$$A_{BSE} = 2\int_0^l (1 - \frac{4\,x^2}{l^2})\,\Delta w\,dx \tag{5.9}$$

gives:

$$= \left[x - \frac{4}{3}\frac{x^3}{l^2}\right]_0^l \Delta w \tag{5.10}$$

$$A_{BSE} = \frac{2}{3}\,l\,\Delta w \tag{5.11}$$

and the area of BSE can be easily converted to a rectangular,

$$A_{BCDE} = w_{mean}\,l \tag{5.12}$$

From the idea of equivalant areas of Eqn 5.11 and Eqn 5.12, the following equation must be satisfied and if they are equated to Eqn.5.13;

$$A_{BSE} = A_{BCDE} \tag{5.13}$$

w_{mean} is found as;

$$w_{mean} = \frac{2}{3}\,\Delta w \tag{5.14}$$

Hence, by using the formula 5.14 once the maximum bulge Δw is measured from

the compressed billet each time this value is converted to an equivalent straight line. At the same time this w_{mean} determines the height of the billet for the next compression step of the 90° rotated billet. This method was used in the relevant section of experiments to evaluate the rotated billet height after every rotation through the incremental compression-rotation process. Considering Fig 5.17 the displaced volume in the axial direction is calculated by substracting the current or remaining volume under the die from the original volume before compression:

$$ie \qquad V_{orig.} = w_0\, h_0\, l$$

Naturally some amount of volume V_{disx} flows from under the die in the longitudinal direction and it can be expressed in general form as follows,

$$V_{disx} = V_{orig} - V_{rem} \tag{5.15}$$

and V_{rem},

$$V_{rem} = 2\, A_2\, h + w_0\, h_0\, l \tag{5.16}$$

The volume which spreads in the lateral direction but which is still under the die is:

$$V_{disy} = 2\, A_2\, h \tag{5.17}$$

$$V_{tot} = V_{disx} + V_{disy} = 2\,(A_1)\,\delta h \tag{5.18}$$

where V_{tot} is the equivalant of the amount of penetration, (e.g. giving 30% of height reduction will cause 30% of total volume displaced in both directions).

Since reduction in height (penetration) is known, once w_{max} is measured, displaced volume in x direction and lateral displaced volume in y direction can be determined. The measurement of w_{max} is made from the centre of the compressed billet where lateral bulging occurs at its maximum. In practice this is unfortunately not always the case and sometimes the measurement of maximum bulging width (w_{max}) cause errors due to the inconsistency and irregularity of the bulging shape.

5.5.2 Calculation of displaced volume based on measuring length

The displaced volume can be calculated by measuring the extension or elongation in the axial direction. The theoretical model again based on a parabolic function but here the assumption was made on only a small part of bulge surface which is shown as S in Fig 5.18. If a finite section of dx is taken from only a small part of the forged billet where material moved from under the tools to axial direction the volume of this small part δV can be expressed as follows;

$$\delta V = \dot{w}\, t\, dx \tag{5.19}$$

The billet profile is assumed to conform to a parabolic function;

$$y = a\, x^2 + b \tag{5.20}$$

From the profile of the billet,

at $x = 0 \qquad y = w_{max}$

at $x = D + S \qquad y = w_0$

Therefore:

$$b = w_{max} \qquad and \qquad a = \frac{w_0 - {w_{max}}^2}{D + S} \tag{5.21}$$

But,

$$\dot{w} = a\,x^2 + b \tag{5.22}$$

and from the geometry of the forged shape, substituting Eqn 5.21 into 5.22 and,

$$t = t_1 + \frac{t_0 - t_1}{S}.(x - D) \tag{5.23}$$

Substituting Eqn 5.22 and 5.23 into Eqn 5.19 and integration of it gives:

$$\delta V = \left[a\,\frac{x^3}{3} + w_{max}\,t\right]_D^{D+S} \tag{5.24}$$

$$t = c + g\,x \tag{5.25}$$

where;

$$g = \frac{t_0 - t_1}{S} \tag{5.26}$$

and

$$c = t_1 - g\,D \tag{5.27}$$

then substituting these values δV from Eqn 5.24 becomes as follows:

$$\delta V = a\,(x^2 + b)\,(c + g\,x)\,dx \tag{5.28}$$

$$= (a\,c\,x^2 + a\,g\,x^3 + b\,c + b\,g\,x)\,dx$$

By integrating Eqn 5.28 V is obtained:

$$V = \left[\frac{1}{4}a\ g\ x^4 + \frac{1}{3}\ a\ c\ x^3 + \frac{1}{2}\ b\ g\ x^2 + b\ c\ x\right]_D^{D+S} \qquad (5.29)$$

By expanding 5.29, V becomes;

$$V = [K_1(D^4 - (D + S)^4 + K_2\,(D^3 - (D + S)^3 + K_3(D^2 - (D + S)^2$$

$$+ K_4\,(D - D + S)] \qquad (5.30)$$

where:

$$K_1 = \frac{(t_0 - t_1)}{4\ S}\ \frac{w_0 - w_{max}}{D + S^2}$$

$$K_2 = \frac{(w_0 - w_{max})\ t_1 - \frac{D}{S}\ (t_0 - t_1)}{3\ (D + S)^2}$$

$$K_3 = \frac{w_{max}\ (t_0 - t_1)}{2\ S}$$

$$K_4 = w_{max}\ \frac{(t_1 - (t_0 - t_1)\ D)}{S}$$

$$and \quad S = \frac{l - l_0}{2}$$

then substituting K_1 , K_2 , K_3 and K_4 into Eqn 5.30 the final equation of displaced volume becomes as follows:

$$V = (t_0 - t_1)\frac{w_0 - w_{max}}{\left[4\,S(D + S^2)\right]}\left((D^4 + D\,S)^4\right) + (w_0 - w_{max})$$

$$\left[\frac{t_1 - \frac{D\,(t_0 - t_1)}{S}}{3\,(D + S)^2}\right]\{((D^3 - (D\,S)^3) + \frac{(t_0 - t_1)}{2}((D^2 - (D\,S)^2)$$

$$+ w_{max}\left[t_1 - \frac{D\,(t_0 - t_1)}{S}\right](D - (D + S)) \qquad (5.31)$$

Where S and w_{max} are determined directly by measuring the final ends and maximum sideways spread of width on the compressed billet. Then, by computing Eqn. 5.31, the displaced volume can be worked out for each single compression step. It should be noted that accurate length measurements are considerably difficult to make because of bent and distorted workpieces. The advantage of the method is that it gives the volume displaced in axial direction within the minimum of assumptions. Thus the calculation error will be small and also the method seems reliable but it does however need accurate displaced length measurements.

In order to evaluate these possible solutions for finding displaced material volume in lateral and axial directions a series of experiment was carried out. 12 groups of specimens were machined to have different aspect ratios of (w_0/h_0). Each group consists of 5 specimens each to be given 5 different penetrations of 10% , 15%

, 20% , 25% and 30%. The height and the length of billets were constant, the width (w_0) being used to change the aspect ratio of (w_0/h_0).

5.6 Results and Discussion

The experimental forging undertaken under dry conditions was directed mostly to validate the theoretical metal flow and forging load predictions. The experimentally obtained results were compared with the theoretical predictions in the working range by examining the critical characteristics such as spread, remaining cross-sectional area under dies and the material volume displaced into the axial direction and load. In pressing a small part of the bar which has a rectangular cross-sectional area the profile of sideway flow is approximately a parabola. The only parameters which were used to calculate the maximum volume between two flat dies were the maximum width of spread, displaced length, die width and billet height. It is also useful to show the reduction of cross-section after each compression step. Fig 5.19 shows the plotted experimental results of maximum remaining cross-sectional area with predicted theoretical curves for various aspect ratios and friction factors. Three billets having the same initial dimensions of width w_0, height h_0 and length l_0 were subjected to incremental compression. Then a series of billets were machined and compressed separately by given different height reductions starting from 5% up to 50%. These two different cases are illustrated in the same figure by the symbols of 'O,Δ,$\square$,' for incremental compressed billets and '*' for separately compressed ones. It is clear from the graph that the cross-sectional area of the billet after compression decreases while

the width increases and height reduces. It is also seen that while the trend shows that billets compressed in an incremental manner give a little higher spread than those which deformed in one step, the difference is small and virtually negligible.

The theoretical load predictions for the first set of experiments of incremental forging of the rectangular long bars are shown in three different graphs for different solutions together with the experimental results; Fig 5.20 based on the rectangular velocity field, (SODIREC), Fig 5.21 based on the triangular velocity field, (SODITRI), and Fig 5.22 which is based on a parabolic velocity field, (SODIPAR). As it can be seen from those graphs the predictions are in good agreement with the experimental results against various aspect ratios of the billet at each stage of incrementation process in relating the initial aspect ratios,IAR. As the number of squeezes increases, the pressing area/contact area between dies and workpiece also increases together with the forging load. Friction and billet aspect ratio have a major influience in determining forging load. From the theoretical curves it is seen that the effect of friction is increasing with increasing aspect ratio. For example in Fig 5.21 at $m = 0$ and $w_0/h_0 = 2$ the forging load $= 200kN$ but; at the same aspect ratio of w_0/h_0 and $m = 0.6$ the forging load goes up to ˜ $500kN$.

The correlation for SODIREC in Fig 5.20 seems better for high initial aspect ratios but in practical terms for block forming the working range mostly used is $0.5 < w_0/h_0 < 2$. In that sense the second and third solutions give better correlation with experimental results. From those graphs it can be seen that the

prediction values are higher than the experimental results and this is probably due to the nature of the upper bound method which always gives overestimates. It has also to be noted that the tool width is one of the characteristics which affects the forging load due to the change in contact area whilst pressing.

Prediction of spread was investigated in the past years theoretically and experimentally by producing some empirical formulas or so-called spread coefficients [83, 16, 84, 14]. When dies press the material locally by a given amount of height reduction, material spreads from between those dies in the lateral and longitudinal directions. These are the most important characteristics of deformation pattern which need to be predicted. Fig 5.23 and 5.24 show the first set of experimental results and corresponding theoretical maximum spread and spread in percentage predictions plotted against initial aspect ratios separately for single step compressed billets with different height reductions. From the figures it can be seen that the theoretical curves are reasonably in good agreement especially for lower height reductions. Because the workpieces were compressed under dry conditions then as the penetration level increases the bulge shape becomes difficult to measure due to workpiece distortions and nonlinear flow in both lateral and axial directions. This case is seen in the same figure for 30% height reduction level. The amount of material expressed as percentage, in both free lateral directions decreases with increasing initial aspect ratio. However this means that the material flows in the axial direction increases while the percent of remaining material under tools decreases. The actual profiles of the theoretical spread predictions and experimental values in the lateral side along a quarter of the billet deforming zone are given in Fig 5.25 for four different aspect ratio billets. The

results show that the spread profile lines and curves increase with increasing IAR and penetration. As it is seen the predictions are in fairly good agreement with the experimental values.

The effect of tool width on metal flow was also investigated. The experimental results for spread are plotted in Fig 5.26 as direct measurement of spread in *mm* and in Fig 5.27 the total percentage of metal flow in both free lateral sideway directions is shown and compared with the theoretical predictions of SODITRI and SODIPAR. The results show that for billets of the same aspect ratio when the tool width is small the amount of percent material flow into the lateral direction increases.

Material elongation was predicted and tested against experiments. In Fig 5.28 the predicted and experimental values of elongation were plotted against different aspect ratios and penetrations. From these results it can be seen that the amount of material elongated in the axial direction increases with increasing aspect ratio and penetration. These results can also be translated into the displaced volume which has a crucial role in terms of controlling the whole process continuously. This parameter was investigated in two ways. First, as described earlier a group of billets having different aspect ratios were compressed with various height reductions. The volume displaced in the axial direction was calculated for each billet. In Fig 5.29 and 5.30 the experimental results and theoretical predictions were plotted against the variation of material displaced in the longitudinal direction against initial aspect ratio at various penetration levels. In fact this may be one of the most difficult issues to work out experimentally due to the shape

complexity and irregularity of forged workpieces. Various displaced volume calculation methods were investigated and details are given in Appendix-A. In this chapter the experimentally plotted values in the relevant figures were provided by using the method described in 5.4.6. It was shown that the displaced material moved away from under tools in the axial direction increases with increasing initial aspect ratio of the billet and also with the penetration level. Secondly as described earlier, a series of billets having the same aspect ratio of $w_0/h_0 = 1$ were subjected to a continous multi-cycle compression and rotation 90° process . The other parameter which has an effect on the volume dispacement is tool width. The effect of tool width on volume displaced in the axial direction was also investigated experimentally and compared with the predictions by the SODIPAR for different tool widths. Both experimental and theoretical results are given in Fig 5.31 and 5.32 from where it can be seen that while the tool width increases the percentage of volume moved into the axial direction becomes smaller as the penetration given to those billets remains at 25%. This was however hampered by the difficulty in measuring the bulge shape particularly for the billets which were compressed by smaller tool widths. Nevertheless both theory and experiment show similar trends. Fig 5.33 shows the variation of displaced volume with the number of compression cycles and height reductions for continously compressed and rotated billets.

Since the workpiece initial aspect ratio and cross section changes and the deforming cross sectional area reduces after each compression step the volume displaced into longitudinal direction increases. The theoretical predictions are a little higher than those experimental plotted results due to the difficulties in measuring the

final dimensions.

The final dimension requirements in open die forging can only be achieved if the volume of material between the tools remains, at all times, greater than that of the final product. Therefore it is very useful to present the data in terms of the local initial and final aspect ratios after each compression step. In Fig 5.34 and 5.35 the experimental results and corresponding predictions of the final aspect ratio after the each compression are plotted against the initial aspect ratio before compression for the SODITRI and SODIPAR solutions respectively. The final maximum aspect ratio increases with increasing initial aspect ratio and the penetration level for the same tool width. The relation between IAR and FAR appears to be almost linear. In addition some experiments were carried out for various tool widths to examine the change in final aspect ratio and the results were plotted in Fig 5.36 and 5.37 for the solutions of SODITRI and SODIPAR respectively. As it can be seen from these graphs the test results and predictions are in a very good agreement.

Up to now the cases described and the results discussed have been for billets which were subjected to compression only on one side, no rotation was involved. In most cases in open die forging the final required dimensions are achieved by reducing the cross-section of the workpiece gradually by rotating it stepwise by 90^0 during the process. As the cross-section of deformed part of the billet is reducing after each compression-rotation cycle the initial aspect ratio also changes locally. That means that the aspect ratio after compression of the locally deformed billet will always be changing through the cycles and the final aspect ratio, after the

rotation, will be the initial starting aspect ratio for the following compression step of the process. The aspect ratio after compression and 90^0 rotation was named as CRAR and the results of SODIPAR theoretical predictions and experimental values are plotted in Fig 5.38 against IAR. Here it should be pointed out that the information from this figure will become an important determining parameter and be used in the following chapter for controlling the process in a continous manner. In Fig 5.42 the variation of predicted and experimental volume displaced values with IAR for multi cycled compression-rotation process against the number of compression step is shown. The corresponding pictures of deformed workpieces was also shown earlier in Fig 5.14 and in Fig 5.15 for one and multi cycled compression rotation process individually.

If it is necessary to make a comparison between those solutions one could say that each method has some advantages and disadvantages depending up on the experimental set up, holding device, forged shape geometry and measurement facilities. From the overall results it can be concluded that the parabolic solution appears to give the closest results to those of the experiments. The results of these unitary tests between flat tools forms the basis for an incremental open die forging strategy described in the following chapter. The trends of these curves indicates that it is viable to pre-design production routes for feature making and that rapid execution of such programme could be accommodated via a computer controlled set up.

a)

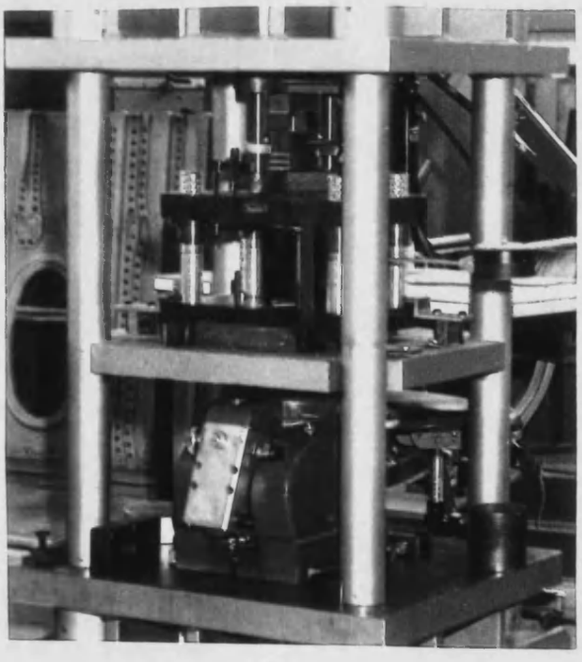

b)

Figure 5-1: Hydraulic Forging presses with tool set a)Numerically controlled b) manually operated.

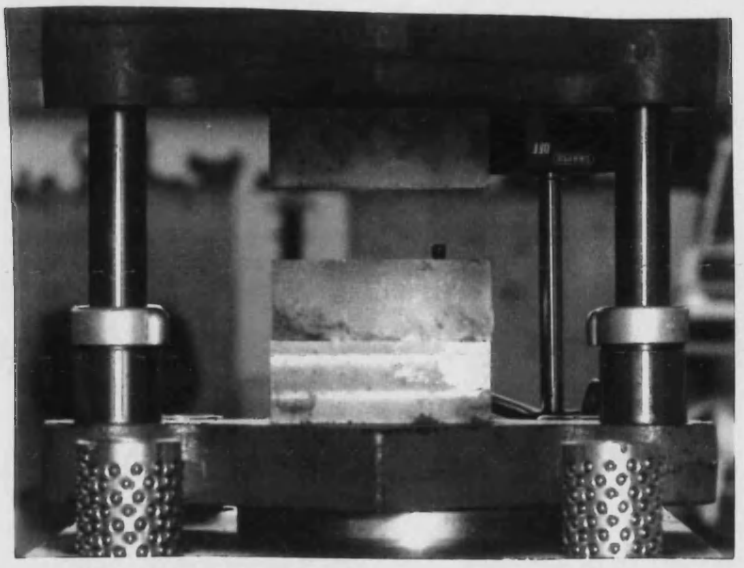

a)

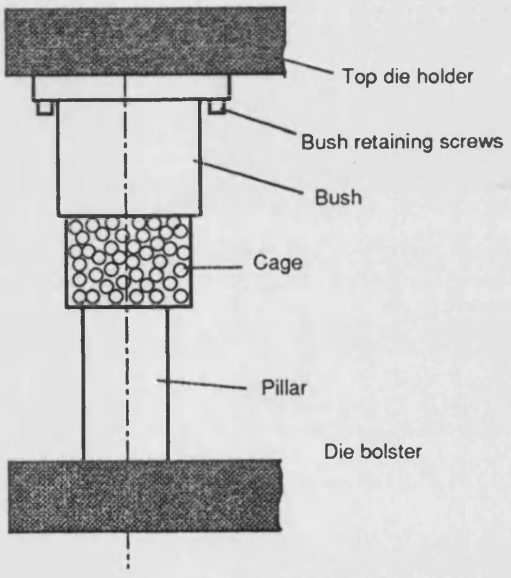

b)

Figure 5-2: a)Tool set with simple flat tools b)Tool set showing only one side of pillar.

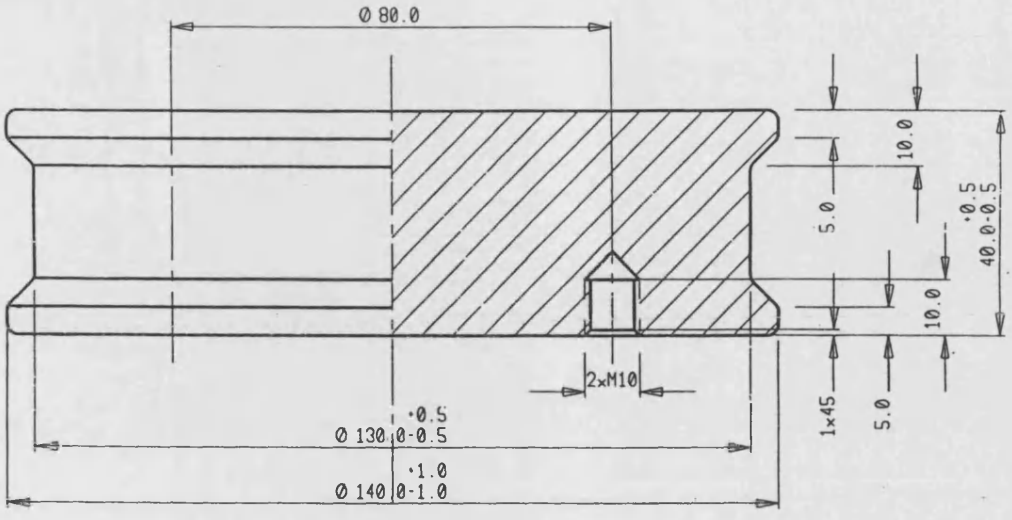

Scale: 1/1

Material: Tool Steel

Figure 5-3: Load cell.

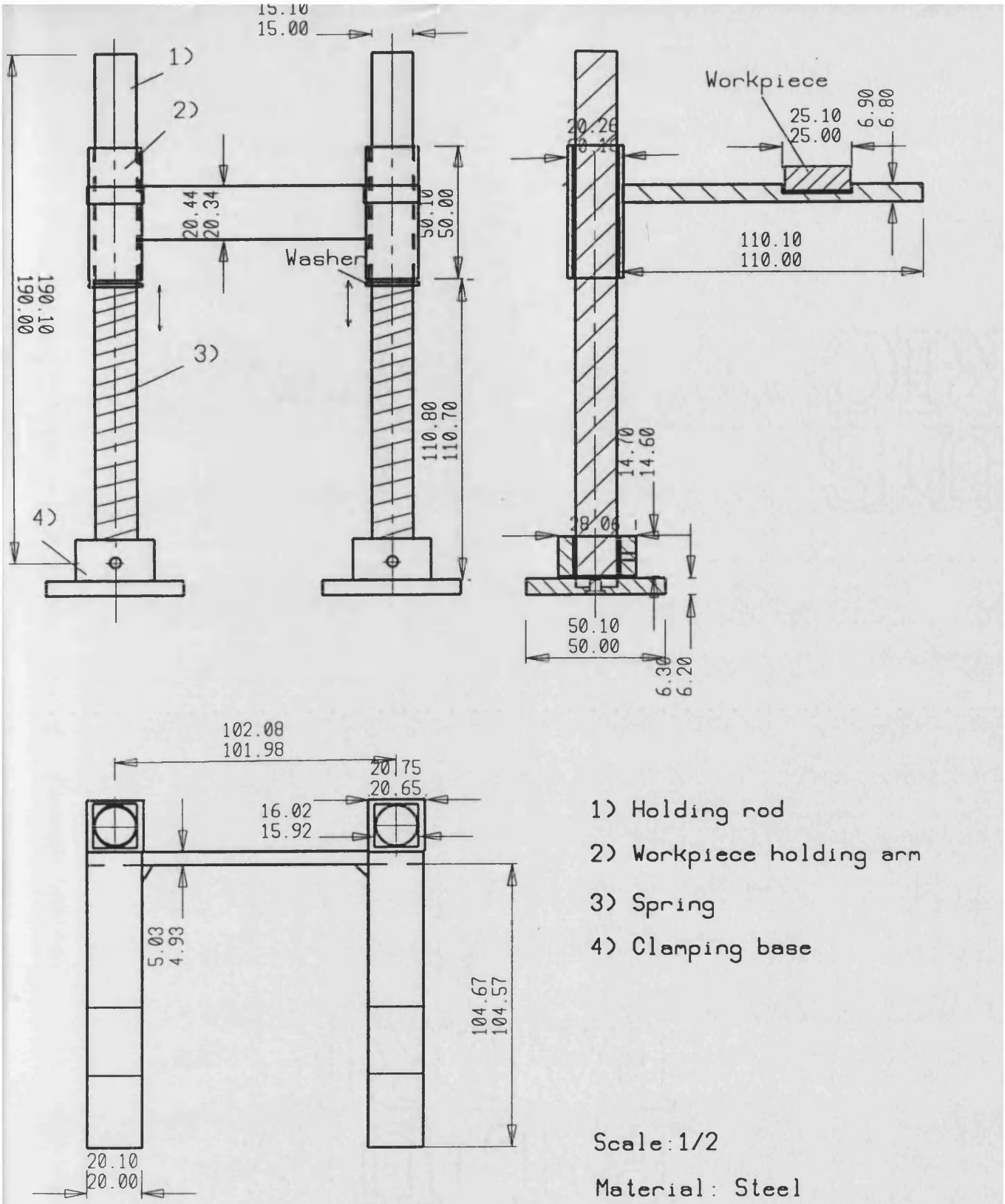

Figure 5.4: Workpiece holder-I.

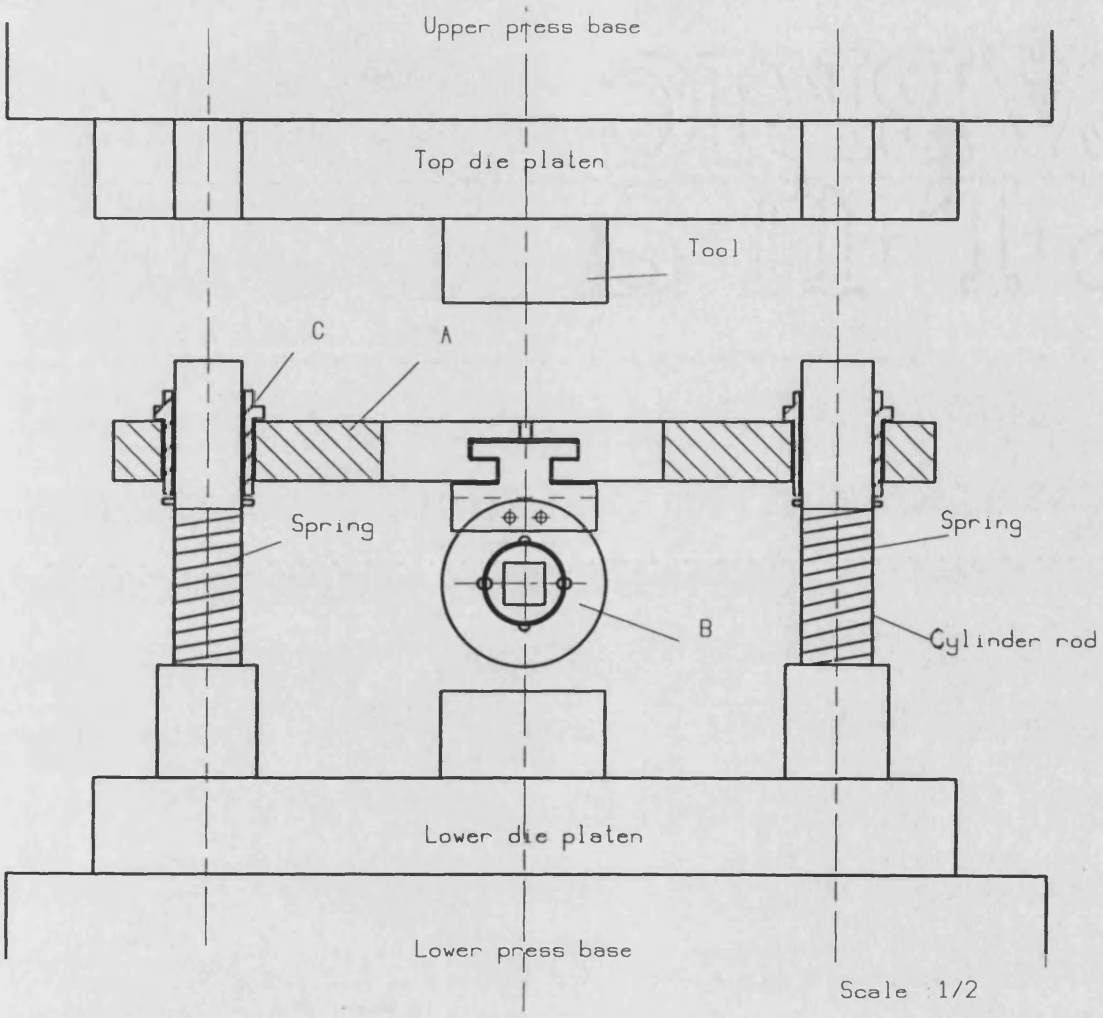

Figure 5-5: Dieset and workpiece holder-II.

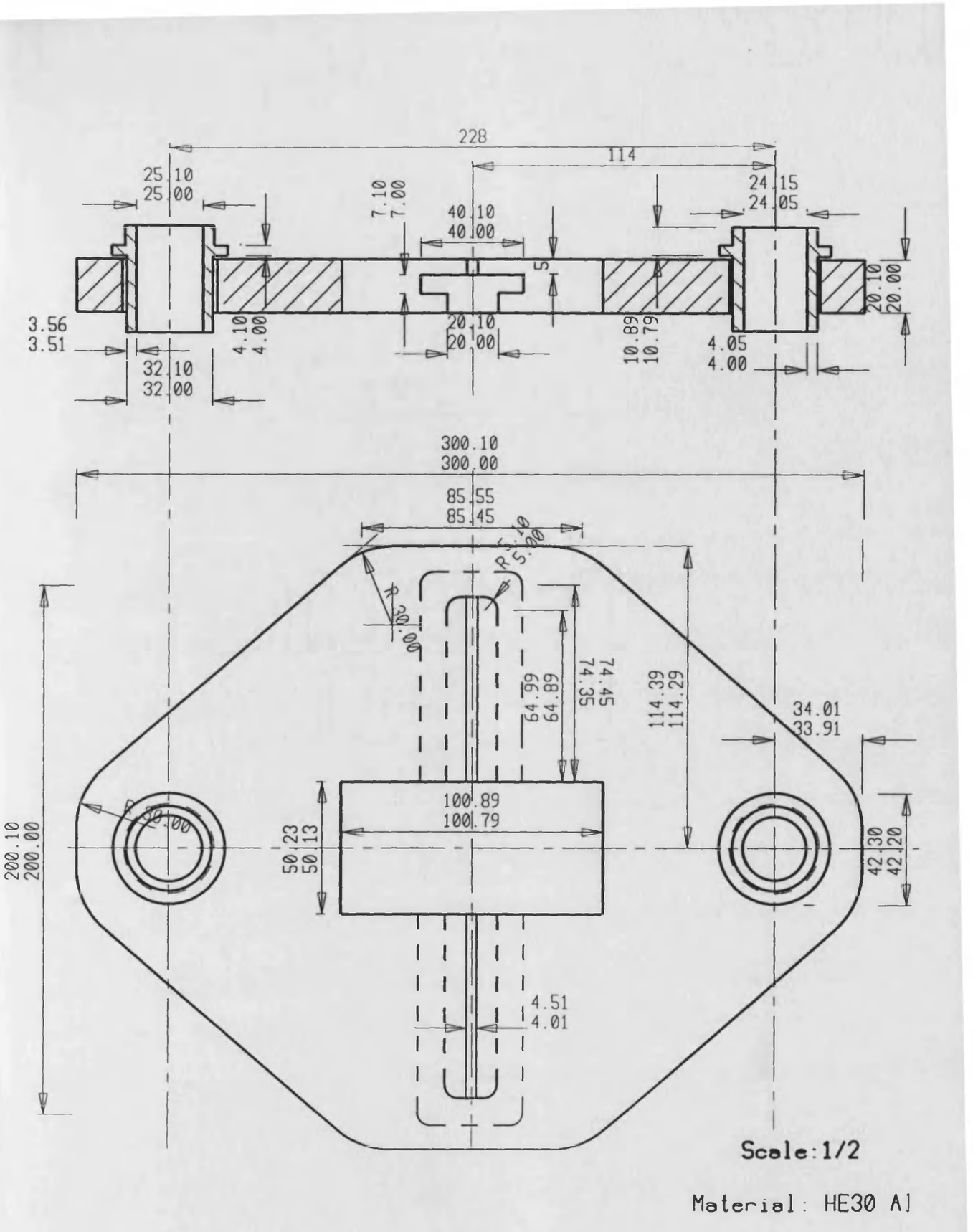

Figure 5-6: Workpiece holder plate-II.

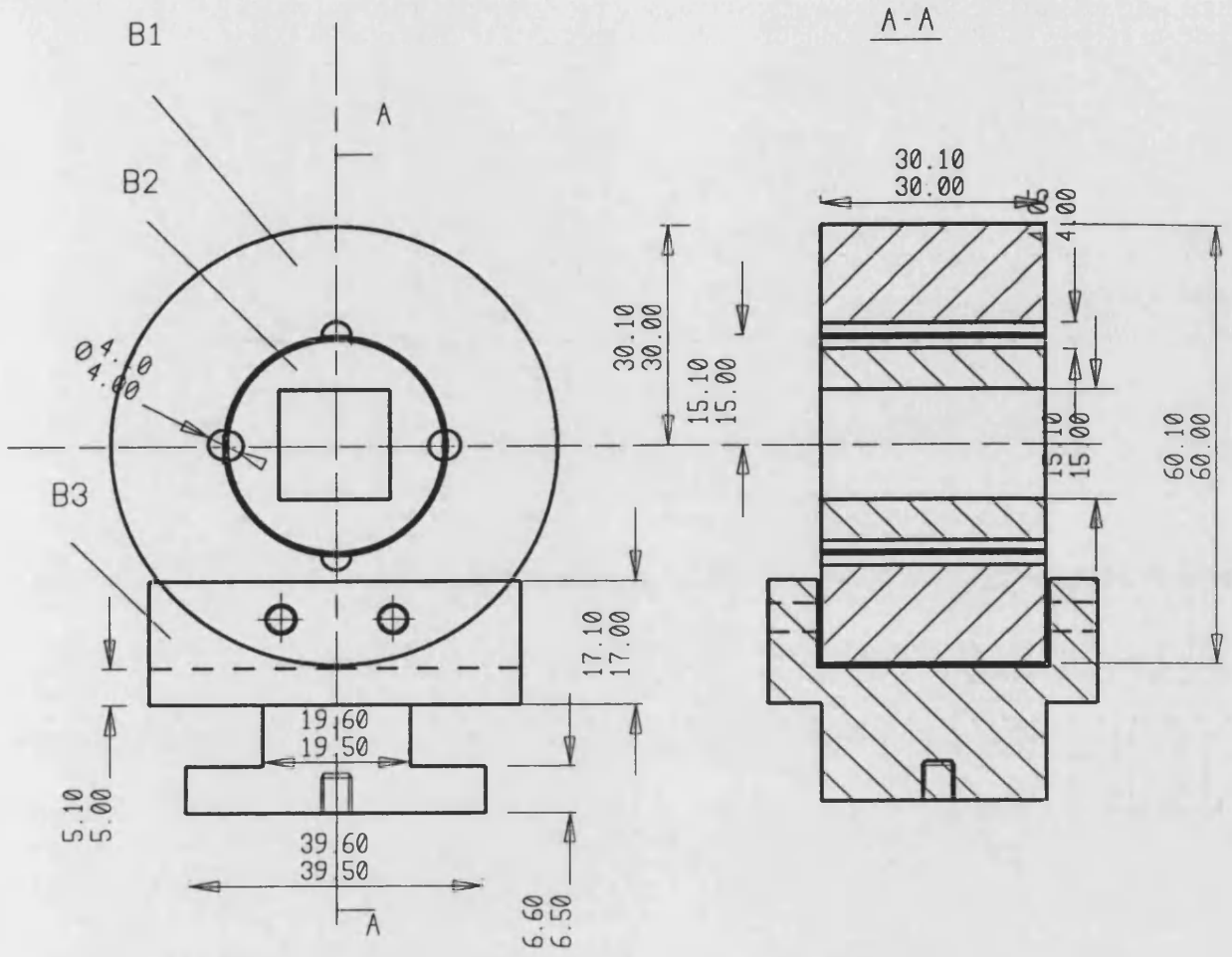

Figure 5-7: Workpiece holder-II.

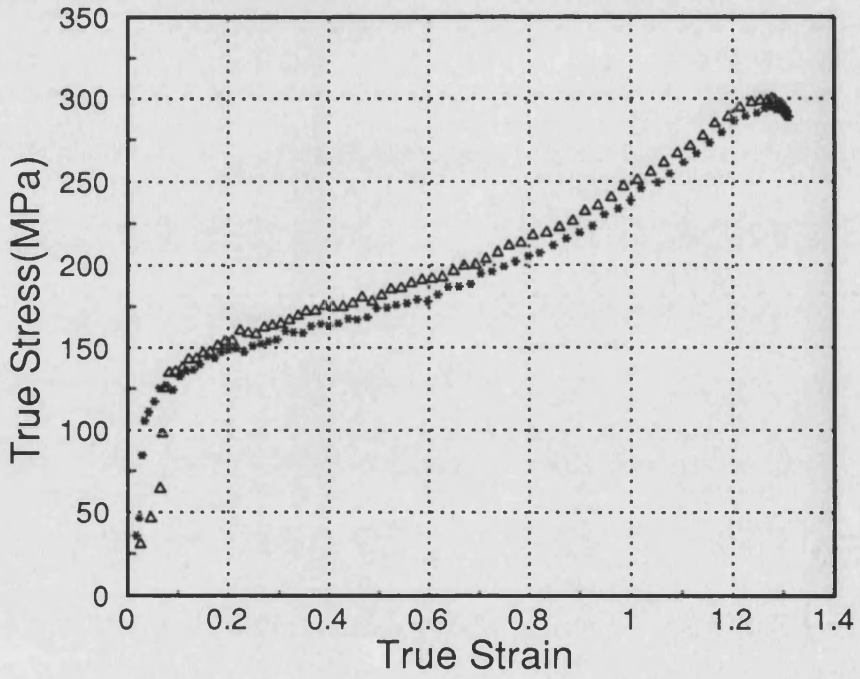

Figure 5-8: Progressive stress-strain curve for 6082Al.

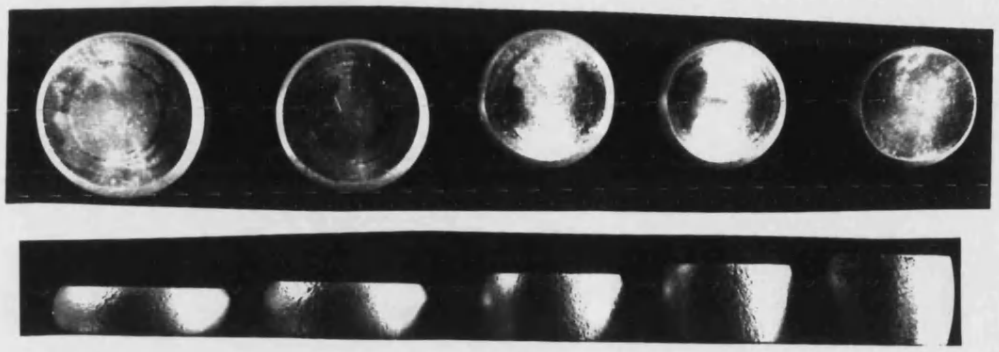

a)

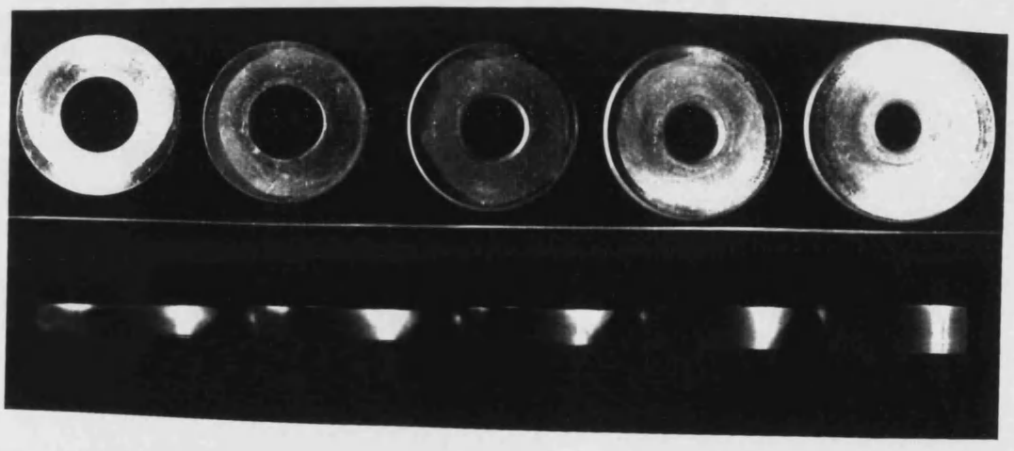

b)

Figure 5-9: A series of deformed a)compression and b)ring specimens.

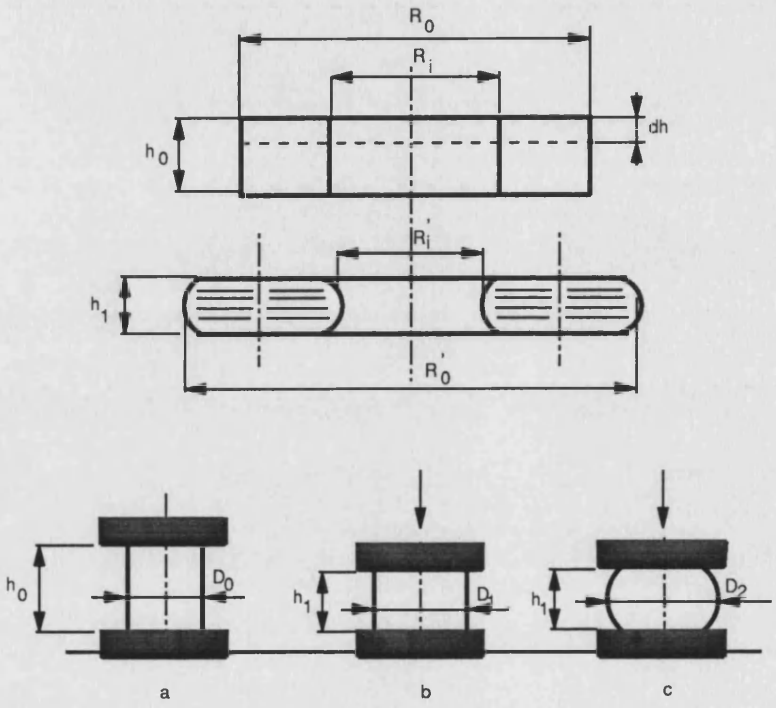

Figure 5-10: Schematic illustration of dimensions in ring test.

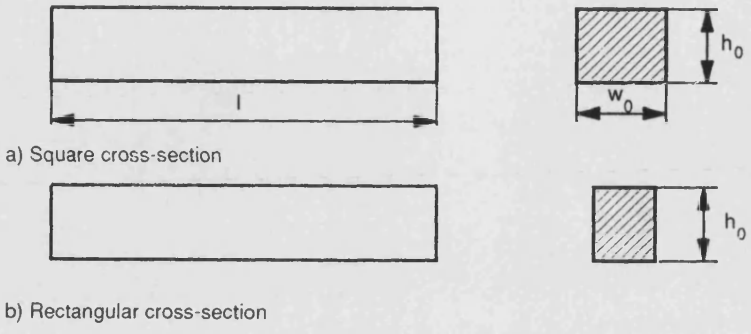

Figure 5-11: Aluminium (6082) specimens

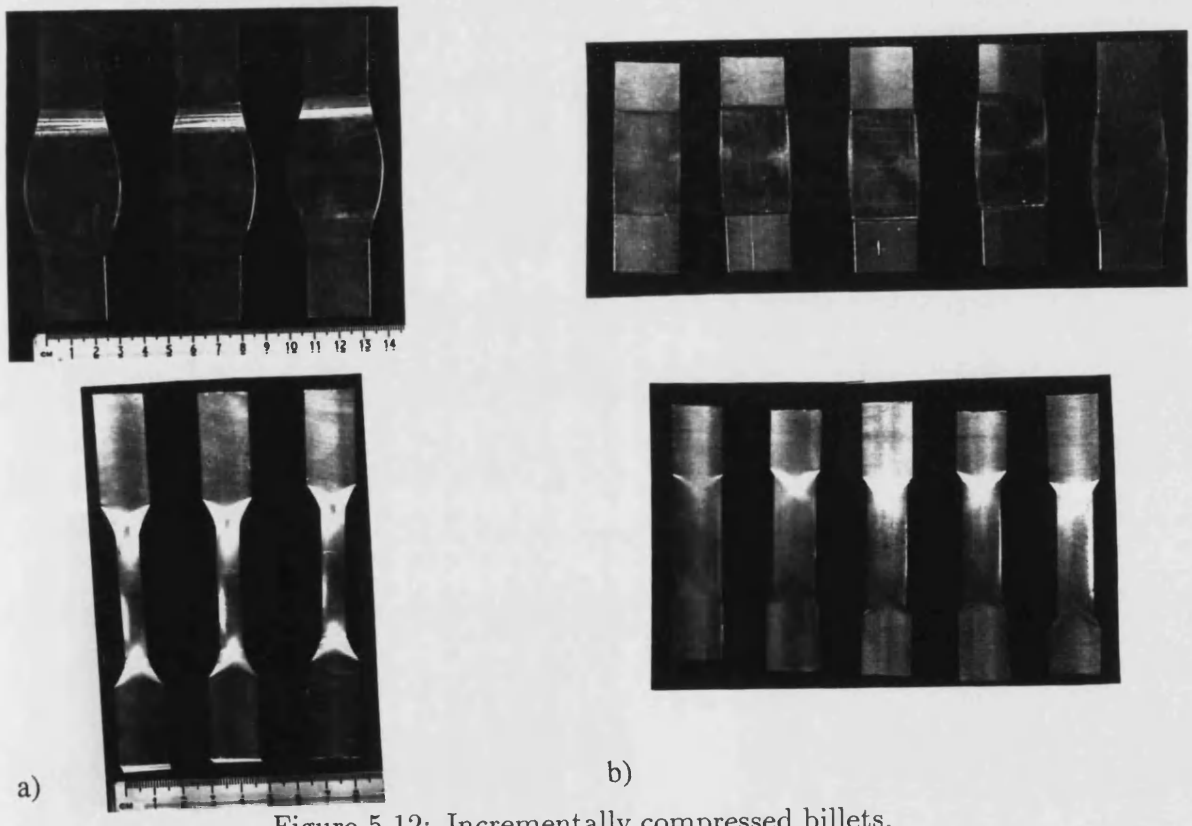

a) b)

Figure 5-12: Incrementally compressed billets.

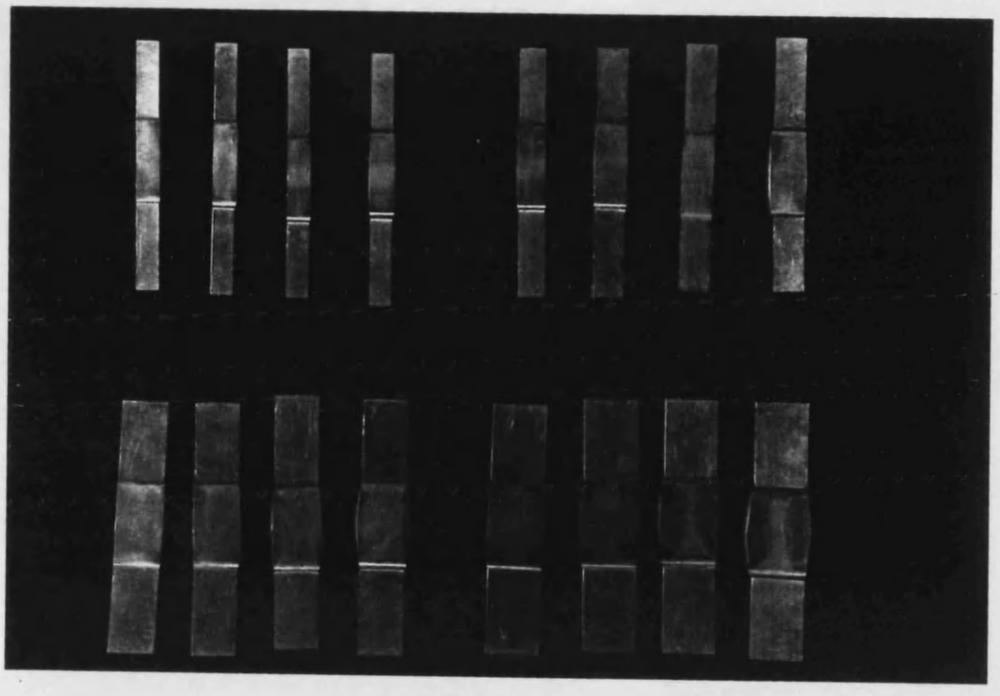

a)

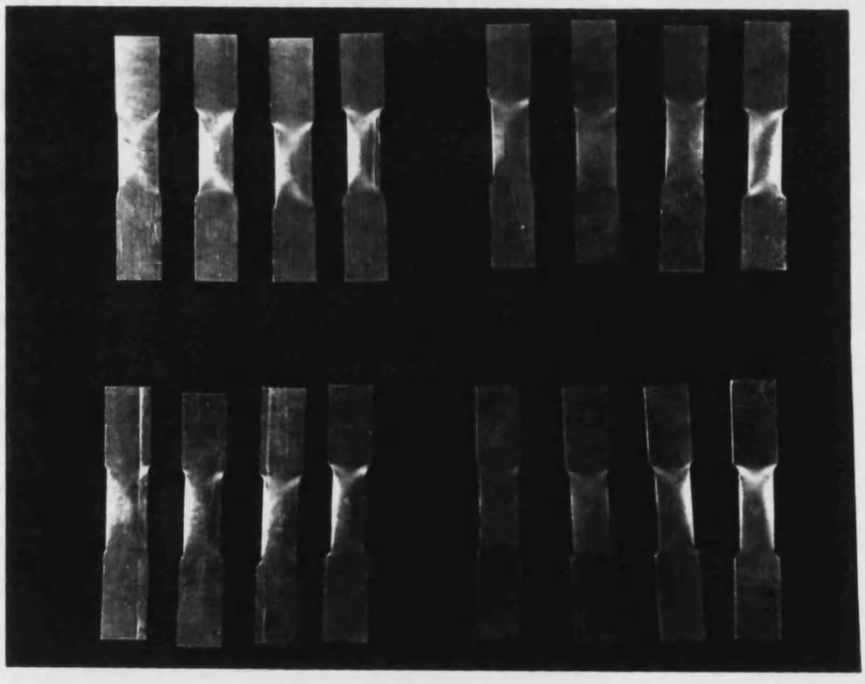

b)

Figure 5-13: A series of compressed billet from different initial aspect ratios. a)horizontal view b)vertical view

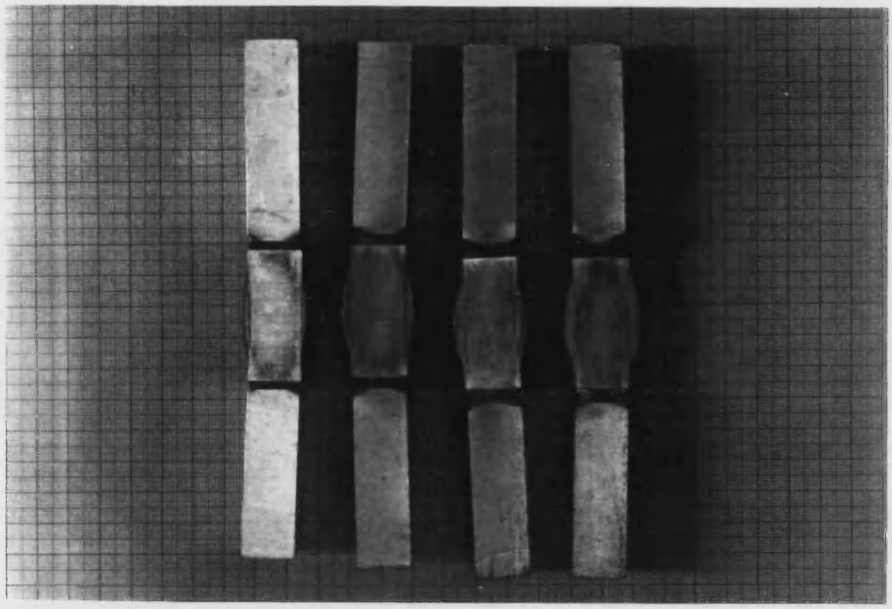

Figure 5-14: Specimens each one subjected to one compression-rotation-compression process.

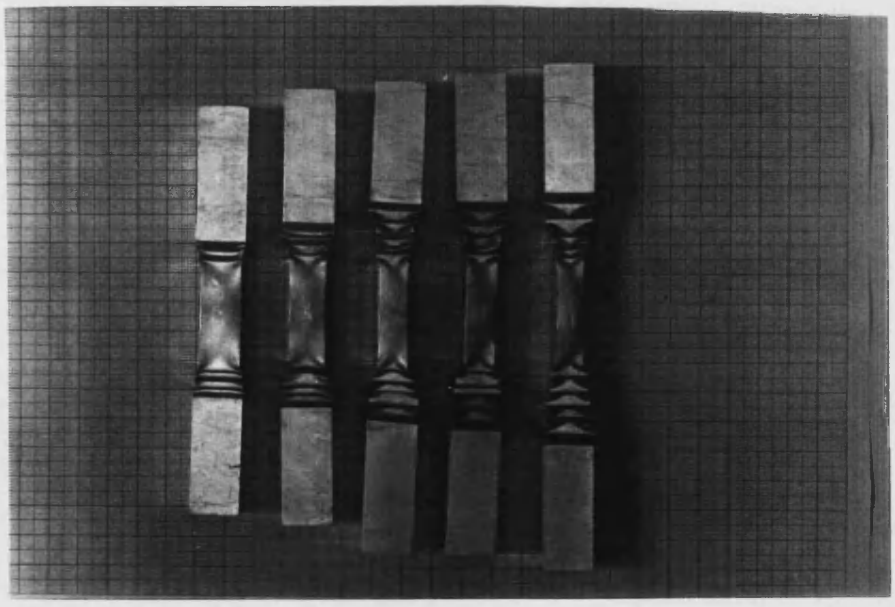

Figure 5-15: Specimens each one subjected to a few compression-rotation cycles

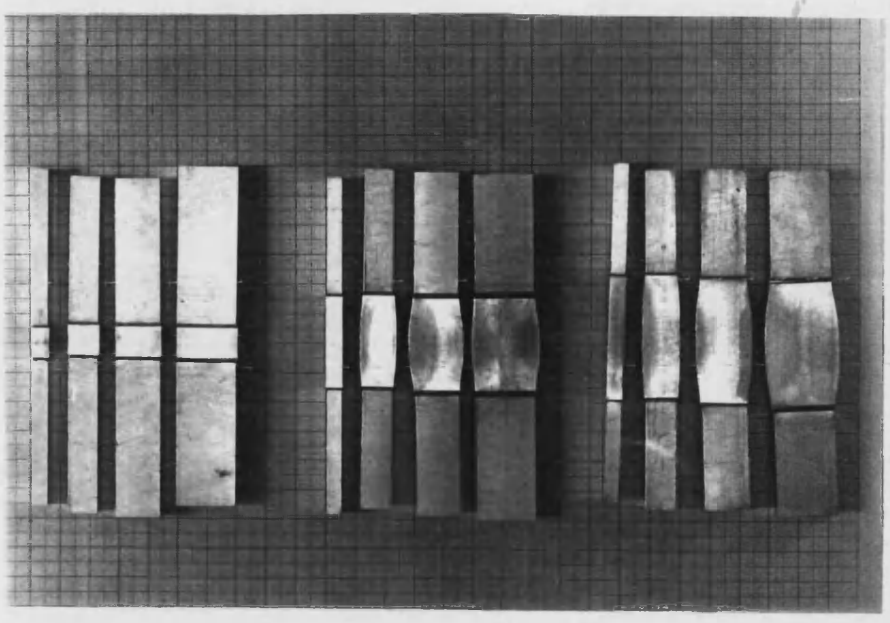

Figure 5-16: Specimens each group subjected to compression using different tool widths.

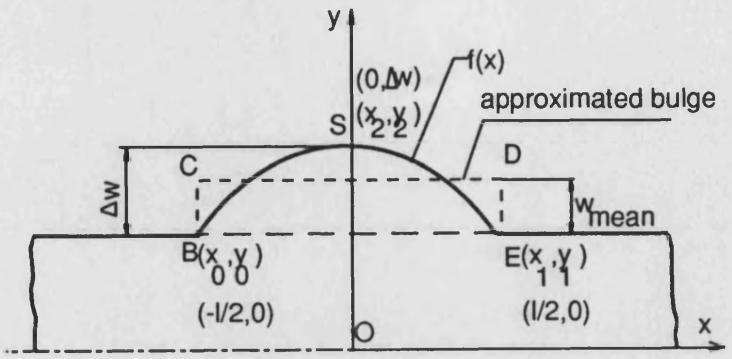

Figure 5-17: Actual lateral bulging and its idealised equivalant.

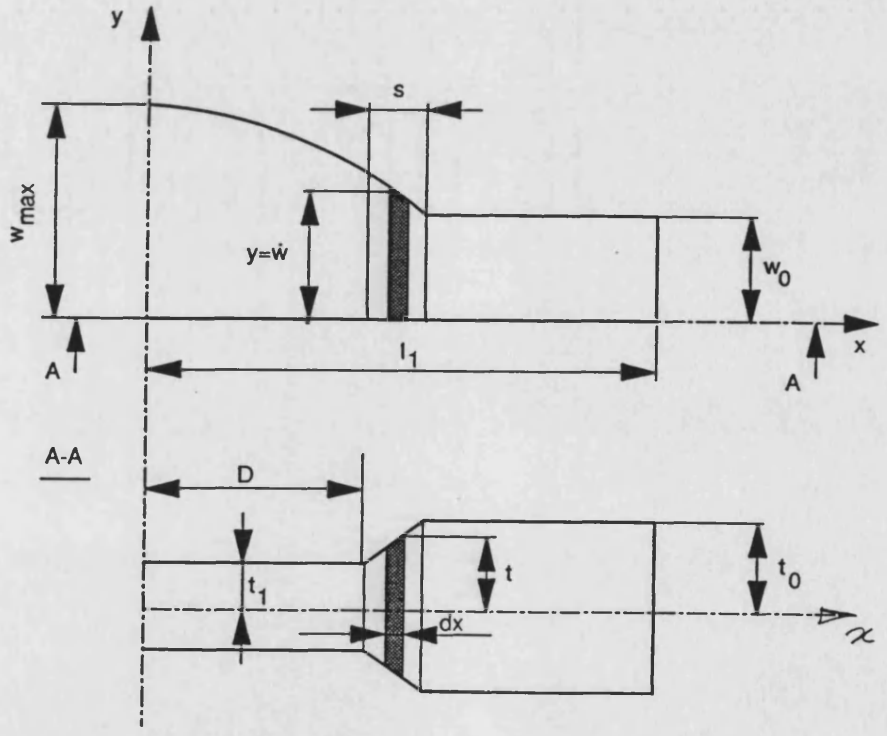

Figure 5-18: A locally compressed billet with two view.

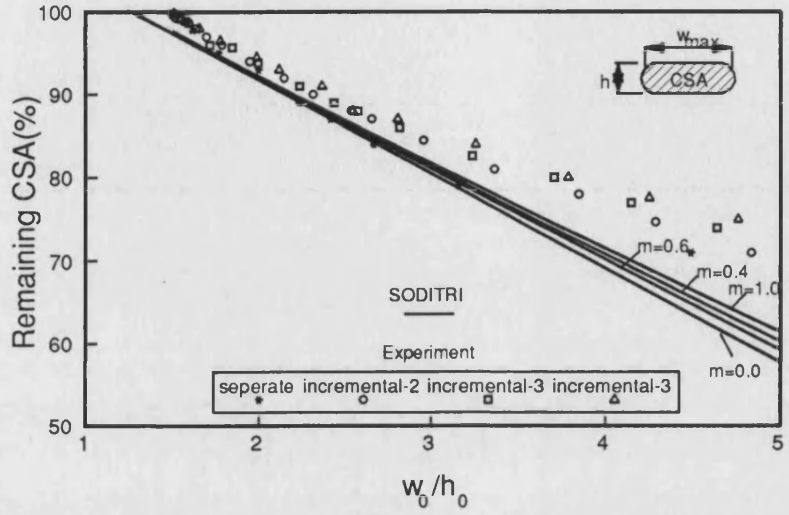

Figure 5-19: Variation of cross-sectional area remained under tools with aspect ratio of w_0/h_0 after compression.

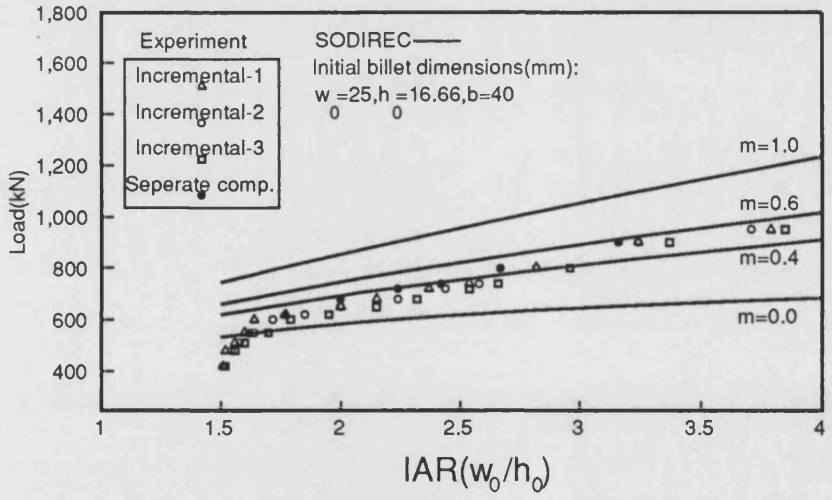

Figure 5-20: Variation of load with the initial aspect ratio and different friction factors for the SODIREC.

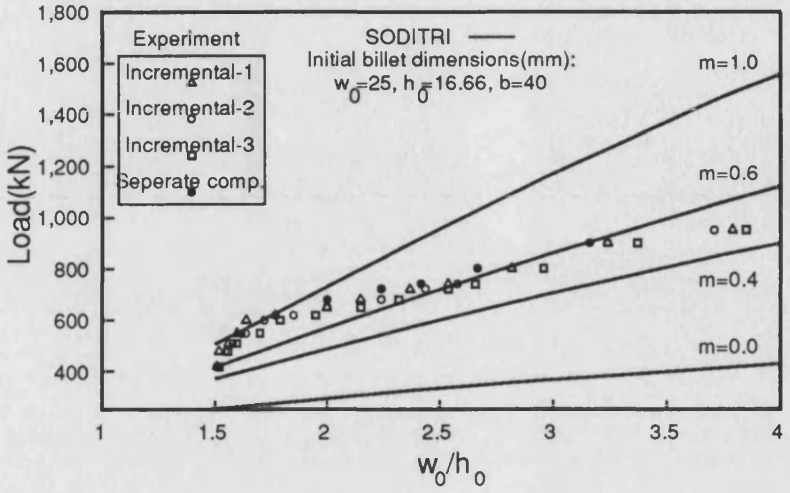

Figure 5-21: Variation of load with the initial aspect ratio and different friction factors for the SODITRI.

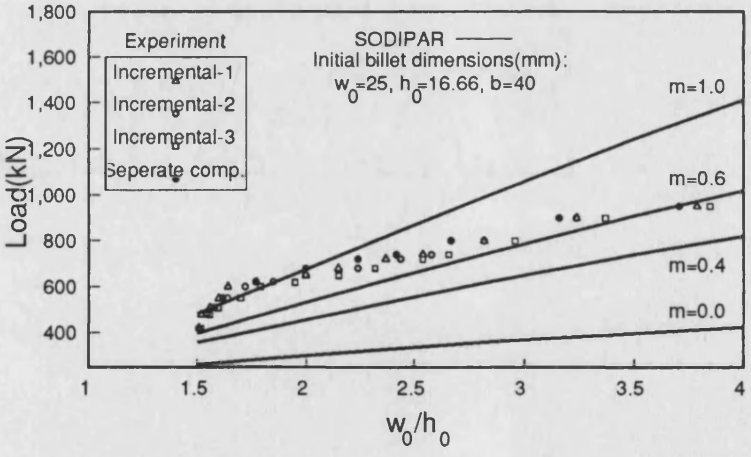

Figure 5-22: Variation of load with the initial aspect ratio and different friction factors for the SODIPAR.

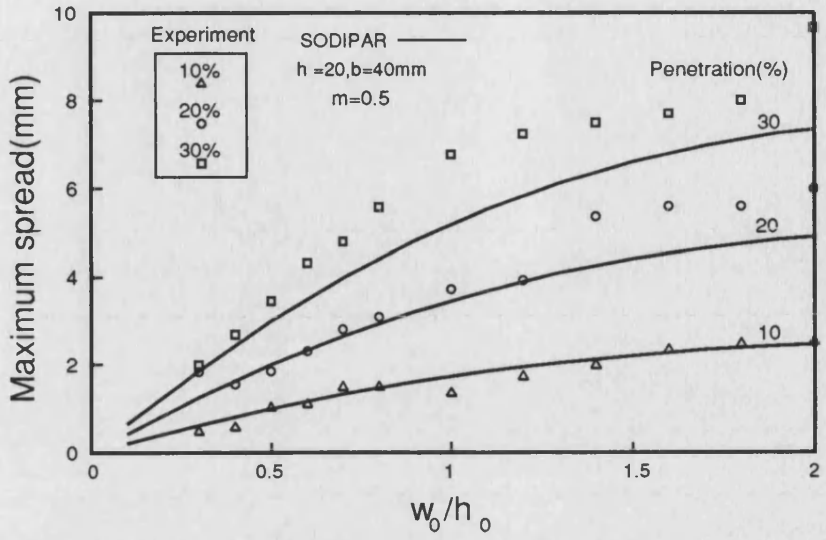

Figure 5-23: Relationship between the spread and the initial aspect ratio of the billet for different height reductions.

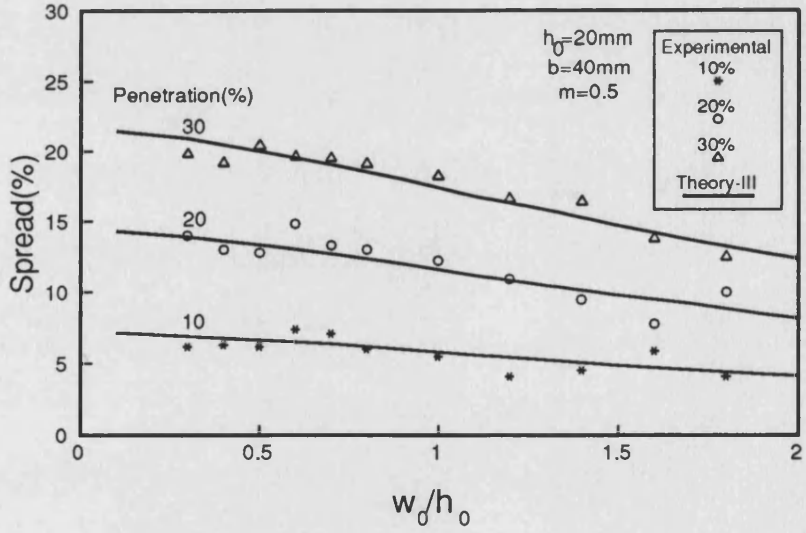

Figure 5-24: Relationship between the percentage spread and the initial aspect ratio of the billet for different height reductions.

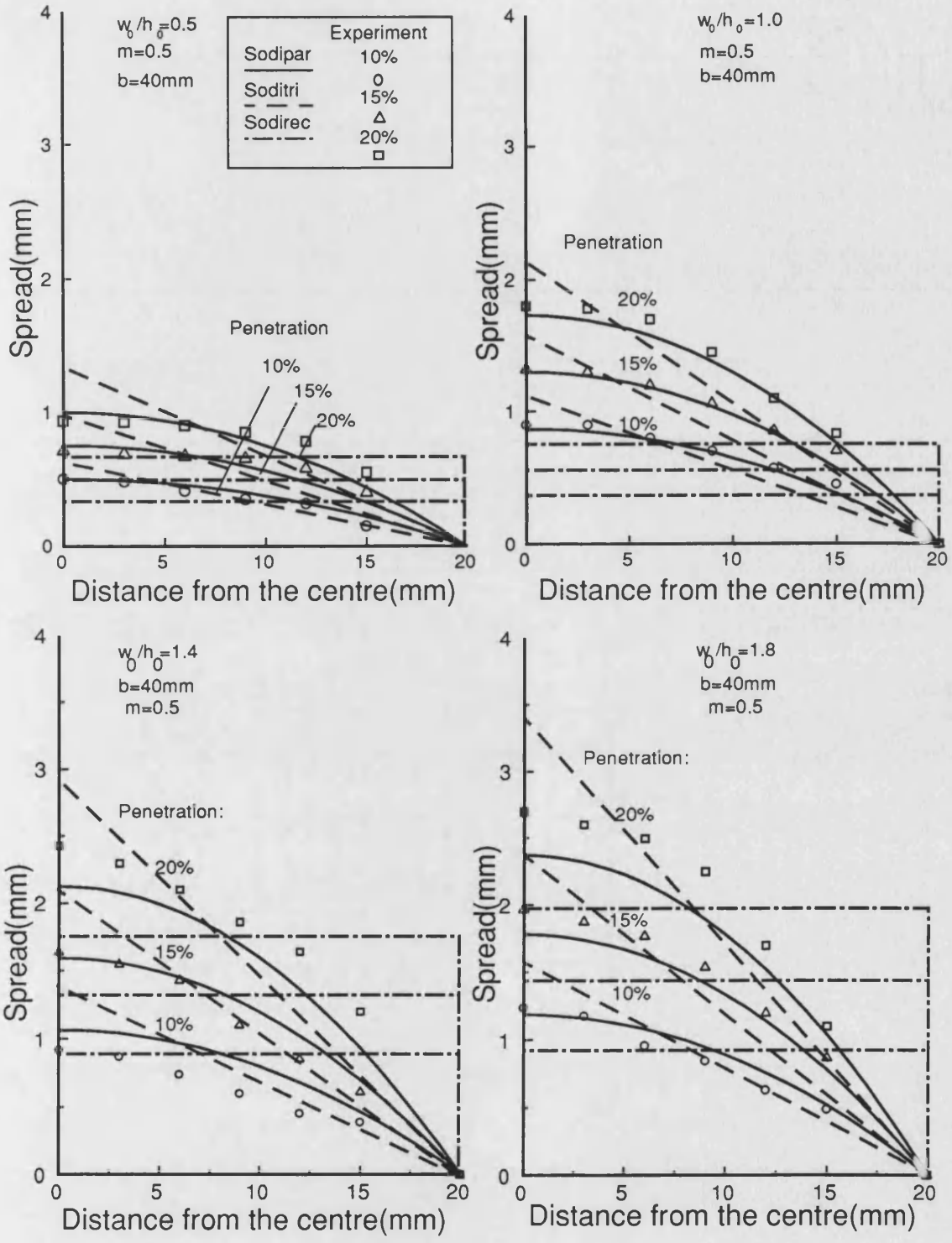

Figure 5-25: Predictions and experimental values of a quarter of bulge profile along the axial axis.

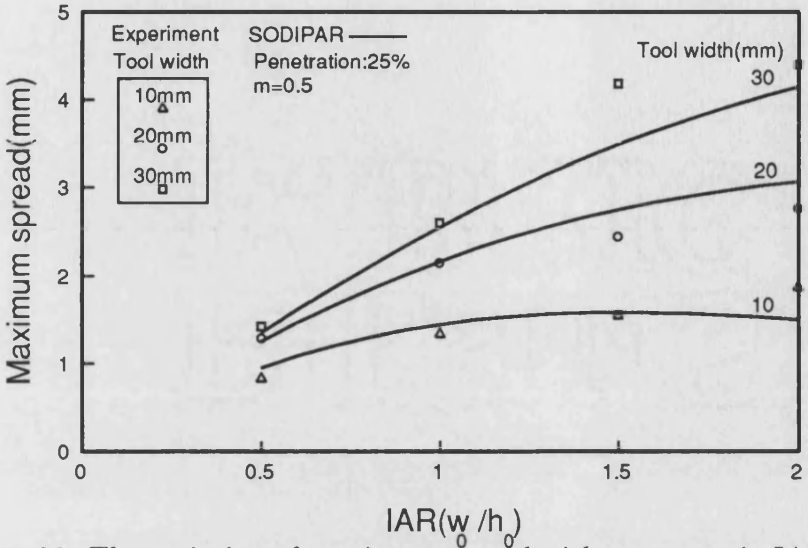

Figure 5-26: The variation of maximum spread with aspect ratio,IAR for different tool widths.

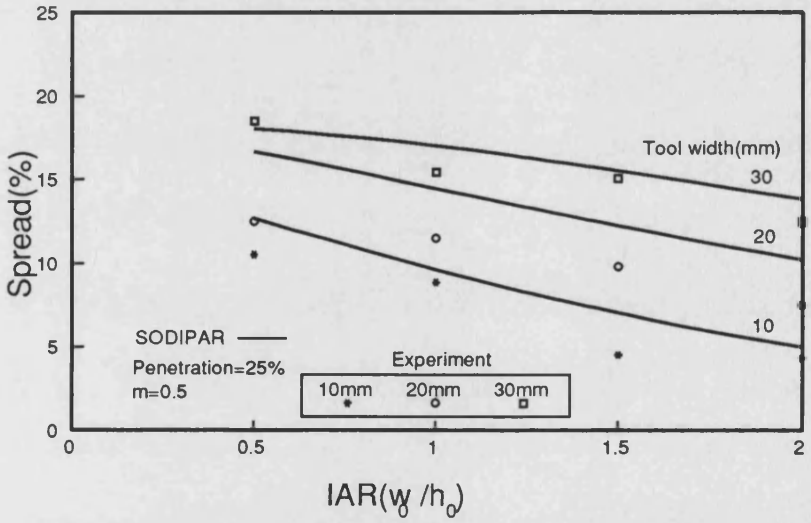

Figure 5-27: Relationship between the spread volume and the initial aspect ratio of the billet for various tool widths and different height reductions.

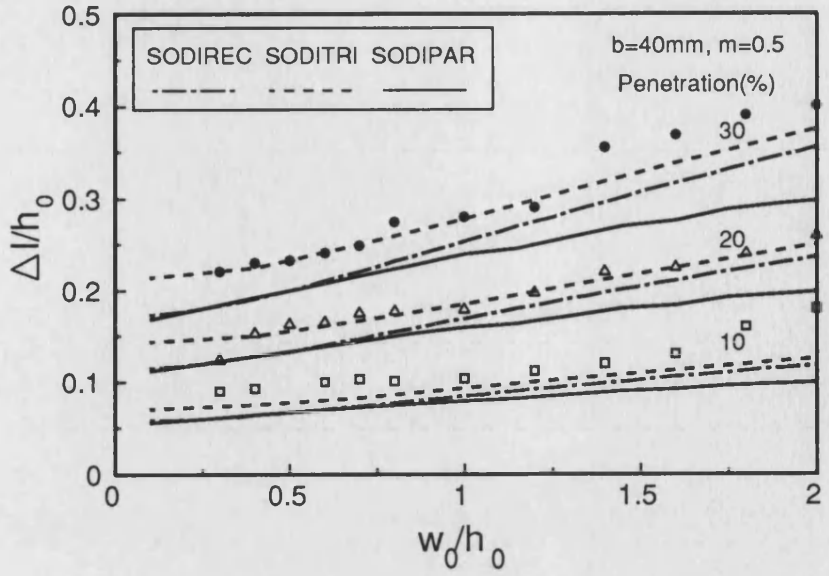

Figure 5-28: The variation of elongation with aspect ratio.

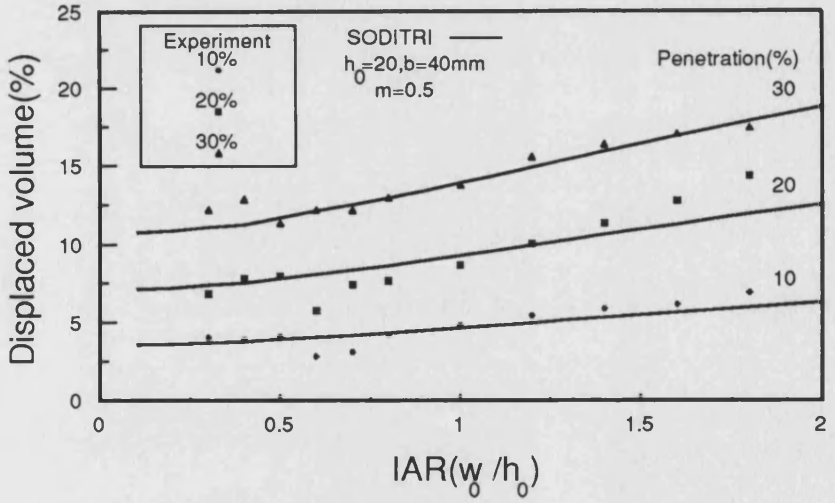

Figure 5-29: Relationship between displaced volume and the initial aspect ratio of the billet,SODITRI.

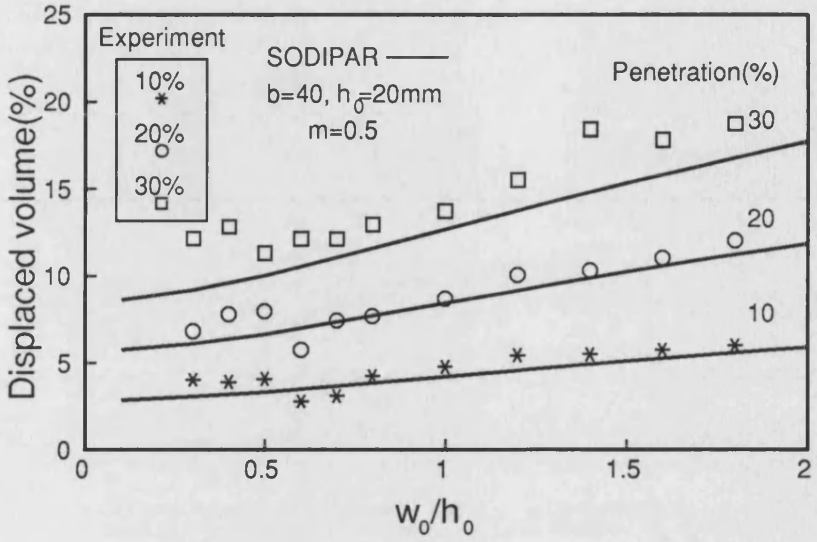

Figure 5-30: Variation of displaced volume with initial aspect ratio and penetrations,SODIPAR.

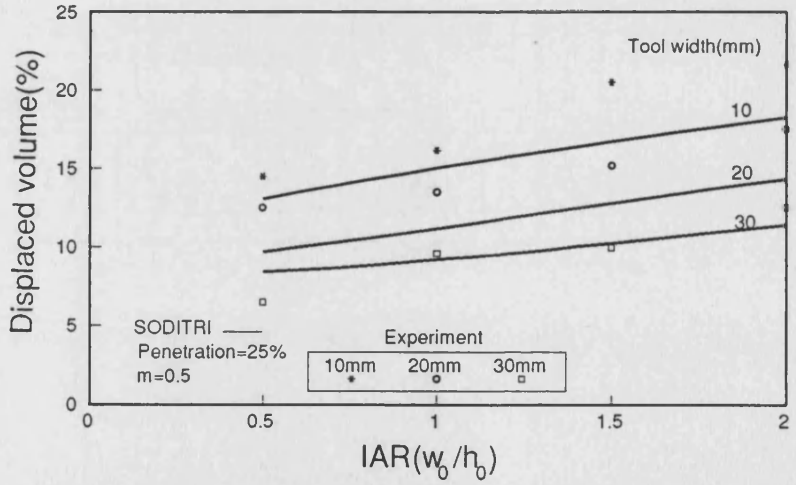

Figure 5-31: Variation of volume displaced volume with initial aspect ratio and penetrations for different tool widths,SODITRI.

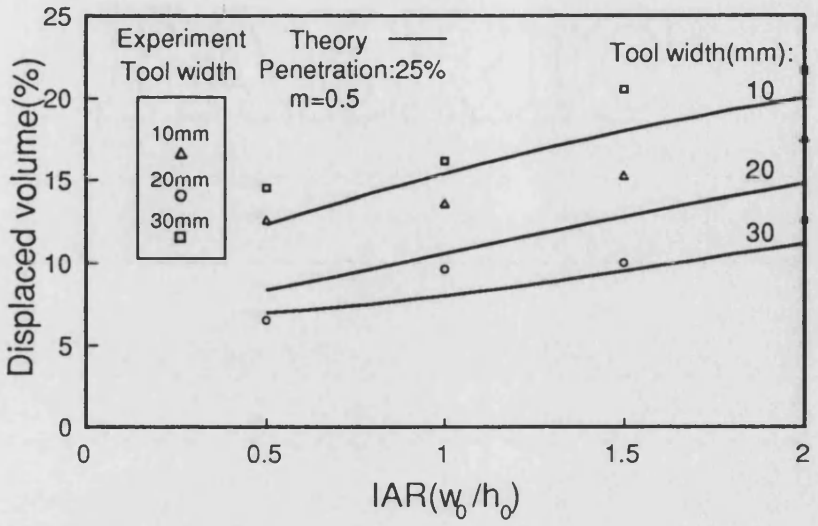

Figure 5-32: Variation of volume displaced between tools into axial direction with initial aspect ratio and penetrations for different tool widths.

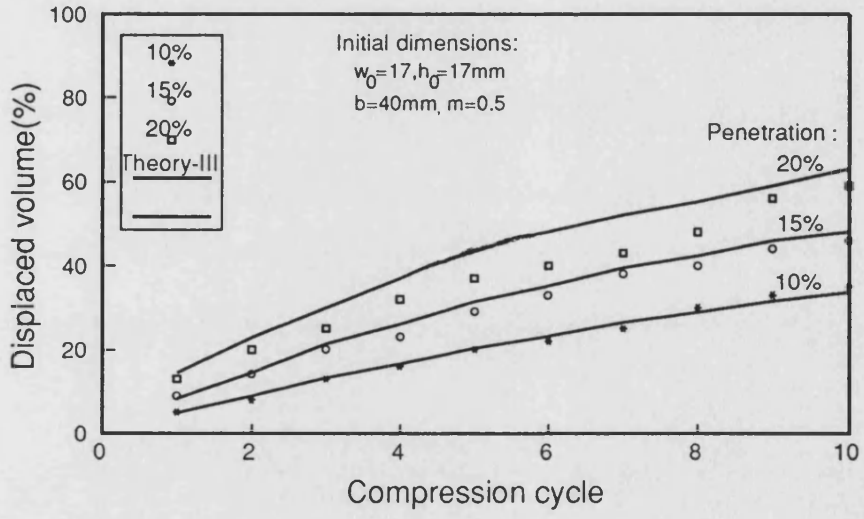

Figure 5-33: Variation of displaced volume with the number of compression turn for a continously compressed and rotated long bar.

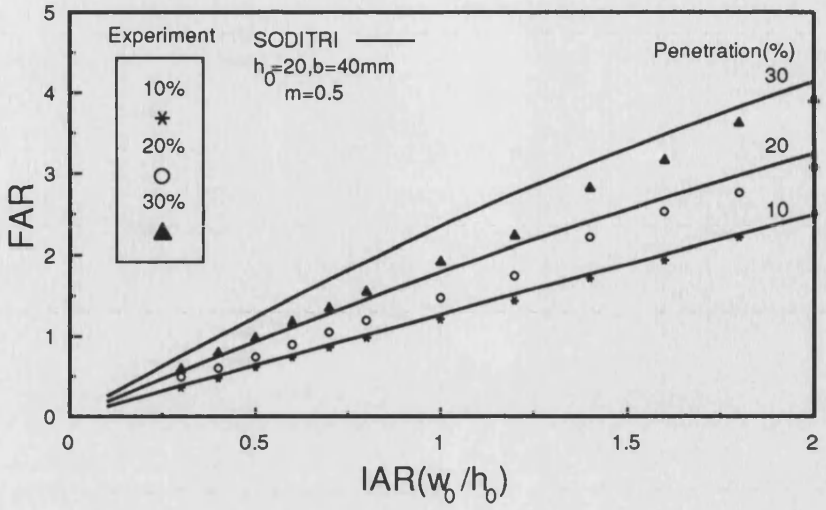

Figure 5-34: Variation of initial aspect ratio with the final aspect ratio and different penetrations.

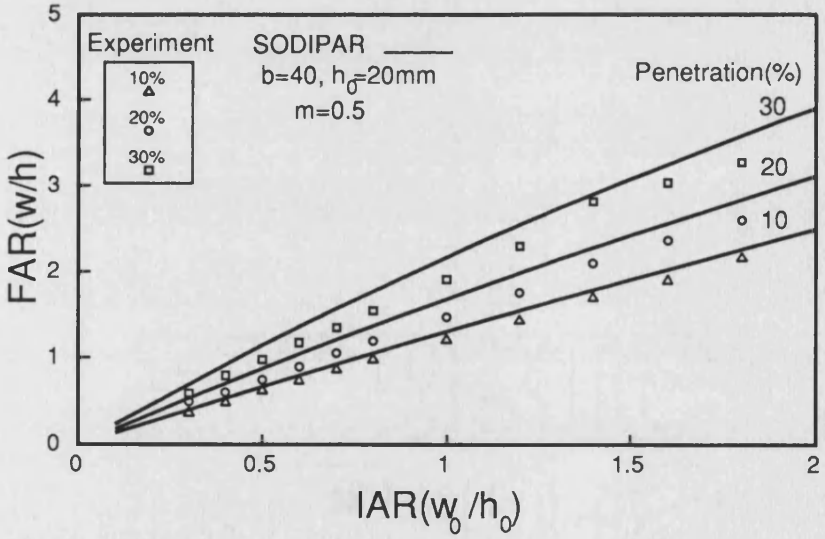

Figure 5-35: Variation of initial aspect ratio with the final aspect ratio and different penetrations

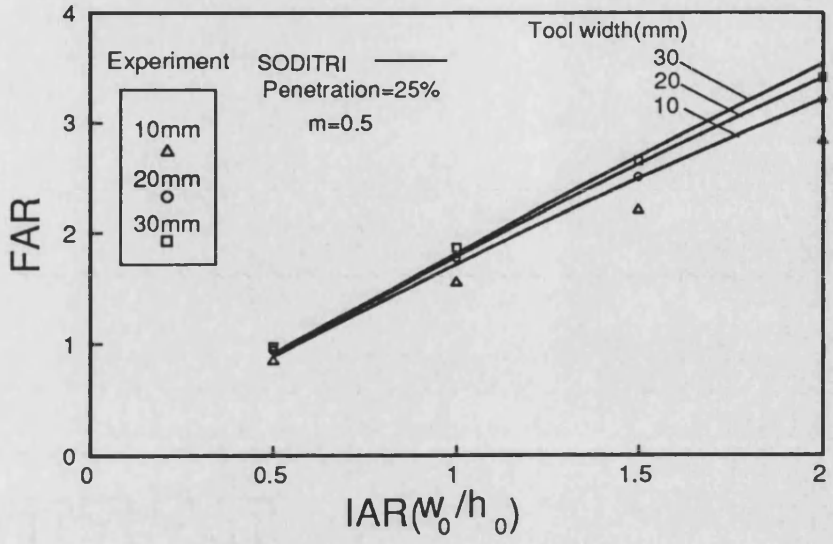

Figure 5-36: Variation of initial aspect ratio with the final aspect ratio and different penetrations

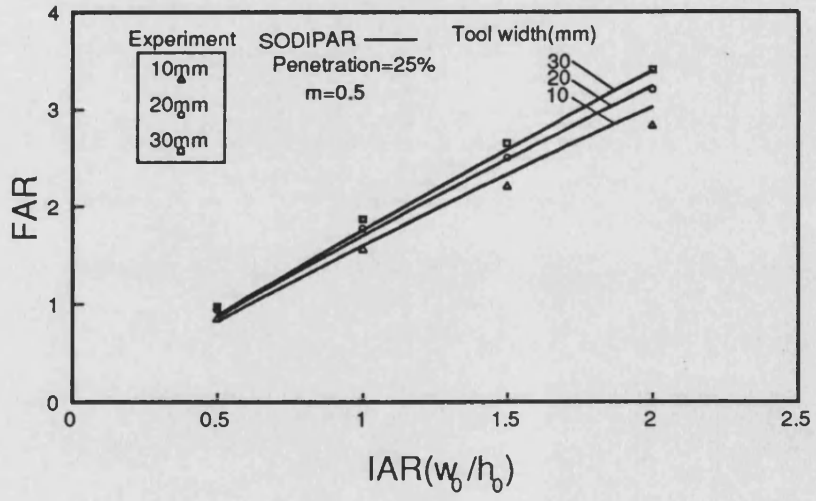

Figure 5-37: Variation of initial aspect ratio with the final aspect ratio for different tool widths.

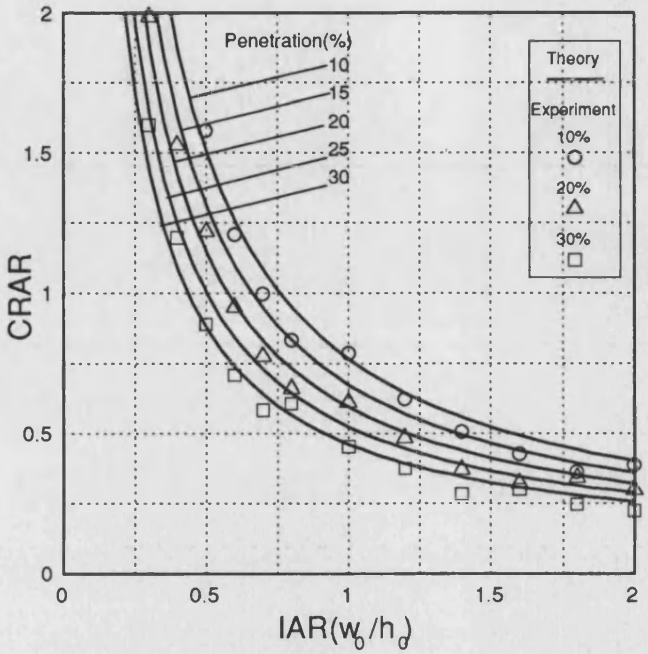

Figure 5-38: Variation of compressed and rotated aspect ratio(CRAR) with initial aspect ratio(IAR) for a continously compressed and rotated long bar.

Chapter 6

BAR PROFILING METHOD WITH FLAT TOOLS

6.1 Introduction

Open die forging and swaging type processes are long established methods used to produce either very large and/or one-off components for which the closed die forging process would not be viable. The characteristic feature of these processes is that the workpiece is being worked at any one time. As a consequence the forging load and energy requirements are very much less than that which would be required if the component was to be made by closed die forging. Where open die forging processes are still used there is always a heavy reliance on manual skill and previous experience. Billet usually worked over its entire length by applying axial and rotational manipulation to the workpiece.

The analysis of deformation pattern for long bars was given in previous chapters. Here only one of them, SODIPAR, will be used in order to construct a schedule

of forging steps. The foregoing sections indicated that a forging schedule must be kept within geometrical bounds so that a symmetrical pattern of deformation is achieved through the operational cycles. Thus, the overall strategy can now be reduced to repetitive compression of a long bar of square sections. The process is somewhat simplified and reduced to the prediction of either the volume remaining between tools or that which is displaced in the longitudinal direction. Relevant figures for a partially deformed long bar, and theoretical predictions of volume displacement ΔV and initial aspect ratio,IAR have already been given earlier in both chapter three and four.

In this chapter the results from the theoretical predictions will be used for the purposes of establishing a method of incremental open die forging for long bars-MODIF. It forms the basis for an incremental open die forging strategy and its use in setting up a more fundamental approach to design of a processing route or sequence is described in the following section. The overall correlation between experiment and the analysis is sufficiently good to suggest that the analysis could be used for an on-line modelling system. A strategy of the Method of Open Die Incremental bar Forging ,MODIF for profiling long bars is described based on the theoretical analysis given in chapter three and some experimentally produced profiles are examined.

6.2 Implementation Strategy of the MODIF

A successful execution of a processing strategy for an automated/computerised open-die forging schedule depends to a large extent on the operational require-

ments for workpiece manipulation and positioning. Longitudinal and rotational movement of the workpiece is vital while reducing the cross-section at each compression step. As it was given in chapter five, a workpiece holder was designed and manufactured which accommodates sufficient flexibility to allow free vertical and longitudinal movement of the workpiece during deformation. In order to present a profiling strategy the operational definitions given below are used.

Geometrical and Operational Definitions:

n = Number of compression-rotation cycles,

a = The constant aspect ratio in all cycles,

r = One step reduction ratio,

x = Overall required height reduction in multi-cycle operation,

h_0, h = height before and after compression in cycle n,

w_0, w = width of before and after compression in cycle n,

l_0, l = length before and after compression in cycle n,

Fig 6.1 shows a schematic illustration of the proposed automated bar profiling system, simple tool profiles and the type of products that could be manufactured by such a system. A strategy of the process in its simplest form may be explained schematically in Fig 6.2 for the production of stepped and tapered type shapes. Conceptually, all that is involved is the repetition of the elementary deformation step described in previous chapters. A crucial feature of the process is the volume of material displaced from between the tools in each deformation step. It is necessary to ensure that more material is not displaced than is required to make

up the desired cross section of any particular portion of the workpiece.

The parameters employed in this figure are the initial aspect ratio,IAR, and the final aspect ratio after rotation,CRAR and the volume displaced in the longitudinal direction, ΔV. It is clear from that graph that the initial aspect ratio,IAR at the end of cycle 'n' on the vertical axis can be transposed to the horizontal axis through a 45^0 line, for the start of cycle 'n+1'. Any particular starting shape is defined by volume V_i and IAR. The limiting values for these parameters in any squeeze during a complete cycle are taken as; Penetration $=$ 30% and IAR $=$ 2

In order to execute the whole process using the minimum number of steps. Point A is the starting point for compression rotation cycle, B is the penetration level, C is the value for aspect ratio- w_1/h_1 after compression and 90^o rotation of the workpiece. Point A is projected each time into the volume change characteristics ΔV enabling the volume displaced in the longitudinal direction to be determined. Also the volume displacement at any step, ΔV_i is added to the displaced volume accumulator along the left side of the horizontal axis. It can also be used to update the current volume between the tools by substracting its value from the volume prior to the incremental step. A repetitive cycle is now engaged as symbolised by the route A-B-C. The penetration level at each squeeze, is checked off at point D. Also, at each cycle the current volume, that is the initial volume less ΔV_1, is checked against its proximity to the final required volume V_f. This will enable the last cycle to be defined so that the shape closest to the required dimensions is produced, point E. With this strategy, absolute dimensions of the required

shape may not be possible to achieve. However, if the processing schedule is optimised with respect to IAR and penetration the final step can be chosen to produce the required dimensions. This implementation is based on the uniformity of deformation at each step, but in practice the actual profile in some cycles will deviate from the predicted values due to inevitable inaccuracies in the modelling.

An actual graphical explanation of the method is shown in Fig 6.3 which gives the CRAR values for a range of penetrations being applied to billets of various IAR values. This family of curves is valid for particular values of tool width and friction factor. The figure illustrates the interesting concept of an operating region outside of which the billet aspect ratio is too high for stable deformation, ie buckling or nonuniform deformation will probably occur. It also suggests that for a given IAR value, there will be a unique operating point corresponding to a particular step penetration value of r, which enables the same percentage reduction to be applied at each step of the process; with the billet aspect ratio, after the first cycle, remaining constant. To enable this, the operating point must fall on the 45^0 line. Fig 6.4 shows how these optimum reduction ratios vary with IAR values. Clearly the aspect ratio of a square section cannot be retained as no deformation will occur. In order to understand the operating strategy consider Fig 6.6 and the case of a portion of a bar whose initial cross-section w_0/h_0 is reduced to x (w_0/h_0) by executing a number of compression and rotation cycles at the optimum reduction ratio.

The aspect ratio at the beginning of each cycle remains the same for the multi-cycle reduction and this is represented by the triangle DEC in Fig 6.3. The height

reduction ratio at any step can also be expressed by:

$$r = \frac{h_{ic}}{h_i} \tag{6.1}$$

where h_{ic} is the height after compression and before the billet is rotated. After 'n' cycles (compression followed by rotation) we can write:

$$ie \quad r^n = x\, a^n \tag{6.2}$$

where;

$$a = \frac{w_0}{h_0} \tag{6.3}$$

is the constant aspect ratio in all cycles. The step height reduction ratio effected in all steps can now be expressed by:

$$r = e^{\frac{1}{n}\,[lnx + nlna]} \tag{6.4}$$

Fig 6.5 shows the derived relationship between the parameters x,r,a and n. Thus for a required overall reduction in the cross-section of a billet in a multi-cycle operation, it is possible to determine an approximate operating aspect ratio, corresponding step reduction and number of cycles. For reduction of square section stock, an initial and final reduction will be required to "set" the operating aspect ratio and the terminating return to a square section. Only for these starting and finishing points can the aspect ratio approach the limiting value of 2. For example to achieve an overall height reduction of 40% in the dimensions of the billet an aspect ratio of $a = 0.72$ must be established and then 5 steps

each with $r = 0.6$ should be applied to reach the required terminating point. In Fig 6.3 the overall strategy and sequence are depicted by starting with a square billet at A which is reduced by approximately 20% ie point B after which the height is progressively reduced by 40% for 5 cycles corresponding to the circuit DECD. Finally a reduction of approximately 20% would return the aspect ratio to unity corresponding to point F.

The analysis can thus be used to establish an overall process planning and control strategy. On-line measurement and adjustment would of course be required to accommodate the inevitable variation in predictions caused by uncertain friction values and inaccuracies in the analysis. The CPU time for ten cycles was completed in less than half a minute on a $SUN\ SPARC1^{+}$ workstation which may be fast enough to enable on-line control of the process.

6.2.1 Implementations of the MODIF

Fig 6.7 shows a chart for the overall comparison between experiment and theory for multi cycle compression-rotation process in which two graphs were combined to provide the prediction of shape changes. From this chart the compression-rotation can be started at any individual initial aspect ratio value and the process followed step by step systematically. For this example, A was chosen as starting point,IAR=1.0. The material is compressed up to a penetration value eg 10% ie point B. The new value of the aspect ratio of the compressed and 90^0 rotated billet is read on the vertical axis at point C. This point is then transformed onto the horizontal axis ie point D by a 45^0 line as a new starting point for compression. The volume displaced in the axial direction can also be read from

the lower right hand graph at point D'. The process can also proceed in the same way by applying any other chosen penetration levels, ie 20% and 30%. If the route is followed for these penetrations the compressed and rotated aspect ratio can be read at F and H and transferred onto the horizontal axis by 45^0 lines. To reach a desirable cross-section the number of steps can also be optimised depending on the penetration level at the operating point.

The process in its simple form can be used for the production of stepped and tapered type shapes by applying multi-compression and rotation cycles via computer control. The single step analysis described earlier can be applied in a consequitive manner on alternate faces of the workpiece thus causing reduction in the cross section and an increase in the component length. Various profiles can be generated by effecting different penetration levels and also by employing tools with varying widths at different locations along the working length of the workpiece. The sequence of operations including the workpiece manipulation can be implemented and optimised using a computer controlled press and manipulator type of arrangment.

In Fig 6.8 another example chart is given through the analysis for producing a profile this time using two different flat tools one having 40mm the other 20mm tool width. The chart consists of three individual parts. In this example, two different tool widths were used and multi-compression and rotation cycles were applied in a consequitive manner on an initially square cross sectioned billet. The stepped shaft to be produced is shown in Fig 6.8(a).

The vertical axis of figure 6.8(b) represents the aspect ratio of the bar after

compression and 90^0 rotation,CRAR whilst the horizontal axis shows the various initial aspect ratios,IAR of the bar before any compression step. Figure 6.8(c) presents the volume of material displaced into the longutidunal-x direction against the number of the compression-rotation cycle. Considering a 15mmx15mm initial cross-section of a billet the process starts from point A in Fig 6.8(b) and the initial aspect ratio is at unity and tool width $b_1 = 40mm$. After the application of 20% penetration, the compressed and rotated aspect ratio,CRAR of the bar becomes the new initial aspect ratio of the billet at B. The next compression step, 20% penetration, is identified by point C, this can be followed on the chart by drawing a 45^0 line from point B to meet the horizontal axis at C. The aspect ratio at B and C is identical. The volume of material displaced in the longitudinal direction can be determined from figure 6.8(c) at point D' for the first cycle. Five compression-rotation cycles were applied for the tool width of $b_1 = 40mm$. The total volume displaced can be read at point P'. The cyclic compression-rotation process continues from point P, using the tool width of $b_2 = 20mm$, and applying 20% penetration for further six cycles thus generating a stepped shaft whose the final dimensions are shown in Table 13:

The idealised quarter cross-section of workpiece using this systematic schedule is shown in figure 6.8(a) of the chart. Experimental measurements of final dimensions of profiles are found to be fairly close with theoretical, especially the SODIPAR solution, predictions. However the practical results indicates that the final product may need to have some final machining. In Fig 6.9 some of the profiles produced in this way are shown.

Experimental measurements of final dimensions of profiles are found to be fairly close with theoretical predictions. For a further development of the process a vision system comprising a set of sensors or probes could provide instant description of the deformation pattern. Monitoring the deformation pattern is essential if the feedback loop is to be incorporated in the set up.

6.3 Limitations and workpiece distortions

Open die forging has various workpiece/die geometrical limitations, the quality of the final product being rather sensitive to the occurrence of metal flow defects in the form of foldover. The basic geometrical parameters in this type of process are in height and width of the deforming volume and the die width. An initial aspect ratio of w_0/h_0 smaller than 0.3 generates two types of undesirable features, workpiece buckling along the height between the dies and non-uniform deformation characterised by a double bulge while the central portion of the workpiece remains rigid. During experiments at $w_0/h_0 = 0.3$ non-uniform patterns of deformation were observed. Similar effects are also reported in [84] for b/h_0 greater than 3. Excessive side spread is also undesirable in order to reduce the incident of laps between the deforming and rigid parts of the workpiece. Such features will inevitably cause internal defects due to surface fold over when the workpiece is squeezed on alternate surfaces in one cycle. However, for practical reasons experiments were limited to the aspect ratio, w_0/h_0 of 2.

The manipulation and positioning of the workpiece is of vital importance and if it cannot be centralised around the tool width properly, distortions will occur.

Distortions caused by off-centre positioning of the workpiece length under-going deformation can take many forms, but in general, it is exhibited by variations in the displacement of the workpiece edges containing the deforming volume, unsymmetrical edge displacement inevitably causing workpiece bending. Such a type of distortion is more pronounced when the workpiece is manipulated manually or being positioned under its own gravitational forces thus causing workpiece tilting and hence an unsymmetrical deformation pattern. Also, the penetration level in one squeeze makes the distortions greater. However, there are four basic patterns of bending that can occur in each plane. Fig 6.10 illustrates the interesting concept of the operating region and limitation zones in open die forging. It is characterised by four zones. The impossible zone which is bounded by the limiting aspect ratio and zero penetration curve. The impractical zone gives a tall billet that is susceptible to buckling or non uniform deformation. The single step zone does not permit rotation due to limiting billet aspect ratio after rotation. The operational zone enables full cycle operation; that is continuous compression followed by rotation. In this zone an optimum operation line is defined which enables continuous and infinite number of cycles for a range of aspect ratios $0.5 < w_0/h_0 < 1$. The other billet aspect ratios must be subjected to an initial compression in order to bring the dimensions of the billet to within the continuous cycle line. Also, a final compression step will be required in order to achieve final specified dimensions. Fig 6.11 shows schematically the basic patterns of distortions that might occur during compression. Under ideal working conditions the edge points A, A', B and B' are displaced away from the centre of the workpiece with equal amounts. It is reasonable here to assume that the overhanging parts of the workpiece remain rigid around their local axes if such

edge distortions occur. During rotational compression the IAR should be kept within the allowable range all the time. Otherwise, the possibility of ending up with some undesirable features is very high.

Fig 6.11i and (ii) show distortion that causes symmetrical bending of the two overhanging parts of the workpiece while Fig 6.12iii and (iv) show opposite bending resulting from rhombic distortion of the workpiece edges. Similar effects on the other planes are also possible, the total distortion is a combination of the three parts and the directional movement of each edge of the quadrapiped element under going deformation. Fig 6.12 shows some distorted specimens caused by these effects. However, such secondary distortion is detectable by the use of suitable sensing devices that could be attached to the workpiece manipulator with a feedback system incorporated in the processing scheduling strategy for corrective action to be taken.

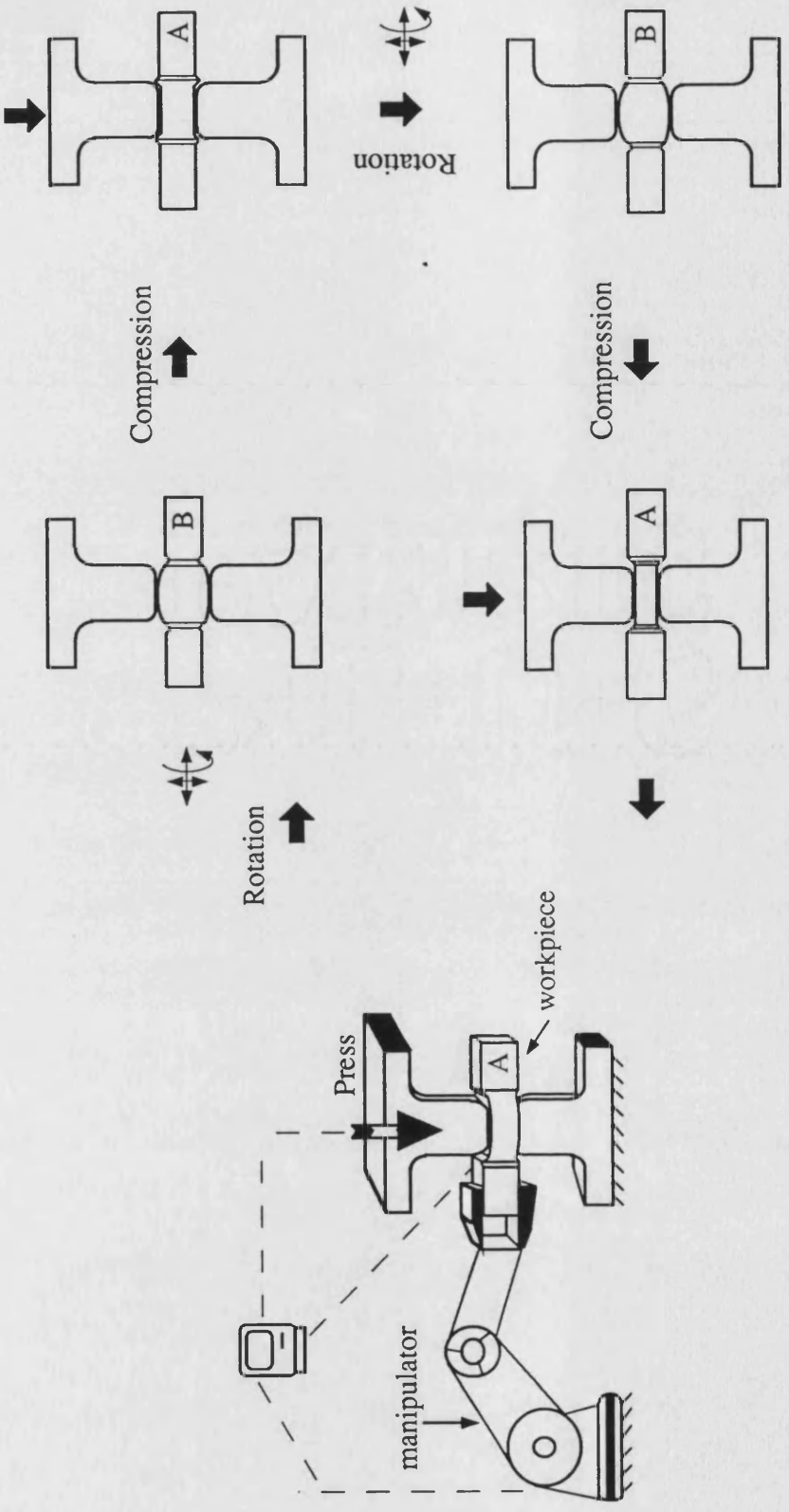

Figure 6-1: Automated bar profiling process

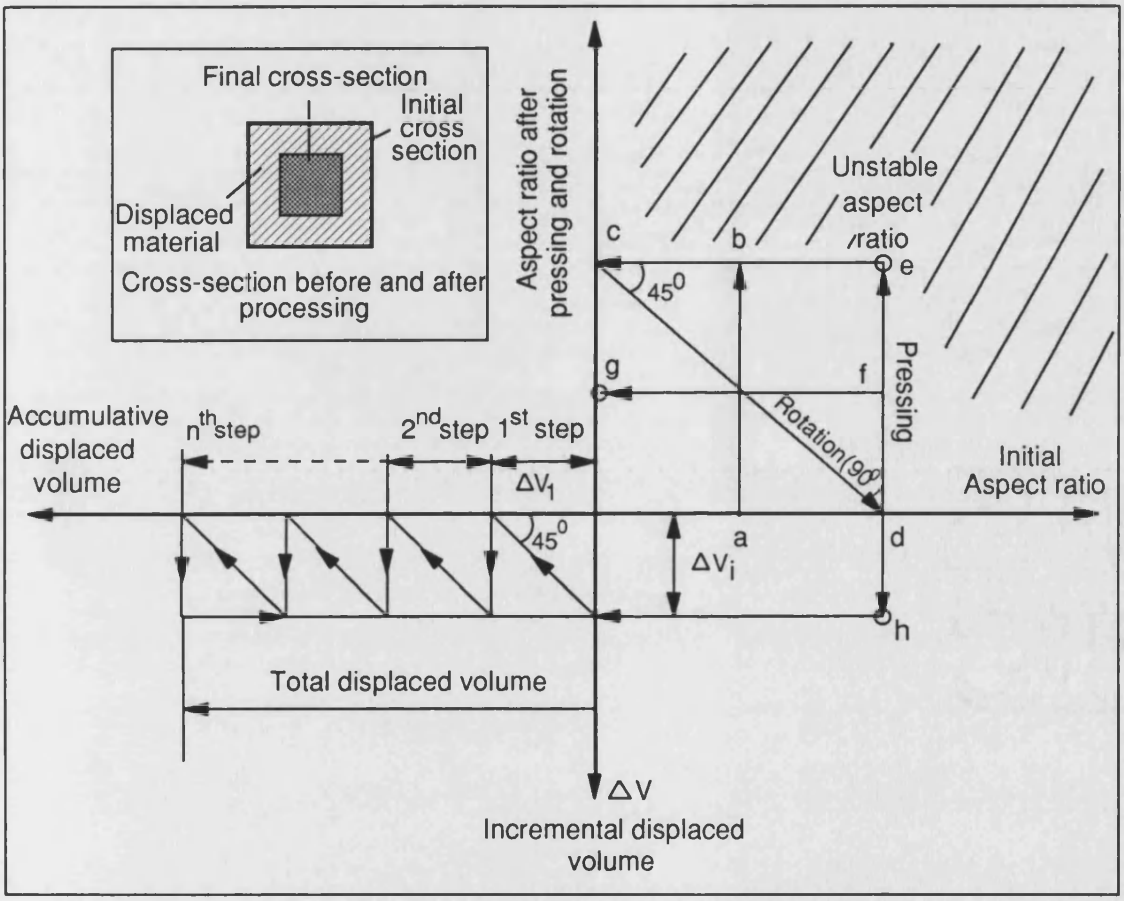

Figure 6-2: A schematic implementation strategy to produce a stepped feature.

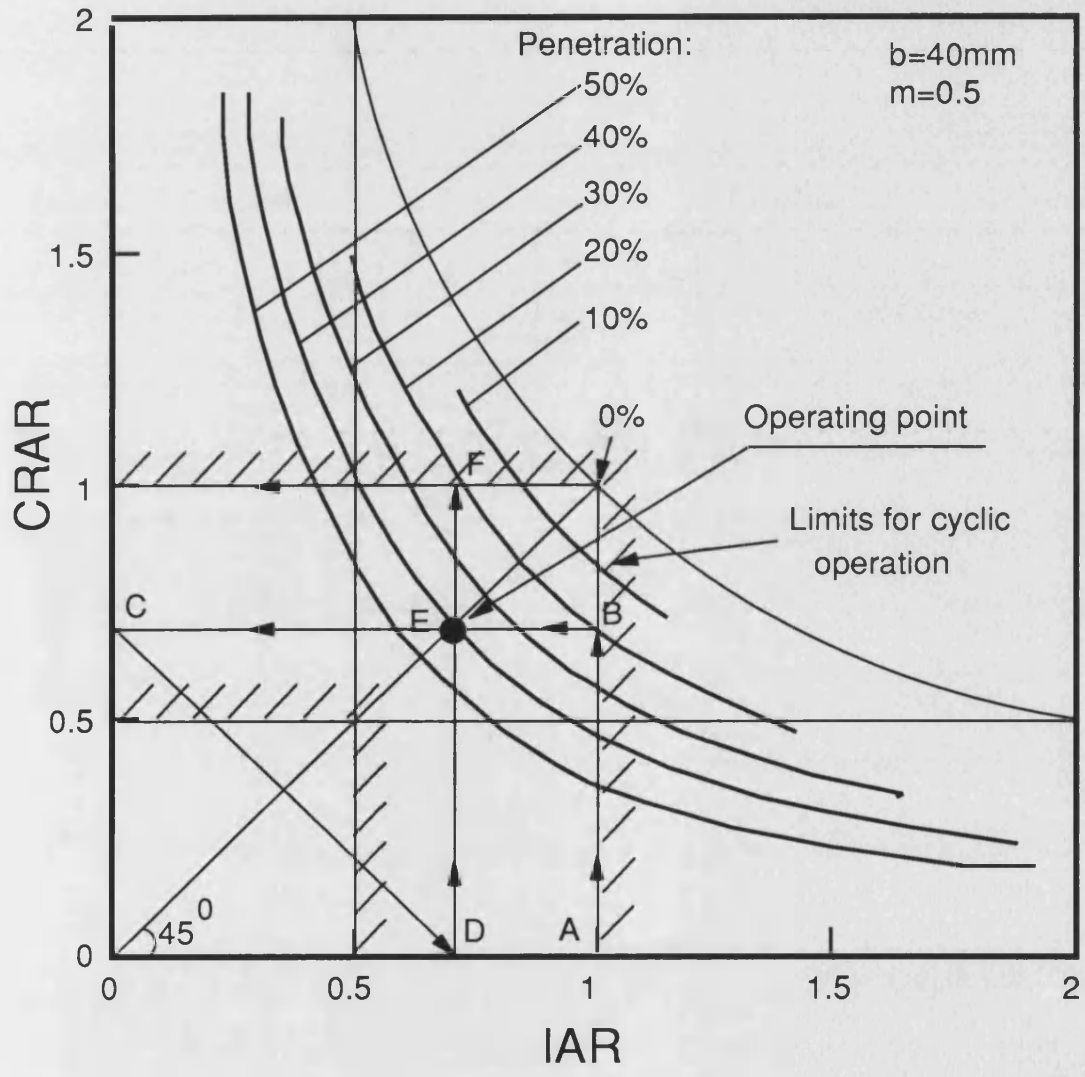

Figure 6-3: A sequential diagram for implementing of strategy for producing tapered shapes

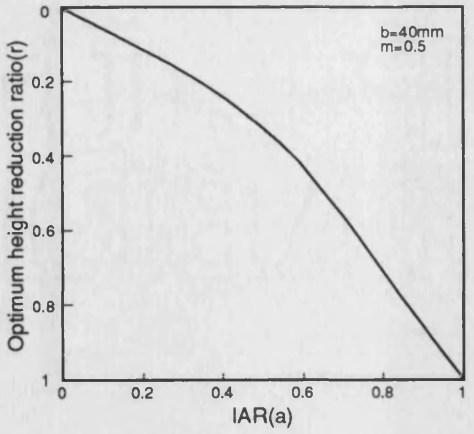

Figure 6-4: Optimum penetration per step for a given aspect ratio of billet.

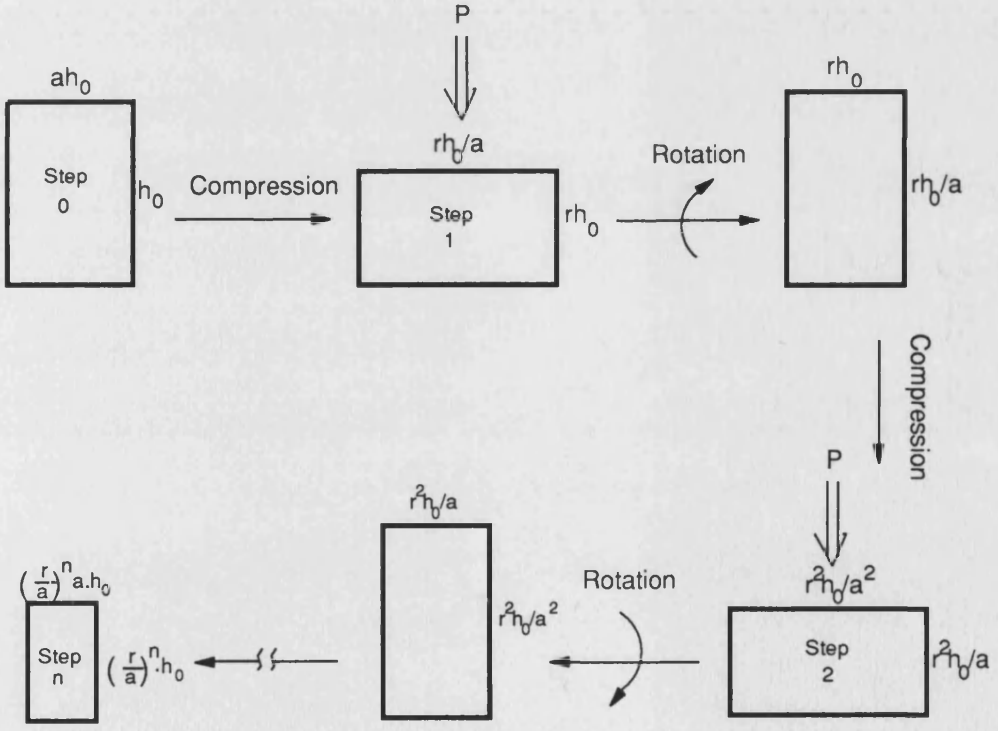

Figure 6-5: A schematic sequential cross-section changes during compression-rotation cycle.

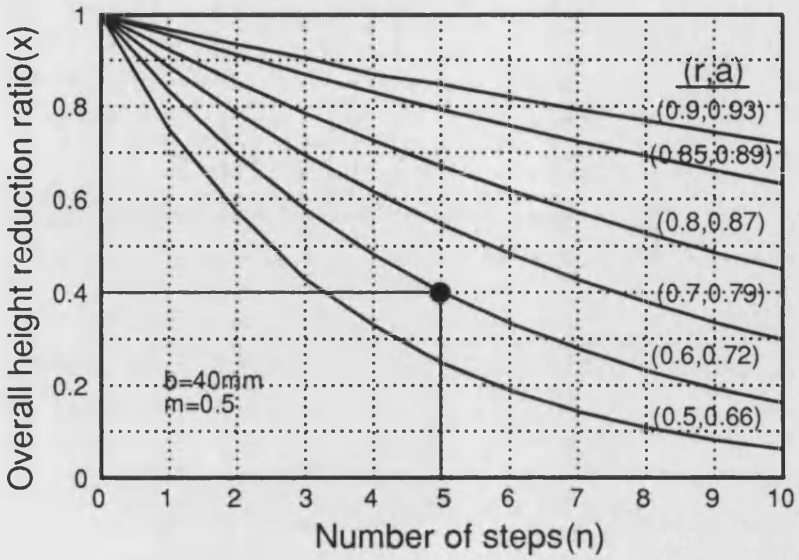

Figure 6-6: Optimum operating point per step for a given aspect ratio of billet.

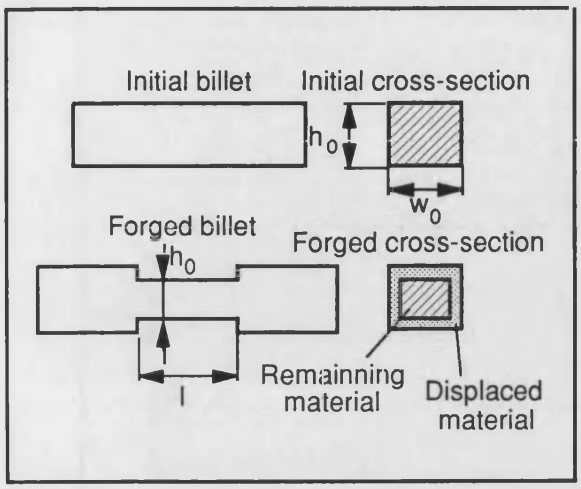

a)

Experimental Penetration(%)	Number of cycles									
	1	2	3	4	5	6	7	8	9	10
*	10.6	10	11	10	10.5	10	10	10	10	10.5
□	21	20	21	20	21	19	19	20	20	20
●	31.5	34	30	30	30	30.1	30	30	30	30.5

d)

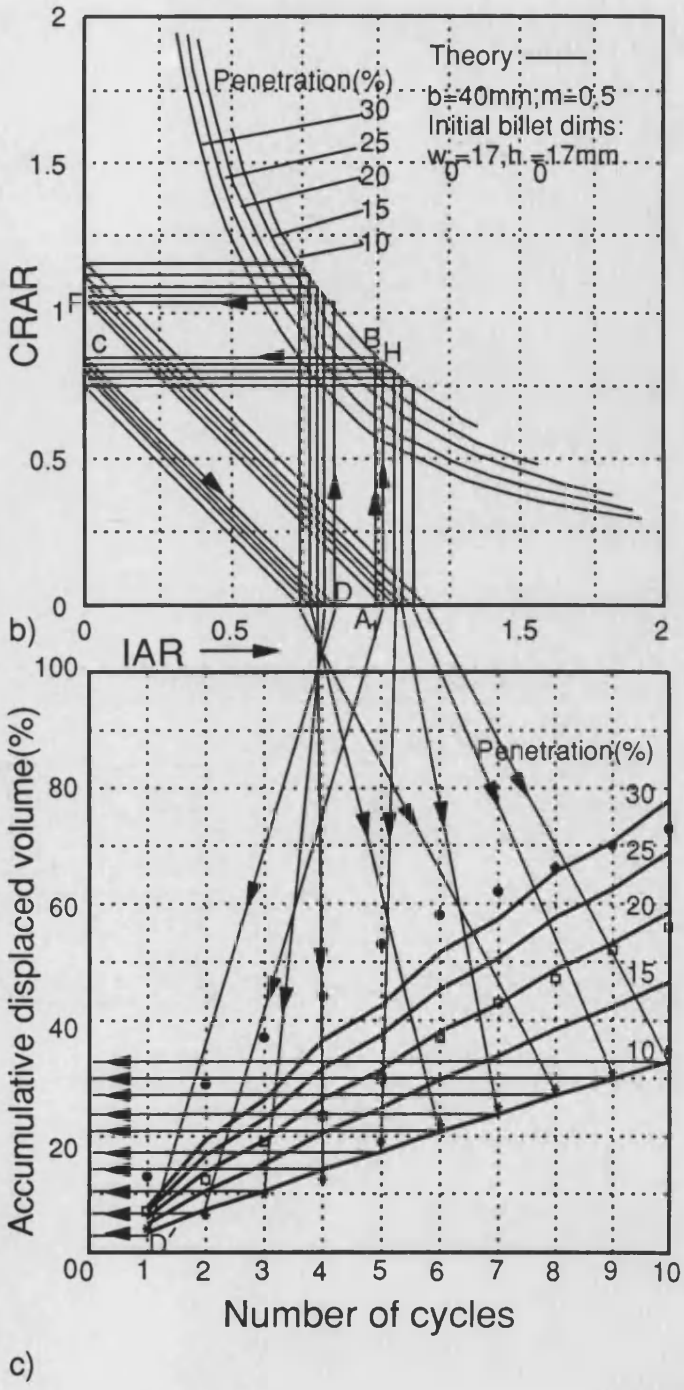

b)

c)

Figure 6-7: A chart for producing tapered shape using one fixed tool width

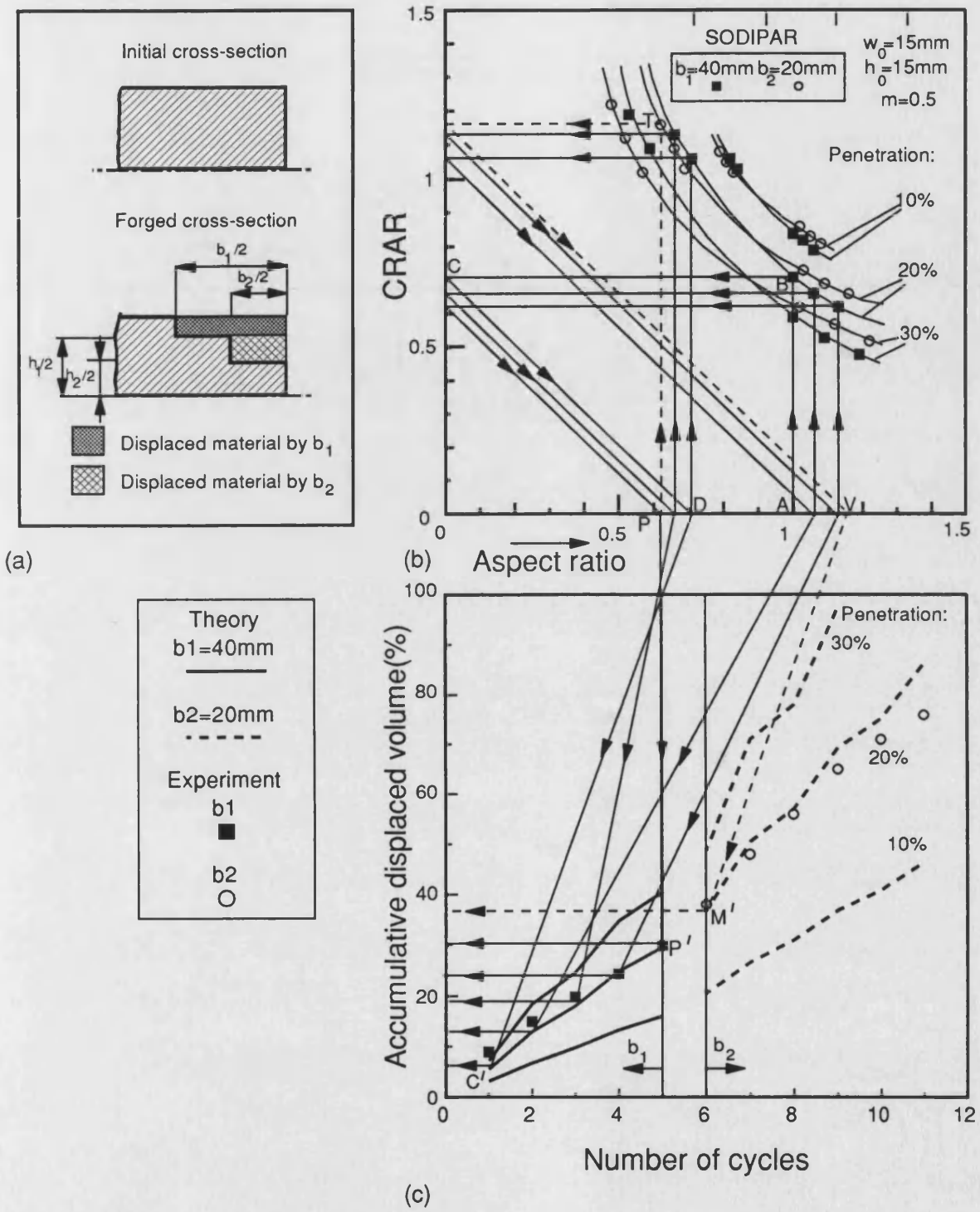

Figure 6-8: A chart for producing a tapered shape using two different tool widths.

Chapter 7

CONCLUSIONS and RECOMMENDATIONS for FUTURE WORK

7.1 Conclusions

Through this research, the objectives proposed at the beginning are basically achieved. The core of work has been focused on three main points. One was to examine a number of analytical solutions which could be used to simulate of deformation steps and predict the material flow and forging load through single step and continuously compression-rotation process. The second was to develop a method which can be used as the basis of a process controlling system for producing specific shapes by providing a system for the sequence of the compression steps. Finally it was aimed to check the validity of these analyses and verify them against experiments in single and cyclic compression plus rotational

sequences using a basic quadrapiped workpiece with various flat tool widths. In metal forming operations, it is of great interest to predict a force that will surely cause the body to deform plastically to produce the desired shape change and metal flow in an incremental manner. Since the programming of the open die forging process can be accomplished with the press and workpiece manipulator first and foremost the characteristic data of the material must be determined by theoretical and experimental analysis. It was seen from the literature survey that there is no existing systematic and detailed analysis for supporting automation of open die forging. Some of the existing empirical formulae were compared with the analysis with respect to spread and elongation. It was demonstrated convincingly that the current analysis can provide very reliable results rapidly.

In this research, a number of upper bound solutions for predicting metal flow and load in open die forging were introduced as SODIREC, SODITRI and SODIPAR. By considering the process as a single step and incrementally the total power consumption was minimised at each increment and so the load was determined and the prediction of metal flow was evaluated. The effect of processing parameters such as aspect ratio, tool width, penetration and friction factor on metal flow has been investigated. It was demonstrated that these methods of analysis form of a basis of establishing an overall process planning and control strategy in automating of open die forging. From the analysis a method of open die incremental forging(MODIF) has been introduced. In this system the single step analysis described earlier was applied in a consequetive manner on the faces of the workpiece thus causing reduction in the cross section and an increase in the component length. Various profiles have been generated by effecting differ-

ent penetration levels along the length of the workpiece and also by employing tools with varying widths at different locations along the working length of the workpiece. The sequence of operations including the workpiece manipulation can be implemented and optimised using a NC press and manipulator type of arrangement. It was demonstrated how this method can be used to produce an idealised desired profile of given dimensions at an intermediate position on the workpiece. The final desired cross-section can be achieved by applying a number of compression-rotation cycles from a given initial aspect ratio of the billet.

The theoretical results indicate that it is viable to pre-design a production route for feature making and provide executable rapid programs using a computer controlled set-up. The computational time required for the calculations was found to be more than adequate to enable on-line control of the process. For example the CPU time required for 10 incremental steps was found to be less than half a minute on a SUN SPARC1$^+$ workstation with 12 MB of memory. Such speeds would enable the proposed on-line application using a faster PC and incorporating a feed back mechanism to reschedule the sequence at each increment. The actual implementation for the profiling will be alongside a computer based planning algorithm. On-line measurement and adjustment would of course be required to accommodate the inevitable variation in predictions caused by uncertain friction values and inaccuracies in the analysis.

Some difficulties were experienced during the experimental work in measuring the bulge into lateral direction, elongation or displaced material volume in the axial direction due to workpiece bending and distortions. These problems appear

because of the difficulty in holding the workpiece between the tools and can lead to the occurrence of nonsymmetrical flow and undesirable features. To overcome these problems some of the investigations took place using a workpiece holder which accommodated the vertical, lateral and axial movement of the workpiece during single and multi-cycle compression-rotation process. In order to avoid these features, the concept of process operating regions and limitation zones in open die forging, characterised by four zones, has been proposed to overcome the difficulty in measuring elongation. A number of methods were also developed for calculating the displaced material volume into the axial direction.

In the whole of this work the applications of the theoretical solutions were limited to relatively simple but realistic open die forging process configurations with various aspect ratios of rectangular cross-section of aluminium bars. The analytical solutions have been tested against a wide range of experiments carried out using flat tools in open die forging. The capability of the solutions was demonstrated to be sufficiently adequate for automation of small batch manufacture. Arising from some of these investigations four papers have been published(1,2,3,4)

7.2 Recommendations for future work

It would be of great benefit if the following proposed outline procedures are achieved and utilised for further developments of an automated manufacturing system using open die forging.

- 1) Developing improved velocity fields, for predicting metal flow for cylindirical and hexagonal cross-sections. These billets can be compressed and ro-

tated through both 45^0 and 90^0 in which the number of steps need to be determined to reach the final shape. Hence a larger variety of shapes can be produced.

- 2) To investigate the range of products that can be produced using a small range of tools of V and curve shaped types hence the possibility of a range of profiles can be increased. This could then open up the area of experimental pre-forming, with the ultimate possibility of abandoning pre-form dies altogether for small scale production.

- 3) Investigation could be made into the possible combination of squeezes along the longitudinal direction of a long bar using various tool widths.

- 4) The flexibility and cost effectiveness are increasingly becoming important in the utilisation of material and time. Therefore for the purpose of automatisation in open die forging an automatic tool changing system could be set up. This would result in lowering the production time, cost, especially in the case of small batch sizes.

- 5) The modelling software needs to be extended to cope with the full range of engineering materials.

- 6) A computer program could be generated which enables the linking of a robot arm which provides the workpiece manipulation. Furthermore the image processing analyser can be introduced to establish a working prototype with feed back loop.

- 7) Since there are some inevitable inaccuracies in the modelling, the concept of in process corrections needs to be investigated with appropriate on-line

feedback. In addition an effective transmit/receive system could be incorporated into the NC press microprocessor for effective data transmission.

- 8) For a further development, a process vision system comprising a set of sensors or probes could provide instant description of the deformation pattern and interfaced to the controller to facilitate effective quality assurance. Monitoring the deformation pattern is essential whilst the feedback loop is incorporated in the set up.

APPENDIXES

Appendix-A: Displaced volume calculation methods for the experimental purposes

1. Cutting off the partially forged material and weighing its mass

This is one of the simplest ways of working out the volume remained under dies, but it requires an accurate cutting-off system. If a partially compressed billet is sawn off from the forged specimen, as seen in Fig A-1, is weighted and the volume of it can easily be determined,

$$V_t = \frac{m_1}{\rho_{material}} \tag{1}$$

The displaced volume is given by;

$$V_{disp.} = V_2 + V_3$$

is worked out by substructing V_1 from the original volume before compression as follows;

$$V_{disp.} = V_{orig.} - V_1 \tag{2}$$

There are some disadvantages of this method; one is that the workpiece is wasted and second; it needs very careful workpiece cutting off.

2. Use of Archimedes' principle

The volume of an irregular solid can be found by determining the apparent loss of weight when the body is immersed in a liquid of known density, this is known as Archimedes' principle. Any weight, floating or immersed in a liquid, is acted

as Archimedes' principle. Any weight, floating or immersed in a liquid, is acted upon by a "buoyant force" equal to the weight of the displaced liquid. If an irregular solid which weighs $m = 50kN$ in air when is immersed into water as shown in Fig A-2 weighs $30kN$

The total weight of 50N acting downward, the tension of 20N upward, and the net buoyant force P_v acting upward. From

$$\Sigma Y = 0$$

and,

$$50 - 30 - P_v = 0 \tag{3}$$

Hence the buoyant force P_v becomes,

$$P_v = 20N$$

Thus the volume of the solid V_{solid}

$$V_{solid} = \frac{P_v}{\rho_{water}} \tag{4}$$

$$V_{solid} = \frac{20N}{9810\ N/m^3} = 0.00203\ m^3$$

Applying this simple principle for finding the remaining volume of a partially forged billet; a tube of water is placed on a digital weigh scale with the workpiece

which is bounded by *gidc* is immersed. The mass of this part of material is recorded in grams and then second part of material is immersed into water and the mass of this part of material is also recorded. The difference of those two masses (Eqn.5) is actually the mass of material remained (m_{rem}) under tools after compression.

$$m_{rem.} = m_2 - m_1 \tag{5}$$

Thus the remaining volume V_{rem} under dies can be expressed as follows;

$$V_{rem.} = \frac{m_{rem.}}{\rho_{water}} \tag{6}$$

where ρ_{water} is the density of water.

By substructing remaining volume $V_{rem.}$ from the original volume ($V_{orig.}$) bounded dies before compression, the displaced volume ($V_{disp.}$) into axial direction is worked out.

$$V_{disp.} = V_{orig.} - V_{rem.}$$

This may well be seen okay but obviously when the amount of displaced volume is too small, then effective measurements become very difficult and also as a whole process it is not practical enough for rapid analysis.

3. Use of imaging machine

For this method the "Joyce-Loebl Magiscan 2" imaging machine has been used. The specimen is placed under a camera and the imaged picture of primary and secondary bulge are drawn manually on the screen and then the bounded surface area is calculated automatically through a software which based on one of the

numerical area calculations as shown in Fig A-4a.

The disadvantage of this method is that the displaced volume is calculated through the average of primary and secondary bulge line images. If the secondary bulge is eliminated by taking the average area as shown in the above figure and the calculations are made on this bounded area line the method is reliable. However it is a time consuming process and is not therefore practical enough for this work.

4 Use of the Coordinate Measurement Machine(CMM)

A programme was written based on minimum and maximum probing points of the bulge to manipulate the CMM by a PC computer and digitise the partially compressed workpiece by giving number of reading points along the profile. The process starts by placing a workpiece on the basis of the CMM which it is the original starting point. By giving a start command the digital probing device moves horizontally in the y direction and probes onto the primary bulge shape at the starting point and the numerical values of bulged surface are recorded. Fig A-4b illustrates the process schematically. This can be expressed by following equation;

Moving distance in x direction = Tool width / Number of points

The the digitised area is then multipled by the current height the remaining volume under dies is calculated and substructed from the original volume(between tools before compression) the volume displaced in the axial direction is determined. This process also takes a considerable time and does not appear to be practical enough for this type of work.

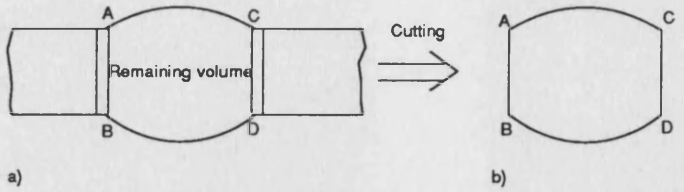

Fig A-1: A compressed billet(a) and its cutting area(b).

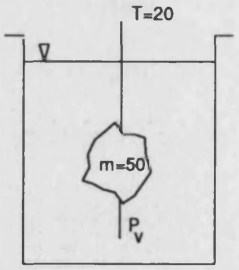

Fig A-2: A floated irregular solid.

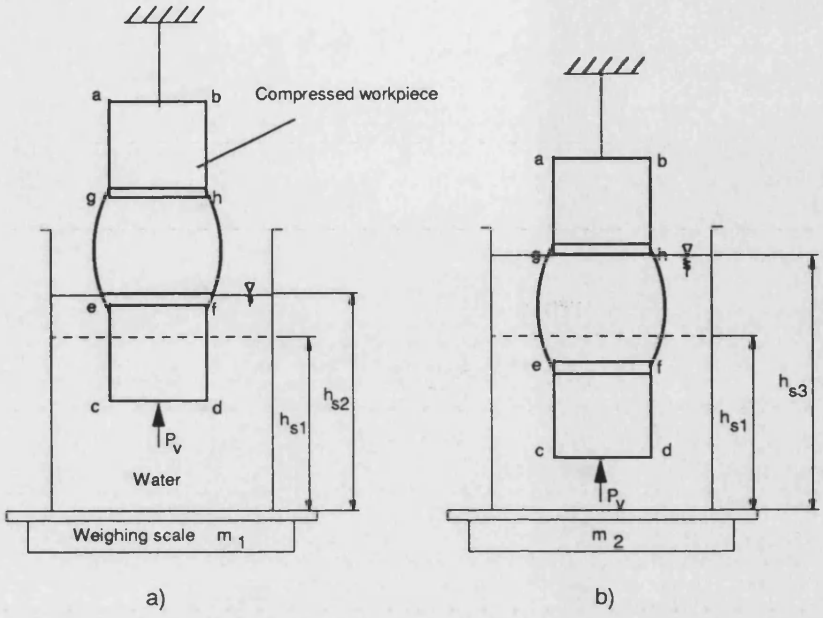

Fig A-3: Floating a partially compressed workpiece into water

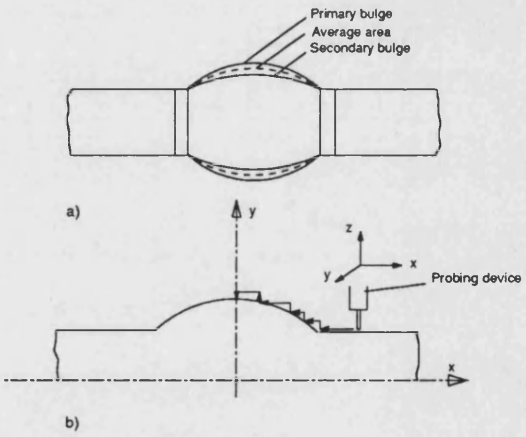

Fig A-4: Probing the forged surface of billet

APPENDIX-B

Experimental data tables

Specimen Group	w_0/h_0=0.5	w_0/h_0=1.0	w_0/h_0=1.5	w_0/h_0=2.0
Tool width(b)	10mm 20mm 30mm 40mm	10mm 20mm 30mm 40mm	10mm 20mm 30mm 40mm	10mm 20mm 30mm 40mm

Table 3. Experimental data for different tool widths.

No:	Load(kN)	$R_{i(mm)}$	$R_{o(mm)}$	H.red(%)	Red. R_i %	$\frac{p}{\sigma_0}$	m
1	120	19.32	40.91	7	1	1.25	0.2
2	170	17.67	42.74	19	8	1.50	0.40
3	240	15.97	45.05	29	15	1.55	0.55
4	330	13.50	46.33	35	27	1.90	0.60
5	420	12.52	47.79	41	31	2.00	0.70

Table 4. Experimental data for the ring test.

Spc.no	Actual Load(kN)	h (*mm*)	w_{max}(*mm*)	*H.red.* (%)	*Rem.CSA* (mm^2)
1	420	16.55	25.11	1.0	99.7
2	480	16.35	25.3	2.0	99.2
3	510	16.14	25.53	3.2	98.9
4	550	15.8	25.98	5.2	98
5	600	15.3	26.44	8.2	95.7
6	620	14.65	27.2	12	95.7
7	650	13.83	28.25	17	93.8
8	680	12.96	29.45	22	91.0
9	720	12.29	30.42	26	89.0
10	740	11.85	31.14	29	88
11	800	11.21	32.14	33	86
12	900	10.23	33.81	39	82.6
13	950	9.41	35.6	44	80
14	1000	8.73	37	48	74
15	1050	8.13	38.3	52	74

Table 5. Experimental results for incrementally compressed billet-I.

Spc.no	Actual Load(t)	h (*mm*)	w_{max}(*mm*)	*H.red.* (%)	*Rem.CSA* (mm^2)
1	42	16.58	25.1	1.0	99.8
2	48	16.5	25.18	1.2	99.7
3	51	16.33	25.36	2	99.3
4	55	16.05	25.65	3.4	98.6
5	60	15.7	26.06	5.8	98
6	62	15.06	26.81	10.0	96.5
7	65	14.08	28.74	19	93
8	68	13.51	28.74	19	93
9	72	12.65	30.04	24.1	91
10	74	12.1	30.85	27.4	88
11	80	11.38	31.98	32	87
12	90	10.35	33.69	44	84
13	95	9.4	35.69	44	80
14	100	8.72	37.11	48	77.6

Table 6. Experimental results for incrementally compressed billet-II

Spc.no	Actual Load(kN)	h (*mm*)	w_{max}(*mm*)	*H.red.*(%)	*Rem.CSA* (mm^2)
1	420	16.58	25.1	1.0	99.8
2	480	16.5	25.18	1.2	99.7
3	510	16.33	25.36	2	99.3
4	550	16.05	25.65	3.4	98.6
5	600	15.7	26.06	5.8	98
6	620	15.06	26.81	10.0	96.5
7	650	14.08	28.74	19	93
8	680	13.51	28.74	19	93
9	720	12.65	30.04	24.1	91
10	740	12.1	30.85	27.4	88
11	800	11.38	31.98	32	87
12	900	10.35	33.69	44	84
13	950	9.4	35.69	44	80
14	1000	8.72	37.11	48	77.6
15	1050	8.09	38.55	52.0	75.0

Table 7. Experimental results for incrementally compressed billet-III

Spc.no	Actual Load(kN)	h (*mm*)	w_{max}(*mm*)	*H.red.*(%)	*Rem.CSA* (mm^2)
1	550	15.93	25.83	4.4	97.7
2	620	15.16	26.8	9.0	95.0
3	680	14.06	28.43	16	93
4	720	13.23	29.72	20	89
5	740	12.63	30.64	25	87
6	800	11.89	31.76	29	84
7	900	10.69	33.83	36	79
8	950	8.41	37.76	50	71

Table 8. Experimental results for separatly compression of a series of billet having different aspect ratios of w/h.

Spc.group	h.red(%)	h (*mm*)	$w_{prim.}$	$w_{sec.}$	$w_{ave.}$	Length (*mm*)	Load(kN)
$\frac{w_0}{h_0} = 0.3$	10	18.00	6.34	6.60	6.47	111.80	80
	15.3	16.94	6.60	7.10	6.85	112.32	90
	20	15.98	6.66	8.00	7.33	112.49	90
	25.2	15.04	6.79	8.19	7.41	113.11	90
	30	14.00	7.57	8.42	7.99	114.43	90
$\frac{w_0}{h_0} = 0.4$	10	18.04	8.34	8.82	8.53	111.85	90
	15	17.05	8.46	9.42	8.94	112.49	100
	20.35	16.08	9.05	10.02	9.55	113.06	110
	25	14.97	9.68	10.63	10.11	113.82	115
	30	14	9.82	11.55	10.69	114.67	120
$\frac{w_0}{h_0} = 0.5$	10	17.96	10.47	11.11	10.79	112.5	90
	15.35	16.93	10.70	11.82	11.26	112.55	90
	19.5	16.1	10.95	12.7	11.83	113.27	100
	26	14.8	11.41	13.54	12.47	113.62	110
	30	14	12.08	14.37	13.23	114.67	120
$\frac{w_0}{h_0} = 0.6$	10	18	12.66	13.53	13.1	111.5	110
	16.4	16.71	12.91	14.21	13.56	112.42	110
	19	16.11	13.30	15.24	14.22	113.3	120
	25.25	14.95	13.93	16.05	15.0	113.90	130
	30	14	15.04	17.22	16.13	114.02	135
$\frac{w_0}{h_0} = 0.7$	10.8	17.84	14.56	15.76	15.16	111.57	110
	16.1	16.78	15.08	16.72	15.9	112.55	120
	20	16	15.67	17.77	16.08	113.50	140
	25.9	14.82	16.5	18.90	17.7	114.0	150
	30	14	17.45	20.18	18.8	114.99	160

to be continued...

Table 9. Experimental data for single squeeze compression for different aspect ratios and penetration levels.

Spc.group	h.red(%)	h (mm)	$w_{prim.}$	$w_{sec.}$	$w_{ave.}$	Length (mm)	Load(kN)
$\frac{w_0}{h_0} = 0.8$	10	18.00	16.83	18.11	17.45	111.82	120
	15.25	16.95	17.11	19.16	18.06	112.49	140
	19.9	16.03	17.96	20.15	19.03	113.54	160
	25.1	14.97	19.13	21.45	20.25	114.23	180
	30	14.00	20.26	22.90	21.6	115.50	190
$\frac{w_0}{h_0} = 1.0$	10.1	17.98	21.16	22.22	21.70	112.09	150
	15.1	16.97	22.09	23.60	22.85	112.82	180
	20.2	16.06	22.52	24.9	23.71	113.58	200
	25.6	14.88	24.34	26.47	25.42	114.35	220
	30	14.00	25.33	28.42	26.80	115.60	230
$\frac{w_0}{h_0} = 1.2$	10	18.00	25.35	26.1	25.73	112.00	160
	16	16.80	26.28	27.44	26.86	113.30	190
	20.65	15.87	26.60	29.18	27.9	113.65	210
	25.9	14.82	28.70	30.40	29.55	114.60	240
	32	13.60	29.99	32.50	31.25	115.50	270
$\frac{w_0}{h_0} = 1.4$	9.3	18.14	29.13	30.40	29.76	112.16	175
	15	17.03	30.29	32.18	31.23	113.18	200
	20.5	15.90	32.16	34.56	33.36	114.10	220
	25	15.00	33.37	36.27	34.82	115.25	270
	33	13.30	35.90	39.12	37.5	117.10	320
$\frac{w_0}{h_0} = 1.6$	10	18.00	33.62	35.02	34.32	112.26	200
	14.75	17.05	35.03	36.68	35.85	113.30	280
	20.3	15.94	36.30	38.89	37.60	114.61	300
	25	15.00	37.97	40.95	39.46	115.96	340
	32	13.70	39.84	43.35	41.60	117.60	360
$\frac{w_0}{h_0} = 1.8$	10.0	18.00	37.81	39.11	38.46	112.53	220
	15.0	17.00	39.05	40.76	39.90	113.68	270
	20.25	15.95	40.26	42.78	41.52	115.20	320
	25.40	14.92	41.61	44.62	43.11	116.36	350
	30.75	13.85	43.65	47.17	45.41	117.98	400

Table 9 (continued).

Spc.no	Load(t)	w (*mm*)	h (*mm*)	m_{ave} (*gr*)	H.red(%)	Ds.vol(%)
1	15	28.9	14.29		14	5
		22.62	17.9	13.6	38	19
2	17	30.2	13.83		17	6
		25.4	15.35	12.87	49	23
3	18	30.05	13.75		18	12
		25.9	14.67	12.0	51	28
4	20	30.4	13.45		19	16
		26.65	14.0	11.8	54	29
5	23	31.5	13.0		22	16
		29.0	12.5	10.87	59	35
6	25	33.22	12.30		26	17
		31.5	11.05	10.2	67	39

Table 10. Experimental data for a series of compressed billets with having one rotation.

Spc.no	N. of turn	w_{ave}	h (mm)	$\frac{w_{ave}}{h}$	$h_{eq.}$	Pentr.(%)	$CRAR$	Acc.Dis.vol(%)
	0	17.00	17.00	0.0	0.0	-	-	-
	Comp.1	18.58	15.34	1.17	18.00	10	-	4
	Rot.1	15.34	18.00	-	-	-	0.85	-
	Comp.2	17.57	16.10	1.044	16.82	10.6	-	6.3
	Rot.2	16.10	16.82	-	-	-	0.95	-
	Comp.3.	17.85	15.19	1.136	17.26	10	-	10
	Rot.3	15.19	17.26	-	-	-	0.88	-
	Comp.4	16.90	15.43	1.045	16.13	11	-	12.5
	Rot.4	15.43	16.13	-	-	-	0.956	-
1 (10%)	Comp.5	17.00	14.51	1.128	16.37	10	-	19
	Rot.5	14.51	16.37	-	-	-	0.886	-
	Comp.6	16.27	14.67	1.044	15.33	10.5	-	22
	Rot.6	14.67	15.33	-	-	-	0.957	-
	Comp.7	16.50	13.82	1.109	15.75	10	-	25
	Rot.7	13.82	15.75	-	-	-	0.901	-
	Comp.8	15.4	14.17	1.037	14.7	10	-	28
	Rot.8	14.17	14.70	-	-	-	0.964	-
	Comp.9	15.9	13.22	1.149	15.2	10	-	31
	Rot.9	13.22	15.20	-	-	-	0.87	-
	Comp.10	15.0	13.57	1.039	14.11	10.5	0.962	35
	0	17.00	17.00	0.0	0.0	-	-	-
	Comp.1	19.10	14.45	1.270	18.40	15	-	8
	Rot.1	14.45	18.40	-	-	-	0.787	-
	Comp.2	17.2	15.6	1.043	16.28	15.3	-	12
	Rot.2	15.6	16.28	-	-	-	0.958	-
	Comp.3	18.2	13.86	1.255	17.4	15	-	17
	Rot.3	13.86	17.40	-	-	-	0.796	-
	Comp.4	16.27	14.72	1.050	15.46	15.5	-	27
	Rot.4	14.72	15.46	-	-	-	0.952	-
2 (15%)	Comp.5	17.8	12.65	1.324	16.75	18	-	29
	Rot.5	12.65	16.75	-	-	-	0.755	-
	Comp.6	15.02	14.3	1.002	14.23	15	-	30
	Rot.6	14.20	14.23	-	-	-	0.988	-
	Comp.7	16.5	12.05	1.307	15.76	15	-	34
	Rot.7	12.05	15.76	-	-	-	0.765	-
	Comp.8	14.25	13.4	1.008	13.51	15	-	37.5
	Rot.8	13.40	13.51	-	-	-	0.998	-
	Comp.9	15.96	11.3	1.361	15.39	16.3	-	40
	Rot.9	11.30	15.39	-	-	-	0.734	-
	Comp.10	13.37	13.1	0.967	12.68	15	1.034	42
	0	17.00	17.00	0.0	0.0	-	-	-
	Comp.1	21.55	13.42	1.467	19.7	21	-	7
	Rot.1	13.42	20.03	-	-	-	0.681	-
	Comp.2	17.45	15.73	1.023	16.1	20	-	12.5
3 (20%)	Rot.2	15.73	16.10	-	-	-	0.97	-
	Comp.3	20.0	12.63	1.470	18.57	21	-	19
	Rot.3	12.63	18.57	-	-	-	0.68	-
	Comp.4	15.84	14.85	1.030	14.77	20	-	23.5
	Rot.4	14.95	14.77	-	-	-	0.97	-

Table 11. Experimental data for continously rotated billets by given a certain amount of penetration. (to be continued)

Spc.no	N.of turn	w_{ave}	h (mm)	$\frac{w_{ave}}{h_0}$	$h_{eq.}$	Pentr(%)	$CRAR$	Acc.Dis.vol(%)
	Comp.5	18.95	11.80	-	17.80	22	-	30
	Rot.5	11.80	17.80	-	-	-	0.699	-
	Comp.6	15.01	13.13	-	13.78	19	-	37
	Rot.6	13.13	13.78	-	-	-	0.987	-
3 (20%)	Comp.7	17.14	11.18	-	15.60	19	-	40
	Rot.7	11.18	15.60	-	-	-	0.75	-
	Comp.8	12.51	12.22	-	12.22	20	-	47
	Rot.8	12.22	12.51	-	-	-	1.023	-
	Comp.9	13.89	9.76	-	13.43	20	-	53
	Rot.9	9.76	13.43	-	-	-	0.8	-
	Comp.10	12.10	10.74	-	11.04	20	-	56
	0	17.00	17.00	0.0	0.0	-	-	-
	Comp.1	20.55	12.7	-	19.36	25.3	-	10
	Rot.1	12.70	19.36	-	-	-	0.655	-
	Comp.2	16.45	15.17	-	15.20	22	-	16
	Rot.2	15.17	15.20	-	-	-	0.988	-
	Comp.3	19.18	11.40	-	17.84	25	-	24
	Rot.3	11.40	17.84	-	-	-	0.64	-
	Comp.4	13.38	13.38	-	14.61	25	-	33
	Rot.4	13.38	14.61	-	-	-	0.91	-
4 (25%)	Comp.5	16.92	10.00	-	15.88	31	-	41
	Rot.5	10.00	15.88	-	-	-	0.632	-
	Comp.6	13.48	11.91	-	12.62	25	-	48
	Rot.6	11.91	12.62	-	-	-	0.94	-
	Comp.7	15.60	9.46	-	14.61	25	-	52
	Rot.7	9.46	14.61	-	-	-	0.647	-
	Comp.8	12.74	10.95	-	11.80	25	-	55
	Rot.8	10.95	11.80	-	-	-	0.927	-
	Comp.9	14.54	8.85	-	13.44	25	-	59
	Rot.9	8.85	13.44	-	-	-	0.658	-
	Comp.10	11.65	10.01	-	10.82	25.5	-	62.5
	0	17.00	17.00	0.0	0.0	-	-	-
	Comp.1	21.10	11.64	-	19.6	31.5	-	13
	Rot.1	11.64	19.6	-	-	-	0.56	-
	Comp.2	15.26	14.54	-	14.00	34	-	29
	Rot.2	15.54	14.00	-	-	-	1.038	-
	Comp.3	20.42	9.80	-	18.58	30	-	37
	Rot.3	9.80	18.58	-	-	-	0.527	-
	Comp.4	13.22	13.00	-	12.00	30	-	46
5 (30%)	Rot.4	13.00	12.00	-	-	-	1.083	-
	Comp.5	18.67	8.4	-	16.90	30	-	51
	Rot.5	8.40	16.90	-	-	-	0.497	-
	Comp.6	11.27	11.80	-	10.21	30	-	58
	Rot.6	11.80	10.21	-	-	-	-	-
	Comp.7	15.40	8.44	-	13.85	30	-	62
	Rot.7	8.44	13.85	-	-	-	-	-
	Comp.8	12.00	9.70	-	10.85	30	-	66
	Rot.8	9.70	10.85	-	-	-	-	-
	Comp.9	14.16	7.60	-	12.67	30	-	70
	Rot.9	7.60	12.67	-	-	-	-	-
	Comp.10	11.00	9.90	-	-	30.5	-	72

Table 11 (continued)

Tool(mm)	N.of cycles	$w_{ave.}$	h (mm)	$h_{eq.}$	Δh (%)	Δl	Load(kN)
	-	15.00	15.00	-	-	-	-
	Comp.1	17.89	12.06	16.92	20	3.10	100
	Rot.1	12.06	16.92	-	-	-	-
	Comp.2	15.14	13.47	14.11	20	1.80	95
	Rot.2	13.47	14.11	-	-	-	-
$b_1 = 40$	Comp.3	17.21	11.26	15.96	20	1.45	102
	Rot.3	11.26	15.96	-	-	-	-
	Comp.4	14.40	12.73	13.35	20	1.00	87
	Rot.4	12.73	13.35	-	-	-	-
	Comp.5	15.95	10.63	14.87	20	1.10	100
	Rot.5	10.63	14.87	-	-	-	-
	-	10.63	14.87	-	-	-	-
	Comp.1	12.98	11.87	12.19	20	2.19	50
	Rot.1	11.87	12.19	-	-	-	-
	Comp.2	13.93	9.80	13.24	20	1.21	50
	Rot.2	9.80	13.24	-	-	-	-
$b_2 = 20$	Comp.3	11.69	10.58	11.06	20	1.25	40
	Rot.3	10.58	11.06	-	-	-	-
	Comp.4	13.90	8.00	12.79	20	1.70	50
	Rot.4	8.00	12.79	-	-	-	-
	Comp.5	10.19	9.72	9.46	20	1.30	40
	Rot.5	9.72	9.46	-	-	-	-
	Comp.6	12.03	7.57	11.26	20	0.65	35

Table 12. Experimental data compressed-rotated continously using two different tool widths.

Theory (mm)					*Experiment*				
w_1	w_2	h_1	h_2	l_f	w_1	w_2	h_1	h_2	l_f
8.76	9.02	14.07	8.88	128.4	10.63	9.46	14.87	9.72	126.7

Table 13. Final dimensions of the stepped shaft.

APPENDIX-C

Published papers from the work

1) **Aksakal B., Osman F.H., Bramley A.N.**, "Analysis of Open die Forging", Procc. of 29th.Int.Matador Conf.,pp 415-419,1992

2) **Aksakal B., Osman F.H., Bramley A.N.**, "Analysis for the automation of small batch manufacturing using open die forging", to be published in CIRP annals.

3) **Aksakal B., Osman F.H., Bramley A.N.**, "An open die forging methodology for the production of bars with stepped pofiles", to be published.

4) **Osman F.H., Aksakal B., Bramley A.N.**, "Computer aided flexible system for open die forging", to be published in Proc.9th National Conf. on Manuf.Research, Bath, 7-9 September, 1993

Bibliography

[1] **Aksakal B., Osman F.H.,Bramley A.N.,** "Analysis of Open die Forging", Procc. of 29th.Int.Matador Conf.,pp 415-419,1992

[2] **Aksakal B., Osman F.H.,Bramley A.N.,** "Analysis for the automation of small batch manufacturing using open die forging", September-1993, to be published in CIRP annals

[3] **Aksakal B., Osman F.H.,Bramley A.N.,** "Analysis for the automation of small batch manufacturing using open die forging, September-1993, to be published in ICTP proceeding.

[4] **Appleton E. et al,** "Open die forging with industrial robots", J.of Ind. Robot Vol.6,N.4, 191-194, 1979

[5] **Appleton E.and Heginbotham W.B.,**"Experimental study into the use of an industrial robot as a manipulator for open die forging of light workpieces",Proc. 9th I.S.I.R Washington, 709-728 (1979)

[6] **Appleton E. et al,**"Design study and feasibility trial for a robot blacksmith",Proc.8th. I.S.I.R.,Stuttgart,1978

[7] **Avitzur B.**, "Metal Forming processes and analysis" McGraw Hill Book Coop., New York, 1968.

[8] **Avitzur B.**, "Metal Forming" Marcel Dekker,inc, New York,1980.

[9] **Avitzur B.**, "Forging of hollow discs", Israel J.of tech., Vol.93, 295-304, 1964

[10] **Alexander J.M., Brewer R.C. and Rowe G.W.**, "Manufacturing Technology", Ellis Horward series, John Willey and sons Lmtd.,1987

[11] **Avitzur B.**, Metal Forming: Processes and Analysis, McGraw-Hill Book Comp.,N.Y.,1968

[12] **Avitzur B.**, Metal Forming Proceses and analysis, Robert E. Krieger Publishing company, Huntington,N.Y,1979

[13] **Baraya G.L.**, "Flat bar forging and the yield criteria",PhD Thesis,Victoria University of Manchester,1964

[14] **Baraya G.L.and Johnson W.**, "Flat bar forging", Proceedings of the fifth int.Tool Des. Conf. 449-469 (1964)

[15] **Bramley A.N.,Abdul N.A**, "Stress strain curves from the ring test',

[16] **Braun-Angot and Berger B.**, "An Upper Bound Aproximation for spread and pressure in flat tool forging", Proc. Int.Conf. on Numerical Methods in Ind. Forming Processes, Swansea, UK,1982.

[17] **Cramphorn A.S and Bramley A.N.**, "Computer aided forging design with UBET" Proc. 18. MTDR Conf., London, 1977.

[18] **Christensen P.**, "Computer Aided Design for forging dies using the upper bound elemental technique", PhD thesis, Techniqal Univ. of Denmark, Inst. of Manufac. Eng.,1987

[19] **Drucker D.C.**, "Plasticity theory , strength-differential(S-D) phenomenon, and volume expansion in metals and plastics", Metall.Trans. 4, 667, 1973.

[20] **Green and Johnson W.**, "A theoretical investigation of the compression of a ductile material between smooth flat dies", Phil. Mag.,42, 1951, 900-918

[21] **Ewans C.W.**, Engineering Mathematics, Van N.Reinhold Co.Ltd.,1989

[22] **Hill R.**, "A general method of analysis for metal working processes" J.Mech. Phys.solids 11, 305-326 (1963).

[23] **Hill, R.**, The Mathematical Theory of Plasticity, Clarendon Press, Oxford,1983

[24] **Dudra S.P. and Im Y.T.**, "Investigation of metal flow in open die forging with different die and billet geometries", J.Mat.Process.Tech., Vol.21, 143-154(1990)

[25] **Erman E. and et al.**, "Physical modelling of blocking process in open die press forging",J.Mech.Working Tech.,Vol.19, 165-180, 1989

[26] **Erman E. and et al.**, "Physical modelling of the upsetting process in open die press forging",J.Mech.Working Tech.,Vol.19, 195-210, 1989

[27] **Ewans C.W.**, Engineering Mathematics, Van N.Reinhold Co.Ltd.,1989

[28] **Hosford W.F., and Caddell R.M.**,Metal Forming Mechanics and Metallurgy, Prentice-Hall Inc.,Englewood Cliffs,N.Y,1983

[29] **Heginbotham, W.B., Dooner,M., Kennedy,D.N.,** "Robot machine interfacing by computer graphics" 3rd CISM IFTOMM Symposium, Udine, Italy(1978)

[30] **Heginbotham, W.B., Dooner,M., Kennedy,D.N.,** "Computer graphics simulation of industrial robot interactions", Proc. 7th.ISIR, Tokyo,(1977)

[31] **Hartley P., Pillinger I. and Sturgess C.,** "Numerical Modelling of Material deformation Processes", University of Birmingham, Pringer-Verlag London,1992

[32] **Ewans C.W.,** Engineering Mathematics, Van N.Reinhold Co.Ltd.,1989

[33] **Hill, R.,** The Mathematical Theory of Plasticity, Clarendon Press, Oxford,1983

[34] **Foster, G.,** Proc. of 4th Int. Conf. on J.I.T Manufacturing, "J.I.T's managing for success", 1989, London,UK

[35] **Drucker D.C.,** "Coulomb Friction, Plasticity and Limit Loads", J. of Applied Mech.,Trans.,ASME,Vol.21, 71-74(1954)

[36] **Johnson W.,** "Estimation of Upper Bound loads and coining operations" Proc. Inst.Mech.Engs., 173, 1959, p61

[37] **Johnson, Mellor** ,Engineering Plasticity, Van Nostrand Reinhold Comp.Ltd.,London,1980

[38] **Lange K.,** Metal Forming Processes, Handbook of Metal Forming", McGraw-Hill Book Comp.,NY, 1985

[39] **Calladine C.R.** ,Engineering Plasticity, Pergamon Press, Oxford,1969

[40] **Rowe G.W.**, Principles of Industrial Metalworking Processes, Edward Arnold Ltd.,London,1977

[41] Metals Handbook,ASM, Open Die Forging, Vol.5,pp 41-48,1970

[42] **Kudo H.** "An Upper Bound approach to plane strain forging and extrusion-I" Int. J .Mech. Sci,1, 1960, pp,57-83.

[43] **Kudo H.**, An Upper Bound approach to plane strain forging and extrusion-II" Int. J .Mech. Sci,1, 1960, pp,229-252.

[44] **K.F Kennedy**, "A method for analysis spread, elongation and bulge in flat rolling" J.of engineering for industry.Vol.109, ASME, August 1987 pp 248-256.

[45] **Juneja B.L.** "Forging of Rectangular Plates", Inst.J.Mach.Tool.Des.Res Vol 13, pp 141-153, 1973

[46] **Juneja B.L.**, "Forging of polygonal discs with barrelling", Int.J.Mach.Tool Des.Res.,Vol.13, 87-97(1973)

[47] **Juneja B.L.** , "Forging of rhombus shaped discs", Int.J.Mech.Sci.Vol.13, 99-110(1973)

[48] **Sagar R. and Juneja B.L.**, "An upper bound solution for flat tool forging taking into account the bulging of sides", Int.J.Mech.Sci.Vol.19, 253-258, 1979

[49] **Sagar R. and Juneja B.L.**, "Open die forging of a four sided irregular discs", Int.J.Mech.Sci.Vol.31, 315-328(1991)

[50] **Kiefer B.V. and Shah K.N.**, "Three-Dimensional simulation of open die forging", J. of Eng.Mat.Tech., Vol.112, 477-485 (1990)

[51] **Kanacri F., et al.**, "Plastic compression of rectangular blocks between two parallel platens", Int.J.Mech.Sci.Vol.13, 481-490 (1972)

[52] **Kim J.H.**, "A study on the three-dimensional upset forging of prismatic blocks", PhD Thesis, Dept.of Production Eng. Korea Adv. of Sci.,1985

[53] **Lakshmipaty R. and Sagar R.**, "Effect of die surface topography on die-work interfacial friction in open die forging", Int.J.Mach. Tools Manufact., Vol.32,No.5. 685-693 (1992

[54] **Kemp I.**, "Modelling of three dimensional metal forming processes using the Upper Bound elemental technique, BHP research and new technology, Melbourne Research Laboratories, technical Note-MRL/MAT/89/027Johnson W., "Estimation of Upper Bound loads and coining operations" Proc. Inst.Mech.Engs., 173, 1959, p61

[55] **Kopp R.**, "Incremental Forging with integrated open-die forging presses" Metall.plant and Techn.6, pp 76-81, 1982.

[56] **Johnson W.and Mellor P.B.**, "Engineering Plasticity" The Camelot Press ltd., southampton, 1973.

[57] **Li Y.and Zhou D.**, "An upper bound strip technique for predicting three dimensional spread", Dept. of Metal Eng. jilin Univ. of Techn.,China,1988

[58] **Lange K.**, "NC-Radial forging -a new concept in flexible automated manufacturing of precision forging in small quantities", 25th MTDR Conf.,Birmingham,157-162, 1985

[59] **Lange K.**, Handbook of Metal Forming, Mc Graww-Hill Book Comp.,1985

[60] **Lugora G., Bramley A.N.**, "Three dimensional analysis of closed-die forging processes 1,2", Proc.Instn.Mech.Engrs.Vol 203, pp 33-42,1989.

[61] **Male A.T. and Cockcroft M.G.**, "A method for determination of friction of metals under conditions of bulk plastic deformation", J. of the Inst. of Metals, Vol.93, 38-46, 1964

[62] **Male A.T.**, "The effect of temperature on the frictional behaviour of various metals during mechanical working", Vol.93, 489-494, 1964

[63] **Male A.T.**, "Variations in Friction coefficients of Metals during compressive defoemation", J. of the Inst. of Metals, Vol.94, 121-125, 1966

[64] **Male A.T. and DePierre, V.**, "The validity of mathematical solutions for determining friction from the ring compression test", ASME Journal of lubrication Tech. Vol.92, 389-397, 1970

[65] **Mc Dermott R.P and Bramley A.N.**, "An elemental upper bound technique for general use in forging analysis", Proc. 15. Int. MTDR conf., 1974

[66] **Mulc A. and Milcic B.**, "Contribution to Modelling of Forging with Flat Tools", Annals of the CIRP,Vol.32, 215-217, 1983

[67] **Neuborn A. and Faber**, Forging Handbook, Arnold Ltd., London, 1959

[68] **Osman F.H.**, "Computerised Simulation of Forging Processes" Ph.D Thesis The university of Leeds Mech.eng dept. september 1981.

[69] **Osman F.H and Bramley A.N.**, Proc. 20. Int.Mach.Tool Des.Res.Conf. Birmingham,1980.

[70] **Pahnke H.J.**, "Fundamentals of programmed forging", MPT Met.Plant and Tech.Vol.6.,No.5, 92-101, 1983

[71] **Pahnke H.J.**, "Fundamentals of programmed forging", Stahl Eisen, V.103,N.11, June, 547-552, 1983

[72] **Prager W. and Hodge P.G.**, "Theory of perfectly plastic solids", John Wiley, New York(1951).

[73] **Pillinger I.**, "The Prediction of metal flow and proporties in three- dimensional forgings using the finite element method" Ph.D Thesis Dep. of Mech. Eng. Univ.of Birmingham, December 1983.

[74] **Park J.J. and Kobayashi S.**, "Three dimensional finite element analysis of block compression", Int.J.Mech.Sci.Vol.26,No.3, 165-176(1984).

[75] **Raughunathan and Sheppard**, "A new method for predicting spread in rolling processes", J.Mech.Working Tech.,Vol.19, 195-202, 1979

[76] **Schonberger J.R.**, "World Class Manufacturing", The Press Macmillan, NY.,1986.

[77] **Shimizu T. and et al.**, "Process Design on Multi Ram Forging", Advd.Tech. of Plasticity,Vol.1, 137-142, 1990

[78] **Shiau Y.C and Kobayashi S.**, "Three dimensional finite element analysis of open-die forging", Int.J.Num.Methods in Engng, Vol.25, 67-85(1988)

[79] **Sperry P.R., Bankard M.H.**, Metals Handbook,ASM, "Metallographic technique for aluminium Alloys",Vol.8,pp 120-129,1973

[80] Metallurgy of Aluminium Alloys,ASM Handbook, pp 260-267 and 441-472, 1970

[81] **Soda C., et al.**, "Metal forming machinery development in the national project of FMCS", Proc.1st Int. Conf. of Plasticity,Tokyo, 449-460, 1984

[82] **Stauffer I. and Robert.N.**, "Robot Adds Flexibility in Forging", J. of Rob. Today, V.7,N.1, Feb. 43-44,1985

[83] **Tomlinson A. and Stringer J.D.**, "Spread and elongation in flat tool forging", Journal of The Iron and Steel Institute, Oct.1959 pp 157-162.

[84] **Wistreich J.G.and Shutt A.**, "Theoretical analysis of bloom and billet", Journal of the Iron and Steel Institue Oct.1959 pp 163-176.

[85] **Thornton J.R.**, "Flow and load predictions in forging and extrusion operations" Ph.D Thesis Dept.of Mech.eng. Univ.of Leeds September 1977.

[86] **Zaharoff T.L., Johnson R.E. and Karabin M.E.**, "Spread in sheet rolling: a comparison using experiments, analytical solutions and numerical techniques", Int.J.Mech.Sci.Vol.34,No.6,435-442(1992).

[87] **Wada T. and Dean T.A.**, "An energy method analysis in three dimensions of the compression of a square sectioned block", Int.J.Mech.Sci.Vol.25, 497-503, 1985

[88] **Yang D.Y., et al.**, "Analysis of upset forging of cylindirical billets considering the dissimilar frictional conditions at two flat die surfaces", Int.J.Mach.Tool Des.Res.,Vol.31,No.3, 397-404 (1991)

[89] **Yang D.Y. and Kim J.H.**, "An analysis of three dimensional upset forging of regular polyigonal blocks by using the upper bound method", J. of Eng. for Ind.,Vol.109, 155-160 (1987)

ANALYSIS OF OPEN DIE FORGING

B. AKSAKAL, F.H. OSMAN AND A.N. BRAMLEY
School of Mechanical Engineering, University of Bath

SUMMARY

Open die forging is a long established process which can be used to produce a wide range of shapes. Its characteristic features in relationship to closed die forging processes are that it requires low forming loads, and with a small range of simple tools a wide variety of shapes can be produced. Deforming the workpiece is essentially incremental and manual skill and experience in manipulating the workpiece between the tools plays an important part in producing the required profiled product. This however has resulted in a diminished utilisition of the process. In this paper a general computerised methodology is proposed for small batch manufacture using a programmable press in conjunction with a workpiece manipulator. Elementary analysis, based on the upper bound method, with a simple kinematically admissible velocity field is introduced for restricted block forming, thus enabling the load and metal flow to be predicted for open die forging of rectangular sections locally deformed between two flat dies.

INTRODUCTION

Forged products offer substantial benefits in terms of material utilisation when compared with machined components and often also when compared with castings. Forgings are however invariably associated with large batch-size production where die sinking costs can be amortised to a small proportion of the individual component cost. Open-die forging uses simple flat tools and low energy machines but requires a great deal of experience and manual skill. Shape transformation is achieved by laborious manipulation of the workpiece while repeated blows are effected in order to reduce, locally, the cross section of the workpiece. There are some fundamental difficulties in planning the sequence of operations to achieve the required shape transformations in a systematic way. Some empirical rules exist in fullering type processes and there are a number of examples of so-called automatic/programmed forging sequences. Current methods are manual and applied to very large ingots without strategic planning. Operator knowledge and expertise ensures that workpiece manipulation and bite depth at every location is just sufficient to displace a small volume away from the gap between the two dies. The basic geometry of the cross-section of the workpiece during deformation remains the same with each blow reducing the component height and causing the material to flow laterally. The mode of the flow is characterised by increasing the length in the longitidunal direction and also causing side spread. In 1959 Tomlinson and Stringer/1/ used the results of their experimental work on hot forging of square section bars to simulate a multi-pass rolling process. They introduced a spread coefficient which is the ratio between the lateral and vertical logarithmic strains. It is worthwhile noting that for test carried out the transverse forging of cylindrical billets the bite ratio was the only significant factor. In the same year Wistreich and Shutt/2/ presented a comprehensive study on techniques for automated forging in which square blooms and billets were forged with aim of finding the best working procedure by considering the required load capacity of the press and cost of production. They considered only press cogging operations in which the billet cross-section was reduced in size but remained rectangular. In their study a general concept for cogging schedules which comprised finite sequence of squeeze ratios and workpiece rotations through 90 was presented. Braun-Angott and Berger/3/ presented an upper bound numerical solution for rectangular bar hot cogging process, they used a velocity field which was formulated using polynomials; linear in the direction of lateral spread but of higher order in the loading and longitidunal directions. Their results showed that while the width of the billet decreased the spread coefficient increased and the pressure on the tools decreased.

The authors are developing a system to automate the open-die forging processes using a robot to manipulate the workpiece and a numerically controlled press linked together via a controlling computer as shown in Fig 1. The system needs to be programmed and controlled to enable a given shape to be produced by a series of operations and workpiece manipulations. In order to provide such automation, a complete schedule of various formed features and profiles is necessary. This requires a reasonably accurate and rapid analysis of the deformation pattern for each individual bite so enabling on-line feedback. An analytical approach based on the upper bound method is introduced in this paper in order to predict flow and load and to set the foundation for a "process planning" algorithm.

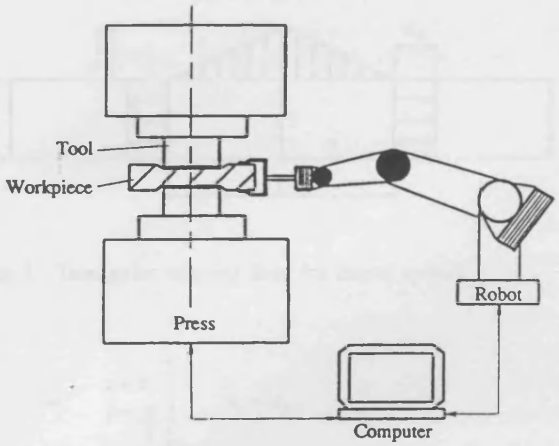

Fig 1. A proposed system for open-die forging

List of symbols

h : height of the billet

l : length of the billet

m : Friction factor,

w : width of the billet

p_{ave} : Mean forging pressure

$\dot{u}_x$, $\dot{u}_y$,$\dot{u}_z$: Velocities in the x,y,z directions respectively,

$\dot{u}_{max}$: Maximum velocity in the y-direction

$\dot{v}_p$: The upper tool velocity

J^* : Rate of total energy dissipation ,

$\dot{W}_d$: Deformation power or internal power,

$\dot{W}_f$: Friction losses,

$\dot{\varepsilon}_x$: Strain rate in x direction,

$\dot{\varepsilon}_y$: Strain rate in y direction,

$\dot{\varepsilon}_z$: Strain rate in z direction,

σ_0 : Yield strength of the deformed material ,

ANALYTICAL SOLUTION

In order to construct a methodology for the automation of open-die forging, a reasonably accurate metal flow analysis is required. The deformation pattern in this type of operations is a basic block quadrapiped element of width of w, thickness h and length l squeezed between two flat dies. When the billet is compressed there exist both primary and secondary bulges as Fig 2a. A theoretical model based on the upper bound theorem employing a triangular flow field is proposed and shown in Fig 2b. The elongation and the spread that occur during compression are estimated using a kinematically admissible velocity field which is optimised to yield the minimum power requirements.

The actual profile, however, is usually curved and symmetrical with maximum spread at the centre of the deformed section. The total power is minimised with respect to a pseudo independent parameter that is the maximum flow rate $\dot{u}_{max}$ in the direction of lateral spread. The secondary bulge being small compared to the primary bulge is not considered in this analysis.

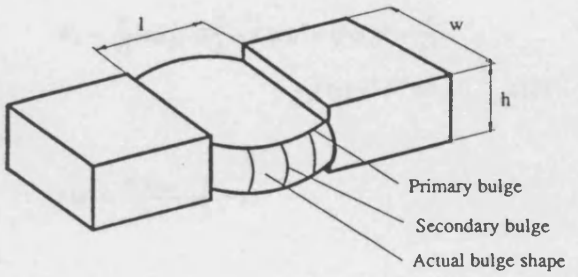

a)

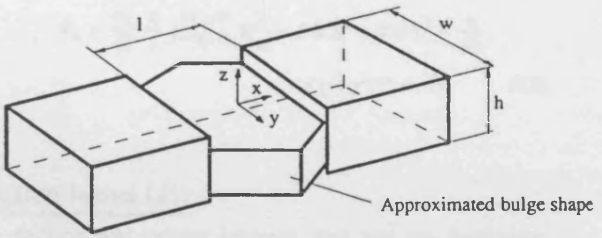

b)

Fig 2. Partially compressed block element

The velocity field

Fig 3 shows the velocity distribution at the boundary of the deforming section. Assuming that the dies approach the billet at unit speed and that the velocity in the z direction will vary linearly through the deforming zone, the following equations can be written:

$$\dot{u}_z = -\frac{2}{h} z$$

$$\dot{\varepsilon}_z = \frac{\partial \dot{u}_z}{\partial z} = \dot{\varepsilon}_z = -\frac{2}{h} \qquad (1)$$

The velocity $\dot{u}_y$ in the direction of lateral spread can be written as:

$$\dot{u}_y = \frac{4\,\dot{u}_{max}}{w\,l}\left(\frac{l}{2} - x\right) y \qquad (2)$$

This velocity distribution satisfies the boundary conditions, that is,

$$at \quad \left.\begin{matrix} x = 0 \\ y = 0 \end{matrix}\right\} \qquad \dot{u}_y = 0$$

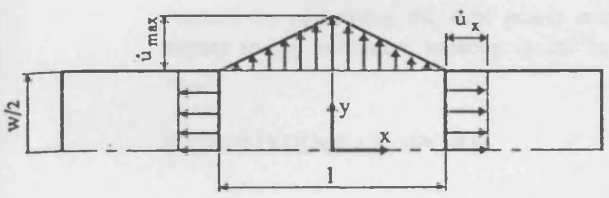

Fig 3. Triangular velocity field for lateral spread.

$$\left.\begin{array}{ll} at & x = 0 \\ & y = \dfrac{w}{2} \end{array}\right\} \quad \dot{u}_y = \dot{u}_{max}$$

$$\left.\begin{array}{ll} at & x = \dfrac{w}{2} \\ & y = \dfrac{l}{2} \end{array}\right\} \quad \dot{u}_y = 0$$

the strain rate $\dot{\varepsilon}_y$ becomes,

$$\dot{\varepsilon}_y = \frac{4\,\dot{u}_{max}}{w\,l}\,(\frac{l}{2} - x) \tag{3}$$

if the volume constancy equation is introduced;

$$\dot{\varepsilon}_x + \dot{\varepsilon}_y + \dot{\varepsilon}_z = 0 \tag{4}$$

then,

$$\dot{\varepsilon}_x = \frac{2}{h} - \frac{4\,\dot{u}_{max}}{w\,l}\,(\frac{l}{2} - x) \tag{5}$$

and the longitudinal velocity distribution $\dot{u}_x$ becomes,

$$\dot{u}_x = x\left[\frac{2}{h} - \frac{4\,\dot{u}_{max}}{w\,l}\,(\frac{l}{2} - \frac{x}{2})\right] \tag{6}$$

$$\dot{\varepsilon}_{xy} = \frac{1}{2}\left[\frac{\partial \dot{u}_x}{\partial y} + \frac{\partial \dot{u}_y}{\partial x}\right] \tag{7}$$

$$\dot{\varepsilon}_{xy} = -2\,(\frac{\dot{u}_{max}}{w\,l})\,y \tag{8}$$

The other strain rate components, $\dot{\varepsilon}_{yx}$ and $\dot{\varepsilon}_{yz}$, are zero.

Power analysis

The Upper bound theorem formulated by Prager and Hodge/4/ without traction forces is as follows:

$$J^* < \frac{2}{\sqrt{3}}\,\sigma_0 \int_V \sqrt{\frac{1}{2}\dot{\varepsilon}_{ij}^2}\; dV + \int_S \tau\,\Delta\dot{v}\; dS + \frac{m}{\sqrt{3}} \int_S \sigma_0\,\Delta\dot{v}\; dS \tag{9}$$

The first term of equation 9 is deformation power, the second term is shear power at surfaces of velocity discontinuity . And the third term represents the friction on the tool/workpiece interface where m is the friction factor $(0 < m < 1)$.

Deformation power ($\dot{W}_d$)

The deformation power is written as follows:

$$\dot{W}_d = \frac{2}{\sqrt{3}}\,\sigma_0 \int_z \int_y \int_x \sqrt{\frac{1}{2}(\dot{\varepsilon}_x^2 + \dot{\varepsilon}_y^2 + \dot{\varepsilon}_z^2) + \dot{\varepsilon}_{xy}^2}\; dV \tag{10}$$

Substituting for the strain rate components, from equations 1,3 and 5, gives:

$$\dot{W}_d = \frac{1}{\sqrt{3}}\,\sigma_0 \int_V [(\frac{2}{h} - f(x))^2 + (f(x))^2 + \frac{4}{h^2} + f(y)\,y^2\,]^{1/2}\, dV \tag{11}$$

where,

$$f(x) = \frac{4\,\dot{u}_{max}}{w\,l}\,(\frac{l}{2} - x)$$

and,

$$f(y) = \frac{4\,\dot{u}_{max}^2}{w^2\,l^2}$$

Considering one quarter of the billet the equation of the deformation power becomes,

$$\dot{W}_d = \frac{\sigma_0}{\sqrt{3}}\,\frac{h}{2} \int_{x=0}^{l/2} \int_{y=0}^{w/2} [(\frac{2}{h} - f(x))^2 + (f(x))^2 + \frac{4}{h^2} + f(y)\,y^2]^{1/2}\, dx\, dy \tag{12}$$

Friction losses ($\dot{W}_f$)

The friction that occurs between tool and the workpiece material is given by,

$$\dot{W}_f = \sigma_0\,\frac{1}{\sqrt{3}}\,m \int_A \Delta\dot{v}\; dA \tag{13}$$

The relative velocity $\Delta\dot{v}$ along the friction surface is;

$$\Delta\dot{v} = \sqrt{\dot{u}_x^2 + \dot{u}_y^2} \tag{14}$$

Substituting the velocity components in the x and y directions equation 2 and 6 respectively into (14) $\Delta\dot{v}$ becomes,

$$\Delta\dot{v} = \left[x^2\,(\frac{2}{h} - (l - x)\,\frac{2\,\dot{u}_{max}}{w\,l})^2 + (y\,f(x))^2\right]^{1/2} \tag{15}$$

Therefore the power required to overcome friction is,

$$\dot{W}_f = \frac{\sigma_0}{\sqrt{3}}\,m \int_{x=0}^{l/2} \int_{y=0}^{w/2} [\,x^2[\frac{2}{h} - (l - x)\,\frac{2\,\dot{u}_{max}}{w\,l}\,]^2 + (y\,f(x))^2]^{1/2} dx\, dy \tag{16}$$

The total power $\dot{W}$ is:

$$\dot{W} = \dot{W}_d + \dot{W}_f \tag{17}$$

and equals to the external power supplied by the tools $(p_{ave}\,w\,\frac{l}{4}\,\dot{v}_p)$ where $\dot{v}_p$ is the tool speed. The relative pressure $(\frac{p_{ave}}{\sigma_0})$ can therefore be obtained by proper substi-

tution into equation 17. The upper bound solution is obtained by optimising the total power numerically with respect to the maximum velocity in the lateral direction ($\dot{u}_{max}$).

EXPERIMENTAL WORK

In order to determine the validity of the theoretical analysis a series of experiments were carried out using a 100 tons Rhodes N.C hydraulic press provided with a load cell. Billets of 100mm in length 25mm in width and 16.66mm in height were machined from half hard aluminium 6082(HE30). The stress-strain curve for the working material was obtained by means of a compression test at room temperature. Fig 4 shows the experimental set up which was used for these experiments. Two sets of experiments were carried out, firstly, billets were deformed incrementally by giving 5% of height reductions at each blow. In the second test each billet was subjected to one deformation step, varying from 5% to 50% height reduction. Fig 5(a) shows examples of the incrementally deformed billets while 5(b) shows a series of billet subjected to progressive penetration. The dimensions and cross sectional area of the compressed billets were measured after each step. The figures show the primary and secondary bulge and also that both spread and elongation increase with the amount of height reduction.

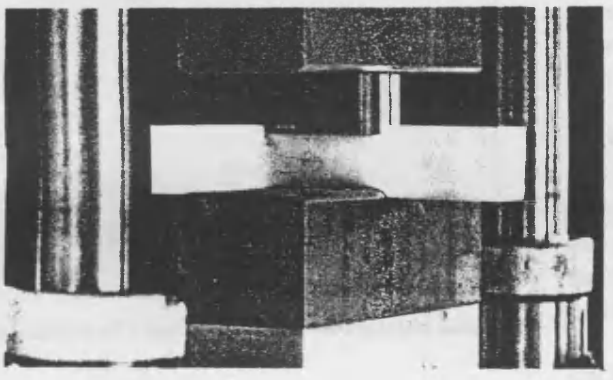

Fig 4. Experimental die set up.

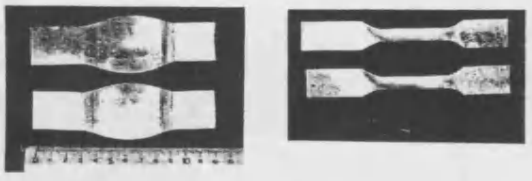

a) Incrementally compressed,

b) Separetely compressed.

Fig 5. A group of compressed specimens

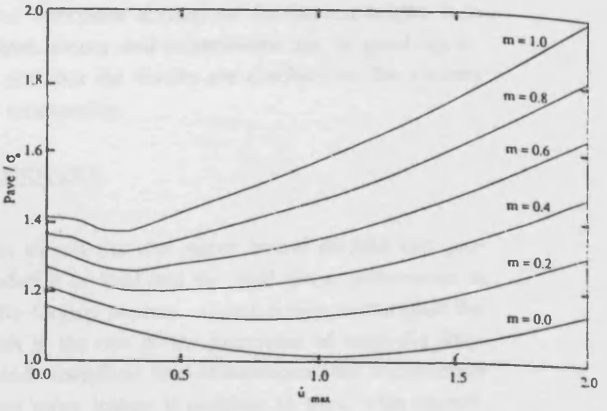

Fig 6. Variation of average pressure with spread

RESULTS AND DISCUSSION

The analytical method proposed earlier is based on the upper bound method and hence successful minimization of the power dissipated due to deformation and friction resistance is essential. Fig 6 shows the characteristic of the minimised function at friction levels between 0 and 1. The prediction of the minimum average relative pressure is very close to unity at frictionless condition and increases as the level of friction increases. Fig 7 shows the prediction of forging load and experimental results against various aspect ratios for the billet. In pressing a small part of the bar which has a rectangular cross sectional area the actual profile of spread is usually parabolic. The essential parameters which define the volume between the tools may be reduced to the maximum width of spread, die width and billet height. The die width is constant through the processes, the height reduction is effected by the tool penetration and therefore the only unknown parameter in this case is the maximum spread. Hence the maximum cross sectional area of the part of the billet remaining under the die is an essential parameter in determining the volume of the material between the two dies. Fig 8 shows the theoretical predictions and the experimental results of the maximum cross sectional area of the part of billet that is being compressed at various height reductions. It is also noted that while the trend shows that billets compressed in an incremental manner gave higher spread than those which deformed in one step the difference is negligible. Also, the trend in the theoretical prediction for this parameter is not sensitive to friction. During the open die

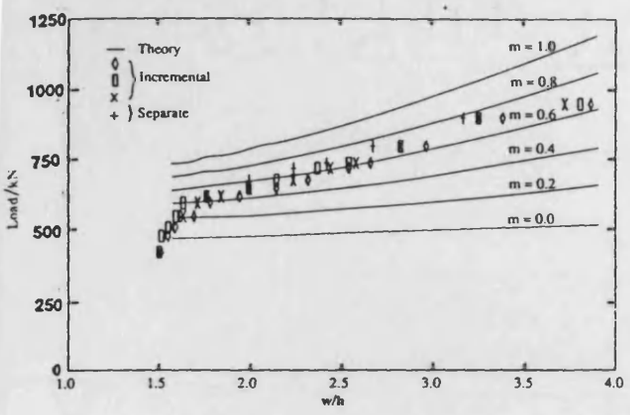

Fig 7. Prediction of forging load.

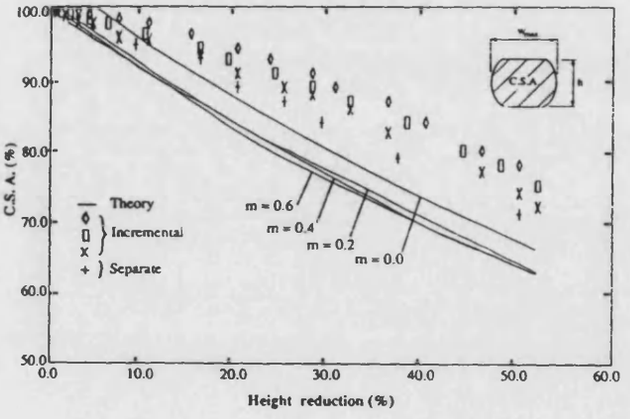

Fig 8. Prediction of billet maximum cross-sectional area.

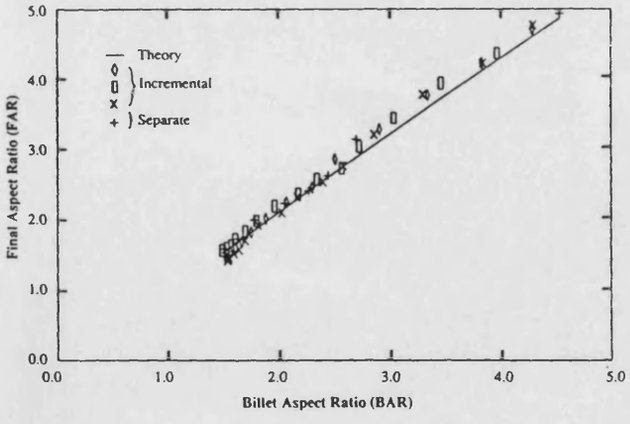

Fig 9. Prediction of final aspect ratio of w/h

forging process the final dimensions requirement can only be produced if the volume of material between the dies remains, at all times, greater than that of the final product. It is however useful to present the data in terms of the aspect ratio of the deformed part before and after each step as shown in Fig 9. The aspect ratio here is defined by the width of the workpiece divided by the current height. It is seen that both theory and experiments are in good agreement and also that the results are confined to the vicinity of a linear relationship.

CONCLUSIONS

It has been shown that the upper bound method can provide a predicton of load and the final shape dimensions in the open die forging process. Using simple rectangular flat tools, which is the one of the principles of open-die forging, load and workpiece final dimensions after incremental compression steps makes it possible to plan, with reasonable accuricy, the sequence of blows and workpiece manipulation for the production of profiles. This basic analysis will enable the method to be used as characteristic of an incremental forging technique in which workpiece is manipulated using a robot and deformation being carried out with simple shaped tools.

ACKNOWLEDGEMENTS

The authors acknowledge the financial support given to Mr. Aksakal by the University of Ataturk in Turkey and the provision of research facilities by the University of Bath.

REFERENCES

1] TOMLINSON AND STRINGER(1959), "Spread and elongation in flat tool forging", Journal of The Iron and Steel Institute, pp 157-162.

2] WISTREICH and SHUTT(1959), "Theoretical analysis of bloom and billet", Journal of the Iron and Steel Institue, pp 163-176.

3] BRAUN, ANGOT and BERGER(1982), "An Upper Bound Approximation for spread and pressure in flat tool forging", Proc. Int. Conf. on Numerical Methods in Industrial Forming Processes, Swansea, UK, pp 165-174

4] PRAGER and P.G.HODGE(1951), "Theory of perfectly plastic solids", John Wiley,New York.

ANALYSIS FOR THE AUTOMATION OF SMALL BATCH MANUFACTURING USING OPEN DIE FORGING

AKSAKAL .B, OSMAN .F.H, and BRAMLEY .A.N(1)
University of Bath
School of Mechanical Engineering, UK

ABSTRACT

Open die forging is a long established process which can be used to produce a wide range of shapes. Its characteristics features in relationship to other types of forging processes are that it requires low forming loads and only a small range of simple tools to make a wide variety of shapes. Whilst the process is generally associated with the production of large forgings, an automated version could be attractive for small batch manufacturing of low weight forgings. Such a system could compete effectively against machining process. This paper examines the process of pressing small size parts by open die forging, reviews existing literature and presents an upper bound based solution for single step and incremental open die forging. The validity of the theoretical analysis is assessed by comparison with experiments and found to be in a good agreement.

Keywords: Open die forging, upper bound, automation.

List of symbols

h_0 : Initial height of the billet (mm)

h : Final height of the billet (mm)

l_0 : Initial length of the billet before compression(mm)

l : Length of the deformed region after compression(mm)

m : Friction factor,

w_0 : Initial width of the billet (mm)

w : Final width of the billet (mm)

b : Tool width (mm)

p_{av} : Mean forging pressure,

$\dot{u}_x, \dot{u}_y, \dot{u}_z$: Velocities in the x,y,z directions respectively,

b : Tool width (mm)

p_{av} : Mean forging pressure,

$\dot{u}_x, \dot{u}_y, \dot{u}_z$: Velocities in the x,y,z directions respectively,

$\dot{u}_{y_{max}}$: Maximum material displacement in the y direction,

$\dot{v}_p$: The upper tool velocity

$\dot{W}_d$: Deformation power or internal power,

$\dot{W}_f$: Friction losses,

$\dot{\epsilon}_x$: Strain rate in x direction,

$\dot{\epsilon}_y$: Strain rate in y direction,

$\dot{\epsilon}_z$: Strain rate in z direction,

σ_0 : Yield strength of the deformed material,

w_0/h_0 : Initial aspect ratio of the workpiece(IAR)

w/h : Final aspect ratio of the workpiece(FAR)

n : Number of compression-rotation cycles,

x : Overall height reduction in multi-cycle operation,

r : One step height reduction ratio.

INTRODUCTION

Open die forging has been in use for many years by relying upon forgemasters' experience and to a certain extent on the use of empirical formulae. Forming a bar with flat tools is one of the simplest processes but there exists no systematic approach to enable flow prediction and provide process planning algorithms. The workpiece is deformed and the cross section reduced using simple tools acting on a small part of the workpiece causing local plastic deformation. Forging loads are therefore much reduced as compared with conventional closed die forging where dies almost totally surround the workpiece and a flash is formed.

A computer -controlled on-line low-cost, incremental flexible forging process would have great benefit if the system were automated for production of small -batch near-net-shape profiles varying from simple stepped shaft to curved and elongated components. The complete system would be comprised of a numerically controlled press interfaced with a robot, which manipulates the small sized workpiece.

Previous research in open die forging has mostly dealt with the prediction of average pressure applied and forging load but for the present work one of the important aspects of the deformation is the analysis of flow which results in sideways spread and elongation. Pioneering work on providing a model which predicts the metal flow was introduced by Tomlinson and Stringer[9]. The effect of temperature, reduction in height, longitudinal extension of the bar and the shape of cross sections were investigated. Reduction in height was also varied in order to examine the proportion of spread to elongation. They developed an empirical formulae from their experiments describing spread as a ratio between the lateral and vertical logarithmic strains for square cross sections. The change in billet dimensions during each step was predicted by this spread coefficient. The effect of friction was not considered and it was pointed out that the coefficient of spread depends mainly on the shape of the tool contact area, as defined by the bite ratio ie the ratio of specimen width to tool width. Also it appears not appropriate for automation of the whole process.

Baraya and Johnson[1] analysed the problems in bar forging using the upper bound method. Three different solutions were suggested to determine the forging load. It was assumed that straight boundaries remain straight after compression but all the three solutions had some restrictions limiting their suitability also, the validity of solutions was dependent on aspect ratio of the workpiece. The analytical solutions did not take into account sideway bulging or friction. The experimental correlation was also poor.

Sagar and Juneja[7] also used the upper bound to derive a solution for compressing rectangular plates of aluminium which determined the average die pressure but did not take the sideway bulging into account. Subsequently they extended the work [3] for the forging of polygonal discs but taking the bulging into account and from this work the influence of aspect and bite ratio and friction on the optimum values of average pressure was shown. They reported that for the same values of bite ratio and aspect ratio, the spread increases with the friction factor on the tool workpiece interface increased and at small bite ratios bulging was increasing.

Kiefer and Shah[5] simulated open die forging by using a three dimensional analysis based on a finite element model. They used the model to show the distribution of internal stresses and strains on a rectangular ingot which was compressed to analyse the effect of different types of flat dies under different height reductions. Kanacri et al.[4] investigated the compression of rectangular blocks between two parallel platens by modifying Hill's[2] theory. It was shown from the flow lines that the amount of spread becomes higher with increased friction values. An experimental investigation into the strain distribution and surface crack formation using a photoelastic technique was carried out by Mulc[6] in a attempt to evaluate the practical workability limits in open die forging.

Recently Shimizu et al[8] presented some work which deals with a process design using the finite element method. In their analysis a multi ram press with a fixed tool width was used to reduce the cross section of circular

aluminium billets in three different ways. Firstly, elongating along longitudinal direction of billet, secondly, hexagonal reducing by rotating 45° and finally, square reducing by rotating the billet 90°. They showed the strain distribution while the cross section of the billet is reducing. During analysis no friction was considered and it was noted that the analysis process is limited by computing time which was given as 40 minutes CPU time for only four steps of cyclic compression and rotation. Such techniques requiring lengthy computing times and are not really suitable for adaptation into on-line modelling systems. The authors believe that the upper bound based methods offer a better prospect.

In order to develop an automated open die forging process it is essential to be able to predict the shape which occurs at each step. This can only be achieved by simulating the process using an incremental three dimensional analysis. In this paper some of the parameters that effect spread and elongation in open die forging using simple flat tools are investigated and a strategy constructed via a theoretical model based on the upper bound method producing rapid predictions of metal flow for continuing incremental deformation.

THEORETICAL ANALYSIS

Fig 1 shows schematically a long bar subjected to local deformation between two flat tools. The upper bound method is used to predict the three dimensional flow. In the analysis the free boundaries are assumed to be of parabolic form. The spread and elongation were predicted after each compression step using a kinematically admissible velocity field optimised to yield the minimum power requirements.

Velocity and strain rate field

In Fig 2 a quarter of the parabolic velocity field distribution is shown with primary lateral bulging. Secondary bulging is ignored and the metal flow in the lateral direction, y, is assumed parabolic reaching a maximum value of $\dot{u}_{y_{max}}$ at the centre and zero at the edge of tool. The term $\dot{u}_{y_{max}}$ will subsequently be used as a pseudo-independent parameter determined by minimization of the total power.

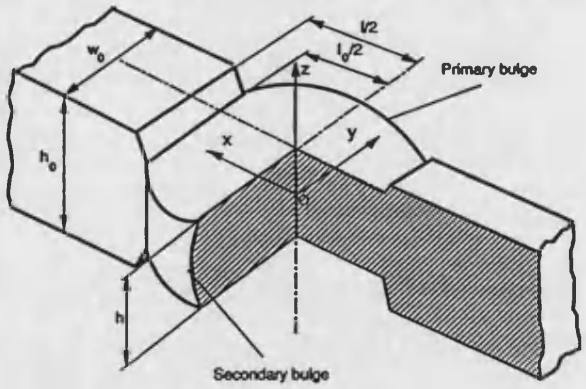

Fig 1. A locally compressed billet showing primary and secondary bulging.

During compression in the z-direction material will flow in the longitudinal direction, x and lateral direction, y . From the boundary conditions metal flow in the y direction can be determined.

$$ie. \qquad \dot{u}_y = \left(\frac{l_0}{2} - \frac{2x^2}{l_0}\right) \dot{v}_p \frac{4\dot{u}_{y_{max}}}{w_0 l_0} y \tag{1}$$

The velocity in the z direction is assumed to be a linear function of z with a maximum value equal to the die velocity, $\dot{v}_p$ at $z = \frac{h_0}{2}$

$$ie. \qquad \dot{u}_z = -\frac{2\dot{v}_p}{h_0} z \tag{2}$$

The strain rates can then be evaluated as:

$$\dot{\epsilon}_y = \frac{\partial \dot{u}_y}{\partial y} = \left(\frac{l_0}{2} - \frac{2x^2}{l_0}\right) \dot{v}_p \frac{4\dot{u}_{y_{max}}}{w_0 l_0} \tag{3}$$

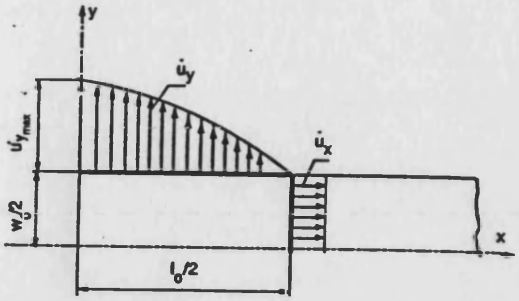

Fig 2. The parabolic velocity field for lateral flow.

$$\dot{\epsilon}_z = \frac{\partial \dot{u}_z}{\partial z} = -\frac{2\dot{v}_p}{h_0} \tag{4}$$

The volume constancy condition enables the strain rate in the x direction to be determined.

$$ie. \qquad \dot{\epsilon}_x = -(\dot{\epsilon}_y + \dot{\epsilon}_z) \tag{5}$$

$$ie. \qquad \dot{\epsilon}_x = \left[\frac{2}{h_0} - \left(\frac{l_0}{2} - \frac{2x^2}{l_0}\right)\frac{4\dot{u}_{y_{max}}}{w_0 l_0}\right] \dot{v}_p \tag{6}$$

By integrating Eqn. 6 the velocity in the x-direction can be obtained,

$$\dot{u}_x = \left[\frac{2}{h_0} x - \left(\frac{l_0}{2} x - \frac{2x^3}{3 l_0}\right)\frac{4\dot{u}_{y_{max}}}{w_0 l_0}\right] \dot{v}_p \tag{7}$$

then

$$\dot{\epsilon}_{xy} = \frac{1}{2}\left[\frac{\partial \dot{u}_x}{\partial y} + \frac{\partial \dot{u}_y}{\partial x}\right] = -\frac{8\dot{v}_p}{w_0 l_0^2} x y \dot{u}_{y_{max}} \tag{8}$$

Deformation power

In general form deformation power $\dot{W}_d$ is given as follows:

$$\dot{W}_d = \frac{2}{\sqrt{3}} \sigma_0 \int_x \int_y \int_z \sqrt{\frac{1}{2}(\dot{\epsilon}_x^2 + \dot{\epsilon}_y^2 + \dot{\epsilon}_z^2) + \dot{\epsilon}_{xy}^2}\, dV \tag{9}$$

Substituting strain rates from Eqn. 4 , 5, 6 and 7 into 8, the deformation power formula becomes:

$$\dot{W}_d = \frac{h_0 \dot{v}_p}{\sqrt{3}} \sigma_0 \int_{x=0}^{l_0/2} \int_{y=0}^{w_0/2} \left[\frac{1}{2}(f'^2(x) + f(x) + 2f'^2(x,y) + \frac{4}{h_0^2})\right]^{1/2} dx\, dy \tag{10}$$

where,

$$f(x) = 4\dot{v}_p \frac{\dot{u}_{y_{max}}}{w_0 l_0^2}\left(\frac{l_0}{2} - \frac{2x^2}{l_0}\right) \tag{11}$$

and,

$$f(x,y) = -\frac{8\dot{v}_p}{w_0 l_0^2} x y \dot{u}_{y_{max}} \tag{12}$$

Friction Power

The friction power occurs between tool and contact area A and is given by,

$$\dot{W}_f = \frac{\sigma_0}{\sqrt{3}} m \int_A \Delta\dot{V}\, dA \tag{13}$$

where the velocity $\Delta\dot{V}$ along the velocity discontinuity is ;

$$\Delta\dot{V} = \sqrt{\dot{u}_x^2 + \dot{u}_y^2} \tag{14}$$

Substituting the velocity components 1 and 2 into Eqn. 14 and then substituting Eqn.14 into Eqn.13, the friction power is determined as;

$$\dot{W}_f = \frac{\dot{\gamma}_\rho \sigma_0}{\sqrt{3}} m \int_{x=0}^{l_0/2} \int_{y=0}^{w_0/2} \left[\left(\frac{2}{h_0^2} x - g(x) \right)^2 + f^2(x)\, y^2 \right]^{1/2} dx\, dy \qquad (15)$$

where $g(x)$,

$$g(x) = \left(\frac{l_0}{2} x - \frac{2x^3}{3 l_0} \right) \frac{4 \dot{u}_{y_{max}}}{w_0 l_0^2} \qquad (16)$$

Optimization of Total Power

The total internal power is given by the sum of the deformation and friction power. The average pressure is then determined by equating the external to internal power.

$$\dot{W} = p_{av}\, \dot{v}_y \left(\frac{w_0 l_0}{4} \right) = \dot{W}_d + \dot{W}_f \qquad (17)$$

Thus,

$$\frac{p_{av}}{\sigma_0} = \frac{4}{\sqrt{3}} \frac{h_0}{w_0 l_0} \int_{x=0}^{l_0/2} \int_{y=0}^{w_0/2} \left(\frac{1}{2} \left[f^2(x) + f(x) + 2 f^2(x,y) + \frac{4}{h_0^2} \right] \right)^{1/2} dx\, dy$$

$$+ \frac{4}{\sqrt{3}} \frac{m}{w_0 l_0} \int_{x=0}^{l_0/2} \int_{y=0}^{w_0/2} \left[\left(\frac{2}{h_0} - g(x) \right)^2 + f^2(x)\, y^2 \right]^{1/2} dx\, dy \qquad (18)$$

The total power given by Eqn. 18 can then be optimised numerically to determine the value of $\dot{u}_{y_{max}}$ for which;

$$\frac{\delta \dot{W}}{\delta \dot{u}_{y_{max}}} = 0 \qquad (19)$$

EXPERIMENT and THEORETICAL CORRELATION

Experiments were performed on aluminium specimens in order to investigate the effects of initial aspect ratio, amount of deformation and tool width on the metal flow in the open die forging process. Metal flow was investigated initially in a single step compression on square cross-sectioned billets then further experiments were performed where the workpiece was subjected to multi-stage compression with 90° rotations around the x axis. Rotational movement of workpiece was controlled mannually at each step to effect the progressive deformation where required on only a small proportion of workpiece. The forging experiments were performed on a 1500kN capacity hydraulic press. The workpiece material was 6082Al and before the deformation process all workpieces were annealed at 425°C for two hours and cooled in air. The workpiece was located in a holder which accommodates longitidunal elongation and vertical movement of the billet centerline during pressing.

The measurement of spread in the lateral direction and so the calculation of displaced material volume into the axial direction are major problems in this type of process. These difficulties arise because of the shape complexity of the deformed material after each compression. Accurate location of the workpiece between the flat tools is also crucial since if it is not well centered by the holder the bulge shape becomes nonsymmetrical and difficult to measure. Thus the calculation of metal volume flow in the longitudinal direction also becomes difficult due to the undesirable bulge shape and workpiece distortions.

The effect of aspect ratio on material flow

To examine this effect experimentally, 12 sets of billets with aspect ratios in the range of 0.5 to 2.0 were used. The aspect ratios for these groups were varied by keeping the height h_0 constant and increasing the width w_0 of the billets. Each set consisted of 5 specimens of similar dimensions and each billet was subjected to different height reductions between 10 and 30%. The deformed height h, and average spread were measured. Elongation of each locally deformed billet was incorporated into material volume displacement by calculating the remaining material volume under tools and then substructing it from the initial volume for each single compression.

The same procedure was followed for the other 11 groups. In open die forging the initial aspect ratio of the billet is one of the effective parameters which determines the load and final dimensions. In Fig 3 the prediction of maximum spread values together with experimental results are shown for different initial aspect ratios of the long billets for a range of penetrations. It can be seen from this figure that the maximum spread initially increases with aspect ratio and its rate of increase tends to become decrease at high aspect ratio values.

It is also necessary to determine the amount of material flow in the axial direction for each single step of compression. This can be presented as elongation which in turn can be converted to the volume of material displaced

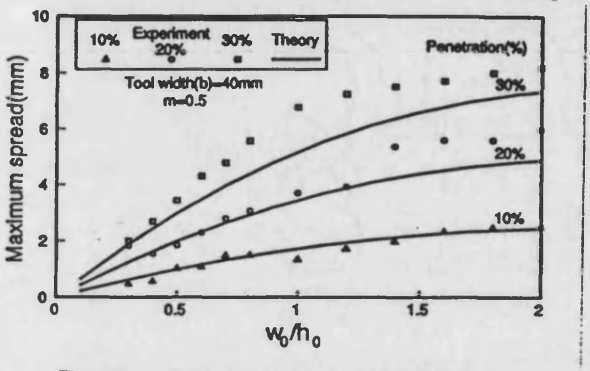

Fig 3 The variation of maximum spread with initial aspect ratio of workpiece.

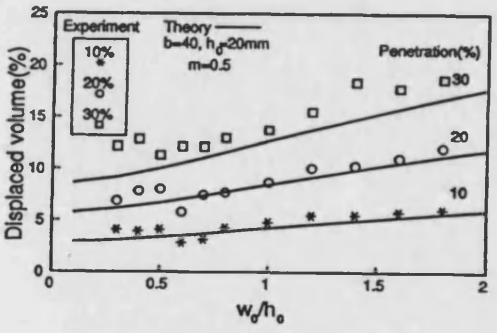

Fig 4 The variation of displaced material volume in axial direction.

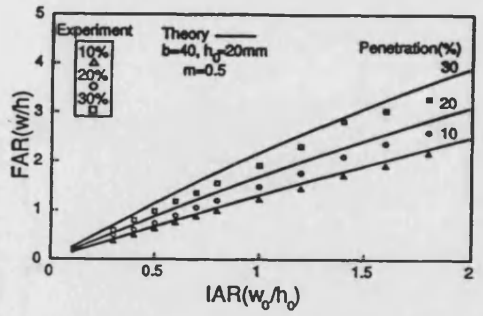

Fig 5 The variation of initial aspect ratio with final aspect ratio.

from between the dies. This has been investigated theoretically and experimentally, the results being shown in Fig 4 for various initial aspect ratio of billets. As can be seen from the graph the material volume displaced in the longitidunal direction increases with increasing initial aspect ratio and penetration. A similar trend in nondimensional form of elongation is also given in [4]. Whilst the displaced volume is of crucial importance in establishing processing routes, information about the resultant aspect ratio is also required.

The final aspect ratio was predicted as a function of various inital aspect ratios as shown in Fig 5. This shows that the final aspect ratio(FAR) increases with increasing initial aspect ratio(IAR).

The effect of tool width on material flow

In order to examine the affect of tool width on material flow, three different sets of billets were machined. Each set having four different aspect ratios of 0.5, 1, 1.5 and 2.0. The billets in each set were subjected to 25% penetration using different tool widths of 10, 20 30mm. After each compression with different tool widths the changes in height and spread were measured. Some experimentally deformed specimens are shown in Fig 6. Fig 7 shows the results in the form of variation of spread with initial aspect ratio of the workpiece and various tool widths. It was shown that at a fixed height reduction

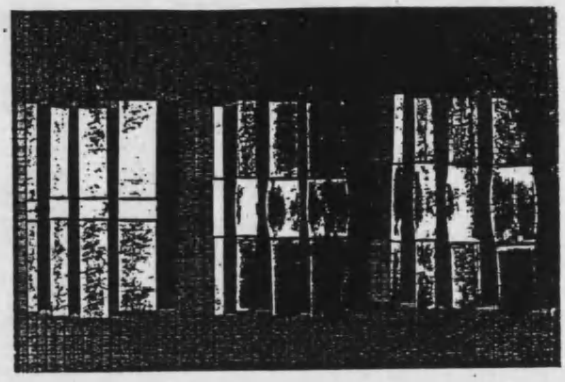

Fig 6. Some specimens locally deformed by tools of different widths.

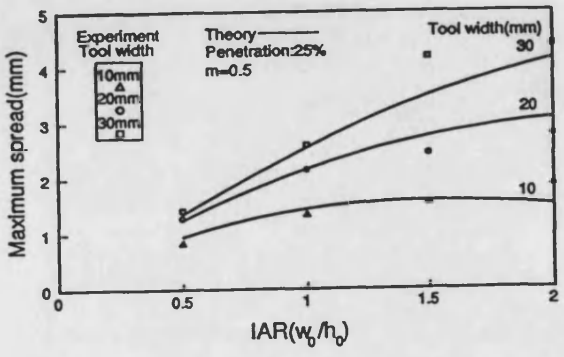

Fig 7. Spread prediction with different tool widths.

the amount of spread in this lateral direction increases with increasing tool width.

The effect of tool width on displaced volume in the longitidunal direction was also predicted, the results being given along with experimental data in Fig 8. The volume displaced in the axial direction increases with reducing tool width and increasing aspect ratio. The effects of tool width and initial aspect ratio on final aspect ratio are shown in Fig 9 and indicate an almost linear relation between initial and final aspect ratios.

Compressing and rotating of square cross-sectioned billets

Up to now the material flow in a single compression step has been considered and results presented. The production of symmetrical profiles in open die incremental forging is only possible by reducing the initial cross-section incrementally and this can be achieved by using workpiece compression and rotation cycles. As a first step for this type of operation a series of long bars were machined to provide a square cross section of 17x17mm. They were then

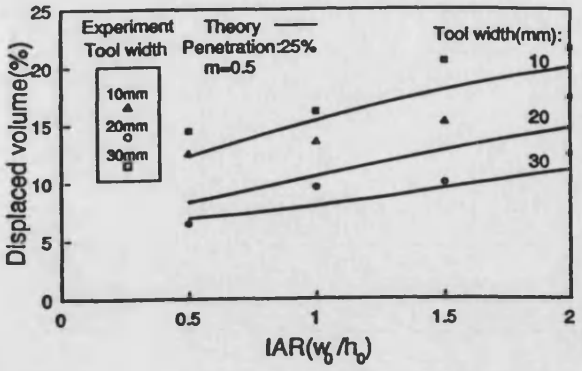

Fig 8. Variation of material volume displacement with various tool widths.

subjected to one compression corresponding to a 20% penetration after which the billet was removed and rotated through 90° then compressed by 25% penetration. Fig 10 shows a schematic drawing of the compression rotation cycle

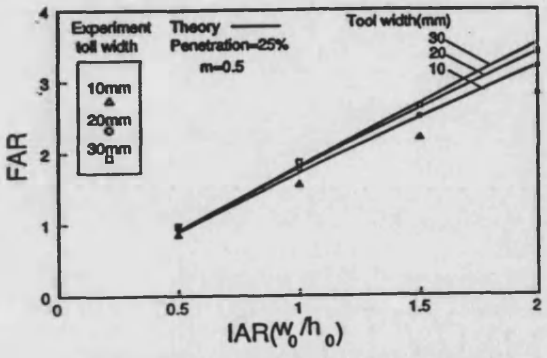

Fig 9. Variation of initial aspect ratio(IAR) with final aspect ratio(FAR) for different tool widths.

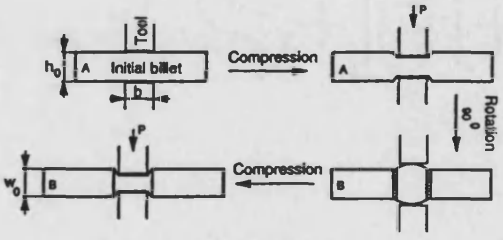

Fig 10. One cycle compression-rotation process

and Fig 11 shows some of these billets that were subjected to one cycle compression-rotation operation.

Many profiles may not be achieved by applying one cycle of this compression-rotation process due to the process limitations explained earlier. Some experiments were therefore carried out to analyse the viability of single and multi-cycle compression and rotation of the workpiece. For this, a number of billets were machined to the same dimensions and each one was subjected to compression-rotation cycles by repeating the process schematically described above in Fig 10 to enable overall reductions in the cross-section. Fig 12 shows some of the billets which were deformed in this way. The dimensions of the forged billet were measured after each compression step thus providing the starting dimensions for the next compression step. Here the determination of the height of the billet is important for the following compression step. It was calculated after every squeeze by assuming an equivalent flat profile for the assumed parabolic bulge. Thus the penetration level to be given for the next step was calculated and applied from this

equivalent height for the compressed and rotated billet. Another one of the crucial parameters of the process is the volume of material displaced from between the tools in each deformation step. It is necessary to ensure that more material is not displaced than is required to make up the desired cross section of any particular portion of the workpiece. In Fig 13 the change in displaced volume with the number of compression cycles for a fixed tool

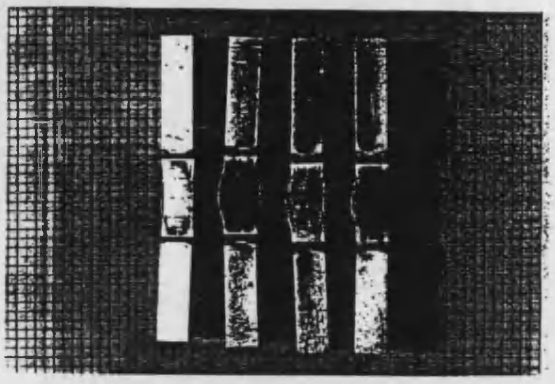

Fig 11. Some specimens locally subjected to one cycle.

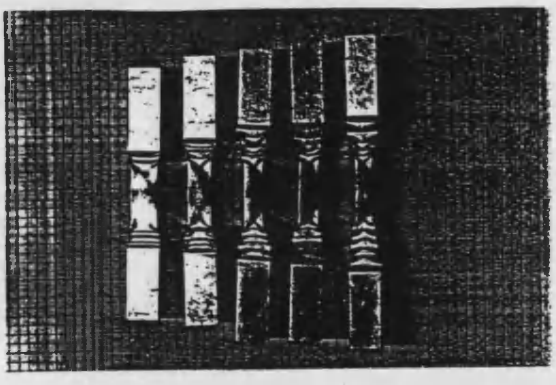

Fig 12 Specimens subjected to multi compression-rotation cycles.

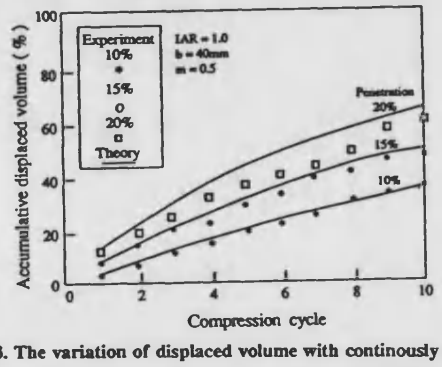

Fig 13. The variation of displaced volume with continously multi cycled compression and 90° rotation of the billets.

width and different penetration levels is seen. This shows that the volume displaced in the axial direction increases with the number of compression-rotation cycles while the process progresses continously with a simultaneous decrease in the cross section.

Implementation Strategy

A successful execution of a processing strategy for an automated/computerised open-die forging schedule depends to a great extent on the operational requirements for workpiece manipulation and positioning. Longitidunal and rotational movement of the workpiece is necessary while reducing the cross-section at each compression step. Conceptually, all that is involved is the repetition of the elementary deformation step described previously. The overall correlation between experiment and the analysis using the parabolic velocity field is suffeciently good to suggest that the analysis could be used for an on-line modelling system for a method of open die incremental forging.

The basis of the system is shown in Fig 14 which gives the compressed and rotated aspect ratio(CRAR) values for a range of penetrations being applied to billets of various IAR values. This family of curves is valid for particular values of tool width and friction factor. Fig 14 also suggests that for a given IAR value, there will be a unique operating point corresponding to a particular value of r, the height reduction which can be applied at each step of the process; with the billet aspect ratio, after the first cycle, remainning constant. To enable this, the operating point must fall on the 45° line. Fig 15 shows how these optimum reduction ratios vary with IAR values. Clearly the aspect ratio of a square section cannot be retained as no deformation will occur. In order to understand the operating strategy consider the case of a portion of a bar whose initial height h_0 is reduced to h by executing a number of compression and rotation cycles at the optimum operating point. The final overall height reduction ratio x for the whole process can be expressed as follows;

$$x = \frac{h}{h_0} \tag{20}$$

The aspect ratio at the begining of each cycle remains the same for the multi-cycle reduction which is represented by the triangle DEC in Fig 14. The height reduction ratio at any step can also be expressed by

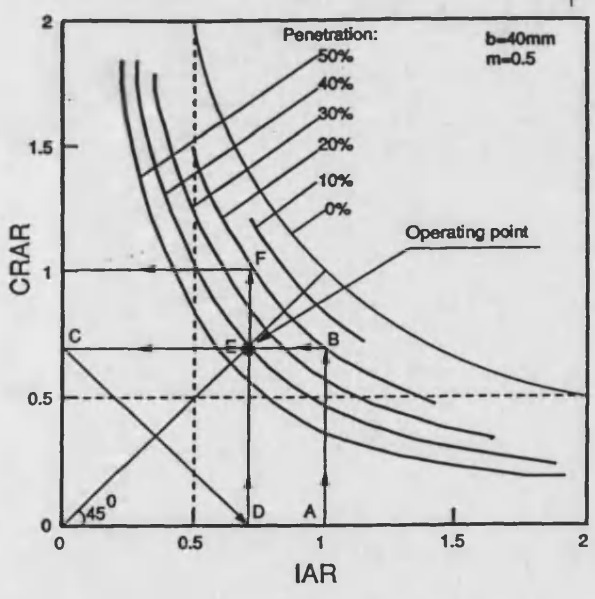

Fig 14. Optimum penetration per step for a given aspect ratio of billet.

$$r = h_{ic}/h_i \tag{21}$$

where h_{ic} is the height after compression and before billet is rotated. After 'n' cycles (compression followed by rotation) we can write:

$$ie \quad r^n = x\, a^n \tag{22}$$

where $a = \frac{w_0}{h_0}$, the constant aspect ratio in all cycles. The step height reduction ratio effected in all steps can now be expressed by:

$$r = e^{\frac{1}{n}\{\ln x + n \ln a\}} \tag{23}$$

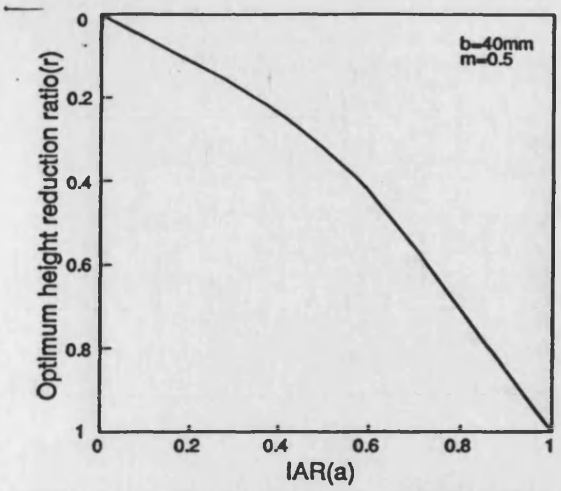

Fig 15. A sequential diagram for implementation strategy in reducing the cross-section of a long bar for a given reduction ratio.

Fig 16 illustrates the interesting concept of the operating region and limitation zones in open die forging. It is characterised by four zones. The impossible zone which is bounded by the limiting aspect ratio and zero penetration curve. The impractical zone gives a tall billet that is susceptible to buckling or non uniform deformation. The single step zone does not permit rotation due to limiting billet aspect ratio after rotation. The operational zone enables full cycle operation; that is continuous compression followed by rotation. In this zone an optimum operation line is defined which enables continuous and infinite number of cycles for a range of aspect ratios $1 > w_f/h_o > 0.5$. The other billet aspect ratios must be subjected to an initial compression in order to bring the dimensions of the billet to within the continuous cycle line. Also, a final compression step will be required in order to achieve final specific dimensions.

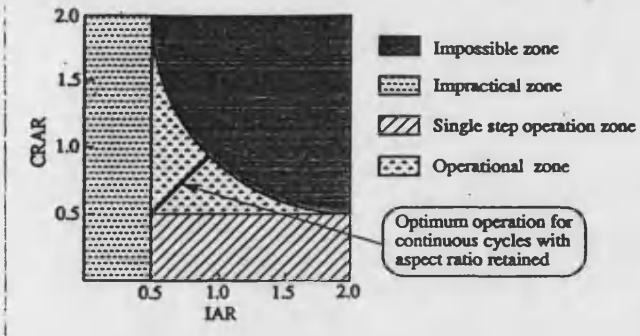

Fig 16. Operating regions for open die forging.

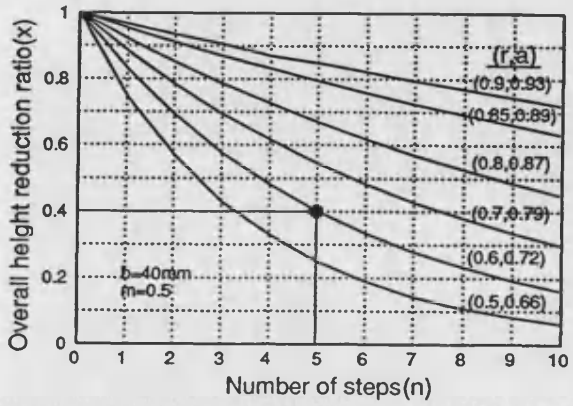

Fig 17. The relationship between overall reduction and the number of compression-rotation step.

Fig 17 shows the derived relationship between the parameters x,r,a and n. Thus for a required overall reduction in the cross-section of a billet in a multi-cycle operation, it is possible to determine an approximate operating aspect ratio, corresponding step reduction ratio and number of cycles. For reduction of square section stock, an initial and final step reduction will be required to "set" the operating aspect ratio and the terminating return to a square section. Only for these starting and finishing points can the aspect ratio approach the limiting value of 2. For example to achieve an overall height reduction of 0.4 in the dimensions of the billet an aspect ratio of $\hat{a} = 0.72$ must be established and then 5 steps each with $r = 0.6$ should be applied to reach the required terminating point. On Fig 14 the overall strategy and sequence are depicted by starting with a square billet at (A) which is reduced by approximately 20% ie point (B) after which the height is progressively reduced by 40% for 5 cycles corresponding to the circuit DECD. Finally a reduction of approximately 20% would return the aspect ratio to the unity corresponding to point (F).

The analysis can thus be used to establish an overall process planning and control strategy. On-line measurement and adjustment would of course be required to accommodate the inevitable variation in predictions caused by uncertain friction values and inaccuracies in the analysis. The computational time required for these calculations is more than adequate to enable on-line control of the process.

CONCLUSIONS

An analysis of the open die forging process based on the upper bound method has been presented as the basis of a process controlling system for producing specific shapes. The validity of the analysis has been checked against single compression steps and also against cyclic compression plus rotation sequences. The correlation has been demonstrated to be sufficiently adequate to enable a viable system for automated small batch manufacture.

ACKNOWLEDGMENTS

The authors acknowledge the financial support given to Mr. Aksakal by the Turkish Government-University of Ataturk and provision of research facilities by the University of Bath.

REFERENCES

1] Baraya G.L. and Johnson W.,1964, "Flat bar forging", Advances in Mach. Tool and Des., Res., Pergamon press, Vol.I, pp 449-469, NY.

2] Hill R., 1963,"A general method of analysis for metal working processes", J.Mech.Phys.solids 11, pp 305-326

3] Juneja B.L., 1973,"Forging of polygonal discs with barrelling", Int.J.Mach.Tool Des.Res., Vol.13, pp 87-97

4] Kanacri F., et al, 1972,"Plastic compression of rectangular blocks between two parallel platens", Int.J.Mech.Sci.Vol.13, pp 481-490

5] Kiefer B.V. and Shah K.N.,1990, "Three-Dimensional simulation of open die forging", J.of Eng.Mat.Tech., Vol.112, pp 477-485

6] Mulc, A., Milcic, B, 1983, "Contribution to modelling of forging with flat tools", Annals of the CIRP, Vol.32, pp 215-217

7] Sagar R., Juneja B.L.,1973,"Forging of Rectangular Plates", Int. J.Mach.Tool.Des.Res., Vol.13, pp 141-153,

8] Shimizu T. and et al, 1990,"Process Design on Multi Ram Forging", Advd.Tech. of Plasticity, Vol.1, pp 137-142

9] Tomlinson A, and Stringer J.D, 1959,"Spread and elongation in flat tool forging", J. of The Iron and Steel Institute, Oct., pp 157-162.

An Open Die Forging Methodology For The Production Of Bars With Stepped Profiles

AKSAKAL .B, OSMAN .F.H, and BRAMLEY .A.N

School of Mechanical Engineering, UK

ABSTRACT

Automation of open die forging systems can be attractive for small batch manufacture of medium-size parts where they can compete against a number of machining processes. The introduction of new manufacturing systems and the associated work-in-progress minimisation technique prompts a consideration of the use of the open die forging for incremental profiling and shaping processes. This paper reviews the open die forging process in this context as a part of a computer controlled robotic flexible forging system for the economic production of small-batch quantities. The metal flow in open die forging is analysed through a number of upper bound solutions and the basis of an on-line analytical modelling system together with experimental correlation and planning system is presented to produce bar profile features.

Keywords: Open die forging, upper bound, automation.

INTRODUCTION

Open die forging and swaging type processes are long established and are used to produce either very large or one-off components for which the closed die forging process would not be viable. The billet is usually worked progressively over its entire length by applying axial and rotational manipulation to the workpiece. The characteristic feature of this type of process is that only a small section of the workpiece is being worked at any one time. As a consequence the forging load and energy requirements are very much lesser than would be required if the component was to be made by closed die forging. Where open die forging processes are used there is a heavy reliance on manual skill and previous experience, although some empirical approaches to modelling the open die forging process have been made[1,2,3]. Park and Kobayashi[6] employed three dimensional finite element method in the analysis of simple block compression which is somewhat different from open-die forging in that the whole of the workpiece is worked on and the aspect of partially deforming the workpiece was not investigated. In addition the computing time was considerably high, hence it seems that the finite element method is yet not viable for applications where on-line processing and feed back monitoring is essential.

Incremental forming type process have been gaining ground in the area of sheet metal working and rotary forming together with various new forms of the swaging process and attempts have been made to automate and systematize the process. For example, in an industrial context, the Siemel Kempf Company in Germany[4] produces a robot and press combination which can be used for automatic open die forging. However whilst the facility is programmable, in order to produce a particular shape the robot has to learn the appropriate sequence of steps prior, these steps are determined by trial and error or from experience etc. The GFM and the MRPM[4] forging machines employ a multi-ram arrangement and exploit the concept of open die forging, but are generally associated with large components and do not offer a great deal of flexibility in setting up for different shapes. Lange[5] developed a four die radial machine, RUMX 2000, suitable for flexible production of medium size components, which was coupled with some analytical modelling work but the concept does not appear to have been taken up commercially.

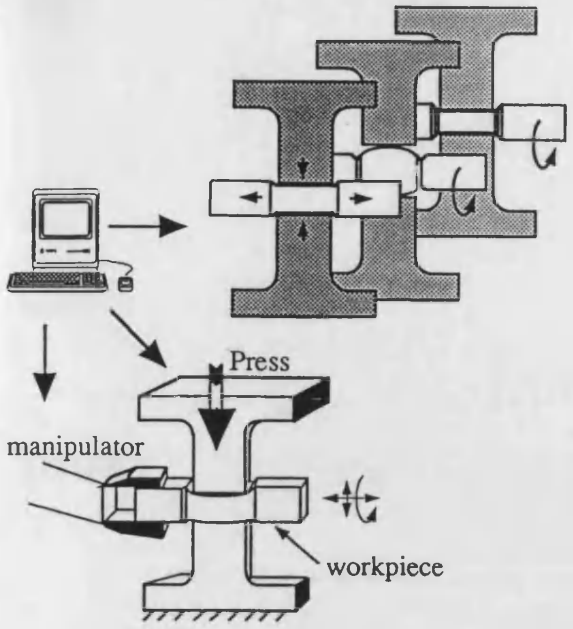

Fig 1. Automated bar profiling in open die forging

The forging industry, like many others, is having to make some significant adjustment to accommodate shorter production runs and a greater variety of parts. The economic benefits of small batch production in manufacturing, and of the forging process itself as a shape maker, suggest that a promising line of development could be to couple an automated open die forging process with a flexible on-line process design and modelling system as shown schematically in Fig 1. This has the potential for making use of existing equipment possibly with the need to retro-fit some form of computer control system to an existing set-up. Current practice and existing empirical formulae are restricted to a limited range of configurations and are not suitable or rapid enough for an on-line process. The main factors affecting the deformation characteristics are the friction, aspect ratio of the workpiece and the tool geometry; the first two which were investigated previously by the authors in a single step [8], and in multi compression and workpiece rotation type of processing[9].

In this paper three upper bound solution are presented for constructing an on-line modelling system in open die forging. The main purpose of this investigation is to enable the rapid prediction of material flow and allow for flexibility in process utilization so as to save material and reduce the total cost of production. Experiments were carried out for both single step squeezing and continuous cyclic compression and rotation of the workpiece.

ANALYTICAL SOLUTIONS

The configuration considered is that of a rectangular cross section billet being squeezed between two flat dies. When the element is compressed flow occurs in both longitudinal and lateral directions. Three different flow patterns have been proposed and evaluated; a simple homogeneous deformation pattern, a nonhomogenous triangular flow pattern and one incorporating a parabolic function in the lateral direction. The analysis for all these solutions in both one step compression with fixed penetration and tool widths are investigated and then extended into incremental compression with various penetration levels, different tool widths and friction levels. Fig 2 shows schematically the deformation patterns for the proposed solutions. Bar extension in the longitudinal direction, due to a deformation step, is assumed uniform and causes an increase Δl in the length of the bar. As a quadrapiped section of the billet is compressed between two flat dies both ends of the bar remains rigid and the height of the deformation zone is reduced.

Flow occurs in the longitudinal and lateral directions, x and y respectively. The actual bulge shape in this type of forming operations is normally of a parabolic type and is affected by forming conditions, friction, aspect ratio and tool width. The quadrapiped element undergoing deformation has an initial width, w_0, thickness, h_0 and length, l_0. Considering symmetry and assuming linear variation of velocity in the z direction. The velocity fields for those three solutions can be expressed as follows:

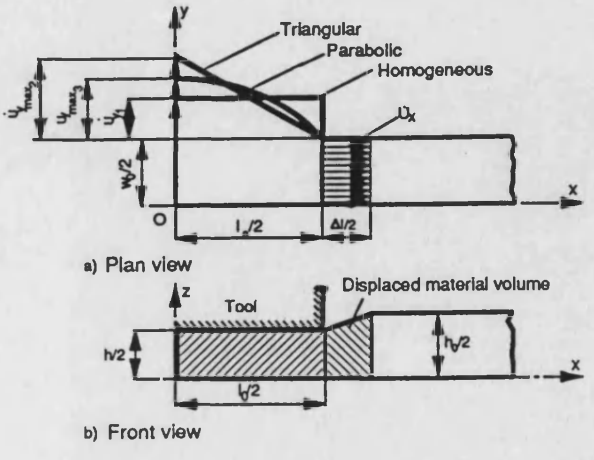

Fig 2. Schematic illustration of the deformation pattern in proposed models.

Homogeneous Velocity Field :

$$\dot{u}_x = \frac{2\,\dot{v}_p}{h_0}\,x \tag{1}$$

$$\dot{u}_y = \frac{2\,\dot{v}_p}{h_0}\,(1-\alpha)\,y \tag{2}$$

$$\dot{u}_z = -\frac{2\,\dot{v}_p}{h_0}\,z \tag{3}$$

where $\dot{v}_p$ is the die velocity and α is the ratio between longitudinal and axial strain rates,

$$\alpha = \frac{\dot{\varepsilon}_x}{\dot{\varepsilon}_z} \tag{4}$$

Triangular Velocity Field:

$$\dot{u}_x = \dot{v}_p\left[\frac{2}{h_0}\,x - \frac{2\,\dot{u}_{y_{max2}}}{w_0\,l_0}\,(l_0\,x - x^2)\right] \tag{5}$$

$$\dot{u}_y = \dot{v}_p\left[\frac{4\,\dot{u}_{y_{max2}}}{w_0\,l_0}\,(\frac{l_0}{2}\,y - yx)\right] \tag{6}$$

$$\dot{u}_z = -\frac{2\,\dot{v}_p}{h_0}\,z \tag{7}$$

Parabolic Velocity Field:

$$\dot{u}_x = \dot{v}_p\left[\frac{2}{h_0}\,x - \frac{4\,\dot{u}_{y_{max3}}}{w_0\,l_0}\,(\frac{l_0}{2}\,x - \frac{2}{3\,l_0}\,x^3)\right] \tag{8}$$

$$\dot{u}_y = \dot{v}_p\left[\frac{4\,\dot{u}_{y_{max3}}}{w_0\,l_0}\,(\frac{l_0}{2}\,y - \frac{2}{l_0}\,yx^2)\right] \tag{9}$$

$$\dot{u}_z = -\frac{2\,\dot{v}_p}{h_0}\,z \tag{10}$$

Rate of Energy Consumption:

The internal power of deformation $\dot{W}_d$ is calculated from the derived strain rate field as follows,

$$\dot{W}_d = \frac{2}{\sqrt{3}}\sigma_0 \int_V \sqrt{\frac{1}{2}\,(\dot{\varepsilon}_x^2 + \dot{\varepsilon}_y^2 + \dot{\varepsilon}_z^2) + \dot{\varepsilon}_{xy}^2}\;dV \tag{11}$$

and the friction power is calculated over the area of contact with the tool, A, using;

$$\dot{W}_f = \frac{\sigma_0}{\sqrt{3}}\,m \int_A \Delta\dot{V}\,dA \tag{12}$$

where,

$$\Delta\dot{V} = \sqrt{\dot{u}_x^2 + \dot{u}_y^2} \tag{13}$$

and m is the friction factor, $1 < m < 0$.

The total deformation power $\dot{W}$ is therefore;

$$\dot{W} = \dot{W}_d + \dot{W}_f \tag{14}$$

The external power supplied by the platens is the force times the platen velocity, thus;

$$\dot{W} = p_{ave}\,A\,\dot{v}_p \tag{15}$$

where p_{ave} is the average tool pressure.

By equating the power supplied by the tool to the power required to effect the deformation, the final expression can be derived for the relative average pressure as follows;

for the homogeneous pattern;

$$\left(\frac{p_{ave}}{\sigma_0}\right)_I = \frac{2}{\sqrt{3}}\left[(\alpha^2 - \alpha + 1)^{1/2} + \frac{4\,m}{h_0\,w_0\,l_0}\int_{x=0}^{l_0/2}\int_{y=0}^{w_0/2}\left[\alpha^2 x^2 + (\alpha^2 - 2\alpha + 1)\,y^2\right]^{1/2}\right] dx\,dy \tag{16}$$

for the triangular solution;

$$\left(\frac{p_{ave}}{\sigma_0}\right)_{II} = \frac{h_0}{\sqrt{3}\,w_0\,l_0}\int_{x=0}^{l_0/2}\int_{y=0}^{w_0/2}\left[\frac{8}{h_0^2} - \frac{4}{h_0}\,f(x) + 2\,f^2(x) + f^2(y)\right]^{1/2} + \frac{4\,m}{h_0}\left[g^2(x) + f^2(x)\,y^2\right]^{1/2} dx\,dy \tag{17}$$

where;

$$f(x) = \frac{4\,\dot{u}_{y_{max2}}}{w_0\,l_0}\,(\frac{l_0}{2} - x) \tag{18}$$

$$g(x) = \frac{2}{h_0} - \frac{2\,\dot{u}_{y_{max2}}}{w_0\,l_0}\,(l_0\,x - x^2) \tag{19}$$

and,

$$f(y) = \frac{4\,\dot{u}_{y\,max2}}{w_0\,l_0}\,y \tag{20}$$

and for the parabolic solution;

$$\left(\frac{p_{ave}}{\sigma_0}\right)_{III} = \frac{h_0}{\sqrt{3}\,w_0\,l_0}\int_{x=0}^{l_0/2}\int_{y=0}^{w_0/2}\left[\frac{8}{h_0^2} - \frac{4}{h_0}\,f_1(x) + 2\,f_1^2(x) + \frac{8}{l_0}\,x\,f_1^2(y)\right]^{1/2} + \frac{4\,m}{h_0}\left[g_1^2(x) + f_1^2(x)\,y^2\right]^{1/2} dx\,dy \tag{21}$$

where,

$$f_1(x) = \frac{4\,\dot{u}_{y_{max3}}}{w_0\,l_0}\,(\frac{l_0}{2}\,x - \frac{2}{l_0}x^2) \tag{22}$$

$$g_1(x) = \frac{2}{h_0}\,x - \frac{4\,\dot{u}_{y_{max3}}}{w_0\,l_0}\,(\frac{l_0}{2}\,x - \frac{2}{3\,l_0}\,x^3) \tag{23}$$

$$f_1(y) = \frac{4\,\dot{u}_{y_{max3}}}{w_0\,l_0}\,y \tag{24}$$

The final energy formulae are then optimized numerically, with respect to the independent parameter α in the homogeneous solution, $\dot{u}_{y_{max2}}$ in the triangular solution and $\dot{u}_{y_{max3}}$, in the parabolic solution. Spread and elongation or volume displaced away from under the pressing tool are then

obtained from these parameters. The CPU time required for 10 incremental steps was found to be less than half a minute on a SUN SPARC1+ workstation with 12 MB of memory. Such speeds would enable the proposed on-line application using a faster PC and incorporating a feed back mechanism to reschedule the sequence at each increment if necessary.

The results of the theoretical analysis for billet aspect ratios up to 10 is shown in Figs 3 and 4 for loading requirement and spread respectively. The homogeneous solution due to its simplicity gives considerably underestimated results for both loading and spread. However, the results of the triangular and parabolic solutions are fairly close to each other. The initial aspect ratio along the x-axis is generated by fixing the billet height, h_0 at 20mm and varying the width w_0. Fig 3 shows that the relative pressing pressure predicted by the triangular and parabolic solutions levels off to a max-

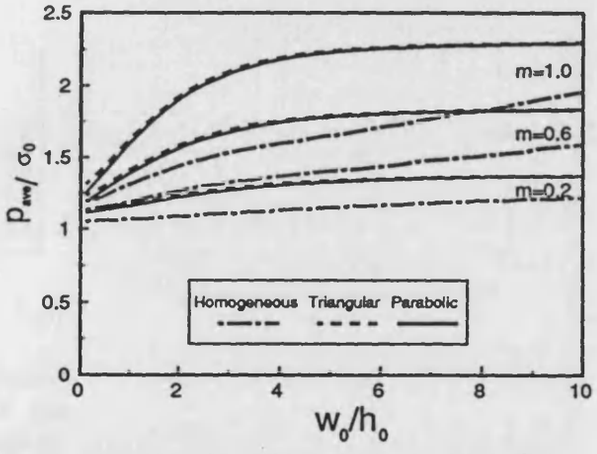

Fig 3. The variation of average pressure with aspect ratio.

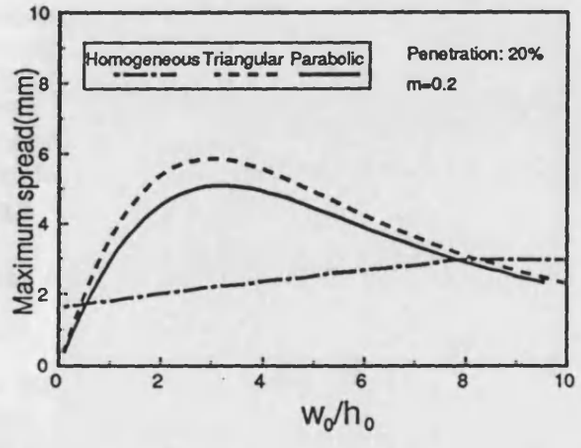

Fig 4. The variation of maximum spread with aspect ratio.

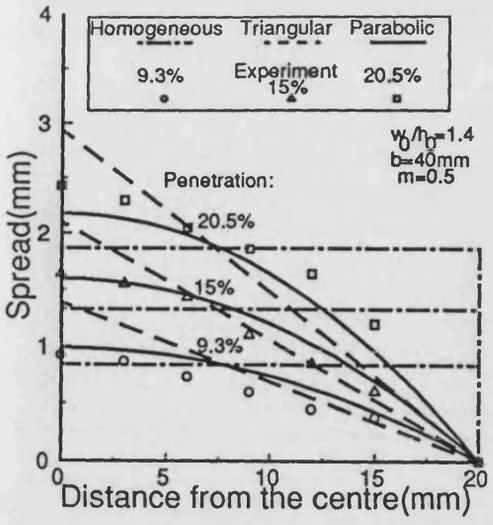

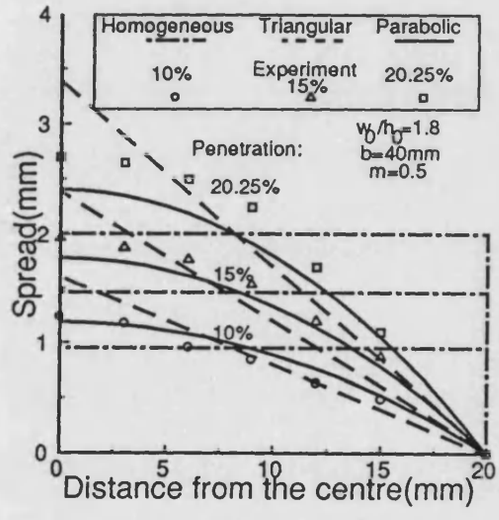

Fig 5. The variation of spread profile with various penetration levels.

EXPERIMENTAL PROCEDURE

In order to validate the theoretical analysis, experiments were carried out on billets made out of 6082 aluminum bars, 110mm long with various initial aspect ratios up to 2. Each specimen was subjected to a specific penetration in a single step and cyclic continous compression up to 30% using two dies with different width. After each compression both the maximum spread and spread profiles were measured.

Fig 5 shows the experimental values and theoretical prediction of the bulge profile for billets compressed with different penetration levels; only one quarter of the deformed billet is shown. As it

can be seen from this figure the amount of spread increases with increasing penetration. The parabolic solution appears to give the closest results to those of the experiments.

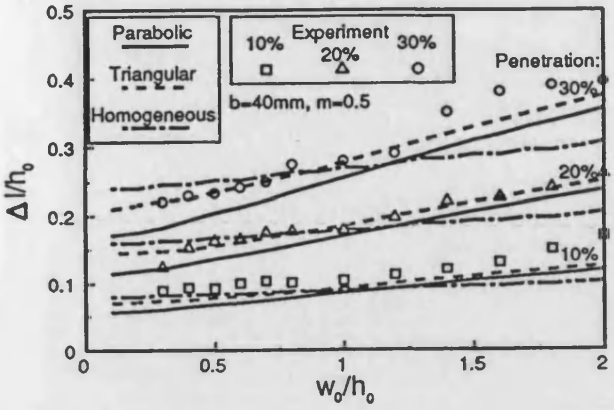

Fig 6. The variation of elongated material with aspect ratio.

	Initial Aspect Ratio(w_0/h_0)											
	0.3	0.4	0.5	0.6	0.7	0.8	1.0	1.2	1.4	1.6	1.8	2.0
Experimental Penetration(%)	10	10	10	10	10.8	10	10.1	10	9.3	10	10	10.2
	20	20.3	19.5	19	20	19.9	20.2	20.65	20.5	20.3	20.25	20
	30	30	30	30	30	30	30	32	33	32	30.75	30.7

Table 1. Experimental penetration levels.

During compression the workpiece also elongates in the longitudinal direction and the effect of aspect ratio, penetration and friction on the increase in billet length is shown in Fig 6, both experiment and theory show that elongation increases with increasing initial aspect ratio and penetration. The penetration levels obtained experimentally are given in Table 1. They are slightly higher than those used for the theoretical predictions. However, the results of this elementary unit compressed between flat tools forms the basis for the following incremental open die forging strategy.

Bar Profiling with Simple Flat Tools

The single step analysis described earlier can be applied in a consequtive manner on alternate faces of the workipece thus causing reduction in the cross section and increase in the component length. Various profiles can be generated by effecting different penetration levels along the length of the workpiece and also by employing tools with varying widths at different locations along the working length of the workpiece. The sequence of operations including the workpiece manipulation can be implemented and optimized using a computer controlled press and manipulator type of arrangment. It is therefore possible to simulate such a sequence using the chart shown in Fig 7 for a simple stepped type profiled component. In this example, a square cross-section billet and two different tool widths were used. Multi compression-rotation cycles were applied in a consequetive manner and to produce the stepped shaft profile shown in Fig 7(a).

The vertical axis of figure 7(b) represents the aspect ratio of the bar after compression and 90^0 rotation, CRAR (compressed and rotated aspect ratio), whilst the horizontal axis shows the initial aspect ratios, IAR (initial aspect ratio), of the bar before the beginning of each compression step. Fig 7(c) presents the volume of material displaced into the longitudinal-x direction against the number of the compression-rotation cycles. The initial billet has a square cross section; 15mmx15mm. The process starts using tool width $b_1 = 40mm$ and initial aspect ratio unity corresponding to point A in Fig 7(b). The billet is then compressed with 20% penetration and rotated 90^0 corresponding to point B. The CRAR becomes the new initial aspect ratio of the billet for the next step, point D. This point is identified by locating point C on the CRAR axis, by drawing a 45^0 line from point C to meet the horizontal axis at aspect ratio D. The aspect ratios at C and D are identical. The volume of material displaced into the longitudinal direction can be determined from Fig 7(c) at point C' for the first cycle. A total of five compression and rotation cycles were applied using a tool width of $b_1 = 40mm$. The total volume displaced at the end of the fifth cycle can be read at point P'. A tool width of $b_2 = 20mm$ is then used and the cyclic compression-rotation process is continued from point P with 20% penetration for a further six cycles. In this way a stepped shaft was produced as shown in Fig 7(a), the final dimensions of the theory and experiment are also given in Table 2.

CONCLUSIONS

A number of upper bound solutions and a method from these analyses were introduced for a bar profiling process which can be implemented alongside a computer based planning algorithm in automated open die forging. It demonstrates how this method can be used to produce an idealized

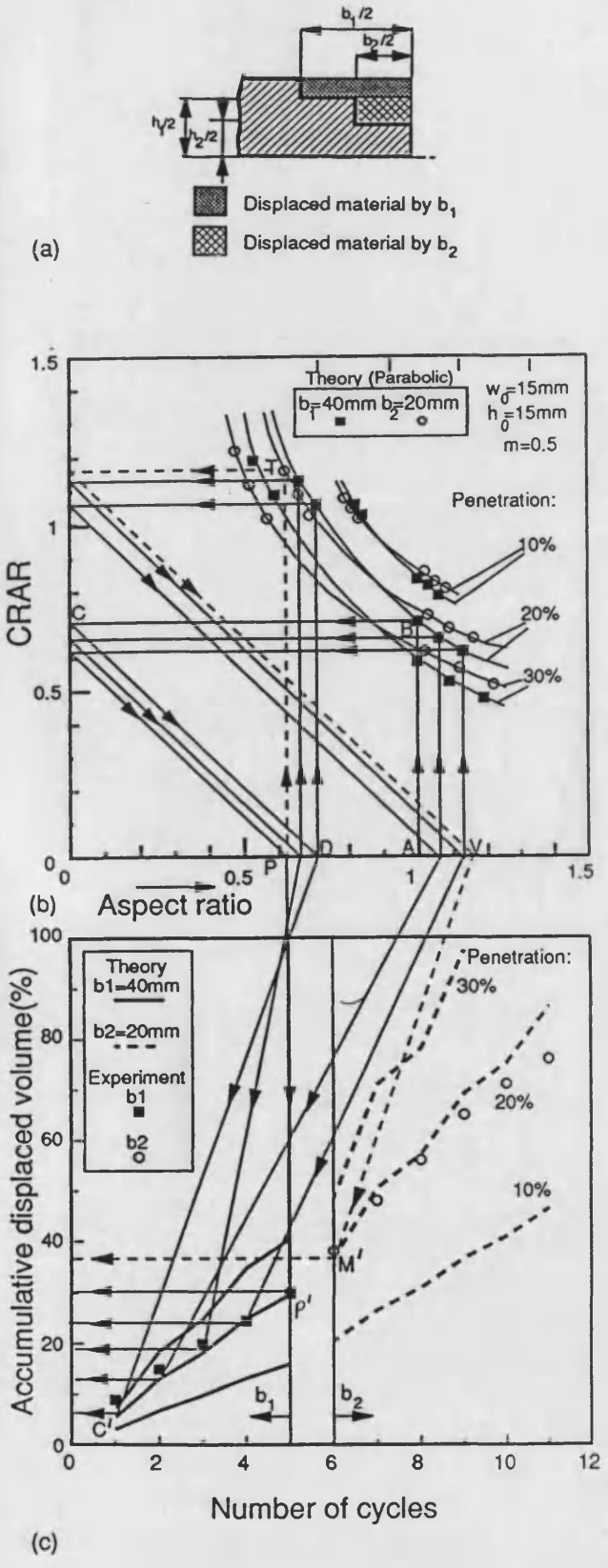

Fig 7. A chart for profiling a bar using flat tools.

Theory (mm)					Experiment				
w_1	w_2	h_1	h_2	l_f	w_1	w_2	h_1	h_2	l_f
8.76	9.02	4.07	8.88	28.4	10.63	9.46	4.87	9.72	126.7

Table 2. Final dimensions of the stepped shaft

dimensions at an intermadiate position on the workpiece. The analytical solutions are found to be in fairly good agreement with the experimental results.

ACKNOWLEDGMENTS

The authors acknowledge the financial support given to Mr. Aksakal by the Turkish Government-University of Ataturk and the provision of research facilities by the University of Bath.

REFERENCES

[1] Tomlinson A, and Stringer J.D, "Spread and elongation in flat tool forging", Journal of The Iron and Steel Institute, Oct. 1959, pp 157-162.

[2] Wistreich J.G.and Shutt A., "Theoretical analysis of bloom and billet", Journal of the Iron and Steel Institue, 1959, pp 163-176.

[3] Kemp I., "Modelling of three dimensional metal forming processes using the Upper Bound elemental technique", BHP research and new technology, Melbourne Research Laboratories, technical Note-MRL/MAT/., 1989.

[4] Soda C., et al, "Metal forming machinery development in the national project of FMCS", Proc.1st Int. Conf. of Plasticity, Tokyo, 1984, pp 449-460.

[5] Lange K. , "NC-Radial forging -A new concept in flexible automated manufacturing of precision forging in small quantities", 25th MTDR Conf., Birmingham, 1985,157-162.

[6] Park J.J. and Kobayashi S., "Three dimensional finite element analysis of block compression", Int.J.Mech.Sci.Vol.26, No.3, 1984, pp 165-176.

[7] Baraya G.L.and Johnson W., "Flat bar forging", Proc. of the fifth Int. MTDR Conf., 1964, pp 449-469.

[8] Aksakal B., Osman F.H. and Bramley A.N. "Analysis of Open Die Forging", Proc. of 29th.Int.Matador Conf., 1992, pp 415-419.

[9] Aksakal B., Osman F.H. and Bramley A.N., "Analysis for the automation of small batch manufacture using open die forging", to be published in CIRP Annals., 1993.